

This work is protected by copyright and other intellectual property rights and duplication or sale of all or part is not permitted, except that material may be duplicated by you for research, private study, criticism/review or educational purposes. Electronic or print copies are for your own personal, non-commercial use and shall not be passed to any other individual. No quotation may be published without proper acknowledgement. For any other use, or to quote extensively from the work, permission must be obtained from the copyright holder/s.

***Cell-based meniscus characterization
and regeneration: basic science, tissue
engineering and clinical applications***

Jingsong Wang

***PhD in Cell and Tissue Engineering
July 2021
Keele University***

Abstract

As a vital part of the knee joint, the meniscus acts to prevent the degeneration of articular cartilage and the onset of knee osteoarthritis (OA). Repairing meniscus injuries in the avascular region is still a challenge in orthopaedics. The current primary option is partial meniscectomy which can significantly increase the risk of developing knee OA. This unmet clinical need has shifted the research focus on the field towards novel cell-based tissue engineering approaches. In this thesis, the chondrogenic and immunomodulatory properties of regional meniscal cells from degenerative meniscus tissue have been investigated, in order to begin to understand more fully the changes in meniscal cells during knee degeneration. In addition, progenitor populations from human meniscus tissues have been isolated and the cell phenotypes characterised, and their proliferation rate and chondrogenic potency for meniscus regeneration analysed as compared their whole mixed population. Then moving to cell-based meniscus tissue engineering, a sheep explant model was used to examine the feasibility of utilising autologous avascular meniscal cells with a fibrin gel delivery system into a clinical grade polyurethane scaffold with the aim of promoting meniscus regeneration. A review has also been undertaken of the mid to long-term outcome of patients who had received combined autologous chondrocyte implantation (ACI) and meniscus allograft transplantation (n=20) or commercial meniscus scaffolds (n=8) treated at RJAH Orthopaedic Hospital (Oswestry).

Herein, it has been demonstrated that both avascular and vascular meniscal cells have chondrogenic capacity *in vitro* and the immunopositivity levels of the integrin markers CD49b and CD49c are valuable in distinguishing avascular, vascular meniscus cell and chondrocyte phenotypes. Histology of degenerated meniscus showed decreased vascularity in “tree-like” transverse collagen fibres, which may indicate that such structures are involved in the meniscus pathological process. This work has also demonstrated that the

human meniscus contains a meniscal progenitor population in both the avascular and vascular regions, based on clonogenicity and chondrogenic differentiation capacity. Results suggested that progenitor meniscal cells from vascular regions exhibit superior regenerative characteristics which are likely associated with the better meniscal healing properties noted in the vascular region of the tissue. The sheep explant experiment proved the feasibility of using fibrin gel to deliver autologous avascular meniscal cells in a clinical grade meniscus substitute *in vitro*. Further, the fibrin seeded scaffolds showed increased cell numbers and more matrix production compared to scaffolds seeded without fibrin.

In the clinical study, the data analysed showed for the first time that combining ACI with meniscal allograft transplantation or synthetic scaffold transplant to treat patients with cartilage defects and meniscal deficiency can provide successful mid-long term clinical outcomes, with 10-year survival rates of 71% in the MAT group and 83% in the scaffold group. Perhaps combining cells in fibrin in the scaffold could lead to even greater successes in the long term .

Table of Contents

Abstract	ii
List of Figures	ix
List of Tables	xii
Abbreviations	xiii
Dissemination	xvii
Acknowledgements	xix
Chapter 1: Introduction	1
1.1 Anatomy of the Meniscus	2
1.1.1 Meniscus Gross Anatomy	2
1.1.2 Extracellular Matrix	4
1.1.3 Cells in the Meniscus	6
1.2 Ageing in the Meniscus	7
1.2.1 Introduction	7
1.2.2 Changes in an Aged Meniscus	8
1.2.3 Cellular Senescence in an Aged Meniscus	10
1.3 Meniscus Injury and Repair in the Clinic	11
1.3.1 Introduction	11
1.3.2 Meniscal Tears: Aetiology and Classification	11
1.3.3 Meniscectomy	14
1.3.4 Repair of Meniscal Tears	14
1.3.5 Meniscus Allograft Transplantation	16
1.3.6 Synthetic Meniscal Scaffolds	18
1.4 Cell-based Meniscus Tissue Engineering	20
1.4.1 Introduction	20
1.4.2 Meniscus Cells	21
1.4.3 Articular Chondrocytes	22
1.4.4 Mesenchymal Stromal Cells	23
1.4.5 Co-culture	25
1.4.6 Combined Autologous Chondrocyte and Bone Marrow Mesenchymal Stromal Cell Implantation in the Knee: Two First-In-Man Cases	26
1.5 Meniscus Scaffolds	29
1.5.1 Introduction	29

1.5.2 Bioabsorbable Synthetic Polymers Scaffolds	30
1.5.3 Hydrogels	31
1.5.4 Biological Component Scaffolds	32
1.5.5 Decellularised Meniscal Scaffolds.....	33
1.6 Aims of PhD Project	35
Chapter 2: Laboratory Material and Method	37
2.1 Cell isolation, cell culture and cell preservation	38
2.1.1 Obtaining patient consent and samples	38
2.1.2 Avascular & vascular meniscal cells and chondrocyte isolation	38
2.1.3 Cell culture in monolayer and cell passaging	39
2.1.4 Cells cryopreservation	40
2.2 Meniscal progenitor cells	40
2.2.1 Meniscal progenitor cells isolation protocol.....	40
2.2.2 Cell-IQ [®] live imaging of progenitor colonies.....	41
2.3 Growth kinetics in monolayer culture.....	43
2.4 Detection of cell surface markers by flow cytometry	44
2.4.1 Flow cytometry introduction.....	44
2.4.2 Preparation for flow cytometry	45
2.5 Three-dimensional pellet culture for chondrogenic differentiation	49
2.6 Biochemical analyses for chondrogenesis within the pellets.....	49
2.6.1 Papain digestion of chondrogenic pellets	49
2.6.2 Dimethylmethylene blue assay (DMMB).....	49
2.6.3 DNA Assay	50
2.7 RNA extraction and Quantitative Real-Time Polymerase Chain Reaction (qRT-PCR).....	51
2.7.1 mRNA extraction	51
2.7.2 mRNA reversed to cDNA	51
2.7.3 Quantitative Real-Time Polymerase Chain Reaction (qRT-PCR).....	52
2.8 Histological analysis	53
2.8.1 Cryosection of chondrogenic pellets.....	53
2.8.2 Wax embedding and sectioning of human meniscus tissue and sheep meniscus explant.....	54
2.8.3 Haematoxylin and Eosin (H&E) staining of human meniscus sections	54
2.8.4 Toluidine blue staining of chondrogenic pellets.....	55
2.8.5 Immunochemical staining of collagen type I and type II	55

2.8.6 Histological grading of human meniscus tissue.....	56
2.9 Fibrinogen and thrombin polymerisation.....	59
2.9.1 Mechanism of Fibrinogen and Thrombin Blood-Clotting Cascade....	59
2.9.2 Fibrin gel in polyurethane scaffold penetration test	60
2.9.3 Chondrocyte viability in polyurethane scaffold with fibrin gel.....	61
2.10 Statistical analysis	62
Chapter 3: Characterisation of Regional Meniscal Cell and Chondrocyte Phenotypes and Chondrogenic Differentiation in Osteoarthritic Donor-Matched Tissues.....	63
3.1 Introduction.....	64
3.2 Experiment design	67
3.3 Results.....	69
3.3.1 Histological scoring and analysis of meniscus sections	69
3.3.2 Growth kinetics	74
3.3.3 Cell surface markers analysis.....	74
3.3.4 Comparing flow profiles and histological analyses	77
3.3.5 Gene expression profiles: Donor-matched analyses of avascular and vascular meniscal cells and chondrocytes.....	78
3.3.6 <i>In vitro</i> chondrogenic pellet analysis	80
3.3.7 Chondrogenic potency analysis	82
3.4 Discussion	83
Chapter 4: Phenotypic characterisation of regional human meniscus progenitor cells	89
4.1 Introduction.....	90
4.2 Experiment Design.....	91
4.3 Results.....	96
4.3.1 Growth Kinetics and Cell Morphology in Mixed Population and Progenitor cells	96
4.3.2 Cell-IQ [®] Analysis	98
4.3.3 Cell Surface Markers	100
4.3.4 Chondrogenic Gene Expression in Cell Pellets	101
4.3.5 <i>In Vitro</i> Chondrogenic Differentiation Analysis.....	104
4.4 Discussion	106
Chapter 5: The influence of fibrin gel on the delivery of autologous meniscal cells in synthetic meniscus scaffold in an ovine meniscus explant model.....	112
5.1 Introduction.....	113
5.2 Experiment design	114

5.3 Results.....	119
5.3.1 Fibrin gel distribution and cell viability in the scaffold.....	119
5.3.2 Imaging of cell-seeded scaffolds in the <i>in vitro</i> explant model	121
5.3.3 Gene expression of meniscal cells in the meniscus explant model ..	122
5.3.4 Matrix formation assessments in the sheep meniscus explant model	123
5.4 Discussion	127
Chapter 6: Concomitant autologous chondrocyte implantation with synthetic meniscus scaffold or allograft transplantation: Mid to long term follow up	133
6.1 Introduction.....	134
6.2 Methods and Materials.....	136
6.2.1 Patient Information	136
6.2.2 Surgical Techniques.....	136
6.2.3 Outcome Assessments	137
6.2.4 Statistical Analysis.....	140
6.3 Results.....	141
6.3.1 Patient Demographics	141
6.3.2 Concomitant and Subsequent Surgical Procedures.....	142
6.3.3 Clinical Outcomes Analysis.....	142
6.3.4 Multilevel Modelling and Estimated Clinical Outcome	144
6.3.5 Radiographic Evaluation.....	145
6.3.6 Post-operative Meniscus Allograft Biopsy Histology Evaluation	147
6.4 Discussion	149
Chapter 7: General Discussion.....	153
7.1 The role the meniscus plays in progression of knee OA	154
7.2 The clinical perspective: translation of meniscus regeneration research to clinical practice	156
7.2.1 Major obstacles limiting cell therapy for meniscus repair in the clinic	156
7.2.2 Future perspectives of translating cell-based meniscus tissue engineering to the clinic	158
7.3 Conclusion	159
Reference	161
Appendices.....	191
Appendix I	191

Appendix II	194
Appendix III.....	195
Appendix IV.....	196
Publications associated with this thesis	198

List of Figures

<i>Figure 1.1: Structural view of the human knee meniscus from above.</i>	3
<i>Figure 1.2: Schematic diagram illustrating the collagen fibre ultrastructure and orientation within the meniscus</i>	5
<i>Figure 1.3: Regional cell populations of the meniscus.</i>	7
<i>Figure 1.4: Schematic diagram of age-related change in the meniscus.</i>	8
<i>Figure 1.5: Examples of Common Meniscal Tears</i>	13
<i>Figure 1.6: Diagram of meniscal tears locations.</i>	13
<i>Figure 1.7: A pyramid schematic describing the repair potential for different types of meniscal injury.</i>	16
<i>Figure 1.8: Schematic representation of the cell-loading of a decellularised ECM meniscus scaffold.</i>	34
<i>Figure 2.1: Schematic diagram of the process used for meniscus dissection</i>	39
<i>Figure 2.2: Schematic diagram of the automated optics module and monitoring system.</i>	43
<i>Figure 2.3: Illustration of the working principle of a flow cytometer.</i>	44
<i>Figure 2.4: Flow cytometry light scattering.</i>	45
<i>Figure 2.5: Diagram of the combination of fluorochrome conjugated antibodies assessed via flow cytometry.</i>	48
<i>Figure 2.6: Macroscopic meniscus assessment</i>	57
<i>Figure 2.8: Schematic representation of fibrin formation.</i>	60
<i>Figure 3.1: Histological grading results of avascular and vascular regions of the meniscus.</i>	70
<i>Figure 3.2: Representative avascular region meniscus histology from donor 9 stained with H&E and TB (Grade 2).</i>	71
<i>Figure 3.3: Representative images of Grade 2 (b-d: donor 4) and Grade 3 (e, f: donor 9) menisci with H&E staining</i>	73
<i>Figure 3.4: Population doubling time (PDT).</i>	74

<i>Figure 3.5: Flow cytometry outcomes</i>	76
<i>Figure 3.6: qRT-PCR outcomes</i>	79
<i>Figure 3.7: The chondrogenic assessment of avascular and vascular meniscal cells and chondrocytes.</i>	81
<i>Figure 4.1: Flow Diagram of the Experimental Plan</i>	93
<i>Figure 4.2: Comparison of progenitor cells morphology on monolayer culture.</i>	97
<i>Figure 4.3: Population doubling time (PDT) of progenitor cells</i>	98
<i>Figure 4.4: Diagram of individual colony proliferation rates over 48 hours in the Cell-IQ®.</i>	99
<i>Figure 4.5: The overall comparison of proliferation rate for avascular, vascular meniscal progenitors and chondroprogenitors.</i>	100
<i>Figure 4.6: Progenitors flow cytometry outcomes</i>	101
<i>Figure 4.7: RT-qPCR outcomes of progenitor cells.</i>	103
<i>Figure 4.8: GAG/DNA quantitation after 28 days of 3D pellet culture</i>	104
<i>Figure 4.9: Collagen type I and II and toluidine blue staining.</i>	105
<i>Figure 4.10: Pellets staining intensity</i>	105
<i>Figure 5.1: Fibrin gel explant experiment workflow diagram.</i>	117
<i>Figure 5.2: Sheep meniscus explant process</i>	118
<i>Figure 5.3: Fibrin gel penetration test</i>	119
<i>Figure 5.4: Live/dead staining of scaffold</i>	120
<i>Figure 5.5 Chondrocytes within fibrin gel distribution in CMI® scaffold (H&E staining)</i>	120
<i>Figure 5.6: Sheep explant culture images</i>	122
<i>Figure 5.7: Gene expression profiles of extracted mRNA in cell only group and fibrin gel seeded scaffold in the meniscus explant model.</i>	123
<i>Figure 5.8: Biochemical component analysis of sheep explant models</i>	125
<i>Figure 5.9: Immunohistochemistry staining of collagen type I in explants and scaffolds.</i>	126
<i>Figure 6.1: Illustration of meniscus extrusion measurement.</i>	139

<i>Figure 6.2: Comparison of pre-operative and one-year post-operative Lysholm score for MAT (A) and Actifit[®] group (B).</i>	143
<i>Figure 6.3: Kaplan-Meier survival curves.</i>	143
<i>Figure 6.4: MRI assessment of meniscus extrusion.</i>	146
<i>Figure 6.5: Represent postoperative MRI (sagittal) of Actifit implants with ACI patient.</i>	147
<i>Figure 6.6: Representative histology of biopsies taken 19 months post-operation with allogeneic meniscus</i>	148

List of Tables

Table 1.1: CMI [®] and Actifit [®] implantation indications and contraindications	20
Table 1.2: Mechanical and biological criteria required for a meniscus scaffold	29
Table 1.3: the biomechanical and viscoelastic properties of human health or degenerate meniscus and clinical scaffold	30
Table 2.1: The Cell-IQ [®] components.....	42
Table 2.2: Cell surface molecules for flow cytometry.....	47
Table 2.3: Primers used for qRT-PCR.....	53
Table 2.4: Macroscopic meniscus scoring system.....	57
Table 2.5: Microscopic meniscus scoring system.....	58
Table 3.1: Demographics of donors from which samples were sourced.	69
Table 3.2: Correlation between surface markers and histology scores.....	78
Table 3.3: Multilevel modelling	82
Table 4.1. Patient Demographics.	92
Table 4.2: Tukey's multiple comparisons test.....	100
Table 4.3: Meniscal progenitor cells isolation protocols	109
Table 6.1: Patient Demographics	141
Table 6.2: Meniscus allograft transplantation failures.....	144
Table 6.3: Fixed Effects in the Longitudinal Multilevel Model	145
Table 6.4: Estimated Post-operative Lysholm Scores	145

Abbreviations

AC	Articular Chondrocytes
ACAN	Aggrecan
ACI	Autologous Chondrocyte Implantation
ACL	Anterior Cruciate Ligament
ACLR	Anterior Cruciate Ligament Reconstruction
AGEs	Advanced Glycation End-products
AKA	Above Knee Amputation
aME	Absolute Meniscal Extrusion
APC	Allophycocyanin
BMI	Body Mass Index
BMLs	Bone Marrow Lesions
BM-MSCs	Bone Marrow Mesenchymal Stromal Cells
BSA	Bovine Serum Albumin
BV	Brilliant Violet
CCCI	Coronal Cartilage Coverage Index
CMI	Collagen Meniscus Implant
CTGF	Connective Tissue Growth Factor
DAB	Diaminobenzidine
DFO	Distal Femoral Osteotomy
DMEM	Dulbecco's Modified Eagle Medium
DMM	Destabilisation of the Medial Meniscus
DMMB	Dimethylmethylene Blue
ECM	Extracellular Matrix
EDTA	Ethylene Diamine Tetraacetic Acid

FACS	Fluorescence-Activated Cell Sorting
FBS	Foetal Bovine Serum
FGF-2	Fibroblast Growth Factor-2
FSC	Forward Scatter
IKDC	International Knee Documentation Committee
IL	Interleukin
IPA	Isopropanol
ISCT	International Society for Cellular Therapy
ITS	Insulin-Transferrin-Selenium
GAGs	Glycosaminoglycans
GAPDH	Glyceraldehyde-3-phosphate Dehydrogenase
GMP	Good Manufacturing Practice
HLA-DR	Human Leukocyte Antigen-D Related
HTO	High Tibial Osteotomy
KOOS	Knee injury and Osteoarthritis Outcome Score
LFC	Lateral Femoral Condyle
LTP	Lateral Tibial Plateau
MAvas	Avascular Meniscal Mixed Cells
MCF	Minced Cartilage Fragments
MChs	Mixed Chondrocytes
MCs	Meniscus Cells
MFC	Medial Femoral Condyle
MHRA	Medicines and Healthcare Products Regulatory Agency
MOCART	Magnetic Resonance Observation of Cartilage Repair Tissue
MRI	Magnetic Resonance Imaging
MTP	Medial Tibial Plateau

MVas	Vascular Meniscal Mixed Cells
NHS	National Health Service
NICE	National Institute for Clinical Excellence
OA	Osteoarthritis
ORKA	Oswestry Risk of Knee Arthroplasty
PAvas	Avascular Meniscal Progenitors
PBS	Phosphate Buffer Saline
PChs	chondroprogenitors
PCL	Polycaprolactone
PDT	Population Doubling Times
PE	Phycoerythrin
PercP-Cy5	Peridinin-chlorophyll-protein-Cyanine
PGA	Polyglycolic acid
PLA	Polylactic Acid
PLGA	Polylactic Co-glycolic Acid
PVA	Polyvinyl Alcohol
PVas	Vascular Meniscal Progenitors
PU	Polyurethane
qRT-PCR	Quantitative Real-Time Polymerase Chain Reaction
RJAH	Robert Jones and Agnes Hunt Orthopaedic Hospital
rME	Relative Meniscal Extrusion
SD	Standard Deviation
SDS	Sodium Dodecyl Sulphate
SF	Silk Fibroin
SSC	Side Scatter
TB	Toluidine Blue

TGF	Transforming Growth Factor
TKR	Total Knee Replacement
TNF	Tumour Necrosis Factor
WORMS	Whole Organ Magnetic Resonance Imaging Score

Dissemination

Publications related to this thesis:

1. Wang J, Wright KT, Perry J, Tins B, Hopkins T, Hulme C, McCarthy HS, Brown A, Richardson JB. Combined Autologous Chondrocyte and Bone Marrow Mesenchymal Stromal Cell Implantation in the Knee: An 8-year Follow Up of Two First-In-Man Cases. *Cell transplantation*. 2019 Jul;28(7):924-31. doi: 10.1177/0963689719845328
2. Wang J, Roberts S, Kuiper JH, Zhang W, Garcia J, Cui Z, Wright K. Characterization of regional meniscal cell and chondrocyte phenotypes and chondrogenic differentiation with histological analysis in osteoarthritic donor-matched tissues. *Scientific reports*. 2020 Dec 10;10(1):1-4. doi: 10.1038/s41598-020-78757-6

Published abstracts:

1. Jingsong Wang, K. Wright, J. Perry, C. Hulme, T. Hopkins, A. Brown, H. McCarthy, B. Tins, J. Richardson. Combined Cultured Autologous Chondrocytes and BM-MSCs Implantation: Two case report, 9 and 8 years follow-up. *Cartilage*, 10135 (2018)
2. Jingsong Wang; Sally Roberts; Weiguo Zhang; Karina Wright. Discrimination of Regional Meniscus Cell And Chondrocyte Phenotype In Osteoarthritic Donor-matched Tissues. *Journal of Orthopaedic Research*, PS2-071 (2020)

Podium Presentation:

1. UK-China Workshop for Regenerative Dentistry, Leeds 2018
2. Research day. The Robert Jones & Agnes Hunt Hospital, Oswestry, April 2019
3. Postgraduate symposium. Keele. May 2019
4. British Orthopaedic Research Society. Online. September 2020

Poster Presentations :

International Cartilage Repair and Joint Preservation Society. Macau, China 2018

Tissue and Cell Engineering Society. Keele, UK. 2018

Postgraduate Symposium. Keele, UK. 2018

Research day. The Robert Jones & Agnes Hunt Hospital, Oswestry, UK 2018

MERCIA Stem Cell Alliance Meeting. Birmingham, UK 2018

International Cartilage Repair Society. Vancouver, Canada 2019

MERCIA Stem Cell Alliance Meeting. Chester, UK 2019

Orthopaedic Research Society. Phoenix, USA 2020

Acknowledgements

First and foremost, I am extremely grateful to my supervisors, Dr. Karina Wright and Professor Sally Roberts for their invaluable advice, continuous support, and patience during my PhD study. Their knowledge and plentiful experience have encouraged me in all the time of my academic research and daily life. I wish to express my sincere appreciation to another of my supervisors, Professor James Richardson and his family, who offered me kindness help and advice throughout my PhD. I would like to thank all the members in the Cartilage Repair and Spinal Studies Group in RJA Orthopaedic Hospital. It is their kind help and support that have made my study and life in the UK a wonderful time. Finally, I would like to express my gratitude to my parents, especially my Mom. Without her taking care of my daily life during the COVID-19 pandemic, it would have been impossible for me to complete my study.

I would also like to show my gratitude to the Orthopaedic Institute of the RJA Orthopaedic Hospital, the Chinese Scholarship Council and Professor Zhanfeng Cui from Oxford University, for their funding of my research at Keele University and RJA. Without their support, this project could not have reached its goals.

I would like to dedicate this thesis to my supervisor, Professor James Richardson and his wife Shona Richardson, for their guidance, support and encouragement during my studies in Oswestry.

Chapter 1: Introduction

1.1 Anatomy of the Meniscus

1.1.1 Meniscus Gross Anatomy

The medial and lateral menisci in the knee joint are two crescentic-shaped wedges of fibrocartilage located between the femoral condyle and tibial plateau ¹. The menisci's superior concave surface allows the convex femoral condyles to articulate, while their inferior flat surfaces accommodate the tibial plateau ². Both play a crucial role in the maintenance of a healthy knee. However, there are macroscopic differences between the medial and lateral menisci (Figure 1.1).

In adult humans, the medial meniscus is approximately 40-45mm long and 27mm wide, while the lateral meniscus is 32-35mm long and 26-29mm wide. The medial meniscus covers less of the corresponding area of the tibial plateau (51-74%) in comparison to the lateral meniscus (75-93%) ³. The medial collateral ligament, menisiofemoral ligaments, transverse ligament and the anterior and posterior horns maintain the stability of the menisci ⁴. The menisiofemoral ligaments are also known as the ligaments of Humphrey and Wrisberg which run from the posterior horn of the lateral meniscus to the lateral aspect of the medial femoral condyle ⁵. The medial meniscus displays greater immobility compared to the lateral meniscus as it more firmly attaches to the deep medial collateral ligament at the midpoint and continuously attaches to the joint capsule on both sides ⁶.

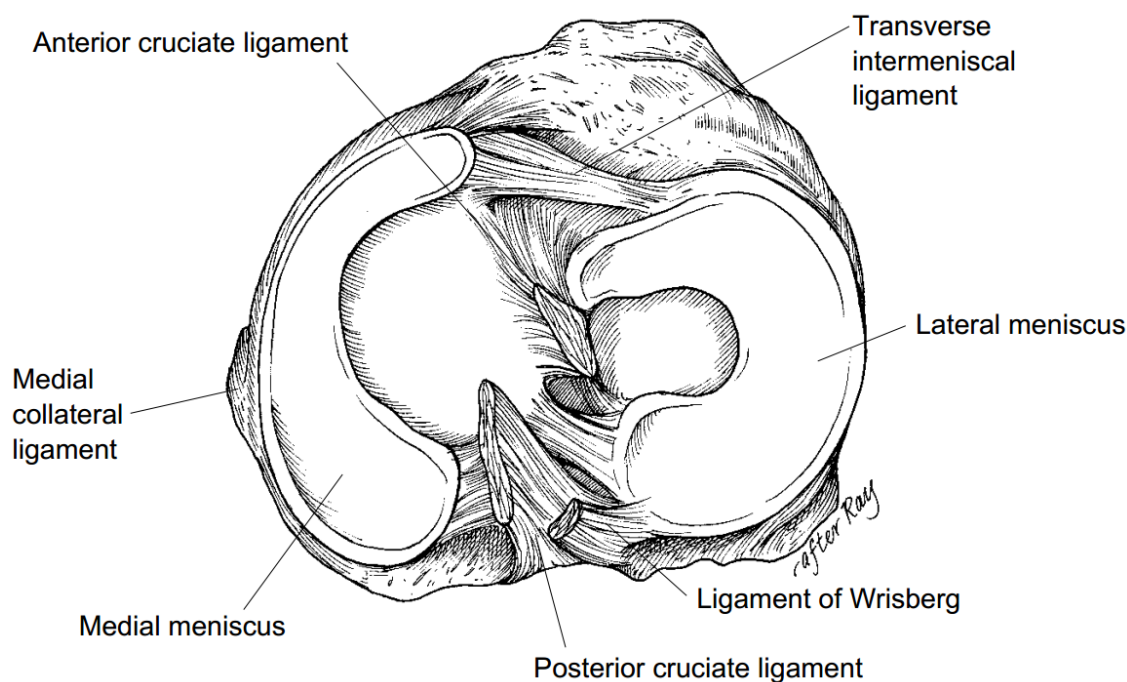


Figure 1.1: Structural view of the human knee meniscus from above.

The shape and position of medial and lateral menisci are distinct. Reproduced from Greis et al. ⁴ (reprint permission from Wolters Kluwer Health, Inc)

As the vascularity of the meniscus continues to reduce after birth, only 10-25% of the peripheral area of the mature meniscus contains vessels and nerves (red-red zone) ⁷. The larger completely avascular zone of the inner meniscus is known as the white-white zone. A transition area between the two also exists, which is called the red-white zone. The healing capacity of a meniscus has direct relevance to its vascularisation. There is evidence that vascularised tissues heal more quickly than avascular tissues. For example, there is no blood supply in the cornea and an incision in the avascular cornea will heal in approximately 6 weeks, whereas sutures can be removed at 2 weeks from a vascular skin incision ⁸. In the menisci, a tear in the red zone may heal spontaneously, but a tear in the white-white region will not heal and will predispose to permanent post-traumatic and degenerative lesions ⁹.

1.1.2 Extracellular Matrix

A normal meniscus is primarily composed of water (72%) and collagens (22%), interspersed with meniscal cells. The remaining dry weight is composed of proteoglycans and matrix glycoproteins ¹⁰. These proportions fluctuate depending on the age of the individuals and the locations within the meniscus structure ¹¹.

Collagens

Collagens play an important role in maintaining the tensile strength of the menisci. They make up 75% of the dry weight of the extracellular matrix (ECM) including type I collagen, which accounts for over 90%, and variable amounts of types II, III, V and VI ¹². The distribution of each collagen varies in different regions within the tissue. In the menisci, type I collagen is predominate with trace amount (<1%) of types III and V in the outer two-thirds zone, whereas in the inner zone 60% is collagen type II and 40% is collagen type I ¹³. The collagen fibres in the meniscus run in three layers (Figure 1.2), the majority of collagen fibres are orientated circumferentially in the middle layer which is ideal for transferring vertical loading into hoop stress. In the superficial layer, collagen fibres are oriented in a more radial direction and act as “ties” providing the meniscus with rigidity and preventing longitudinal splitting, whereas some radially oriented fibres also interweave among the circumferential fibres to provide further stability ^{14,15}.

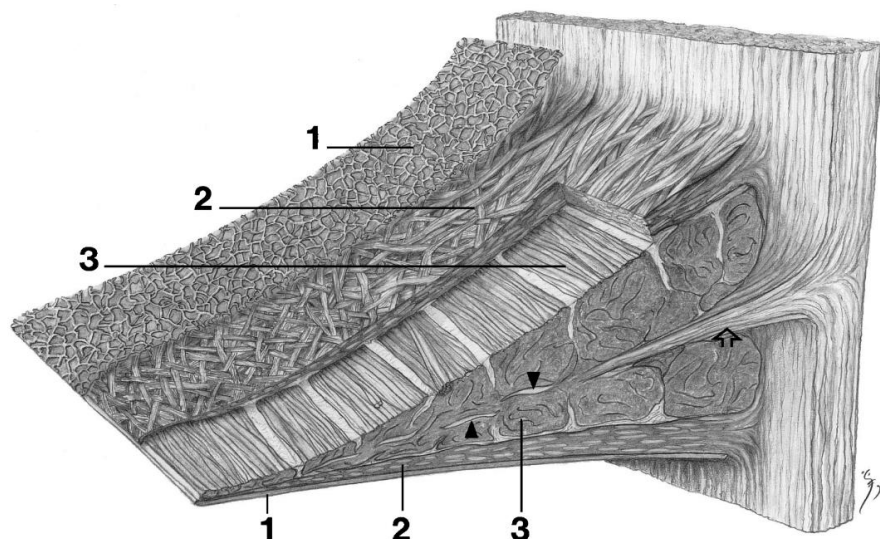


Figure 1.2: Schematic diagram illustrating the collagen fibre ultrastructure and orientation within the meniscus

1, 1st surface layer; 2, 2nd surface layer (radial fibres); 3, middle layer (circumferential fibres). Closed arrowheads, radial interwoven fibres; open arrowhead, loose connective tissue. Reproduced from Petersen et al. ¹⁵ (reprint permission from Springer Nature)

Proteoglycans

Proteoglycans are highly hydrophilic and heavily glycosylated molecules, which contribute less than 1% of the meniscus dry weight ¹⁶. They are composed of one or more glycosaminoglycans (GAGs) chains attached to a core protein. The GAGs in the human meniscus are composed of chondroitin-6-sulphate (40%), dermatan sulphate (20-30%), chondroitin-4-sulphate (10-20%), and keratan sulphate (15%) ¹². The amount of proteoglycan in articular cartilage is eight fold higher than that present in the meniscus ¹⁷. Aggrecan is the major proteoglycan in the meniscus, whereas decorin, biglycan and fibromodulin are found in smaller quantities. Proteoglycans in the meniscus are mainly responsible for absorbing water to resist compressive load ¹⁸.

Therefore, proteoglycans are mainly distributed in the meniscal horns and the inner two-thirds of the meniscus which is the primary weight-bearing zone ¹⁶.

Matrix glycoproteins

Meniscal cartilage contains a large range of matrix glycoproteins and their functions have not been fully identified. The molecular weights vary from a few kilodaltons (kDa) to more than 200-kDa ¹⁰. These matrix proteins include the link proteins that stabilize proteoglycan hyaluronan aggregates and a 116-kDa protein of unknown function. This protein is involved in the formation of a disulphide-bonded complex of large molecular weight ¹⁹. The adhesive glycoproteins are a subgroup of matrix glycoproteins. These macromolecules bind with other matrix components and/or cells, including fibronectin and thrombospondin ^{10,20}.

1.1.3 Cells in the Meniscus

The cells within a meniscus are regarded as fibrochondrocytes, since they seem to possess characteristics of both fibroblasts and chondrocytes ². They are classified into three types according to their shape and location (Figure 1.3). The superficial zone cells have a small and round appearance and a recent study suggested that these cells are a possible progenitor population with regenerative capabilities ^{21,22}. The outer zone cells have an oval, fusiform shape and are described as fibroblast-like cells, whereas the inner zone cells appear to have a more rounded shape and are described as chondrocyte-like cells ²¹. The metabolism of the three types of cell is mainly anaerobic with the cells having abundant endoplasmic reticulum, Golgi complexes, and few mitochondria. The main role of fibrochondrocytes in the menisci is the synthesis and maintenance of the ECM ²³.

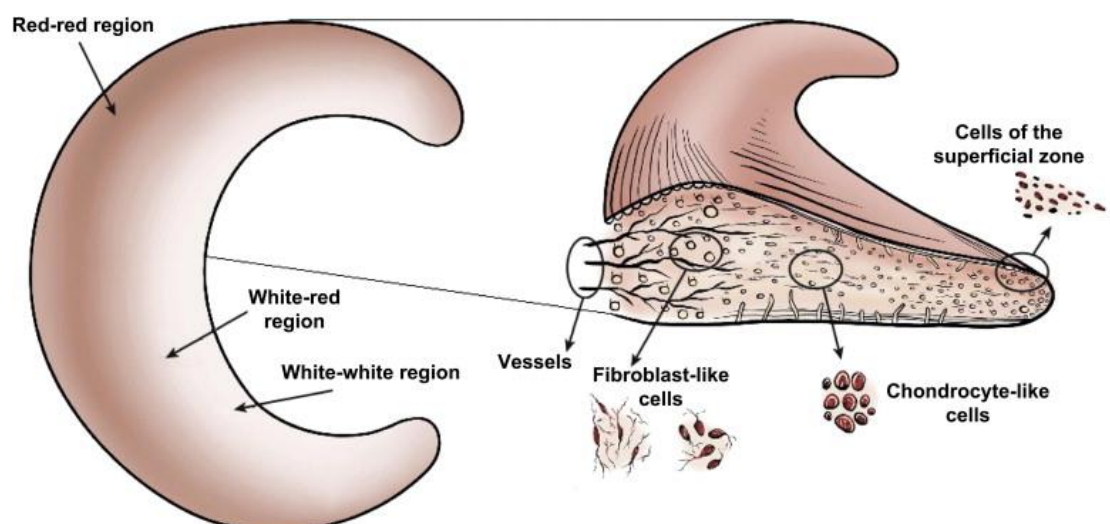


Figure 1.3: Regional cell populations of the meniscus.

Cells in the red-red region (vascular) are spindle-shaped and more fibroblast-like in morphology, while cells in the white-red and white-white region (avascular) are more chondrocyte-like. Cells in the superficial layer of the meniscus are round and small. Reproduced from Makris et al. ²⁴ (reprint permission from Elsevier)

1.2 Ageing in the Meniscus

1.2.1 Introduction

Ageing is an irreversible process, which can be defined as an accumulation of molecular and cellular damage over time. It has been suggested that degeneration should be considered separate from ageing since degeneration is defined as the failure in tissue structure and function which can occur also in young individuals ²⁵. The distinction has been accepted in articular cartilage ²⁶ and intervertebral discs ²⁷. Human knee menisci similarly exhibit changes associated with ageing. The age-related changes in the menisci consist of tissue ageing and cellular ageing (cellular senescence) ²⁵. These changes contribute to the pathogenesis of the meniscus, comparable to those seen in articular cartilage ²⁸. Therefore, it is important to understand the biological processes

involved in the ageing of the meniscus.

1.2.2 Changes in an Aged Meniscus

Macroscopically, young and healthy menisci appear translucent, white, and with a smooth surface, whereas the surface of aged menisci become roughened with fibrillation and appears more opaque with a dark yellowish colour (Figure 1.4). These colour changes are caused by non-enzymatic glycation similar to age-related changes seen in the intervertebral disc ²⁷. In addition, the whole meniscus becomes harder and loses its elasticity, although it retains its shape and looks almost normal except for the more obvious colour change ²⁹.

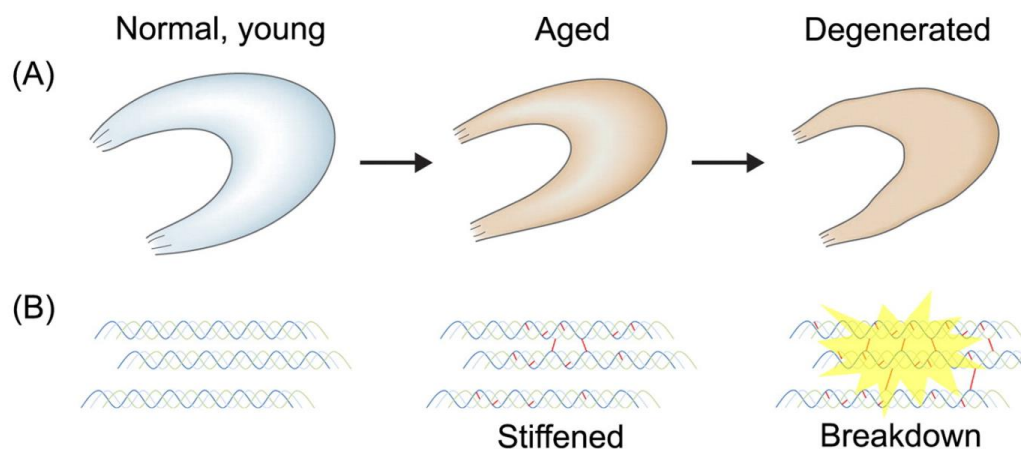


Figure 1.4: Schematic diagram of age-related change in the meniscus.

(A) Macroscopic changes; (B) Increasing cross-link associated changes in collagens;

Reproduced from Tsujii et al. ²⁵ (reprint permission from Elsevier)

Microscopically, the histology of an aged meniscus (with no or minimal OA) demonstrates decreased cell density, with some completely acellular zones being identified. Increased Safranin-O staining intensity is observed in the central area of avascular zones, as well as mucoid degeneration and the loss of collagen fibres ²⁹. The increased Safranin-O staining may represent a shift from a fibroblastic to chondrocytic

phenotype in meniscal cells during the meniscus ageing process. The earliest age-related changes in the meniscus are observed in the innermost rim, in which the diameter of collagen fibres tends to increase with age ²⁹. A cadaver study showed that beyond the age of 50, blood vessels were only present in the outer quarter of an aged meniscus. Immunohistochemical (IHC) analyses demonstrated that blood vessels were also present in the dense connective tissue insertion, but not in the fibrocartilage itself ³⁰. In addition, no change in blood supply was shown in degenerative and torn menisci compared with a normal meniscus in another cadaveric study (specimens obtained from 40-80 years of age) ³¹.

Collagens

The collagen content in normal menisci increases from birth to 30 years of age, after which the content remains steady until 80 years of age, when there is a gradual decline ¹⁶. The cross-linking of collagen molecules plays a crucial role in physiological and pathological processes. Non-enzymatic glycation and deposition of advanced glycation end-products (AGEs) increase with age, which is an irreversible process ³². Accumulation of AGEs was demonstrated to increase tissue stiffness, as well as affecting many cellular processes, such as adhesion of cells to the ECM and cell proliferation ³². Pentosidine is known as a mature cross-link and a marker of glycations and is found to be significantly increased with age ³³. Eventually, menisci with increased levels of AGEs become more vulnerable to mechanical damage (Figure 1.4).

Proteoglycans and fibronectin

The proteoglycan content in the meniscus appears to increase from birth to maturity, and then remains relatively steady. In the adult meniscus, the proteoglycans comprises only 2.7 mg/g of the wet weight, compared to 20 mg/g wet weight in adult articular cartilage ¹⁷. Further, the mRNA expression of decorin and aggrecan in the human

meniscus increases with age but does not change in articular cartilage³⁴. The differences in age-related changes observed between the meniscus and articular cartilage are likely to be a result of functional and morphological differences between the two tissues²⁵.

Fibronectin is a glycoprotein that enhances adhesion in the ECM. It has been found to decrease with ageing in articular cartilage, which leads to fibrillation³⁵. Similar processes may occur in the meniscus and hence the observed surface roughening and fibrillation associated with ageing in the meniscus might similarly be due to a loss of fibronectin, but this theory is yet to be proved²⁵.

1.2.3 Cellular Senescence in an Aged Meniscus

Cellular senescence can be described as the onset of irreversible cellular growth arrest, whereby cell division ceases as a result of persistent stress. It has been demonstrated to play an important role in complex biological processes associated with tissue repair and age-related disorders such as OA³⁶. There are broadly two types of cellular senescence: replicative senescence where progressive telomere deterioration is observed and stress-induced premature senescence which can be induced by a variety of extrinsic factors such as ultraviolet light, reactive oxygen species, chemotherapeutics and ionizing radiation^{36,37}. Meniscus cells have the potential for cell division, and cell growth and proliferation have been observed in primary culture³⁸. Although telomere deterioration of meniscal cells has not been reported, the senescence of chondrocytes is considered to lead to a shift in the balance between ECM synthesis and degradation which eventually results in the disruption of tissue homeostasis³⁹. Moreover, long-term compressive stress could also cause premature senescence for meniscus cells³⁶. In addition, increasing cell size has been observed in the aged meniscus, which is a characteristic of senescent cells²⁹. To date, however, cellular senescence has only been

reported in chondrocytes in articular cartilage and intervertebral disc cells⁴⁰. Thus, further evidence is required to prove its role in the meniscus cell cycle.

1.3 Meniscus Injury and Repair in the Clinic

1.3.1 Introduction

Meniscus injuries are the most commonly observed intra-articular knee injury. In the United Kingdom, the mean annual incidence of meniscus injury is 60-70 per 100,000⁴¹. These tears usually happen within the tissue body or the tibial attachment and in areas of tissue degeneration¹¹. There are different types of meniscal tear, such as longitudinal tears, radial tears and complex tears. Arthroscopic meniscectomy is the most commonly performed orthopaedic surgical procedure. However, partial or total resection of a torn meniscus is known to significantly increase the risk of early onset of OA^{42,43}. Therefore, preserving the native menisci where possible is important for the long-term function and health of the knee joint. There is a wide variety of meniscus repair techniques used in the clinic which will be the focus of the reviewed literature in this chapter.

1.3.2 Meniscal Tears: Aetiology and Classification

Meniscus injuries can be found in all age groups, although they have been shown to have a peak incidence in individuals aged 20 to 29 years, with a male to female ratio of between 2.5:1 and 4:1⁴⁴. Meniscus injuries are also mostly likely to occur in the right knee.

The aetiological factors involved in meniscal injury vary depending on the patient's age⁴⁵. More than a third of meniscal tears in young people are caused by twisting sports such as American football, basketball, soccer, and skiing; these injuries are referred to as traumatic tears. The mechanism of these injuries are usually the result of

hyperextension forces, and there is a high risk of an accompanied anterior cruciate ligament (ACL) rupture^{46,47}. Tears in middle-aged and elderly patients usually occur as a result of long-term degeneration, which lead to joint swelling, pain and locking; these injuries are known as degenerative meniscal lesions⁴⁸. There is a high prevalence (68-90%) of OA accompanying meniscal lesions as identified in radiographic findings^{49,50}. This high correlation brings with it difficulties for the clinical diagnosis of symptomatic meniscal tears, since some symptoms may be caused by the OA, while others may due to the meniscal tear itself²⁴.

Meniscal tears can be divided into two basic types: vertical and horizontal. Vertical tears consist of longitudinal, radial and flap tears⁵¹. Different combinations of these basic shapes can combine in various patterns to form complex tears (Figure 1.5)⁵². “Bucket handle” tears (as they are often referred to clinically) are longitudinal and vertical tears of the periphery of the meniscus. It is important clinically to locate the tear zone exactly since different locations of tears lead to different preferred treatment options. The locations can be divided into red-red zone (0-3mm from periphery), red-white zone (3-5 mm) and white-white zone (>5mm) as demonstrated in Figure 1.6. The plethora of treatment regimens available for meniscal tears will be reviewed in the following sections.

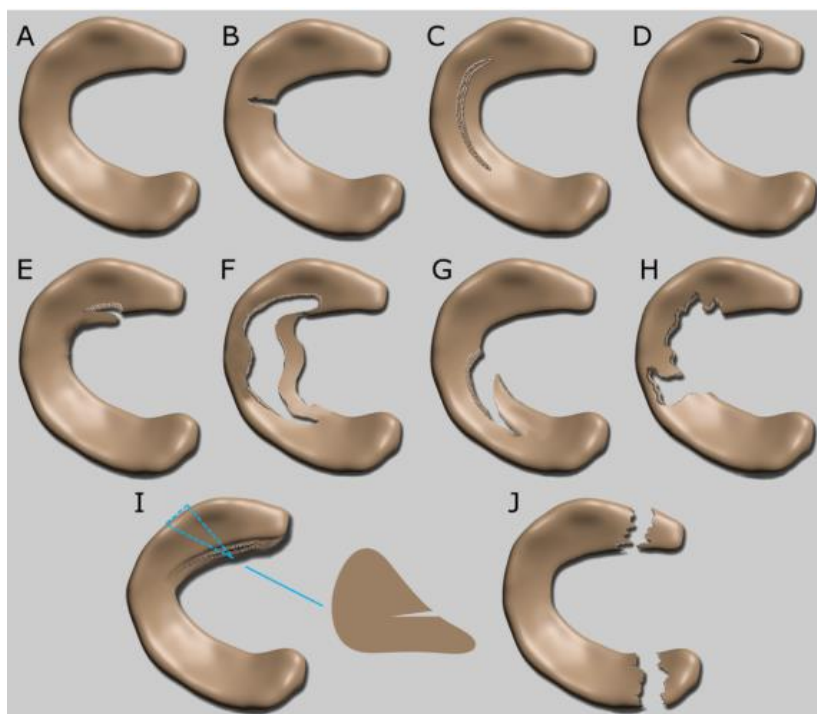


Figure 1.5: Examples of Common Meniscal Tears

Illustration of a normal meniscus (A), and common types of meniscal tears: radial tear (B), longitudinal tear (C), horizontal flap (D), vertical flap (E), bucket-handle tear (F), oblique/parrot-beak lesion (G), complex degenerative (H), horizontal tear (I), root tears (J). Reproduced from Cengiz et al. ⁵² (reprint permission from Springer Nature)

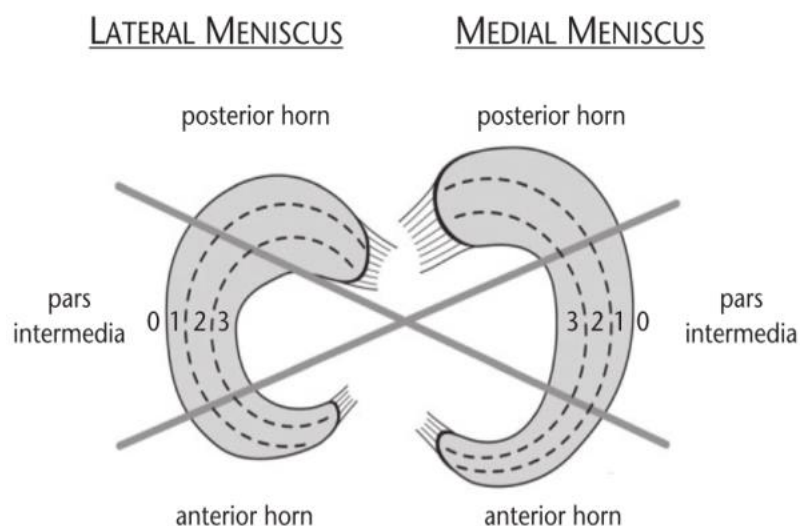


Figure 1.6: Diagram of meniscal tears locations.

1: red-red zone; 2: red-white zone; 3: white-white zone. Reproduced from Beaufils et al. ⁵¹ (reprint permission from Springer Nature)

1.3.3 Meniscectomy

Meniscectomy is one of the most widely used orthopaedic procedures globally ^{42,43}. However, resection of the meniscus leads to greater stress being applied to the articular cartilage, which increases 14-fold the risk of OA after 21 years ⁴³. Similarly, arthroscopic partial meniscectomy (APM) has shown poor clinical results at long-term follow-up. Partial meniscectomy is usually performed in the avascular zone and has the advantage of a quicker rehabilitation period compared to proposed meniscus repair techniques. The concept of meniscal preservation has been promoted and researched for many years ⁵³. So far, there is no clear consensus in the published literature to conclude which meniscal tears should be repaired, but certainly, most experts agree that preservation of as much native meniscus as possible will result in better patient outcomes ⁵⁴. It is also thought to be important to preserve the majority of the circumferential collagen fibres which are essential to the effective transfer of vertical load, hoop stress and shock-absorption ¹⁵.

It is interesting to note that even while the majority of publications indicate the benefits of meniscus repair, there is still a considerable gap between what is recommended in the literature and what happens in the clinic. Reasons for this may arise from historical surgical perspectives: “I always did this operation as it works” and from patient pressure: “Rehabilitation of repair is too long, I need to return to sport” ⁵¹.

1.3.4 Repair of Meniscal Tears

As previously discussed, meniscus repair represents the most ideal solution for treatment. However, not all kinds of tear can be repaired. The reference indication for repair is usually longitudinal vertical tears in the vascular zone (Figure 1.7). Final clinical judgement depends on a surgeon’s experience, the condition of the patient’s tissues and the pattern of the tear itself ⁵⁵.

There are three techniques used for arthroscopic suture repair of the meniscus: outside-in, inside-out and all-inside. The outside-in technique is passing sutures percutaneously through spinal needles across the meniscus rim and the torn meniscus body; then, retrieving the sutures under arthroscopic observation, another spinal needle penetrates over the meniscus to retrieve the suture end and tie outside the capsule⁵⁶. The inside-out technique involves fixation of a tear by placing sutures from inside the knee to an area outside of the joint capsule, then cannulas are used to pass the sutures through the joint and across the tear, a small incision is used to retrieve the sutures and tie them off directly on the capsule⁵⁶. All-inside suture is passing a suture with a suture hook device and the suture would be tied intraarticularly⁵⁶. For successful meniscal healing, all of these techniques need reliable primary fixation⁵⁷. Most surgeons prefer all-inside repair because of the low risk of neurovascular damage and the short surgical time that is required for this procedure⁵⁸. Tears in the anterior and middle segments are usually repaired by outside-in sutures in conjunction with posterior all-inside sutures. Posterior meniscal capsular lesions which contribute to rotational laxity cannot be easily detected on the anterior arthroscopic portal^{59,60}. They are usually exposed by a posteromedial approach and fixed by an all-inside hook suture⁶¹. Open meniscus suturing can be considerable in horizontal cleavage in young athletes, while traumatic root tears can be repaired by trans-osseous pull-out reinsertion⁵⁷.

Additional techniques include puncturing the meniscus with a needle to enhance fibrovascular healing in the avascular zone, shaving the parameniscal synovium⁴⁶ and MSCs or growth factors⁶² have also been applied to promote the meniscal healing process.

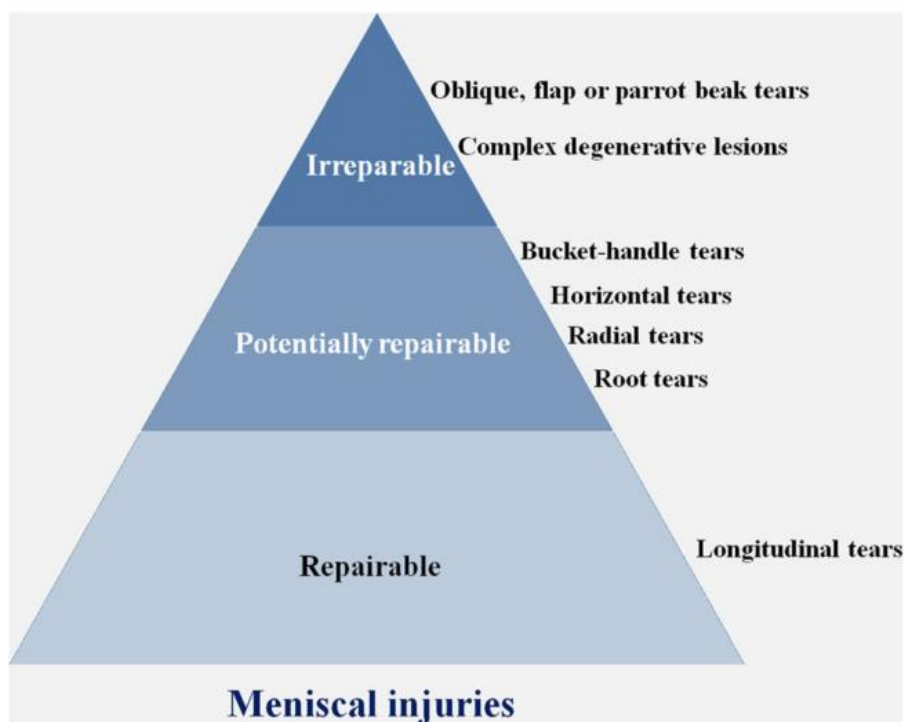


Figure 1.7: A pyramid schematic describing the repair potential for different types of meniscal injury.

Reproduced from Cengiz et al. ⁵² (reprint permission from Springer Nature)

1.3.5 Meniscus Allograft Transplantation

Patients who present with symptomatic knee pain several years after meniscectomy can be provided with the surgical option of meniscus allograft transplantation (MAT). The first MAT surgery was performed in 1984 in response to the effect of prior meniscectomy ⁶³. Many MAT systematic reviews have shown a significant improvement in knee function and symptom release in the midterm and long-term follow-up after MAT, with acceptable complication and failure rates ⁶⁴⁻⁶⁷. There is a consensus that MAT should only be considered in patients with localized pain and a stable and well-aligned knee joint. There is no clear evidence, however, to determine whether this procedure is chondroprotective. A systematic review based on radiological outcomes showed that some evidence supports MAT for reducing the progression of

OA, although there is a need for some well-designed randomized control trials to fully ascertain the efficacy of MAT ⁶⁸.

Several meniscus transplantation systematic reviews have been published. Lee et al. ⁶⁹ evaluated 24 studies with clinical outcomes compared between isolated MAT and MAT combined with other procedures. No significant differences were found between these two groups. However, more data was thought to be needed to draw accurate conclusions about the procedures in terms of complication, reoperation and failure rates, as well as in verifying the effects of MAT combined with osteotomy and cartilage procedures. A systematic review of 12 studies comparing the clinical outcomes of medial and lateral MAT has also been undertaken ⁷⁰. These results showed that lateral MAT provides better clinical outcomes compared with medial MAT, with regards to KOOS (Knee Injury and Osteoarthritis Outcome Score) and IKDC (International Knee Documentation Committee) outcome scores. Moreover, the medial MAT group experienced a greater incidence of graft extrusion. Although no significant differences were observed between the two groups, the medial MAT patients were more prone to failure compared with lateral MAT patients. However, few accurate conclusions can be drawn as this study lacked evidence from high-quality prospective randomized trials.

It is interesting to note that there is a wide variability of terms used to define MAT failure in different studies. Some authors have defined failure as no improvement of knee function or no patient satisfaction; alternatively, failure can be based on secondary arthroscopic findings and magnetic resonance imaging (MRI) parameters. Other authors have defined failure as removal of the graft or subsequent knee replacement. The differences in descriptions of failure that are used make it difficult to evaluate MAT failure for a systematic review. Thus, a Delphi investigation using a specialist panel might help to draw a consensus amongst experts in defining MAT failure ⁷¹.

1.3.6 Synthetic Meniscal Scaffolds

In the last decade, many different types of tissue engineered meniscal scaffolds have been developed for meniscus regeneration, with the aim of improving knee joint function and delaying the onset OA. These scaffolds are usually porous structures and are manufactured using biodegradable materials ⁷². However, many of these scaffolds are still investigated only *in vitro* or are in the preclinical phase of evaluation. Only two synthetic and commercially available meniscus implants are currently used to treat partial meniscus deficiencies in the clinic: Collagen Meniscus Implant (CMI[®]; Ivy Sports Medicine, Montvale, NJ) and Actifit[®] (Orteq Ltd., London, UK) ⁷³.

CMI[®] is composed of 97% purified type I collagen isolated from bovine Achilles tendon, the remaining portion consists of GAGs which include chondroitin sulphate and hyaluronic acid ⁷⁴. CMI[®] has been used in the clinic since the year 2000 and it can be implanted arthroscopically ⁷⁵. Its porous structure encourages cellular proliferation and differentiation, as well as ECM deposition. As the regenerative meniscal-like tissue grows into the scaffold, the scaffold gradually degenerates. A prospective study reported that patients receiving this medial meniscus implant showed significant improvement in pain, activity level and radiological outcome measures compared to individuals treated using partial medial meniscectomy at 10 year follow-up ⁷⁶. Several studies have confirmed these findings, demonstrating similar clinical results ^{77,78}.

Actifit[®] is a biodegradable synthetic polymer scaffold composed of 80% polycaprolactone (PCL) and 20% of polyurethane (PU). The scaffold was produced based on the combination of thermally induced phase separation and crystallization and salt leaching using PCL/ 1,4-butanediol/1,4-butanediisocyanate-based PU. The compression moduli of scaffold varies from 200kPa to 1MPa with a variation in porosity between 76% and 84%, while higher porosity lead to decreased compression

modulus of foam ⁷⁹. The softer PCL segments contribute to scaffold flexibility and initiate hydrolytic degradation at a consistent rate, whereas the more rigid polyurethane component provides mechanical strength and serves to make the scaffold more biocompatible and uniform in structure ⁷⁴. The Actifit® scaffold had a very low degradation rate which take in place of the presence of water through the hydrolysis of ester bonds in the PCL soft segments. The PCL segments is expected to be degraded in 4-6 years. The polyurethane segments were removed by macrophage phagocytosis or became integrated with surrounding tissue. In vitro degradation testing showed that the molecular weight of PU decreased 50% while the implant weight was not reduced in phosphate buffer at pH 7.4 ⁸⁰. A rabbit study demonstrated that the polyurethane foam appeared to be resorbed completely after three years ⁸¹. However, no relevant human studies have shown the similar results. Actifit® has been developed more recently than CMI®, therefore there are no long-term study results that have been reported to-date. The safety and feasibility of Actifit® has been demonstrated in short-term outcome studies ⁸², while Dhollander et al. ⁸³ reported at 5 years, midterm clinical outcome, showing significant improvements of knee joint function and reduced pain in response to Actifit®.

A recent systematic review showed that both CMI® and Actifit® meniscal scaffold implantation can significantly improve postoperative outcomes, and those injuries treated with associated anterior cruciate ligament reconstruction (ACLR) or high tibial osteotomy (HTO) demonstrated better outcomes. However, no significant difference between these two groups was reported. The failure rate of the Actifit® scaffold (mean follow-up: 40 months) is 9.9%, whereas CMI® (mean follow-up: 44 months) is 6.7%. Failure rates are difficult to compare across studies as there are no uniform failure definitions, with reported rates varying between 0 to 31.8%. ⁸⁴. Table 1.1 presents the

main indications and contraindications for CMI[®] and Actifit[®] meniscal scaffold implantation in the clinic ⁷⁴.

Table 1.1: CMI[®] and Actifit[®] implantation indications and contraindications

Indications	Contraindications
<ul style="list-style-type: none"> • Irreparable meniscal tears with partial meniscectomy, • Loss of meniscus tissue >25%, • Intact circumference rim (except area of popliteal hiatus for lateral meniscus), anterior and posterior attachments. 	<ul style="list-style-type: none"> • Grade IV degenerative osteoarthritis, • Posterior cruciate ligament insufficiency and posterior knee instability, • Local infection or osteonecrosis.

1.4 Cell-based Meniscus Tissue Engineering

1.4.1 Introduction

As detailed above, successful surgical treatments for meniscal injury in the vascular zone have been developed, whereas there are still no satisfactory strategies for meniscal injury in the avascular zone, due to its poor self-healing capacity ⁴². Therefore, to improve outcomes in surgical meniscal repair, cell-based regenerative strategies have recently received more attention ⁸⁵. A previous systematic review identified 19 studies of preclinical model using cell-based meniscus tissue regeneration ⁸⁶. All these studies used acellular controls to compare different cell sources including MSCs, chondrocytes, meniscal fibrochondrocytes. Sixteen studies concluded that cellular based techniques demonstrate better outcomes, whereas three studies did not find a superior outcome when cells were used. Kon et al. ⁸⁷ did not find any macroscopic or histology difference, but cell-based group was found to have better chondroprotective results. Mizuno et al. ⁸⁸ implanted synovial MSCs but no significant difference was found in histological

scoring between experiment and control group. Port et al.⁸⁹ added fibrin clots and MSCs in suturing longitudinal meniscal tears, but not significant different outcome was found when compare with acellular group. No adverse outcomes were reported with the implantation of cells. Overall, studies that used cellular techniques suggest that cell-based techniques produce better results than acellular techniques. However, there is still no published consensus to-date regarding which kind of cell is the most appropriate cell type for meniscal regeneration.

1.4.2 Meniscus Cells

The obvious advantage of using primary meniscus cells (MCs) in meniscal tissue engineering strategies is that the MC phenotype will produce an ECM which is most like that of the native meniscus^{24,90}. Baker et al.⁹¹ isolated MCs from ten patients' surgical debris (seven partial meniscectomies and three total knee replacement (TKR) from 18-84 year-old donors). Cells were expanded in monolayer culture until passage two and seeded onto a PCL scaffold fabricated via electrospinning and cultured for over 10 weeks. The results showed that fibrochondrocytes from all donors seeded onto scaffolds increased the proteoglycan and collagen content within the scaffold over time. There was also a strong positive correlation between collagen content and the mechanical properties of the scaffolds seeded, but no significant difference was observed between the different donor age groups. This study indicated that autologous MCs isolated from meniscal tissue debris could be a potential cell source for meniscus tissue engineering. However, cell-based meniscus therapy is likely to require a large population of cells for seeding scaffolds. To achieve this, an expansion of primary cells to passage two or three is often required, which can lead to increased expression of collagen I and decreased expression of collagen II and COMP with the number of passages increase in meniscal fibrochondrocytes⁹². Esposito et al.⁹³ seeded

fibrochondrocytes isolated from rabbit menisci on PLDLA/PCL-T scaffolds and cultured them for three weeks; at this time point cell-seeded scaffolds and cell-free scaffolds were implanted back into the rabbit medial meniscus. Histologically, the constructs showed good integration with surrounding tissues and evidence of more, predominantly fibrocartilaginous, tissues were observed at 24 weeks compared to control groups. Several studies have shown that culturing MCs under hypoxic conditions (which is consistent with the microenvironment in the human knee joint) can enhance the capacity of MCs to express an ECM-forming phenotype. In addition, supplementation with TGF β 1 (transforming growth factor beta 1) and FGF-2 (fibroblast growth factor-basic) can further increase this effect up to 10 fold⁹⁴⁻⁹⁷. These findings indicate that MCs may be an ideal cell source for tissue engineering repair strategies for the avascular zone of the meniscus.

1.4.3 Articular Chondrocytes

Articular chondrocytes (AC) and MCs have similar cell membrane markers and high expression levels of collagen and other components of the meniscus ECM²³. ACs have been successfully used in ACI for over 20 years^{98,99} ACI has been demonstrated for safety, efficacy and cost effectiveness as a cartilage repair strategy, having been recommended as a treatment option for NHS patients (NICE technical appraisal 477, published Oct 2017 <https://www.nice.org.uk/guidance/ta477>). These similarities and advantages make ACs a promising alternative cell source for meniscus repair. Marsano et al.¹⁰⁰ demonstrated that ACs produced higher amounts of GAGs and collagens and the regenerated tissues were more akin to the inner and outer meniscus tissues compared to MCs, fat pad cells and synovial membrane derived cells. Vedicherla et al.¹⁰¹ compared fresh chondrocytes (isolated by a rapid digestion method) or minced cartilage fragments seeded onto Actifit[®] scaffolds. These constructs were implanted back into a

caprine model. The results showed that both fresh chondrocytes and minced cartilage fragments improved the scaffold integration at the tissue-scaffold interface and the mechanical strength of the scaffold was increased 4-fold and 2.5-fold, respectively, compared with the acellular group. This experiment demonstrated the feasibility of an intraoperative one-stage repair strategy, which avoids the high costs and specialised expertise (as well as regulatory constraints) involved in cell culturing in good manufacturing practice (GMP) laboratories. In addition, single-stage repair surgery decreases the risk of infection and other complications for patients. A study comparing the capacity of autologous and allogeneic chondrocytes in repairing bucket-handle lesions in a porcine model showed no statistically significant differences between the cell types¹⁰². Together, these findings indicate the potential for the further study and application of chondrocytes in meniscus tissue engineering.

1.4.4 Mesenchymal Stromal Cells

MSCs have the potential to differentiate into fibrochondrocytes and the ability to secrete a plethora of growth factors which might enhance tissue engineered meniscus repair strategies¹⁰³. MSCs, such as BM-MSCs, synovium-derived stromal cells (SMSCs) and adipose-derived stromal cells (ADSCs), have been widely tested for meniscus healing.

Bone marrow-derived mesenchymal stromal cells

Zellner et al.¹⁰⁴ evaluated autologous BM-MSCs or meniscal cells seeded onto collagen-hyaluronan scaffolds and implanted into a punch defect rabbit model. Results showed that both improved meniscal healing, while BM-MSCs significantly increased the gene expression and production of collagen type II compared to meniscal cells. Furthermore, gross joint evaluation demonstrated the disadvantage of using autologous MCs in the presence of donor site morbidity and the restrictions associated with the limited availability of suitable meniscal tissues. Whitehouse et al.¹⁰⁵ conducted a first-

in-man study that repaired avascular meniscal tears using collagen scaffolds seeded with autologous BM-MSCs in five patients. At 24 months' follow-up, three of these patients were asymptomatic with no evidence of recurrent tear according to MRI and improvement of knee function scores, whereas two of the patients required a subsequent meniscectomy due to re-tear or non-healing.

Synovial mesenchymal stromal cells

It was first reported in 1936 that meniscus lesions did not heal without communication with the synovium ¹⁰⁶. The numbers of MSCs found in synovial fluid was found to increase after meniscus injury ¹⁰⁷. In rat ¹⁰⁸, rabbit ¹⁰⁹ and pig ¹¹⁰ meniscal lesion models, intra-articular injection of SMSCs has been shown to promote meniscus regeneration after resection of the medial meniscus. Nakagawa et al. ¹¹¹ made longitudinal tears in the bilateral medial meniscus in 12 micro minipigs, and cultured, passage two SMSCs were injected into the unilateral knee. The results from this study showed that meniscus healing in SMSCs groups was significantly better than that observed in control (sutured-only) groups.

Adipose-derived stromal cells

It has been demonstrated that the population of MSCs in adipose tissues is approximately 500-fold more concentrated than that which resides in bone marrow. Akin to BM-MSCs, ADSCs have multilineage differentiation potential and are capable of secreting therapeutic growth factors ¹¹². Therefore, ADSCs are also a potential candidate cell source for meniscus regeneration. Baek et al. ¹¹³ examined different human cell sources including inner and outer meniscus cells, ADSCs from the infrapatellar fat pad, SMSCs and BM-MSCs for meniscus regeneration *in vitro*. The results of this study showed that ADSCs generated a meniscus-like tissue with higher cell viability and expression levels for collagen type I compared to the other cell types

investigated. Ruiz-Ibán et al. ¹¹⁴ reported complete healing and more meniscal fibrochondrocytes to be present in an avascular meniscus lesion in a rabbit model after the injection of ADSCs (in combination with suturing of the meniscal tear). Moreover, better outcome was observed in acute compared to delayed suture. A case report showed the successful repair of a torn meniscus accompanied with significant pain reduction by intra-articular injection of uncultured autologous ADSCs in the human knee joint ¹¹⁵. Together these studies provide evidence that ADSCs might be an effective and non-invasive cell-based treatment option for meniscus regeneration.

1.4.5 Co-culture

Single cell type meniscus tissue engineering strategies have several potential limitations, such as insufficient cell numbers, single cell phenotypes (more than one cell type resides in the meniscus) and have reported meniscal cell hypertrophy *in vitro*. Therefore, co-cultured cells might improve engineered meniscal properties. Co-culture systems include two types: one is a direct contact system whereby different cell types are mixed directly; another is indirect whereby different cell types reside in the same system but achieve interaction only via paracrine secretions.

As previously described, collagen fibres determine the tensile strength of the meniscus, while GAGs are mainly responsible for the compressive modulus. Articular cartilage chondrocytes produce higher levels of collagen type II and GAGs, whereas meniscus fibrochondrocytes mainly produce collagen type I. Gunja et al. ¹¹⁶ hypothesised that co-culturing MCs and ACs on a poly-L-lactic acid (PLLA) scaffold may produce better results in resembling various regions of the meniscus. The results from this study showed that as the percentage of ACs used increased, the compressive properties of the tissue engineered constructs significantly increased.

MSCs not only have the potential to differentiate into meniscal fibrochondrocytes, but

also have trophic effects in co-culture systems ¹¹⁷. Cui et al. ¹¹⁸ co-cultured MCs with MSCs in different ratios; the results demonstrated that co-culturing MCs and MSCs had a synergistic effect on producing functional ECM components of the meniscus and inhibits hypertrophy of MSCs during chondrogenic differentiation, as well as promoting a meniscal phenotype. The 75% MCs and 25% MSCs co-culture system demonstrated the most promising results of the ratios tested. Similar outcomes were found when co-culturing MCs and BM-MSCs isolated from TKR ¹¹⁹. McCorry et al. ¹²⁰ characterised the fibre formation and matrix production in both MSCs and MCs in monolayer culture and 50/50 co-cultures in collagen gels. This group reported that the MSC monolayer culture group exhibited higher levels of GAGs with reduced fibre diameter, whereas the MC monolayer culture group produced a better collagen organisation. However, the co-culture group achieved intermediate levels of GAGs production and collagen fibre organisation. Hence, co-culture could be utilised to balance the matrix synthesis ability of MSCs and fibre remodelling properties of MCs for future applications.

1.4.6 Combined Autologous Chondrocyte and Bone Marrow Mesenchymal Stromal Cell Implantation in the Knee: Two First-In-Man Cases

Two first-in-man cases treated with combined autologous chondrocyte and BM-MSCs implantation for cartilage repair, with 8 and 9 years follow up have been reported in the literature as a preliminary output of this PhD thesis ¹²¹. In this study patient A (70 years of age) and patient B (65 years of age) presented with International Cartilage Repair Society (ICRS) grade III–IV multiple cartilage lesions (tibia, femur and patella) and underwent a co-implantation of autologous chondrocytes and BM-MSCs between February 2008 and October 2009. In brief, chondrocytes and BM-MSCs were separately harvested and culture-expanded in a GMP laboratory for a period of 2–4

weeks. Cells were then implanted in combination into cartilage defects, while patient B also had a medial Actifit[®] meniscal scaffold implantation. Both patients were clinically assessed preoperatively and postoperatively using the self-reported Lysholm knee score and MRI. The actual post-operative scores were compared with scores predicted using the Oswestry Risk of Knee Arthroplasty (ORKA) score. The ORKA score⁹⁹ is a web-based app that uses baseline information about the patient's age and gender, location of and the number of cartilage defects and baseline knee function score to predict a patient's risk and time of needing knee arthroplasty. Patient A also had a second-look arthroscopy at 14 months after surgery, in which a biopsy of the repair cartilage was taken. Both patients demonstrated significant long-term improvement in their knee function without complications, with their postoperative Lysholm scores being consistently higher than ORKA predictions. Both patients also remained physically active without joint arthroplasty at their last follow-up appointments. The latest Lysholm scores, 8 years after surgery were 100/100 (Patient A) and 88/100 (Patient B), where 100 represents a fully functioning knee joint. Bone marrow lesions (BMLs) volume was shown to decrease on postoperative MRI in both patients. Cartilage defect area increased in patient A, but declined initially for patient B, slightly increasing again 2 years after treatment. The biopsy of repair site taken from patient A at 14 months postoperatively, demonstrated a thin layer of fibrocartilage covering the treated defect site. These two cases suggest that the combination of cultured autologous chondrocytes and BM-MSCs appears to confer improved symptoms, at least in these two patients and at long-term follow-up. However, despite their improvement in clinical outcome scores, physical joint failure as assessed by MRI was seen to progress in both patients. Whether this might have progressed with advancing age at a greater rate had the cells not been implanted, will only be resolved in a full clinical trial with appropriate comparator

cohorts. In summary, these findings support the hypothesis that autologous BM-MSCs stimulate a beneficial host response, reducing pain, perhaps by influencing the subchondral bone and reducing the size of BMLs.

1.5 Meniscus Scaffolds

1.5.1 Introduction

Scaffolds used in meniscus tissue engineering are thought to benefit host tissue integration, new tissue formation and remodelling. An ideal scaffold should meet certain criteria in both appropriate biomechanical and biochemical properties (Table 1.2). Table 1.3 summarized and compared the mechanical properties between health or degenerated human meniscus and clinical scaffolds including Actifit® and CMI®. The current scaffolds can generally be divided into four types: bioabsorbable synthetic polymers, hydrogels, biological component scaffolds and decellularised meniscal scaffolds¹²². The overall objective for the design of these scaffolds is to mimic natural meniscus functions and to stimulate the ingrowth of native tissues.

Table 1.2: Mechanical and biological criteria required for a meniscus scaffold

Properties	Criteria
Mechanical	Provide enough biomechanical function to resist compressive or tensile modulus
	Maintain shape and stability until enough new tissue regenerates
	Produce mechanical stimulation to promote tissue regeneration
Biological	Provide appropriate biocompatibility and nontoxicity to human tissues
	Present suitable surface properties for cell attachment and proliferation
	Provide appropriate porosity and permeability for growth factors and nutrients to reach all of the cells within the scaffold
	Maintain a degradation rate that matches the rate of new tissue regeneration and degradation products should be biocompatible without causing an inflammatory response

Table 1.3: the biomechanical and viscoelastic properties of human health or degenerate meniscus and clinical scaffold

	Human (n = 6)	Human deg. (n = 6)	Actifit (n = 3)	CMI (n = 3)
Stiffness [N/mm], cycle 1	8.54 ± 1.87	7.94 ± 2.25	2.83 ± 0.13	4.66 ± 0.35
Stiffness [N/mm], cycle 5	18.29 ± 2.88	16.59 ± 2.66	3.88 ± 0.17	5.50 ± 0.33
Residual Force [N], cycle 1	2.99 ± 0.63	2.31 ± 0.69	5.93 ± 0.017	5.15 ± 0.31
Residual Force [N], cycle 5	4.26 ± 0.54	3.74 ± 0.35	8.18 ± 0.032	5.58 ± 0.32
Compression [%], cycle 1	19.92 ± 1.36	18.43 ± 0.55	74.7 ± 4.76	72.8 ± 3.86
Compression [%], cycle 5	13.58 ± 1.33	14.38 ± 1.14	65.1 ± 3.38	71.89 ± 7.23

Reproduced from Sandmann et al. ¹²³ (reprint permission from Springer Nature)

1.5.2 Bioabsorbable Synthetic Polymers Scaffolds

Synthetic polymer materials, such as PU, PCL, polylactic acid (PLA), polyglycolic acid (PGA) and polylactic co-glycolic acid (PLGA) have been widely exploited in fabricating meniscal scaffolds ¹²². They have several advantages over other scaffold types; these include the ability to be easily shaped, with varied pore sizes, geometry, fibre size, mechanical properties and adjustable degradation rates ¹²⁴. However, these materials also have some disadvantages, such as hydrophobic properties and poor cytocompatibility. Moreover, their degradation products have been shown to cause aseptic inflammation, immune responses and other negative side effects ¹²⁵.

Kang et al. ¹²⁶ reinforced a meniscus-like PGA scaffold by bonding with PLGA (75:25). The compressive modulus of the bonded PGA/PLGA scaffold was 28-fold higher than the non-bonded scaffold. Allogeneic MCs from rabbits were seeded onto scaffolds and cultured *in vitro* for 7 days and then implanted into medial meniscus-deficient rabbit knee joints. The histological analysis of regenerated fibrocartilage at 10 weeks showed

the formation of abundant proteoglycan and collagen networks. However, lower collagen content and aggregate modulus were observed when compared to the native meniscus.

PCL has indicated its potential utility due to its high tensile modulus, the promotion of cell attachment and proliferation, material plasticity and a slow degradation rate ^{24,127}. Zhang et al.¹²⁸ used PCL meniscal scaffolds fabricated by 3D printing and seeded them with BM-MSCs, constructs were then implanted into a rabbit model of meniscal deficiency. At 12 and 24 weeks postoperative evaluations, the cell-seeded group showed significantly better results in fibrocartilaginous tissue regeneration, levels of cartilage degeneration on the tibia and femur and had a higher tensile compressive modulus compared with the cell-free group.

Multiple synthetic polymers can be mixed in suitable proportions to enhance their compressive, tensile and shear modulus, as well as their cell-attachment properties. As described previously, meniscus substitution Actifit[®] (20% PU and 80% PCL) has already shown promising outcomes in the clinic. “Meniscus-like” tissue ingrowth was also observed at two years post-Actifit[®]-implantation in canine models ¹²⁹.

1.5.3 Hydrogels

Hydrogels have been widely investigated for use in meniscus scaffold engineering. Hydrogels are a crosslinked network of hydrophilic natural or synthetic polymer chains. A large proportion of the hydrogel content is water, (often >90%) ⁷². Hydrogels possess high levels of permeability, good biocompatibility and inherent biodegradability. They can be categorised as natural, synthetic and natural/synthetic hybrid materials. Natural polymers have more desirable biological properties and synthetic polymers tend to possess more appropriate mechanical properties and are easier to reproduce ¹³⁰.

The natural polymers for hydrogels, in the main part, consist of two types: natural proteins and polysaccharides. Natural proteins, such as fibrin¹³¹ and gelatin¹³² have been most widely studied. Polysaccharides include alginate¹³³, chitosan¹³⁴ and chondroitin sulphate¹³⁵ and these have also been developed either alone or mixed with other materials.

The most widely exploited synthetic hydrogel for meniscus tissue engineering is polyvinyl alcohol (PVA). Its biocompatibility and viscoelastic properties are comparable to meniscus tissues¹³⁰. To improve further the mechanical properties of PVA hydrogels, recent studies have developed fibre reinforcement with ultrahigh molecular weight polyethylene^{136,137} and modification with sodium sulphate^{138,139}.

Hydrogel materials play an important role in supporting relevant cell populations for meniscus regeneration, ‘plugging the gap’ in meniscal lesions and retaining bioactive molecules which are crucial for meniscus healing¹³⁰.

1.5.4 Biological Component Scaffolds

Biological component scaffolds can be classified as ECM related and biopolymer scaffolds. ECM component scaffolds are derived from natural tissues and include collagens, proteoglycans and elastin⁷². Different combinations of these molecules have been used, such as collagen-GAGs or combinations of different types of collagen. Nanofibre electrospinning, anisotropic deposition and crosslinking methods have been used to fabricate collagen scaffolds. These methods can strengthen the ECM scaffolds so that they are comparable in strength to synthetic polymer scaffolds. Moreover, the ECM scaffolds can provide a natural environment and bioactivity for seeded cells. The CMI[®] scaffold has been used in the clinic for meniscal implants and belongs to this ECM scaffold grouping. CMI[®] has been shown to significantly relieve pain and improve knee joint function in a ten-year follow-up study⁷⁶. Petri et al.¹⁴⁰ seeded

human BM-MSCs onto CMI[®] scaffolds and placed these into a bioreactor system. Perfusion and biomechanical stimulation were applied to the scaffolds and results showed there to be enhanced cell proliferation under continuous perfusion and improved differentiation under mechanical stimulation.

Other recent studies have focused on making biopolymers, such as silk fibroin (SF) which is derived from silkworms. SF is known to possess attractive biocompatibility and mechanical properties. Pillai et al.¹⁴¹ developed a scaffold using 3:1 SF and PVA reinforced with 3% autoclaved eggshell membrane (AESM) and implanted these scaffolds into a meniscal deficiency rabbit model. This SF-PVA scaffold showed a similar magnitude of compressive and dynamic properties as compared to the natural human meniscus. IHC analyses demonstrated its biocompatibility with minimal inflammatory response. Mandal et al.¹⁴² built a three-layered silk meniscal scaffold by using a salt leaching and freeze-drying method. The scaffolds were seeded with chondrocytes and cultured for 28 days. Results showed an increased production of GAGs and collagens similar to those found in native meniscus tissues. Together these studies suggest that SF is a promising natural material for meniscus tissue engineering applications.

1.5.5 Decellularised Meniscal Scaffolds

Recently, decellularised ECM meniscus scaffolds have drawn a great deal of interest as a method to improve meniscus engineering. Decellularised scaffold composed of natural ECM components and structures, but without immunogenic cells are typically derived from allogeneic or xenogeneic tissues¹⁴³. Decellularisation causes minimal immunogenicity and preserves the ECM, which can protect its biological function. Combinations of physical (e.g. freeze-thaw cycles), chemical (e.g. acids or detergents, such as Triton X-100 and SDS (sodium dodecyl sulphate)) and enzymatic (e.g. DNase

and trypsin) agents are used to lyse cells by solubilizing the cytoplasm and membranes¹⁴⁴. In general, the procedure for meniscus regeneration using decellularised ECM scaffolds involves decellularisation of a meniscus and its reseeding with appropriate cell types (Figure 1.8).

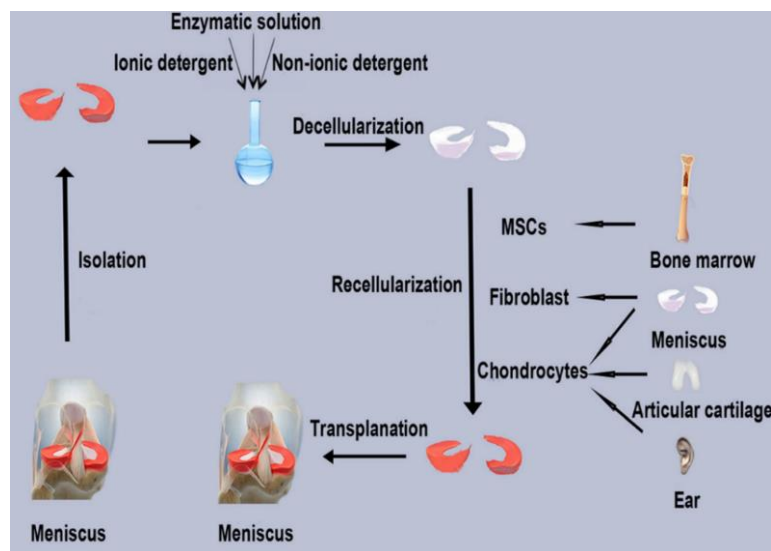


Figure 1.8: Schematic representation of the cell-loading of a decellularised ECM meniscus scaffold.

Reproduced from Chen et al.¹⁴⁴ (reprint permission from Springer Nature)

Maier et al.¹⁴⁵ developed a decellularised ovine meniscus using enzymatic methods including trypsin, collagenase A, protease and EDTA treatments. Histological and IHC analyses showed complete cell removal and high histocompatibility. However, the GAG content was shown to be significantly reduced. Chen et al.¹⁴⁶ investigated the potential of a decellularised porcine meniscus using an acid-based method to decellularise the tissue. They found that formic acid decreased the meniscal DNA content most efficiently compared to other acids, without any adverse effect on GAGs content. These scaffolds were seeded with human primary chondrocytes and after culturing for 28 days, the DNA content was shown to increase 2.62-fold, with cell

populations increasing 10.1-fold. GAGs and total collagen increased by 572.34% and 301.11% respectively, from day 7 to day 21. Finally, the decellularised ECM scaffolds were implanted subcutaneously into rats and no sign of inflammation was observed after 28 days. This study indicated that this decellularised allogeneic meniscus did not cause a significant detectable immune response. Decellularised scaffolds are highly bioactive and provide a natural microenvironment for meniscus repair, although disadvantages to their use have been discussed, which include the poor mechanical properties observed in some studies and the deficiency of suitable menisci for decellularisation¹⁴⁴.

1.6 Aims of PhD Project

From our literature review, we scoped that the histological changes of meniscus from normal to degeneration has well established. However, to our knowledge, the cell phenotype alteration in degenerated meniscus was still not clear. In addition, few studies suggested that meniscus contains a group of progenitor population which involves in the meniscus healing process. There is no clear evidence characterize the progenitor population in meniscus and their origins. This special cell fraction could be a potential treating target in the future. In terms of cell-based meniscus tissue engineering, it has been widely explored including cell sources and scaffold in vitro and preclinical model based on our literature review. However, the application in use of cell-based strategy in treating meniscal lesions in clinic is still under exploration stage. The overall purpose of this PhD project was to provide data that would advance meniscus tissue regeneration approaches using cell-based tissue engineering. This was accomplished through the following basic research and clinical projects:

Basic research studies (focussed on understanding the pathological meniscal cell

phenotypes and characterising potential therapeutic cells):

- (1) Characterisation of the regional meniscal cells and chondrocytes phenotypes and their chondrogenic differentiation capacity from OA donor matched tissues. Investigations were also conducted to analyse the histological features of the OA meniscus (Chapter 3).
- (2) Determination of progenitors in the avascular and vascular region of the meniscus and a comparison of their chondrogenic capacity with their comparator whole mixed populations (Chapter 4).
- (3) Examination of the feasibility of delivering autologous avascular meniscal cells using a fibrin gel into a clinically used polyurethane scaffold to promote meniscus tissue regeneration in a sheep explant model (Chapter 5).

Clinical study (focussed on analysing one of the current combinatorial cell-based and tissue engineering approaches):

- (1) A review of the clinical outcomes of patients who had combined ACI with meniscus allograft transplantation or a polyurethane scaffold implantation assessed at mid- to long-term follow up (Chapter 6).

Chapter 2: Laboratory Material and Method

2.1 Cell isolation, cell culture and cell preservation

2.1.1 Obtaining patient consent and samples

All tissue samples used in this study were obtained from individuals undergoing knee surgery at our centre, the Robert Jones and Agnes Hunt Orthopaedic Hospital (RJAH). Fully informed consent was obtained from patients with ethical approval given by National Research Ethics Committee Northwest Liverpool East (11/NW/0875) (appendix I). All patient consents were obtained prior to surgery. All tissue samples were kept in sterile pots and stored at 4°C prior to use and those for further cell culture were processed within 24 hours.

2.1.2 Avascular & vascular meniscal cells and chondrocyte isolation

Each sample was washed in phosphate buffer saline (PBS, Gibco - Thermo fisher Scientific, USA) three times and photographed before processing. Macroscopically healthy meniscus and full depth cartilage from TKR samples were removed with a sterile scalpel for cell isolation. The meniscus was dissected into the inner (avascular zone), middle and outer (vascular zone) as shown in Figure 2.1. The middle portion was discarded such that only the definite vascular and avascular zones were studied. A section of the meniscus adjacent to that used for cell culture experiments was harvested for histology. Meniscal cells and chondrocytes were isolated following a protocol established in our GMP manufacturing facility for chondrocytes¹⁴⁷. Meniscus and cartilage tissues were digested in type II collagenase (245U/ml; Worthington, USA) in Dulbecco's Modified Eagle Medium (DMEM)/ F12 (1:1) (Gibco, USA) and 1% penicillin-streptomycin (P/S) (ThermoFisher Scientific, USA) for 16 hours at 37°C. The suspension was passed through a 40 µm cell strainer and pelleted at 800g for 10 minutes. Cells were counted with a haemocytometer and trypan blue exclusion (Sigma, Poole, UK).

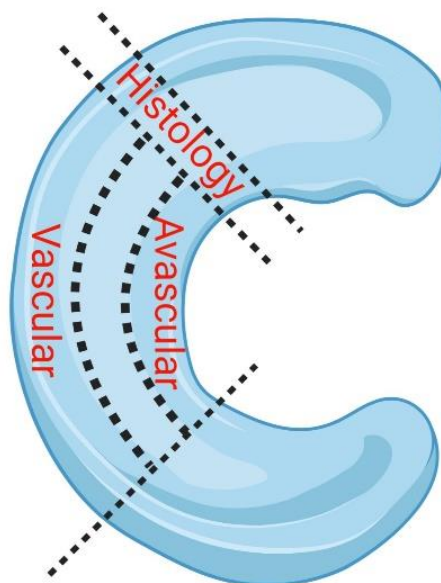


Figure 2.1: Schematic diagram of the process used for meniscus dissection

The central part of the macroscopically “normal” meniscus was longitudinally divided into three parts: the inner third was used to extract avascular meniscal cells, the outer third for the extraction of vascular meniscal cells. The adjacent perpendicular section composed of both inner and outer regions was used for histological grading.

2.1.3 Cell culture in monolayer and cell passaging

Meniscal cells and chondrocytes were seeded into tissue culture flask at a density of 5×10^3 cells/cm³ (passage 0) in complete medium (DMEM/F12 (Gibco, USA), 10% (v/v) foetal bovine serum (FBS) (Gibco, USA), 1% (v/v) P/S (ThermoFisher Scientific, USA), 62.5 µg/ml L-ascorbic acid 2-phosphate (Sigma-Aldrich, USA)). Cells were incubated at 37°C, 5% CO₂ for 4-5 days to allow cell adherence, after which media were replenished every 2-3 days. After reaching 70-80% confluence, cells were washed with PBS and incubated with pre-warmed 0.05% trypsin/EDTA (Gibco - Thermo fisher Scientific, USA) at 37°C for 5 minutes. Cells were observed under a light microscope (Nikon, Tokyo, Japan) and detached by gentle agitation. The remaining active trypsin

was neutralised with an equal volume of complete medium and cell suspension was centrifuged for 10 minutes at 800 g. The supernatant was discarded and the cell pellet was resuspended in 1ml of complete medium. A cell count was performed, and cell viability was recorded. Cells were reseeded at a density of $5 \times 10^3/\text{cm}^2$ in tissue culture flasks. The trypsinisation, counting and reseeding process was referred to as one passage increase.

2.1.4 Cells cryopreservation

Cells required for further experiments were banked by cryopreservation. Following cells trypsinisation and counting, cells were resuspended in 10% (v/v) dimethyl sulfoxide (Sigma-Aldrich, USA) in FBS at 1×10^6 cells/ml. The suspension was gently pipetted into cryovials and stored in a Mr. Frosty™ freezing container (Thermo Scientific, UK) filled with isopropanol (IPA) at -80°C for 24 hours. The cryovials were transferred to liquid N_2 at -196°C for long term storage.

2.2 Meniscal progenitor cells

2.2.1 Meniscal progenitor cells isolation protocol

A fibronectin adhesion assay was used to isolate meniscal progenitor cells from the avascular and vascular regions. This protocol has been well established to extract chondroprogenitor cells from cartilage¹⁴⁸. Progenitor cells, showing the characteristics of stem cells, are selected due to their high expression of $\beta 1$ integrins on the cell surface and rapid adhesion to ECM proteins, such as fibronectin¹⁴⁹.

The definite avascular and vascular meniscal cells and full-depth macroscopically normal articular cartilage from femoral condyles were donor matched, being obtained from the same individual. Samples were digested by sequential pronase (70 U/ml, 1 hour at 37°C) and collagenase type II (245U/ml, 12 hours at 37°C) in serum-free

medium. All three cell types (avascular and vascular meniscal cells and chondrocytes) were cultured under two conditions. The first group was a mixed population of cells including avascular meniscal mixed cells (MAvas), vascular meniscal mixed cells (MVas) and mixed chondrocytes (MChs), which were plated at a density of 5000 cells/cm². The second group was progenitor cells including avascular meniscal progenitors (PAvas), vascular meniscal progenitors (PVas) and chondroprogenitors (PChs), which were subjected to a fibronectin adhesion assay as previously described¹⁴⁸. Briefly, 6 well plates were coated with 10µg/ml fibronectin (Sigma, UK) in PBS, containing 1mM MgCl₂ and 1mM CaCl₂ overnight at 4°C. Each isolated mixed population of cells (1000 cells/well) was seeded onto 3 wells in coated plates for 20 mins at 37°C in complete medium. After 20 minutes, medium and non-adherent cells were removed. Fresh complete medium was added to the remaining adherent cells and incubated at 37°C, 5% CO₂.

2.2.2 Cell-IQ[®] live imaging of progenitor colonies

After three days culture in 6 well plate, progenitor cells were sent in Cell-IQ[®] phase contrast Live Imaging Platform (CM Technologies, Tampere, Finland) to monitor colony formation. The Cell-IQ[®] system is a self-contained cell culturing instrument including environmental control with phase-contrast microscopy and an automation system for repeat imaging of the same location over a defined timescale (Table 2.1). The system consists of an automated optics module (Figure 2.2) and an integrated incubator with two gas flow controllers¹⁵⁰. The imaging system allows continuous imaging of, for example, cell number, motility and morphology in two plates which are controlled under an integrated plate holder. Spare wells and surrounding areas in 6 well plates were filled with distilled water to keep the plate humidified. At least one colony was monitored in each well and each colony was imaged every 30 minutes for 48 hours.

The recorded images were transferred to the Cell-IQ[®] analyser (CM Technologies, Tampere, Finland) to measure the cell number of each colony every 30 minutes.

Table 2.1: The Cell-IQ[®] components

Cell-IQ [®] Vision System		
Phase contrast microscope	Environment control	Automation
<ul style="list-style-type: none"> ▪ Light source ▪ Optics ▪ Digital camera 	<ul style="list-style-type: none"> ▪ Temperature control and logging ▪ Incubation gas control 	<ul style="list-style-type: none"> ▪ Automated cell imaging for selected positions ▪ Label free cell analysis based on morphology ▪ Motorized XYZ translation stages

Table reproduced from Narkilahti et al. ¹⁵⁰ (reprint permission from Springer Nature)

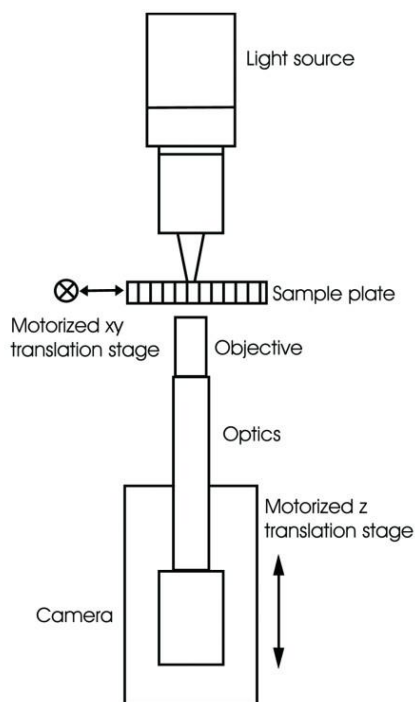


Figure 2.2: Schematic diagram of the automated optics module and monitoring system.

The optics module consists of a digital 768×576 -pixel camera integrated with a phase-contrast microscope and a phase contrast objective with 200mm optics, built onto a motorised z -direction movement stage. The sample plate was allowed to motorise on an xy -direction movement stage to capture images from different locations. A green LED light (530 nm) provides an illumination source for high quality phase-contrast images. Reproduced from Narkilahti et al.¹⁵⁰ (reprint permission from Springer Nature)

2.3 Growth kinetics in monolayer culture

Cell proliferation rate was determined by population doubling times (PDT). PDT was calculated using the following formula:

$$PDT = (t_2 - t_1) * \frac{\ln(2)}{\ln(n_2/n_1)}$$

where t_1 = the time of cell seeding, t_2 = the time of cell harvest and n_1 and n_2 are the

number of cells seeded initially and harvested, respectively.

2.4 Detection of cell surface markers by flow cytometry

2.4.1 Flow cytometry introduction

Flow cytometry uses a sophisticated instrument that rapidly analyses multiple physical characteristics of a single cell (or particles) as the cell suspension flows through a measuring device. The basic working principle of flow cytometry is measuring light scattering and fluorescence emission which is generated by a laser beam striking the moving cells or particles (Figure 2.3). The patterns of light scattering include forward scatter (FSC) and side scatter (SSC). FSC light is diffracted by cells and collected along the same path as the laser beam to identify cell size, whereas SSC light is a measurement of refracted light at approximately 90 degrees to the laser beam to identify cell granularity or internal complexity, as well as the fluorescent light reflected from fluorescent-labelled antibodies (Figure 2.4). Detectors capture the emitted light, which is converted into electronic signals by a computer for analysis.

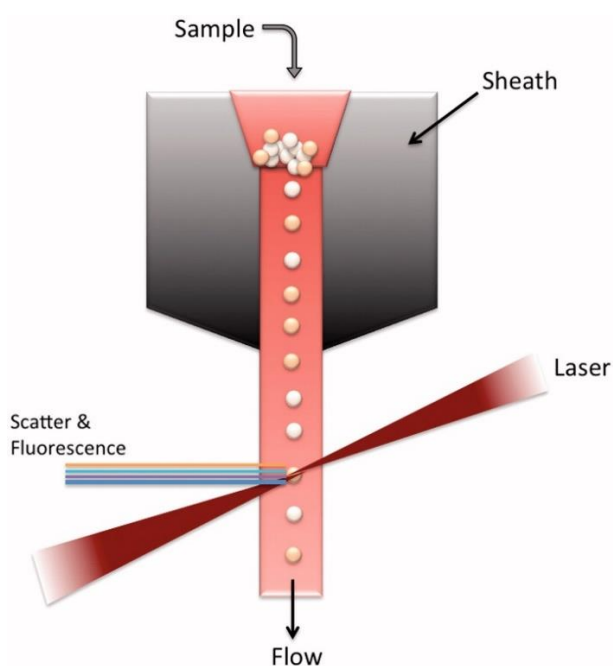


Figure 2.3: Illustration of the working principle of a flow cytometer.

Reproduced from Adan et.al ¹⁵¹ (reprint permission from Taylor & Francis)

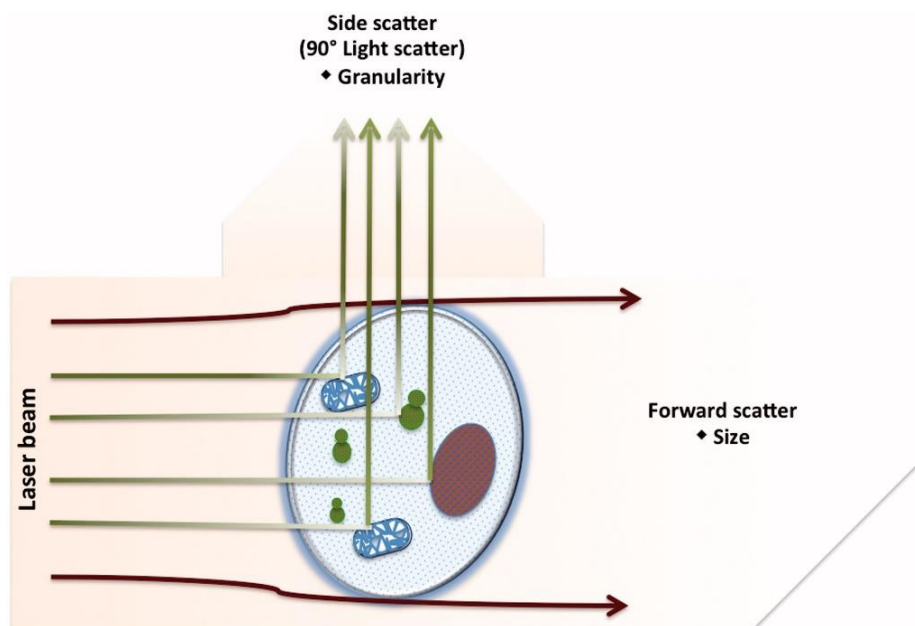


Figure 2.4: Flow cytometry light scattering.

Forward scatter is proportion to size while side scatter is proportional to the cell granularity or internal complexity. Reproduced from Adan et al. ¹⁵¹ (reprint permission from Taylor & Francis)

2.4.2 Preparation for flow cytometry

A profile of cell surface markers were selected based on the International Society for Cellular Therapy (ISCT) criteria for MSC phenotype¹⁵², chondrogenic potency ^{153,154-156} and integrin families ^{157,158}, which were analysed via multi-colour channel flow cytometry. Details of fluorochrome, isotype control and clones are listed in Table 2.2. Different panels which are specific for individual experiments are listed in the experimental design of each chapter.

Experiments were conducted on monolayer cultured cells at passage 0 (P0) or prior to chondrogenesis. Briefly, 160,000 cells were resuspended in 1ml 2% (w/v) bovine serum albumin (BSA, Sigma-Aldrich) in PBS and 10% (v/v) human IgG (Grifols, Spain) and incubated at 4°C for 1 hour to block FC (fragment crystallizable) receptors to help

eliminate non-specific binding. The suspension was centrifuged at 500g for 5 minutes and the cell pellet was resuspended in 2% (w/v) BSA and aliquoted evenly in flow cytometry tubes (100µl per tube). Fluorochrome conjugated antibodies against the ISCT MSC criteria including CD14, CD19, CD34, CD45, CD73, CD90, CD105, HLA-DR (BD Biosciences, Oxford, UK), chondrogenic potency markers including CD44, CD151, CD166, CD271 (BD Biosciences, Oxford, UK) and for the integrins including CD29, CD49b, CD49c (BD Biosciences, Oxford, UK), were added to tubes according to the layout depicted in Figure 2.5. Cells were incubated with antibodies for 30 minutes in the dark at 4°C and washed with 2ml of 2% (w/v) BSA and centrifuged at 350g for 8 minutes. Supernatant was carefully discarded and the pellets were resuspended in 300µl of 2% (w/v) BSA. Samples were analysed using a FACS Canto™ II flow cytometer (BD Biosciences) and with FACS Diva software (BD biosciences, version 7.0).

Table 2.2: Cell surface molecules for flow cytometry

Marker	Fluorochrome	Isotype control	Clones	Description
CD14 ¹⁵²	PerCP-Cy5.5*	IgG2b	MφP9	Monocyte differentiation antigen, LPS-receptor
CD19 ¹⁵²	BV421*	IgG1	HIB19	B lymphocytes antigen
CD29 ¹⁵⁷	APC*	IgG1	MAR4	Integrin β1, cell adhesion
CD34 ^{152,159}	APC	IgG1	581	Hematopoietic progenitor cell antigen
CD44 ¹⁵⁶	PerCP-Cy5.5	IgG2b	G44-26	Hyaluronate Receptor
CD45 ¹⁵²	PE*	IgG1	HI30	Protein tyrosine phosphatase receptor type C
CD49b ¹⁵⁸	BV	IgG2a	12F1	Integrin α2
CD49c ¹⁵⁸	PE	IgG1	C3 II.1	Integrin α3
CD73 ¹⁵²	BV421	IgG1	AD2	5'-nucleotidase
CD90 ¹⁵²	PE	IgG1	5E10	Thy-1
CD105 ¹⁵²	APC	IgG1	266	Endoglin
CD151 ¹⁵⁵	PE	IgG1	14A2.H 1	Raph blood group
CD166 ¹⁵⁴	BV421	IgG1	3A6	Activated leukocyte cell adhesion molecule (ALCAM)
CD271 ¹⁵³	BV421	IgG1	C40- 1457	Low-affinity nerve growth factor receptor
HLA-DR ^{152*}	APC	IgG2b	TU36	Human leukocyte antigens-DR

* PercP-Cy5.5: Peridinin-chlorophyll-protein-Cyanine5.5, BV421: Brilliant Violet 421,

APC: Allophycocyanin, PE: Phycoerythrin, HLA-DR: Human Leukocyte Antigen-D

Related

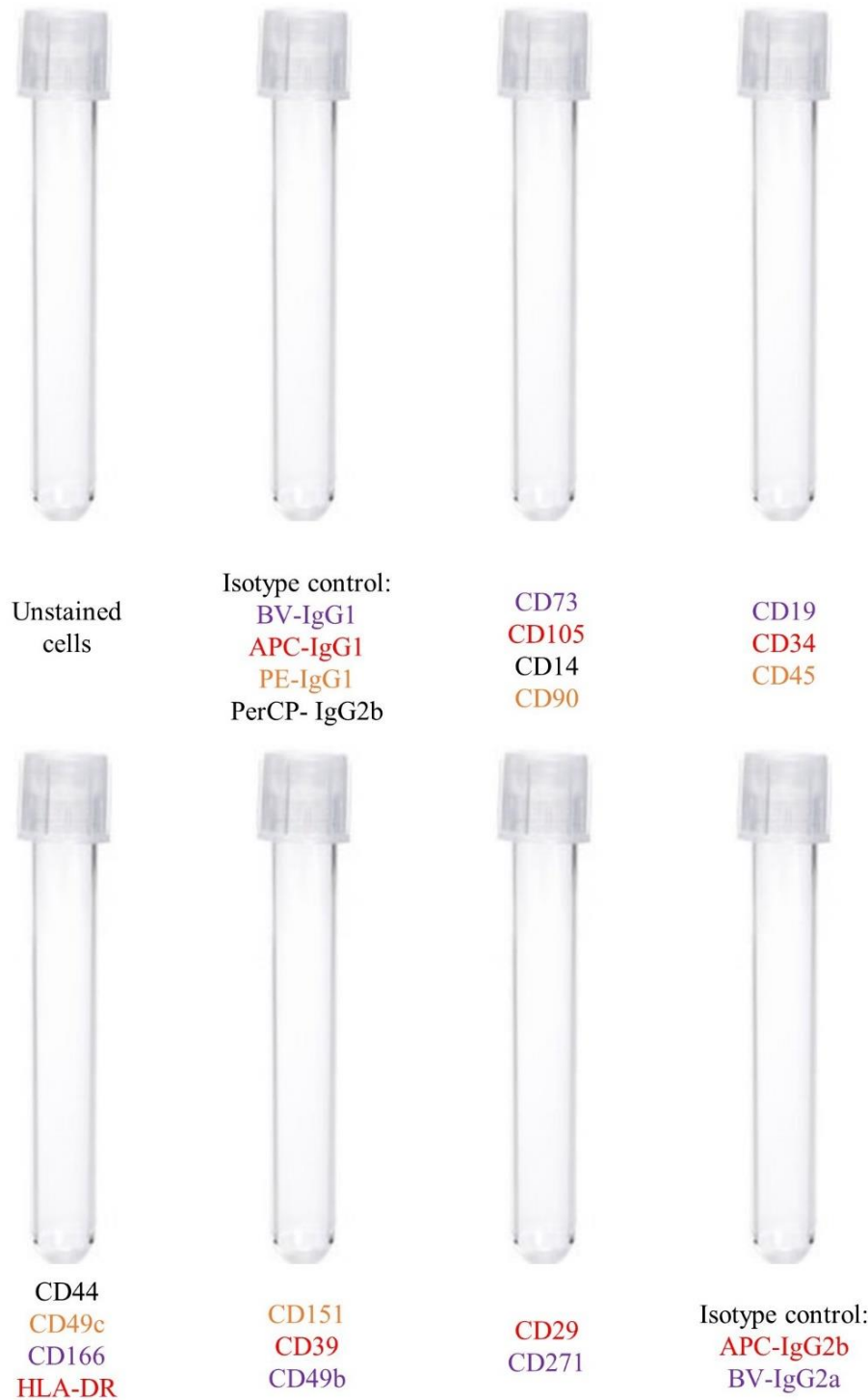


Figure 2.5: Diagram of the combination of fluorochrome conjugated antibodies assessed via flow cytometry.

Fluorochromes are indicated as purple (BV421), red (APC), orange (PE), black (PerCP-Cy 5.5)

2.5 Three-dimensional pellet culture for chondrogenic differentiation

An established 3D pellet culture system was used to assess the chondrogenic potency of donor-matched avascular and vascular meniscal cells and chondrocytes¹⁶⁰. 2×10^5 cells were centrifuged at 350 *g* for 8 minutes into a cell pellet in sterile 1.5 ml microcentrifuge Eppendorf tubes, supplemented with DMEM/F12, P/S (1%), insulin-transferrin-selenium (ITS) (1%), L-ascorbic acid-2-phosphate (1 mM) (Sigma-Aldrich), dexamethasone (100 nM), sodium pyruvate (1 mM) (Sigma-Aldrich) and TGF β 1 (PeproTech, London, UK) (10 ng/ml).

2.6 Biochemical analyses for chondrogenesis within the pellets

2.6.1 Papain digestion of chondrogenic pellets

After 28 days in culture, pellets were digested in papain to release GAGs and DNA. The papain digestion buffer was composed of 50mM sodium phosphate (BDH), 20 mM EDTA (Sigma-Aldrich), 20 mM N-acetyl cysteine (BDH) and adjusted to pH 6.0. Papain was added to the buffer to reach the final concentration of 125 μ g/ml. Each pellet was digested in 200 μ l of the papain solution at 60°C for 3 hours. The digestion samples were vortexed every 30 minutes. Samples were centrifuged at 1000*g* for 5 minutes and stored at -20°C prior to use.

2.6.2 Dimethylmethylene blue assay (DMMB)

The total GAG content in pellets was measured by 1,9-dimethylmethylene blue (DMMB) assay¹⁶¹. The DMMB dye solution was prepared by adding 4mg DMMB (Sigma, Poole, UK), 0.76g glycine (Sigma, Poole, UK) and 0.595g sodium chloride (NaCl) into 250ml distilled water, followed by adjusting to pH 3.0 using 10M hydrochloric acid. Standards were prepared by dissolving chondroitin sulphate (C9819,

Sigma-Aldrich) from bovine trachea in distilled water (stock: 1 mg/ml) and diluted into standards of 0, 0.025, 0.05, 0.075, 0.1 µg/ml. 50 µl of samples or standards were added into 96 well plates in triplicate, with 200 µl of DMMB dye solution. The absorbance results were read immediately at $A_{530\text{nm}}$ and $A_{590\text{nm}}$ on a FluorStar Omega microplate reader (BMG Labtech, Ortenberg, Germany). The standard curve was plotted using the following equation:

$$(A_{530\text{nm}}/A_{590\text{nm}}) - (A_{530\text{nm blank}}/A_{590\text{nm blank}})$$

where $A_{530\text{nm}}$, $A_{590\text{nm}}$ is the absorbance of samples (or standards) at 530nm and 590nm; $A_{530\text{nm blank}}$, $A_{590\text{nm blank}}$ is the absorbance of 0 µg/ml standard at 530nm and 590nm. The total GAGs content of each pellet was calculated using the standard curve equation.

2.6.3 DNA Assay

The PicoGreen[®] dsDNA Assay Kit (Thermo fisher Scientific, Massachusetts, USA) was used to determine DNA content in pellets following the manufacturer's instructions. PicoGreen[®] is a fluorescence probe that binds double-stranded (ds) DNA which forms a highly luminescent complex compared with the free dye in solution¹⁶². 1 x TE buffer (10 mM Tris-HCl, 1 mM EDTA, pH 7.5) was made from 20 x TE stock supplied in the PicoGreen kit. PicoGreen[®] reagent was diluted (1:200) in 1 x TE buffer and protected from light. Standards were prepared by diluting lambda DNA (100 µg/ml) with 1 x TE buffer at a final concentration of 2 µg/ml. The stock solution was then used to create standards at concentration of 0, 25, 50, 100, 200, 300, 400, 500 and 1000 ng/ml. 100 µl of samples or standards were pipetted into 96 well plates in triplicate, with 100 µl of PicoGreen reagent. The microplate was covered with foil and incubated at room temperature for 4 minutes after which the fluorescence value was read at excitation (480 nm) and emission (520nm) wavelengths on the microplate reader. The fluorescence

value of the blank was subtracted from each sample and the DNA concentration was determined using the standard curve. Finally, the total GAG contents in the chondrogenic pellets were normalised to the DNA content of each pellet.

2.7 RNA extraction and Quantitative Real-Time Polymerase Chain Reaction (qRT-PCR)

Avascular and vascular meniscal cells and chondrocytes (2×10^5 cells) cultured in monolayer (P0) or chondrogenic pellets were resuspended in 350 μ l RLT lysis buffer (Qiagen, Hilden, Germany) containing 1% (v/v) β -mercaptoethanol (Sigma, Poole, UK), followed by snap freezing in liquid N₂ and storage at -80 °C in 1.5ml Eppendorf tubes for subsequent RNA extraction.

2.7.1 mRNA extraction

A RNeasy Mini Kit (Qiagen, Hilden, Germany) was used for mRNA extraction from cells or pellets according to the manufacturer's instructions. After samples were thawed, 350 μ l of 70% ethanol (Sigma, Poole, UK) in RNase free water (Sigma, Poole, UK) was mixed with each sample and transferred to a spin column placed in a 2ml collection tube. The collection tube was centrifuged at 10,000g for 1.5 minutes. RWI buffer (700 μ l) and RPE buffer (500 μ l) were used to perform one and two washes of the mRNA respectively and centrifuged at 10,000g for 1.5 minutes. 50 μ l of RNase free water was added and centrifuged at 10,000g for 1.5 minutes to elute the mRNA. The final volume was collected in a 0.5ml Eppendorf tubes and stored at -80 °C.

2.7.2 mRNA reversed to cDNA

mRNA was converted to cDNA using a high-capacity cDNA Reverse Transcription kit (Applied Biosystems, California, USA). 25 μ l of mRNA sample was transferred into a sterile microcentrifuge tube and mixed with 5 μ l of reverse transcriptase buffer, 2 μ l of

dNTP mix, 5µl of random primers, 2.5µl of multiscribe reverse transcriptase (50 U/µl) and 10.5µl of RNase free water. All steps were performed on ice. The tubes were placed in a thermocycler (Techne, Cambridge, UK), which was pre-programmed to 25 °C for 10 minutes, 37 °C for 2 hours and a final holding step of 4 °C. Samples were stored at -20 °C until further use.

2.7.3 Quantitative Real-Time Polymerase Chain Reaction (qRT-PCR)

qRT-PCR was performed using SYBR Green[®] (Applied Biosystems, California, USA) which specifically binds to dsDNA to monitor gene amplification. 2µl of cDNA sample was added into a 96-well PCR reaction plate in triplicate. Subsequently, a reaction mixture consisting of 12.5 µl SYBR Green Master Mix (Taq DNA polymerase, dNTP and SYBR Green dye), 2.5 µl of primers for the target gene and 8 µl of RNase free water were added into each well. The description of target genes is listed in Table 2.3. The plate was then sealed using an optical adhesive film (Applied Biosystems, California, USA) and placed in the Quant Studio3 Real-Time PCR machine (Applied Biosystems, California, USA). The PCR machine was configured to run the following temperature protocol: activation of SYBR Green (10 minutes, 95°C, each for 1 cycle); 40 repeated cycles of denaturation of cDNA (10 seconds, 90°C), annealing (30 seconds, 55°C) and extension (34 seconds, 72°C); dissociation (10 seconds, 94°C; 30 seconds, 55°C; 10 seconds, 94°C, 1 cycle). The Quant Studio Design and Analysis Software (Applied Biosystems, California, USA) was used to determine the cycle threshold (CT) values, which is the cycle number that the fluorescence generated within that reaction crosses the fluorescence threshold. Glyceraldehyde 3-phosphate dehydrogenase (GAPDH) and hypoxanthine phosphoribosyltransferase 1 (HPRT1) were used as reference genes. The relative gene expression was calculated using the comparative CT method ($2^{-\Delta CT}$) ($\Delta CT = CT \text{ gene of interest} - CT \text{ reference genes}$)¹⁶³.

Table 2.3: Primers used for qRT-PCR

Gene:	Official full name	Gene ID (NCBI)
Reference gene		
HPRT1	Hypoxanthine phosphoribosyl transferase 1	3251
GAPDH	Glyceraldehyde-3-phosphate dehydrogenase	2597
Chondrogenic markers		
ACAN	Aggrecan	176
COL2A1	Collagen type 2 alpha 1	1280
SOX9	SRY-box transcription factor 9	6662
De-differentiation markers		
COL1A2	Collagen type I alpha 2 chain	1278
Hypertrophic markers		
COL10A1	Collagen type 10 alpha 1	1300
MMP1	matrix metalloproteinase 1	4312

2.8 Histological analysis

2.8.1 Cryosection of chondrogenic pellets

After 28 days in chondrogenic culture, 3 pellets from each cell population were washed with PBS and imaged under a Hamamatsu digital camera (C4742-95). Pellets were then placed on filter paper and snap frozen in liquid nitrogen cooled hexane and stored at -80 °C until needed. Frozen pellets were mounted onto a pre-cooled chuck with TissueTek® (Sakura Finetek, Zoeterwoude, Netherlands) and frozen with cryospray

(CellPath, Newtown, UK). Pellets were sectioned at a 7 μm thickness using a cryostat (Bright, Luton, UK; Model: OTF) and collected on poly-L-lysine coated slides. Sections were stored at -20°C for future staining.

2.8.2 Wax embedding and sectioning of human meniscus tissue and sheep meniscus explant

Human meniscus tissue obtained from TKR patients or sheep meniscus explants samples were dissected as described in chapter 2.1.2. The cross-section of meniscus was fixed in 10% neutral buffered formalin for at least 48 hours at room temperature. These samples were then processed by the histopathology laboratory at RJA Orthopaedic Hospital as follows. Samples were put in cassettes and placed in the following solutions, for one hour each: 70%, 90%, 95%, 100%, 100% and 100% of methylated spirit (IMS, Gent Medical, York, UK), followed by immersing the samples twice in xylene for one hour prior to immersing twice in Fibrowax[®] (VWR, Pennsylvania, USA) at 65°C for 1 hour. The samples were mounted in a mould with hot Fibrowax and solidified on a cold platform for 30 minutes. The mould was detached from the wax block and sectioned at a 5 μm thickness on a microtome (Leica, Wetzlar, Germany). Sections were then collected onto slides in a warm water container and dried at 37°C for 24 hours.

2.8.3 Haematoxylin and Eosin (H&E) staining of human meniscus sections

The H&E staining is used to assess the general morphology of the meniscus tissues derived from TKR patients. Haematoxylin is a basic dye that is positively charged and so stains the acidic tissue and cell structure (basophilic) purplish blue, whereas eosin is an acidic dye, that being negatively charged, stains the basic structures (acidophils such as cytoplasm and ECM) into pink or red ¹⁶⁴.

To perform the H&E staining for wax sections, slides were dewaxed in xylene x2 for 5

minutes and rehydrated in 100% (x2), 90% and 70% isopropanol for 2 minutes each, followed by rinsing twice in distilled water for 3 minutes. All slides were flooded with Harris's Haematoxylin (ATOM Scientific, Cheshire, UK) for 5 minutes and rinsed with tap water for 5 minutes to allow sections to turn "blue". Slides were then flooded in 1% eosin for 30 seconds and washed in tap water. Slides were dehydrated through an ascending sequence of concentrations of isopropanol: 70%, 90%, 100% x2 for 2 minutes each, after which slides were transferred to clear in xylene twice for 5 minutes. Slides were mounted using Pertex (Histolab, Othenburg, Sweden) and left to dry for at least 1 hour.

2.8.4 Toluidine blue staining of chondrogenic pellets

Toluidine blue is a basic thiazine metachromatic dye used to visualise the presence of GAGs¹⁶⁴. To perform toluidine blue staining for chondrogenic pellets, cryosections were thawed at room temperature. Slides were then flooded with 1% toluidine blue (BDH Lab Supplies, Poole, UK) for 30 seconds and rinsed in running tap water to remove the excess dye. The stained slides were then air dried and mounted using Pertex with coverslips. Once dry, pellets stained with toluidine blue were viewed under a Leitz Diaplan light microscope (Leitz, Stuttgart, Germany) and imaged using the Nikon DS-Fi1 camera (Nikon, Tokyo, Japan).

2.8.5 Immunochemical staining of collagen type I and type II

For chondrogenic pellets, cryosections were pretreated with hyaluronidase (4800U/ml, Sigma, UK) for 2 hours and fixed in 10% formalin for 10 minutes. For sheep meniscus explants, wax sections were dewaxed in Histo-Clear II (NAT1328, National Diagnostic, USA) twice for 5 minutes and successively rehydrated in 100% x2, 90% and 70% isopropanol for 2 minutes each. Sections were then washed with PBS and incubated with a primary mouse collagen type I antibody (1:500, clone I-8H5, MP Biomedicals,

Cambridge, UK) and a collagen type II antibody (1:50, clone CIIC1, DHSB, University of Iowa, USA) in PBS for 1 hour. Negative control sections were incubated with nonspecific, isotype matched antibodies (for collagen type I: IgG2a; for collagen type II: IgG1, Dako, Denmark) instead of primary antibodies at the same concentration. Sections were then washed in PBS before incubation with the secondary biotinylated antibody at 50 µg/mL (goat anti-mouse, VECTASTAIN ABC kit, Vector Laboratories, Peterborough, UK) for 30 minutes. 0.3% (v/v) hydrogen peroxide in methanol (BDH) was applied for 30 minutes to eliminate endogenous peroxidase activity. Labelling was enhanced with incubation of streptavidin-peroxidase (VECTASTAIN Elite ABC kit, Vector Laboratories, Peterborough, UK) for 30 minutes according to the manufacturer's instructions. After washing with PBS, sections were visualised with diaminobenzidine (DAB, ImmPACT, Vector Laboratories, Peterborough, UK). Then sections were dehydrated as described above before mounting under glass coverslips with Pertex mounting medium. The immunohistochemistry staining intensity of collagen type I and type II was quantified using ImageJ Fiji Software (version 1.2; WS Rasband, National Institute of Health, Bethesda, MD) ¹⁶⁵.

2.8.6 Histological grading of human meniscus tissue

All meniscus samples were categorised using the macroscopic meniscus grading system (Figure 2.6 & Table 2.4) and microscopic meniscus grading system (Table 2.5) ²⁹. For both scoring systems, a higher number represents the most degeneration, with 0 being totally normal. The total score from the histological assessment can be converted to a grade system: Grade 1 represents normal tissue with scores ranging from 0 to 4. Grade 2 indicates mild degeneration with scores ranging from 5-9. Moderate degeneration is seen in Grade 3 tissue (scores of 10-14), while Grade 4 represents the most severe degeneration (scores ranging from 15-18). Calcium deposits and cell clusters typically

appeared in Grades 3-4.

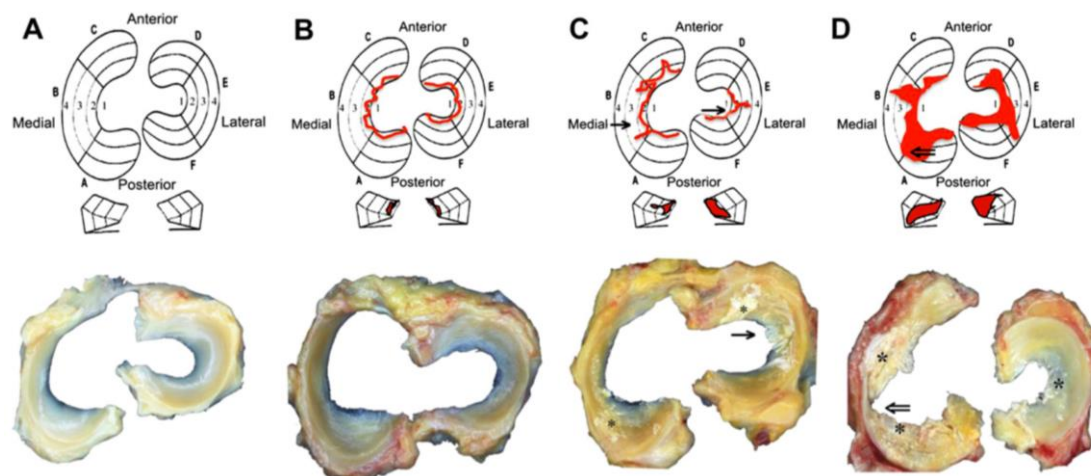


Figure 2.6: Macroscopic meniscus assessment

(A) Grade 1; (B) Grade 2; (C) Grade 3: partial substance tears (right arrow); (D) Grade 4: full substance loss of tissue (left arrow); Red in (B)-(D) indicate the degeneration pattern Reproduced from Pauli et al.²⁹ (reprint permission from Elsevier)

Table 2.4: Macroscopic meniscus scoring system

Grade	Description
1	Normal intact menisci, attached at both ends with sharp inner borders, no meniscal tibia or femoral surface changes
2	Fraying at inner borders, tibial or femoral surface fibrillation, no tears
3	Partial substance tears, fraying, tibial or femoral side fibrillations
4	Full/complete substance tears, loss of tissue, tissue maceration

Table 2.5: Microscopic meniscus scoring system

	<i>Grade</i>	<i>Criteria</i>	<i>Score</i>	
	<i>A</i>	Smooth	0	
Femoral side	<i>B</i>	Slight fibrillation or slightly undulating	1	
	<i>C</i>	Moderate fibrillation or markedly undulating	2	
	<i>D</i>	Severe fibrillation or disruption	3	
	<i>A</i>	Smooth	0	
Surface including lamellar layer	Tibial side	<i>B</i>	Slight fibrillation or slightly undulating	1
		<i>C</i>	Moderate fibrillation or markedly undulating	2
		<i>D</i>	Severe fibrillation or disruption	3
	Inner border	<i>A</i>	Smooth	0
	<i>B</i>	Slight fibrillation or slightly undulating	1	
	<i>C</i>	Moderate fibrillation or markedly undulating	2	
	<i>D</i>	Severe fibrillation or disruption	3	
Cellularity	<i>A</i>	Normal	0	
	<i>B</i>	Diffuse hyper cellularity	1	
	<i>C</i>	Diffuse hypo/acellular regions	2	
	<i>D</i>	Hypocellularity (empty lacuna, pycnotic cells)	3	
Collagen organisation/alignment and fibre organisation	<i>A</i>	Collagen fibres organised, homogenous eosinophilic staining of extracellular matrix	0	
	<i>B</i>	Collagen fibres organised, diffuse foci of hyaline or mucinous degeneration	1	
	<i>C</i>	Collagen fibres unorganised, confluent foci or bands of hyaline or mucinous degeneration, fraying	2	
	<i>D</i>	Collagen fibres unorganised, fibrocartilaginous separation (oedema, cyst formation), severe fraying and tears	3	
Matrix staining (Safranin-O-Fast Green)	<i>A</i>	None	0	
	<i>B</i>	Slight	1	
	<i>C</i>	Moderate	2	
	<i>D</i>	Strong	3	

Cell clusters: present +, ++, +++ Calcium deposition: present +, ++, +++; Total score converted to meniscal grade: Grade 1 (normal) =0-4, Grade 2 (mild degeneration) =5-9, Grade 3 (moderate degeneration) =10-14, Grade 4 (severe degeneration) =15-18. Reproduced from Pauli et al. ²⁹ (reprint permission from Elsevier)

2.9 Fibrinogen and thrombin polymerisation

2.9.1 Mechanism of Fibrinogen and Thrombin Blood-Clotting Cascade

The fibrinogen molecule is a 340kDa plasma glycoprotein, which consists of two sets of $A\alpha$ -, $B\beta$ -, and γ - polypeptide chains linked by 29 disulphide bonds (Figure 2.8)¹⁶⁶⁻¹⁶⁸. $B\beta$ and γ chains together compose a D-region, which is connected with the E-nodule through a coiled-coil segment. The $A\alpha$ chains are the longest, which extend into a high-flexible series followed by a globular α C-terminus that is located close to the E-region¹⁶⁸. Thrombin is a serine protease which is formed by proteolytically cleaved prothrombin (coagulation factor II)¹⁶⁹. Fibrin formation is initiated by thrombin-mediated cleavage of fibrinopeptides (Fp)A and FpB from the fibrinogen. The polymerisation starts with cleavage of FpA into half-staggered, overlapping protofibrils. Subsequently, FpB is cleaved from fibrinogen and fully releases $A\alpha$ -chains from the E-region, which leads to the lateral aggregation of protofibrils into fibres yielding a fibrin meshwork¹⁷⁰.

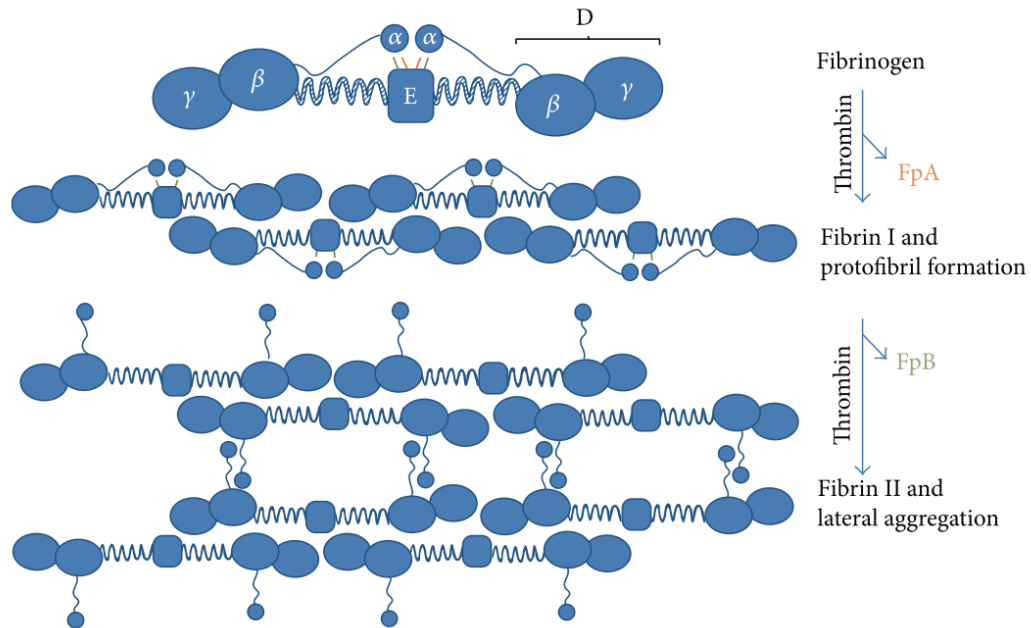


Figure 2.8: Schematic representation of fibrin formation.

Fibrinogen consists of two sets of A α -, B β -, and γ -chains. The A α -chains are connected with the E-region through fibrinopeptide A (FpA, orange) and fibrinopeptide B (FpB, green). The D region is composed of β -, and γ -chains and connected with the E-region by a coiled-coil segment. Fibrin formation initiates with cleavage of FpA by thrombin to polymerises into protofibrils, followed by cleavage of FpB which leads to the release of the α -chain C-terminal and lateral aggregation. Reproduced from Undas et al. ¹⁶⁶ (permission under request)

2.9.2 Fibrin gel in polyurethane scaffold penetration test

To test the feasibility of using a fibrin gel as a carrier to deliver cells into a clinically used synthetic meniscus scaffold, a polyurethane scaffold (Actifit[®]) was selected. Actifit[®] was sectioned vertically into 4 mm thick triangular pieces. Fast green solution was used as an indicator of fibrin gel distribution within Actifit[®] scaffold. It was mixed with 20 mg/ml fibrinogen (F8630, Sigma-Aldrich, USA) and 1500 μ l was injected into scaffold using a 0.5ml syringe (29G, BD). Subsequently, 500 μ l of 100U/ml thrombin

(T4648, Sigma-Aldrich, USA) was added into the scaffold in a ratio of 3:1. After 30 minutes of polymerisation, a scaffold was sectioned horizontally in half to check if the fibrin gel penetrated through the entire scaffold.

2.9.3 Chondrocyte viability in polyurethane scaffold with fibrin gel

Human chondrocytes (P5) were thawed from our cell biobank and cultured until 80% confluence, at which time cells were detached using trypsin and counted. 2mm x 2mm core scaffolds were obtained from Actifit[®] scaffolds using a dermal biopsy punch (2.0mm, Kai Medical, Japan). The experiment was divided into three groups (with triplicates in each group), including (i) scaffold alone (negative control group), (ii) scaffold with chondrocytes group (cell group) and (iii) scaffold with chondrocytes delivered by fibrin gel (fibrin gel group). In the cell group, chondrocytes were resuspended in 100µl of media at a concentration of 2×10^5 cells/ml and loaded onto scaffolds (2×10^4 cells/scaffold). In the fibrin gel group, chondrocytes were resuspended in 75µl of fibrinogen (20mg/ml) at a concentration of 2.7×10^5 cells/ml and injected into scaffolds, followed by the addition of 25µl of thrombin (100U/ml) with 100U/ml aprotinin supplement (resulting in 2×10^4 cells/scaffold). The constructs were placed in 96 well plate and incubated at 37° C for 30 minutes to facilitate cellular attachment and polymerisation of fibrin gel. A pilot experiment was performed to optimise the polymerization time of chondrocytes-fibrinogen and thrombin at 15mins, 30mins and 60mins in a colony ring. The results showed after 30mins or 60mins incubation, the fibrin gel could form firm column to stand on its own without colony ring support, whereas after 15mins incubation, the gel could not maintain its shape after removal of colony ring. Therefore, 30mins incubation time was chosen to facilitate cellular viability and polymerisation of fibrin gel. Subsequently, a further 200 µl of complete media was added to each well. Explants were incubated at 37°C, 5% CO₂.

After 14 days culture, cell viability in the scaffold was assessed using a LIVE/DEAD viability assay kit (Invitrogen, UK). The scaffolds were cut in half, washed in PBS, followed by incubation in 2 μ M calcein AM (live cells, green) and 4 μ M ethidium homodimer-1 (EthD-1, dead cells, red) in culture media. Sections were washed again in PBS and imaged with a Leica TCS SP5 spectral confocal microscope (Leica Microsystems, Milton Keynes, UK).

2.10 Statistical analysis

All statistical analyses were performed in GraphPad Prism (Version 8.30, San Diego, California, USA) or R (The R Foundation, Vienna, Austria). Different statistical tests used for specific experiments are introduced in the experimental design and results section. Shapiro-Wilk normality test was used to determine the distribution of data. Parametric and nonparametric tests were applied for normally and abnormally distributed data, respectively. Data were presented as mean \pm standard deviation (SD) in the graphs and text. For all analyses, $p < 0.05$ was considered statistical significance.

**Chapter 3: Characterisation of Regional
Meniscal Cell and Chondrocyte Phenotypes
and Chondrogenic Differentiation in
Osteoarthritic Donor-Matched Tissues**

3.1 Introduction

Several studies have indicated that degeneration of the meniscus contributes to knee OA pathogenesis¹⁷¹. MRI frequently indicates meniscus degeneration as a key feature in the osteoarthritic knee, which contributes to some of the joint space narrowing that is typically observed¹⁷². Degenerative meniscus tears interfere with the conversion of axial loading into horizontal tensile strain which can increase articular cartilage stress leading to cartilage loss¹⁷³. In combination, this body of evidence indicates that meniscus degeneration is a key contributor in OA disease processes.

In a previous study, degenerate meniscus histological features were described²⁹, these included the identification of cell clusters, hypercellularity (diffuse) and cellular hypertrophy, tears, fraying and calcification. Others have showed there to be collagen fibre disorganization and higher levels of proteoglycans in the matrix as indicated by histological and electron microscopy analyses in end-stage OA patients¹⁷⁴. Further, the degenerated meniscus was shown in another study to be altered in terms of its biochemistry, the extracellular matrix was disorganized and the expression and synthesis of ECM proteins was altered¹⁷⁵. The precise mechanism(s) underpinning the degeneration associated changes remain to be clarified. In this chapter the surface immunoprofile and transcription profile of degenerated meniscus have been characterised, which will add to the scientific literature describing meniscus cell and tissue alteration during the OA disease process.

Three cell types are present within the meniscus itself²⁴. In the avascular zone (inner and middle part of the meniscus), cells with an oval or round morphology reside known as fibrochondrocytes¹⁷⁶. In the outer third of the tissue fibroblast-like cells are present surrounded by dense connective tissue¹⁷⁶. The final cell type is found in the meniscus's superficial zone, these cells have a flattened, fusiform shape and are thought to

represent a sub-population of progenitor cells¹⁷⁷. Meniscal cell phenotypes and transcription profiles have been characterised previously in non-diseased human and animal tissues^{23,178,179}. However, the comprehensive phenotypic and gene profile of degenerate meniscal tissue-derived cells and their immunoprofiles from the distinct regions of osteoarthritic menisci have not previously been described.

Human lateral and medial menisci possess some distinct morphological features²⁴. The lateral menisci demonstrate a wider range of size and thickness variety compared to the medial menisci⁴. Further, the lateral menisci cover a greater portion of the tibial plateau ($59 \pm 6.8\%$ laterally) compared to the medial meniscus ($50 \pm 5.5\%$ medially)¹⁸⁰. However, in this study we have investigated only cells derived from the lateral menisci from lateral compartment in medial OA patients at the time of TKR surgeries, mainly due to the lack of availability of intact medial menisci in these patients.

Meniscus tissue engineering strategies that use cell-based therapies are thought to represent an exciting new tool which may one day be used by clinicians to repair or regenerate damaged or degenerate menisci¹⁸¹. Meniscal cells have been shown to have cartilage matrix forming capacity *in vivo* and *in vitro*^{104,182}. However, meniscal cells derived from patients who have undergone debridement of bucket handle meniscal tears when induced chondrogenic in micromass cultures were able to produce less collagen type II and more collagen type I in comparison to donor-matched MSCs¹⁰⁴. In addition, this study indicated that rabbit meniscus punch defects could be successfully repaired at 12 weeks by transplanting them with meniscus cell seeded hyaluronan-gelatin scaffolds. Further, a sheep meniscus defect study demonstrated that implantation with autologous meniscal cells carried using a CMI[®] produced enhanced repair ECM and vascularisation at 3 months post-op compared to unseeded scaffold controls and in animals that had undergone an meniscectomy without transplantation¹⁸². Together, the

findings from these studies suggest that implanted meniscal cells contributed to the improved repair, although whether or not meniscal cells derived from degenerate tissues can retain this ability to repair is currently unknown.

The work described in this chapter has already been published ¹⁸³ and includes the characterisation of meniscal cell phenotypic markers and chondrogenic capacity. It compares cells derived from the inner (avascular) and outer (vascular) zones also compared to donor-matched articular chondrocytes derived from the lateral femoral condyle, recovered from TKR surgeries from patients affected by medial compartment OA in their knee joints. The findings from this study have the aim of furthering knowledge regarding the OA pathology in these tissues, assessing the potential of cells derived from OA meniscal tissues for regenerative medicine strategies including meniscal tissue engineering.

3.2 Experiment design

All the tissue samples used in this study were obtained from patients who were undergoing TKR for the treatment of medial compartment OA (n=10; mean age 66.4 ± 11.1 ; age range 46-87 years; 4 males, 6 females). Intact lateral menisci and donor-matched articular cartilage from the lateral femoral condyle were harvested and processed to digest avascular and vascular meniscal cells and chondrocytes as chapter 2.1.2 described. PDTs were calculated for each cell type (from passage 0-3) (chapter 2.3). Prior to digestion, a meniscus cross section was embedded in paraffin for histological evaluation using the meniscus microscopic grading system as chapter 2.8.6 described. Flow cytometry was used to assess three cell types of surface markers including MSCs markers (CD14, CD19, CD34, CD45, CD73, CD90, CD105, HLA-DR), chondrogenic potency and cell adhesion molecules (CD29, CD39, CD44, CD49b, CD49c, CD151, CD166, CD271) at day 14 in passage 0 for 10 donors. At passage 2, prior to chondrogenic differentiation, a smaller flow panel including chondrogenic potency molecules (CD39, CD44, CD271) and those in which a marked difference was observed between cell populations at passage 0 (CD49b, CD49c, CD166) were investigated in 6 donors according to chapter 2.4.2. qRT-PCR was performed to assess the gene expression levels of collagen type I (*COL1A2*), collagen type II (*COL2A1*), aggrecan (*ACAN*), *SOX-9* and matrix metalloproteinase-1 (*MMP-1*) and normalised to the housekeeping gene *GAPDH* as chapter 2.7 described. The chondrogenic potency of the three donor-matched cell populations was assessed at passage 2 using a well-established 3D pellet culture system in 6 donors as chapter 2.5 described. After 28 days in culture, n=3 pellets were used for biochemical GAG/DNA quantitation (chapter 2.6), n=3 pellets were snap frozen in liquid nitrogen-cooled hexane and cryosectioned for histological analysis (chapter 2.8.1). Cryosections were stained with TB (toluidine blue,

BDH, UK) to assess the general tissue morphology and GAGs composition of the extracellular matrix. In addition, immunohistochemistry for collagens type I and II was undertaken as chapter 2.8.5 described. The immunohistochemistry staining intensity of collagen type I and type II was quantified using ImageJ Fiji Software (version 1.2; WS Rasband, National Institute of Health, Bethesda, MD) ¹⁶⁵.

All data were inputted into GraphPad Prism (Version 7.04, USA) and Jamovi (Version 1.1.9.0) for statistical analysis. Differences between cell types were assessed by performing one-way ANOVAs with Tukey's multiple comparisons for population doubling time, positive percentage fluorescence signal, gene expression level, GAG/DNA comparisons and semi-quantitative of collagen type II IHC intensity. Two-way ANOVAs were used to compare the positive percentage fluorescence signal of different cell types and histological scores in avascular and vascular regions. The Jonckheere–Terpstra test was used to assess the correlation between the positivity of surface markers and meniscus histological scores. Multilevel modelling was performed to determine whether expressions of cell surface markers were associated with chondrogenic outcome as measured by GAG/DNA content. Cell source and cell surface marker positivity were considered as fixed effects, while the donor was considered as a random effect. Our lab previous data from flow marker reliability test (not published) was used to evaluate the reliability of chondrogenic predictors in multilevel modelling results (appendix II). For all tests, values of $p < 0.05$ were considered statistically significant.

3.3 Results

3.3.1 Histological scoring and analysis of meniscus sections

Ten patients (6 males and 4 females, ages 46-87 years) who were undergoing TKR (Table 3.1) provided donor-matched samples of meniscus and cartilage tissues. Avascular and vascular zones were noted to frequently present with differing states of degeneration and hence, were graded separately using histological analyses. The intensity of matrix metachromatic staining in the vascular zone was found to be significantly elevated compared to the avascular zone of the tissue (Figure 3.1). In addition, the inner zone of the avascular region was shown to score 2 or 3. This data could indicate that the inner region of the meniscus tissue is the first to be affected in the OA disease process. No significant differences were seen when comparing avascular and vascular regions in terms of the other histological parameters measured.

Table 3.1: Demographics of donors from which samples were sourced.

ID	Gender	Age	Meniscus	Microscopic grading
Donor 1	Male	46	Lateral	2
Donor 2	Female	53	Lateral	4
Donor 3	Female	66	Lateral	3
Donor 4	Female	66	Lateral	2
Donor 5	Male	66	Lateral	2
Donor 6	Female	67	Lateral	2
Donor 7	Male	69	Lateral	3
Donor 8	Male	69	Lateral	3
Donor 9	Female	75	Lateral	2
Donor 10	Female	87	Lateral	2

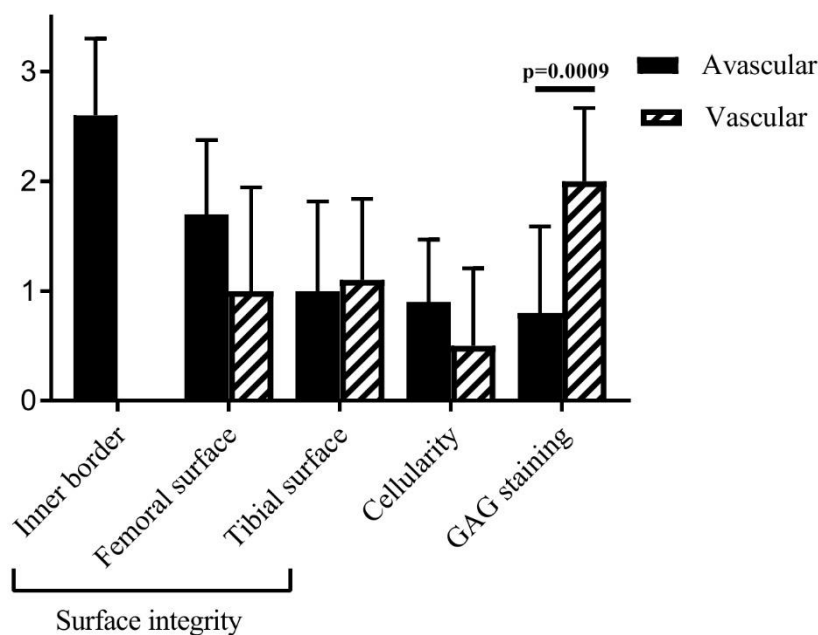


Figure 3.1: Histological grading results of avascular and vascular regions of the meniscus.

Avascular (solid bars) and vascular (hashed bars) regions were scored histologically and compared in terms of significance. The GAGs staining intensity in the vascular region was significantly higher than in the avascular region; (Grade 1: 0-3; Grade 2: 4-7; Grade 3: 8-11; Grade 4: 12-15). The grading criteria was presented in chapter 2.8.6

The histological analyses undertaken revealed several noteworthy observations. Along the inner border fibrillation was apparent with disrupted tissue structures and/or abnormal cellularity observed throughout. These changes seemed to go hand in hand with oedematous matrix changes close to surface (Figure 3.2a). Chondrocyte-like cells were visualised in the swollen oedematous region as well as frequent cell clusters surrounded by an acellular ECM. Further, toluidine blue (TB) staining intensity was stronger in these pericellular regions (Figure 3.2b).

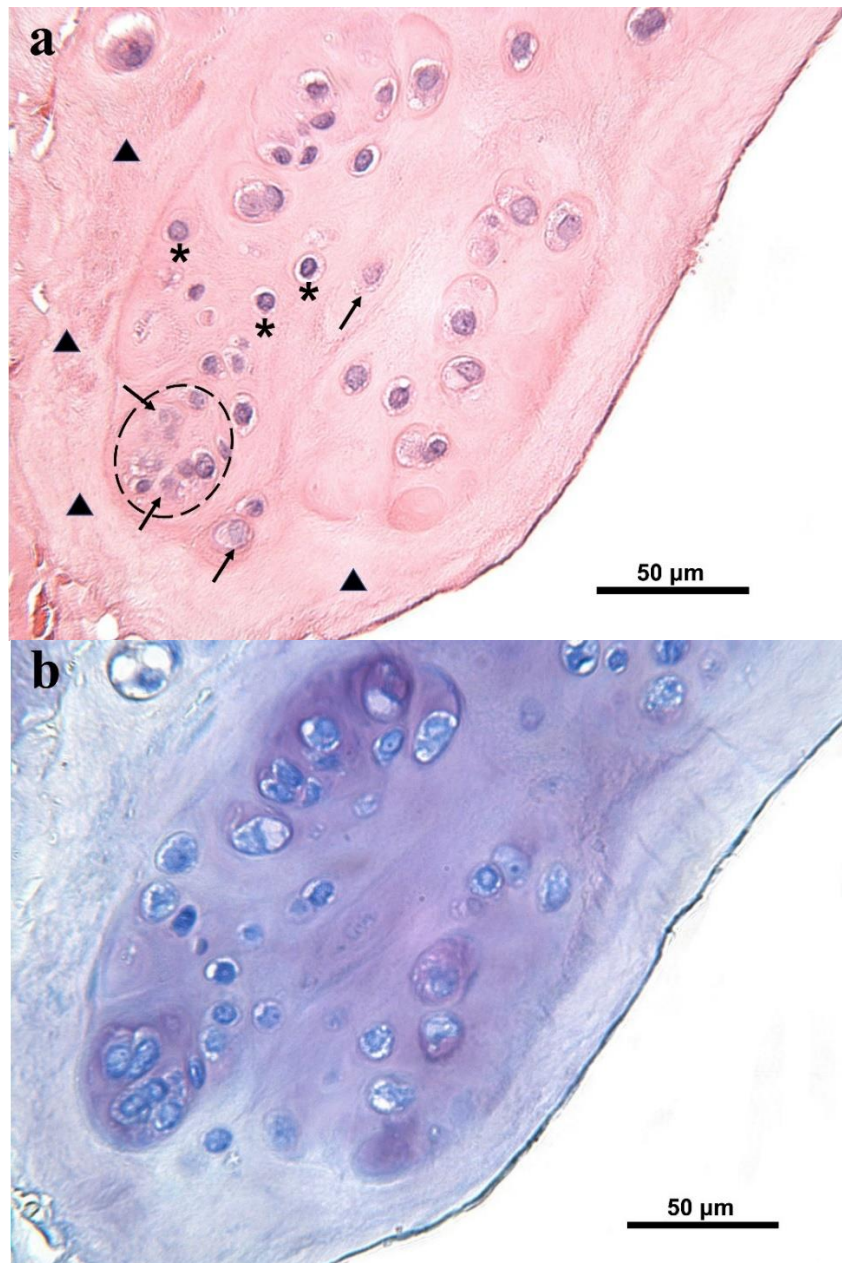


Figure 3.2: Representative avascular region meniscus histology from donor 9 stained with H&E and TB (Grade 2)

(a) Oedematous changes were observed in the meniscus surface zone, where the cells often appeared chondrocytic (*) sometimes forming clusters (dashed line). The area surrounding the oedematous region was typically acellular (▲) Note the necrotic appearance of some cells in this area and within the clusters (↗); (b) A higher intensity of TB staining was observed in the oedematous region.

A bundle of transverse collagen fibres, known as the transverse ligament, were found transcending from the synovial edge (Figure 3.3a) into the vascular region. In all of the 10 patient samples analysed a “tree-like” formation of fibres was observed in the avascular region (Figure 3.3b), which under polarized light was clearly visible (Figure 3.3c). The ligament structure was closely associated with blood vessels in all six of the Grade 2 menisci studied (Figure 3.3d). In the Grade 3 and 4 menisci, however, fewer blood vessels were found observed in connection with this “tree-like” structure (Figure 3.3e-f).

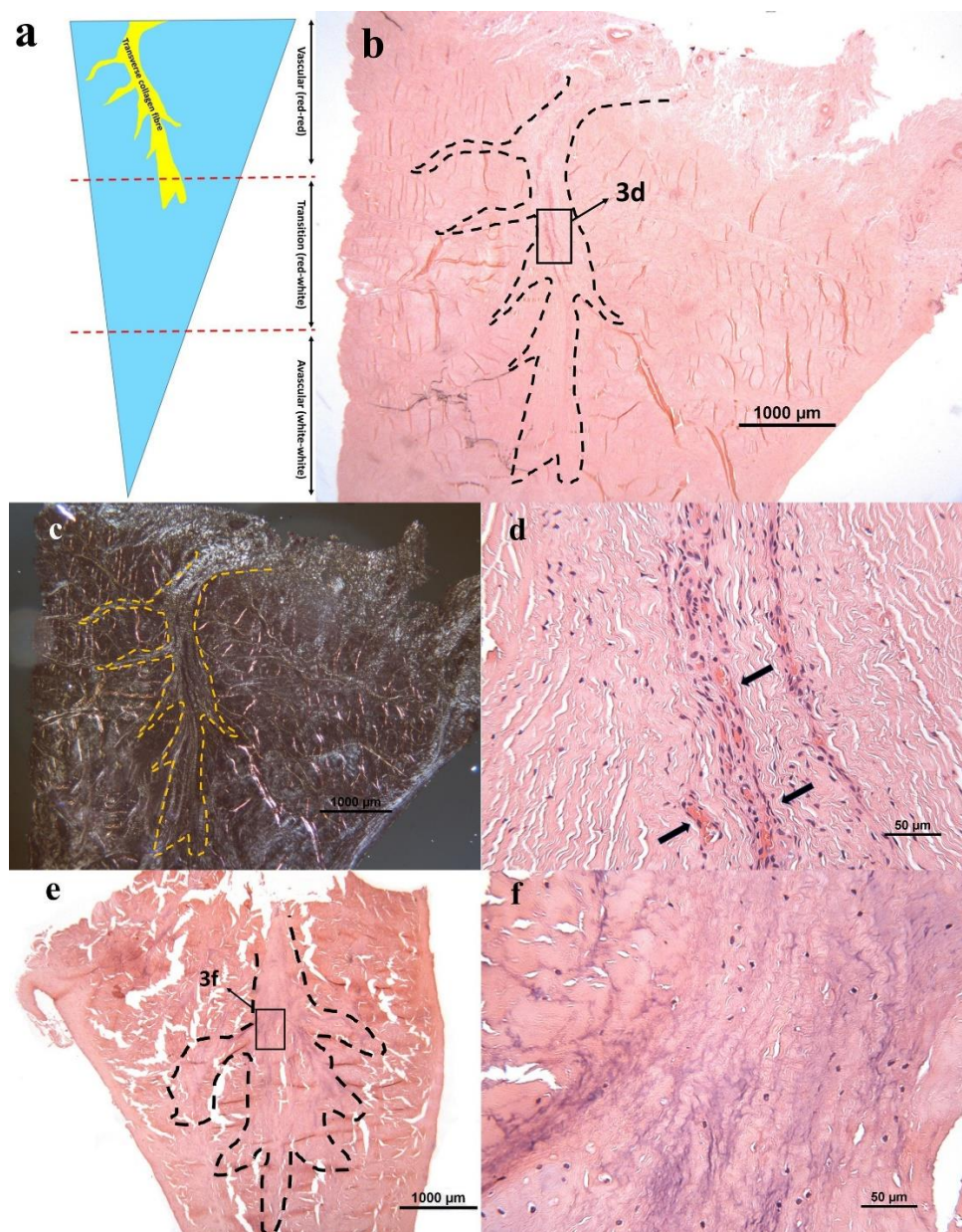


Figure 3.3: Representative images of Grade 2 (b-d: donor 4) and Grade 3 (e, f: donor 9) menisci with H&E staining

(a) Cross-sectional illustration of the meniscus. “Tree-like” transverse collagen fibres (yellow) run into the vascular region radially from the synovial tissue. (b) The “tree-like” structure is indicated with a dotted line; (c) Again, the “tree-like” structure (dotted line) is indicated and visualised using polarized light; (d) Along the “tree” root, blood vessels (arrows) were seen; (e) In the Grade 3 menisci the matrix was fragmented; (f): The “tree-like” structure was without blood vessels and more degenerate in the Grade 3 menisci.

3.3.2 Growth kinetics

Vascular meniscal cells proliferated significantly faster at passage 0-1 compared to avascular meniscal cells ($p=0.0191$) and chondrocytes ($p=0.0057$) (Figure 3.4). Cell PDT decreased as the passage number increased across all cell fractions. However, this observation should be considered a trend, as no significant differences were observed between passages.

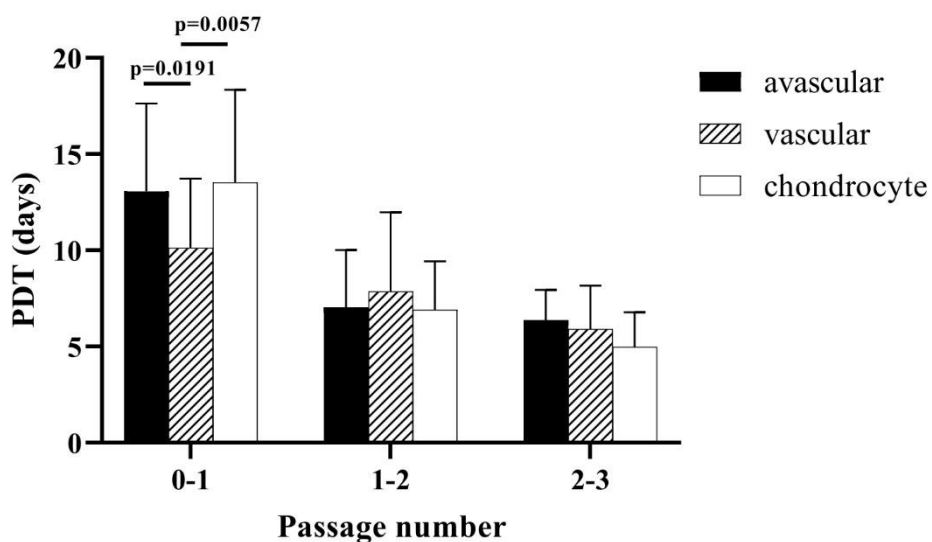


Figure 3.4: Population doubling time (PDT).

Graph depicts the PDT of donor-matched fractions of avascular and vascular meniscal cells as well as chondrocytes (passage 0-3).

3.3.3 Cell surface markers analysis

At passage 0, for all fractions and for all 10 donors, immunopositivity for CD73, CD90, CD105 >95%, adhering to ISCT criteria ¹⁵²; However, ~25% of cells were immunopositive for CD14, which according to the ISCT criteria, should be <2%, but is similar to levels previously reported in MSCs derived from other musculoskeletal tissues ¹⁸⁴. Immunopositivity for CD29 (integrin $\beta 1$) and CD44 (hyaluronate receptor)

was >95% on avascular and vascular meniscal cells and >90% on chondrocytes. Whereas CD19 (B lymphocyte antigen), CD34 (haematopoietic progenitor cell antigen), CD45 (protein tyrosine phosphatase receptor type C), CD271 (low-affinity nerve growth factor receptor) and HLA-DR (human leukocyte antigen-DR) were all <5%, no significant difference was observed between groups. However, CD49b (integrin $\alpha 2$), CD49c (integrin $\alpha 3$) and CD166 (activated leukocyte cell adhesion molecule) displayed significantly different immunopositivity across the three fractions (two-way ANOVA) (Figure 3.5a). At passage 2, similar patterns were observed across the 6 donors tested pre-chondrogenic differentiation, with significant differences between CD49b and CD49c, but not CD166 indicated (Figure 3.5b). Avascular cells showed the highest level of immunopositivity for CD49b at passage 0 ($53.89 \pm 17.41\%$), which was lowest on chondrocytes ($16.80 \pm 7.03\%$) with $41.46 \pm 14.95\%$ of vascular cells being immunopositive. The levels of positivity for CD49b on the three cell fractions followed a similar pattern (avascular: $81.47 \pm 11.88\%$, vascular: $73.03 \pm 11.36\%$, chondrocyte: $47.16 \pm 21.81\%$), although no significant differences were observed. Immunopositivity for CD49c was $73.30 \pm 19.84\%$ on avascular meniscal cells, which was significantly higher than vascular meniscal cells ($60.47 \pm 32.99\%$) and chondrocytes ($53.69 \pm 30.60\%$) at passage 0. Immunopositivity for CD49c on avascular meniscal cells was significantly higher than for the other cell populations, but those from the vascular region were significantly lower than chondrocytes (avascular: $79.99 \pm 14.91\%$, vascular: $54.70 \pm 23.04\%$, chondrocyte: $68.19 \pm 13.46\%$). Further, immunopositivity for CD166 at passage 0 was significantly higher on avascular ($83.47 \pm 14.41\%$) and vascular ($81.68 \pm 16.95\%$) meniscal cells compared to donor matched chondrocytes ($53.47 \pm 21.09\%$). Interestingly, the length of time spent in culture appeared to upregulate CD166 on chondrocytes, from a mean of 53.47% at P0 to 89.82% at P2. CD166 demonstrated no

significant differences across the different cell fractions at passage 3 (avascular: $97.50 \pm 3.26\%$, vascular: $95.50 \pm 3.22\%$, chondrocyte: $89.82 \pm 7.97\%$).

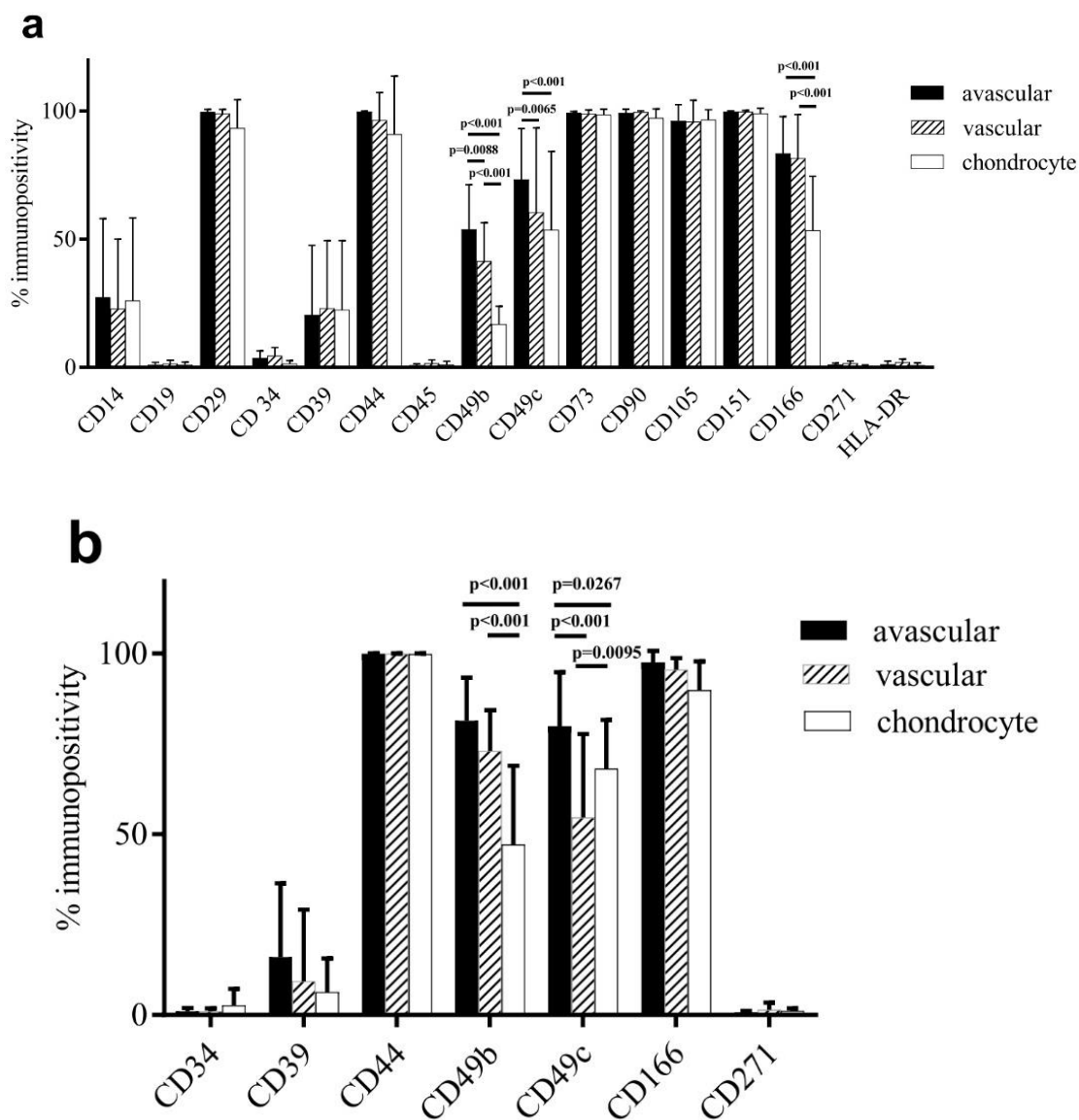


Figure 3.5: Flow cytometry outcomes

(a) All of the donor matched fractions tested showed comparable patterns of immunopositivity for the markers investigated at passage 0. Immunopositivity for CD49b, CD49c and CD166 was greater on meniscal cells compared with chondrocytes (10 donors); (b) CD49b and CD49c immunopositivity showed similar trends across the cell types at passage 2 (6 donors). Data shown are the means \pm SD.

3.3.4 Comparing flow profiles and histological analyses

Histological parameters scored in the avascular and vascular regions were significantly related to the immunopositivity of the six markers tested in the study (Table 5.2).

Jonckheere-Terpstra testing revealed that when the meniscus tibial surface was more severely disrupted in the avascular region, the median number of avascular meniscal cells which were immunopositive for CD49b ($p = 0.009$) and HLA-DR ($p = 0.028$) increased. In addition, when the inner border had more severe disruption in the meniscal tissue, positivity for CD49b was higher in avascular meniscal cells ($p = 0.018$); the same relationship was shown for CD29 ($p = 0.047$). Interestingly, when increased hypocellularity was observed in the vascular zone, the median immunopositivity for CD34 and CD39 in vascular meniscal cells increased ($p = 0.005$ and $p = 0.049$, resp.). Further, in the vascular zone, GAGs intensity increased and more of the vascular meniscal cells were immunopositive for CD19 ($p = 0.024$).

Table 3.2: Correlation between surface markers and histology scores

Region	Tibial			Inner border			Cellularity			GAG intensity			
	<i>p</i>	<i>z</i>	<i>r</i>	<i>p</i>	<i>z</i>	<i>r</i>	<i>p</i>	<i>z</i>	<i>r</i>	<i>p</i>	<i>z</i>	<i>r</i>	
CD19	Avas	0.292	1.054	0.333	0.313	-	-	0.093	1.681	0.532	0.846	-	-
	Vas	0.492	0.688	0.218	-	-	-	0.756	0.311	0.098	0.024	2.261	0.715
CD29	Avas	0.288	1.064	0.336	0.047	1.986	0.628	0.619	-	-	0.667	-	-
	Vas	0.598	-	-	-	-	-	0.657	-	-	0.321	-	-
CD34	Avas	0.151	1.437	0.454	0.093	1.681	0.532	0.911	0.112	0.035	0.699	-	-
	Vas	0.280	1.080	0.342	-	-	-	0.005	2.800	0.885	0.100	1.644	0.520
CD39	Avas	0.151	1.437	0.454	0.313	1.008	0.319	0.575	-	-	0.699	-	-
	Vas	0.202	1.277	0.404	-	-	-	0.049	1.970	0.623	0.681	0.411	0.130
CD49b	Avas	0.009	2.595	0.821	0.018	2.360	0.746	0.911	0.112	0.035	0.627	-	-
	Vas	0.280	-	-	-	-	-	0.756	0.311	0.098	0.537	-	-
HLADR	Avas	0.028	2.203	0.697	0.911	0.112	0.035	0.575	0.560	0.177	0.561	-	-
	Vas	0.377	0.884	0.280	-	-	-	0.254	1.141	0.361	0.150	1.439	0.455

Jonckheere-Terpstra test: Avascular region (grey shading); vascular region (white shading). The significant values are highlighted in bold and italics. The full table content in appendix III

3.3.5 Gene expression profiles: Donor-matched analyses of avascular and vascular meniscal cells and chondrocytes

SOX-9 expression was significantly higher in chondrocytes compared to avascular and vascular meniscal cells (Figure 3.6a). Unsurprisingly, collagen type I expression was significantly higher on the avascular and vascular groups compared to donor matched

chondrocytes (Figure 3.6b). No significant differences were found across the cell fractions in the expression levels of collagen type II (COL II), aggrecan (ACAN) or MMP-1 (Figure 3.6c-e).

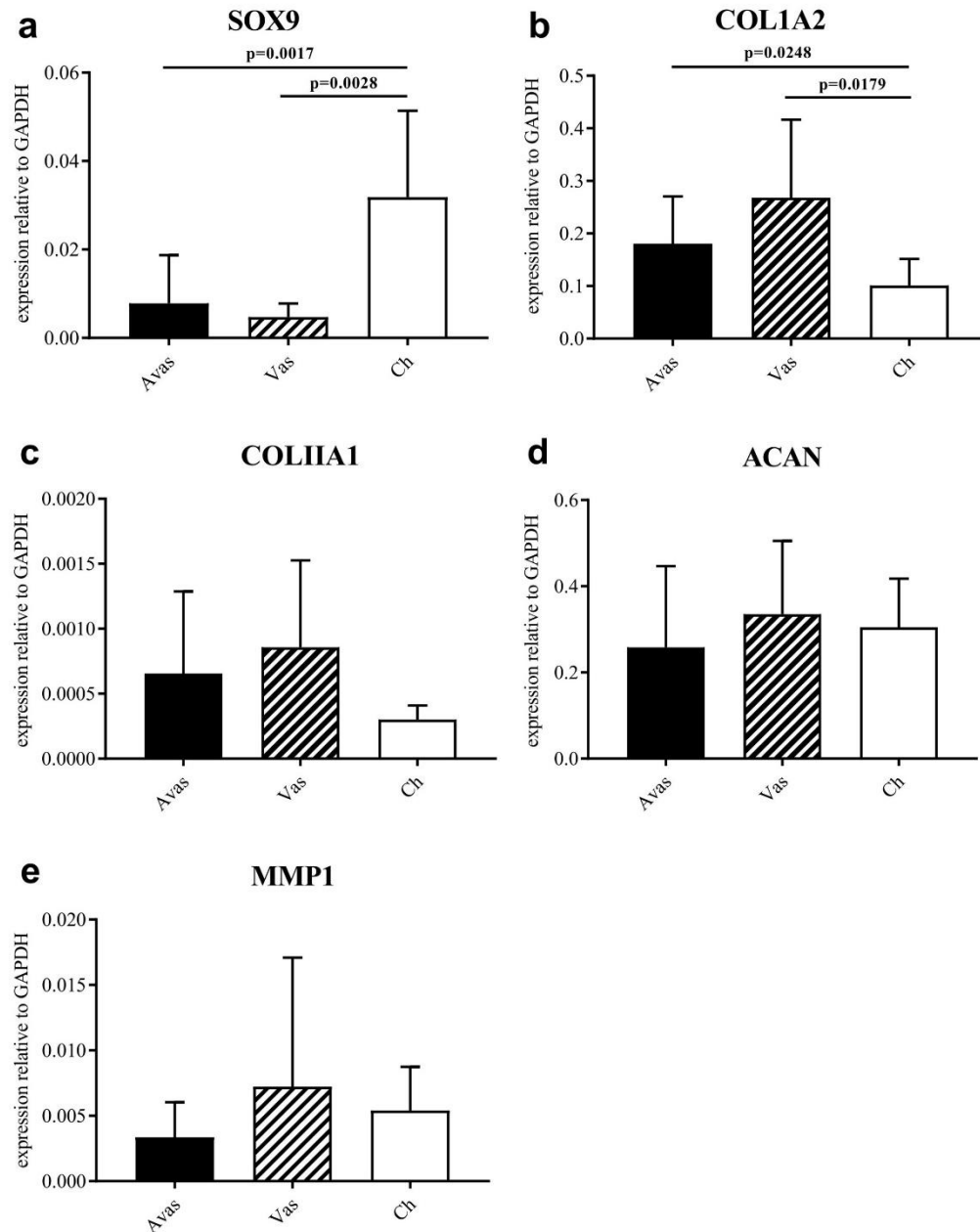
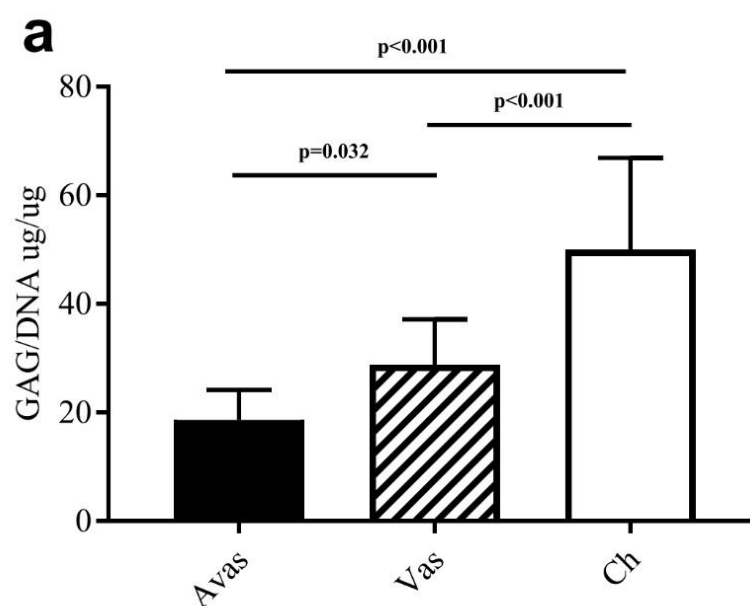


Figure 3.6: qRT-PCR outcomes

The MMP1 and chondrogenic gene expression profiles in Avas, Vas and Chondrocytes after 14 days in monolayer culture (a-e). Data shown are the means \pm SD of n=3 technical replicates and n=10 donors for each cell fraction. Gene expression is shown relative to the house-keeping gene, GAPDH.

3.3.6 *In vitro* chondrogenic pellet analysis

At 28 days post-chondrogenic differentiation GAG/DNA analyses revealed that chondrocytes consistently produced the highest levels of GAGs, avascular meniscal cells also showed lower GAGs levels compared to vascular meniscal cells (Figure 3.7a). The histological grading of TB intensity in the avascular and vascular zones appeared to match this data, in that, the vascular regions demonstrated more pronounced matrix metachromasia compared to avascular regions (Figure 3.1a; Figure 3.7a). Chondrogenic capacity across individual donors was variable. In general, collagen type I staining was observed in all pellets and across cell types after 28 days of chondrogenic induction. The highest staining intensity for collagen type I was seen in the vascular meniscal cell fraction (Figure 3.7b & c), collagen type I gene expression profiles seemed to mirror this pattern for each cell population (Figure 3.6b). In contrast, weak collagen type II staining were detected in all cell fractions, although significantly stronger staining intensity was observed in chondrocyte pellets compared to vascular meniscal cell pellets (Figure 3.7d).



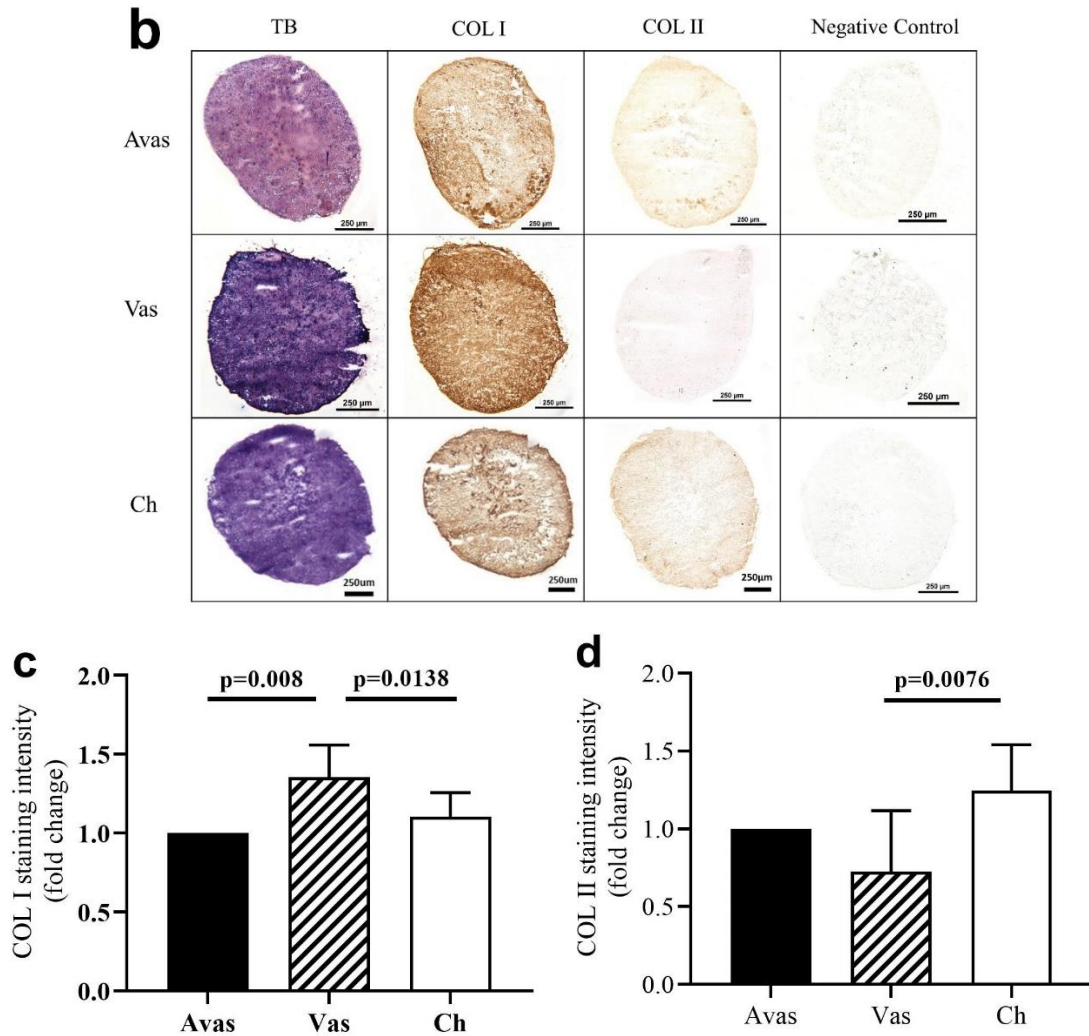


Figure 3.7: The chondrogenic assessment of avascular and vascular meniscal cells and chondrocytes.

(a) A comparison of Avascular (Avas) and Vascular (Vas) meniscal cells and chondrocytes (Ch) in terms of GAG/DNA quantitation after 28 days of culture in pellets. Data shown are the means \pm SD of $n=3$ runs and $n=6$ donors for each cell fraction. (b) Representative donor 6 histological analysis of pellet sections from Avas, Vas, Ch showing toluidine blue (TB), collagen type I (COL I) and collagen type II (COL II) staining. Scale bars represent $250\mu\text{m}$. (c) Collagen type I and (d) collagen type II semi-quantitative IHC analysis, relative fold change is shown compared to avascular meniscal pellets.

3.3.7 Chondrogenic potency analysis

Statistical multilevel modelling was conducted in order to identify chondrogenic potency indicators pre-chondrogenic differentiation (Table 3.3). CD49b positivity was shown to be associated with GAGs levels ($p = 0.035$). Similar to previous chondrogenic analysis (Figure 3.7a), cell types (vascular meniscal cells and chondrocytes) had a significant impact on GAGs quantitation compare to avascular meniscal cells ($p = 0.003$ and $p < 0.001$, respectively). CD44 expression was also shown to be negatively associated with GAGs quantitation in pellets ($p = 0.011$).

Table 3.3: Multilevel modelling

	Coefficient	95% Confidence Interval		<i>p</i>
		Lower	Upper	
CD34	-0.4543	-1.8915	0.983	0.553
CD39	0.277	-0.0109	0.565	0.096
CD44	<i>-77.5159</i>	<i>-123.7309</i>	<i>-31.301</i>	<i>0.011</i>
CD49b	<i>0.4098</i>	<i>0.0922</i>	<i>0.727</i>	<i>0.035</i>
CD49c	0.0606	-0.1577	0.279	0.601
CD166	-0.2386	-0.6014	0.124	0.233
CD271	-2.911	-6.1629	0.341	0.117
Vascular-Avascular	<i>21.0973</i>	<i>11.0721</i>	<i>31.122</i>	<i>0.003</i>
Chondrocytes-Avascular	<i>44.3104</i>	<i>29.7228</i>	<i>58.898</i>	<i><.001</i>

The significant values are highlighted in bold and italics.

3.4 Discussion

It is generally accepted that meniscus degeneration can cause the breakdown of articular cartilage in the knee and the early onset of OA ²⁴. However, the exact mechanisms of early meniscus degeneration are unclear, especially with regards to the cellular phenotypic changes and ECM alterations ¹⁸⁵. This study undertook an extensive characterisation of avascular and vascular meniscal cells derived from the lateral menisci from TKR surgeries. Although we carefully chose regions with an integral morphology, these tissues were certainly influenced by an OA pathological condition for an extended period. In the medial compartment of OA patients, the greater medial loading disturbs the normal mediolateral load distribution balance. This mismatched balance results in lateral compartment lift-off ¹⁸⁶. Consequently, the lateral meniscus undergoes extraordinary decreased loading which decelerates its tissue degeneration ¹⁸⁷. Our histological findings showed that the lateral menisci obtained from such joints have suffered in various degrees of deterioration as was revealed by our use of an established meniscal histological grading system ²⁹.

Petersen et al. ¹⁵ reported on the loosely arranged collagen fibres which developed from the joint capsule and inserted horizontally between the circular collagen fibres of the meniscus. The meniscus sample used in this study has identified these “tree-like” shaped structures in all donors. However, to the best of our knowledge, no previous study has outlined how/if these “tree-like” collagen fibres are involved with the pathological development of knee OA. Arnoczky et al. ⁹ showed there to be radial division of blood vessels originating from the perimeniscal capillary plexus, penetrating the meniscal matrix shortly into the main body of the meniscus, which seemed to associate with the “tree-like” collagen fibres penetrating into the meniscus. Our histological analyses showed that these blood vessels primarily appear along the

“root” of the collagen fibre “tree”. However, the vessels were only discovered in the “root” in the Grade 2 menisci and were rarely present in the same area in Grade 3 or 4 samples. This result matches up with previous research, which noted blood vessel occurrence only in the dense connective tissue but not in the fibrocartilage³⁰. The same study also reported that only 25% of the outer meniscus was vascularised in the aged menisci, whereas the outer one third of the meniscus was vascularised in young adult menisci. Degenerative meniscal tears mostly have a complex pattern, which are generally found in the mid to posterior of the meniscus¹⁸⁵. APM or non-operational treatment is normally selected to handle these patients because of the poor healing ability of the degenerative meniscus⁵⁴. The declined blood supply observed in the vascular zone of the degenerate meniscus may play a major role in the decreased self-healing capacity noted in this region.

The meniscal cells from the OA joint composed of a diverse population, which has not been well characterised previously. In our study, commonalities found in the surface molecules (CD14, CD19, CD29, CD34, CD39, CD44, CD45, CD73, CD90, CD105, CD151, CD271, HLA-DR) on avascular and vascular meniscal cells and chondrocytes imply that they possess similar characteristics and perhaps also chondrogenic potency, as many of these markers have been suggested to be predictive of *in vitro* chondrogenic capacity. Despite these similarities, distinctions in CD49b (integrin α 2), CD49c (integrin α 3) and CD166 (ALCAM) were noticed between meniscal cells and chondrocytes derived from OA joints. Grogan et al.¹⁷⁸ reported, in the normal human meniscus, a higher percentage of meniscal cells that were positive for CD14 (LPS-receptor), CD26 (dipeptidyl peptidase IV) and CD49c in contrast to chondrocytes (n=10). The differences found in our study in comparison may indicate that the OA environment impacts on the cell surface markers expression in meniscus and cartilage.

Grogan et al.¹⁷⁸ highlighted that immunostaining of CD166 was positive on cells that predominately surrounding the blood vessels in the vascular region of the meniscus and on cells at the meniscus surface, which could suggest the presence of progenitors in these regions, as CD166 has previously been used to recognise chondroprogenitors in healthy cartilage¹⁸⁸. A previous study demonstrated that freshly isolated vascular meniscal cells expressed higher positivity of CD34 (stem cell marker) and CD146 (pericyte marker) compared with avascular meniscal cells in the lateral meniscus from knee OA patients. These CD34 and CD146 positive meniscal cells displayed multilineage differentiation capabilities, which also favoured meniscus repair in a rat model¹⁸⁹. Our flow cytometry analysis showed greater expression levels of CD166 in the vascular meniscal cells compared to avascular cells. In addition, the cell growth kinetics analysis showed that the vascular meniscal cell fraction proliferated faster than the other donor-matched cell types. These findings indicate the existence of progenitors associated with the blood vessels or perhaps that the vasculature in the outer zone of the meniscus drives a more progenitor-like phenotype. This is further supported by our theory that the “tree-like” fibres which connects the joint capsule and meniscus together, not only provide the structural support and blood supply to the outer region, but may also contains a conduit for the “progenitors” which may arise from synovium, as CD166 positive progenitor populations have been noted in the synovium tissue of OA knees¹⁹⁰. Ideally, in future work aimed at confirming these hypothesise cell sorting could be used to isolate and analyse CD166 positive populations for progenitor phenotypic characterisation. In the more degenerate meniscus, we noted the shortage of blood vessels in “tree-like” fibres, which may indicate that this structure (consisting of collagen fibres, blood vessels and cells) plays a key role in preventing the meniscus matrix degeneration process in the early OA stages. However, this requires further

investigation before definite conclusions can be drawn. In addition, the progenitor population in the “tree root” may have regenerative features relevant to the improvement of meniscus tissue engineering strategies.

Integrins play an important role in the interactions between chondrocytes and the ECM in the OA pathological process of cartilage degeneration ¹⁹¹. However, the role that integrins have in the deterioration of the meniscus is still uncertain. CD49b and CD49c are integrin- α subunits which were categorized as ECM receptors for collagens, laminins and fibronectin ¹⁵⁸. CD49b expression was reportedly increased in the cartilage of a mouse model after OA induced 45 days compare to normal cartilage ¹⁹². The same study also reported that cell signalling through CD49b was induced by changes in the ECM, which activates the catabolic pathway of chondrocytes and favoured cell apoptosis as a result of elevated MMP activity. Integrin $\alpha 3$ was also found to be abnormally expressed in the knee of a destabilised medial meniscus (DMM) mouse model, which was closely linked with the onset of OA ¹⁹³. Our flow cytometry results demonstrated that the expression levels of CD49b and CD49c were greater in avascular meniscal cells compared with vascular meniscal cells and chondrocytes at both P0 and P2. This might be because the fraying of the avascular rim was found in OA samples in this study, perhaps indicating a more progressive response to OA development in the avascular region of the meniscus compared to the other regions. The correlation results also demonstrated that with more disrupted tissue structures in the meniscal inner rim, the immunopositivity for CD49b and CD29 (integrin $\beta 1$) in the avascular meniscal cells significantly increased. Integrin $\beta 1$ -collagen interaction is a crucial signalling pathway for chondrocyte survival, which prevents chondrocytes apoptosis ¹⁹⁴. Therefore, our results could support the hypothesis that the OA-like ECM changes in the avascular region of the meniscus induced the up-regulation of CD49b,

CD49c and CD29, although additional mechanistic study will be required to draw firm conclusions.

The multilevel modelling analysis carried out to find indicators of chondrogenic potency in this study indicated that greater expression levels of CD49b were significantly associated with higher GAGs production. A previous study showed that gene expression level of CD49b was up-regulated in 3D pellets of human chondrocyte at day 14 compared to monolayer cultures ¹⁹⁵. Another study demonstrated that GAGs quantities were significantly higher in pellet cultures of BM-MSCs compared to monolayer cultures ¹⁹⁶. However, the expression level of CD49b in pre-pellet formation has not previously been proved to correlate with higher post-pellet GAG productions.

Several limitations need to be noted in this study. Firstly, we have focused entirely on the lateral meniscus from the medial compartment of an OA knee. Including the medial menisci from the lateral compartment of osteoarthritic knees would make for a more comprehensive study. However, inadequate samples for this comparison could be achieved because knee OA is less commonly seen in lateral rather than the medial compartment ¹⁹⁷. Another limitation of this study is that the gene expression levels were not checked in chondrogenic pellets but only in monolayer cultures because of limited cell numbers. Such chondrogenic related gene expression analysis would complete the chondrogenic potency analysis conducted in the study.

In conclusion, our study suggests that CD49b, CD49c and CD166 are phenotypic markers which could differentiate cells from avascular or vascular meniscus and cartilage in the OA joint. We observed distinct regional meniscal cell profiles, which relate to histological tissue construct changes. The meniscus “tree-like” collagen fibres noted in the histological analysis in this study may play a key role in supporting the blood supply to vascular zone of meniscus and in maintaining meniscus integrity and

protecting against matrix degeneration. We also showed that meniscal cells derived from the lateral meniscus of knees with medial compartment knee OA have chondrogenic capacity *in vitro* which could be considered as a potential cell source for meniscus tissue engineering.

Chapter 4: Phenotypic characterisation of regional human meniscus progenitor cells

4.1 Introduction

Menisci play a key role in joint congruence, dispersing load and protecting the articular cartilages surface of the femur and tibia ². Although treatment of meniscus tears has developed dramatically including meniscus repair and replacement strategies, these surgical interventions' provide limited protection against the progression of osteoarthritis ^{198,199}. Therefore, there is a demand to develop other treatment to improve meniscus repair.

Mobilization and homing endogenous progenitor cells from the vascular zone of meniscus may be responsible for some of the natural healing noted in the meniscus following injury ²⁰⁰. The meniscus is composed of an outer "vascularised" zone that containing fibroblast-like cells and an inner "avascularised" zone that containing round fibrochondrocytes. It has been long known that the vascular region tears of the meniscus tend to successfully repair themselves after surgical procedure, whereas the inner avascular region has a low healing potential ²⁰¹. The better regeneration of the vascular part of the meniscus might be due to the presence of CD34 and CD166 immunopositive progenitor cells in the blood vessels in this region ¹⁸⁹. Recent studies suggested the presence of progenitor cells in the meniscus that promote meniscus injury repair in bovine, rabbit and mouse models ²⁰²⁻²⁰⁴. In chapter three it was demonstrated that there were fewer blood vessels carried by "tree-like" collagen fibres in the vascular zone of more degenerative menisci compare with healthier ones ¹⁸³. These results suggest that there is a subpopulation of progenitor-like cells in the vascular region. However, there is a lack of studies that decisively identified progenitor cell populations in human meniscus tissue.

Fibronectin-coated flasks have been previously used to extract chondroprogenitors from cartilage and these progenitors have been investigated for their capability for in

terms of cartilage regeneration ¹⁴⁸. Chondroprogenitors are an ideal candidate for cell-based tissue engineering cartilage repair strategies. Human meniscus cells and chondrocytes share similar cell surface markers profiles ¹⁸³. In this study, the chondroprogenitors isolation protocol this is established in the literature ¹⁴⁸ was used to obtain and characterise the progenitors and whole mixed population from donor-matched avascular and vascular regions of the meniscus, as well as cartilage derived chondroprogenitors.

4.2 Experiment Design

Human meniscus (five patients) and cartilage tissues (four patients) were harvested from four patients undergoing TKR and one patient undergoing above-knee amputation (Table 4.1). The general workflow is shown in Figure 4.1.

Table 4.1. Patient Demographics.

Patient	Age	Sex	Procedure	Tissue obtained	Additional Clinical Notes
1	37	male	TKR	Lateral meniscus; cartilage	Previous HTO, artificial meniscus allograft transplant, multiple knee wash out, removal of osteophyte
2	73	male	TKR	Lateral meniscus	Advanced OA with bone-on bone in medial compartment
3	60	female	TKR	Lateral meniscus; cartilage	Indication of OA from MRI imaging assessments
4	65	male	TKR	Lateral meniscus; cartilage	Bone-on-bone medial compartment OA, significant osteophytes
5	59	female	AKA	Lateral meniscus; cartilage	Previous traffic accident, osteoporosis due to lack of use

TKR: total knee replacement; AKA: above knee amputation; OA: osteoarthritis; HTO: high tibial osteotomy.

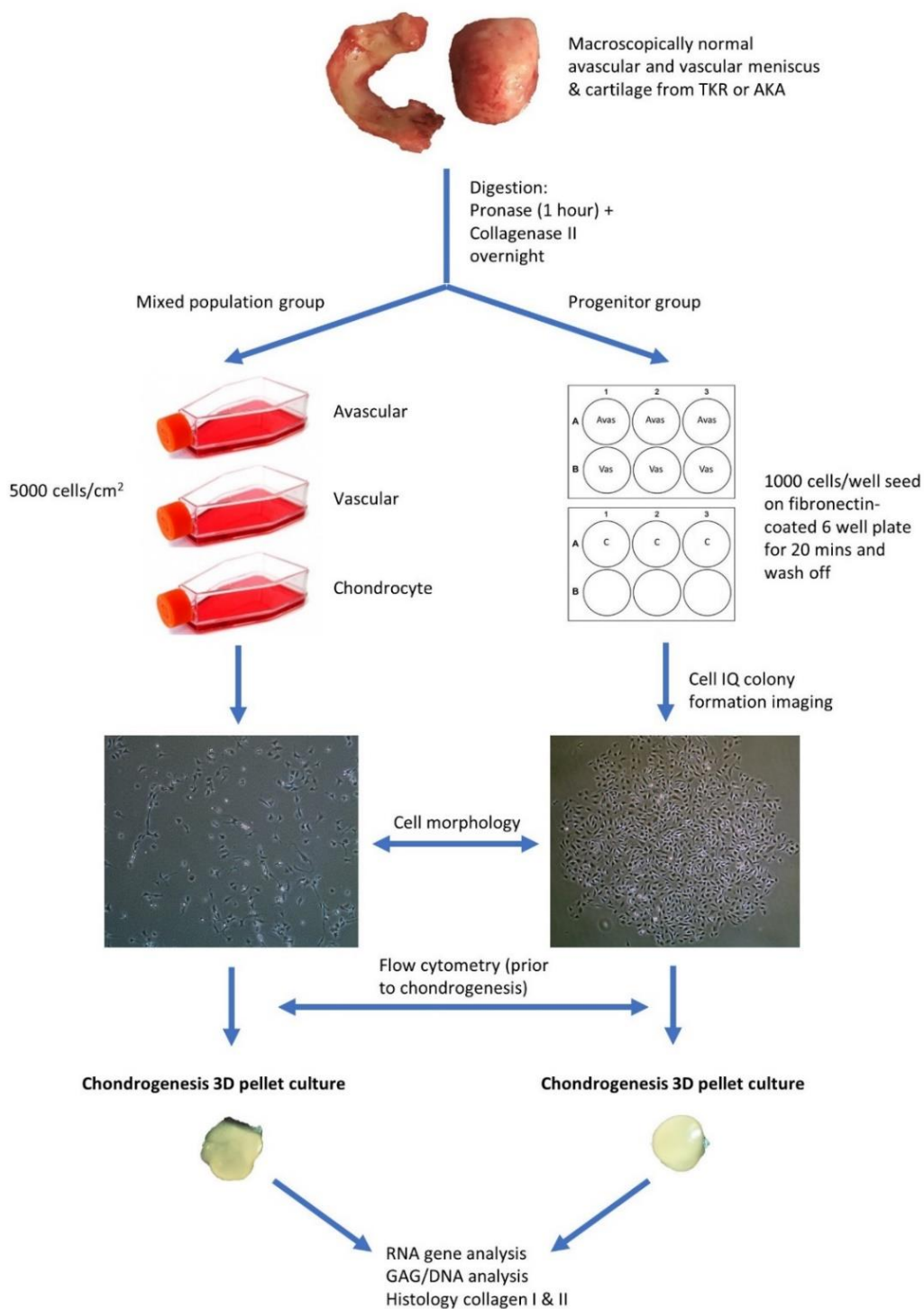


Figure 4.1: Flow Diagram of the Experimental Plan

Avas: Avascular meniscal cells, Vas: Vascular meniscal cells, C: Chondrocytes, TKR: total knee replacement, AKA: above-knee amputation.

The meniscus was dissected longitudinally into three parts: the inner avascular zone, the middle and the outer vascular zone. The middle portion was discarded and only the inner and outer avascular and vascular zones were used to derive meniscal cells. Additionally, full-depth macroscopically normal human articular cartilage from femoral condyles was used to isolate chondrocytes and their progenitors. Samples were digested by sequential pronase (70U/ml, 1 hour at 37°C) and collagenase type II (245U/ml, 12 hours at 37°C). All three cell types (avascular & vascular meniscal cells and chondrocytes) were cultured under two conditions. The first group was mixed population cells including avascular meniscal mixed cells (MAvas), vascular meniscal mixed cells (MVas) and mixed chondrocytes (MChs), which were plated at a density of 5000 cells/cm². The second group was progenitor cells including avascular meniscal progenitors (PAvas), vascular meniscal progenitors (PVas) and chondroprogenitors (PChs), which were subjected to a selective fibronectin adhesion assay as previously described in chapter 2.2.1.

After three days of culture in a 6 well plates, progenitor cells from 5 donors were analysed using the Cell-IQ[®] live cell imager for 48 hours as previously described in chapter 2.2.2. The recorded images were analysed using Cell-IQ[®] analyser software (CM Technologies, Tampere, Finland) in order to count the cell number in each colony at each time point. The number of colonies in each well were also counted under light microscopy post-Cell-IQ[®] analysis (only colonies with over 32 cells were included), the number of colonies counted was considered to be the initial number of progenitors that had adhered to the plate. Each type of polyclonal progenitor population was then trypsinised and cultured in complete medium with TGF-β1 (PeproTech, London, UK) (1ng/ml), FGF-2 (PeproTech, London, UK) (5ng/ml).

PDTs were calculated using the formula: $PDT = (t_2 - t_1) \times \ln(2) / \ln(n_2/n_1)$, where t_1 = the

time of cell seeding, t_2 = the time of cell harvest and n = the cell population at the matching time points. PDTs at passages 0 to 2 and passage 2 to 3 were compared between mixed populations and progenitor cells, as progenitors could not be counted with sufficient accuracy at P0-1.

Prior to chondrogenic differentiation, flow cytometry analysis was performed on avascular meniscal cells, vascular meniscal cells and chondrocytes from both mixed and progenitor populations as described in chapter 2.4.2. Immunopositivity for 6 molecules which are indicative of MSCs profile (CD14, CD73, CD90, CD105), chondrogenic potency or cell adhesion molecules (CD44, CD49b, CD49c, CD166) were evaluated in all five donors.

The chondrogenic potency of the three donor-matched populations in both mixed population and progenitor groups were assessed in all five donors (patient 2 only had matched avascular and vascular meniscal cells). After 28 days in culture, $n=3$ pellets were used for biochemical GAG/DNA quantitation (chapter 2.6) and $n=3$ pellets were used for gene expression analysis (*COL2A1*, *COL1A2*, *ACAN*, *SOX 9*, *COL10A1*) (chapter 2.7). Gene expression levels were calculated in progenitor cell pellets as a ratio compared to donor matched mixed population pellets, using the comparative threshold method. A 2-fold up- or downregulated change was considered biologically significant. In addition, $n=3$ pellets were snap frozen in liquid nitrogen-cooled hexane and used for immunochemistry stained with collagens type I and II.

GraphPad Prism (Version 8.30, San Diego, California, USA) was used for statistical analysis. Two-way ANOVA analysis with a multiple comparisons test was used to analyse flow cytometry, population doubling time, RNA gene analysis, GAG/DNA assay and collagen staining intensity.

4.3 Results

4.3.1 Growth Kinetics and Cell Morphology in Mixed Population and Progenitor cells

Figure 4.2 shows the representative mixed population and progenitor cell morphologies. At passage 0 (Figure 4.2A), mixed population cells were distributed randomly on tissue culture plastic, whereas progenitor cells were organised into round tightly packed colonies. PAvas and PChs had a similar oval chondrocyte-like morphology whereas PVas were fibroblastic spindle-shaped cells. At passage 2 (Figure 4.2B), the majority of the mixed population cells possessed extensive cytoplasmic processes of varying length²⁰⁵. However, this was much less observed in progenitor cells.

Mixed population cells demonstrated a slower growth rate in monolayer culture compare to progenitor cells from both passage 0 to 2 and passage 2 to 3. The mean PDT of MAvas, MVas and MChs at P0-2 were 15.46 ± 13.05 days, 35.40 ± 36.62 days and 9.47 ± 3.21 days compare with 1.27 ± 0.14 days, 1.25 ± 0.11 days and 1.33 ± 0.20 days for PAvas, PVas and PChs. A smaller difference in PDT between mixed and progenitor cells was seen at P2-3 with MAvas, MVas and MChs having a PDT of 15.45 ± 13.16 days, 7.18 ± 3.20 days, 9.39 ± 1.16 days and 2.91 ± 0.66 days, 3.25 ± 0.57 days and 3.19 ± 0.77 days for PAvas, PVas and PChs. However, the only statistically significant difference was found between MVas and PVas at P0-2 ($P=0.011$) ($n=5$ for MAvas, MVas, PAvas, PVas; $n=4$ for MChs, PChs) (Figure 4.3).

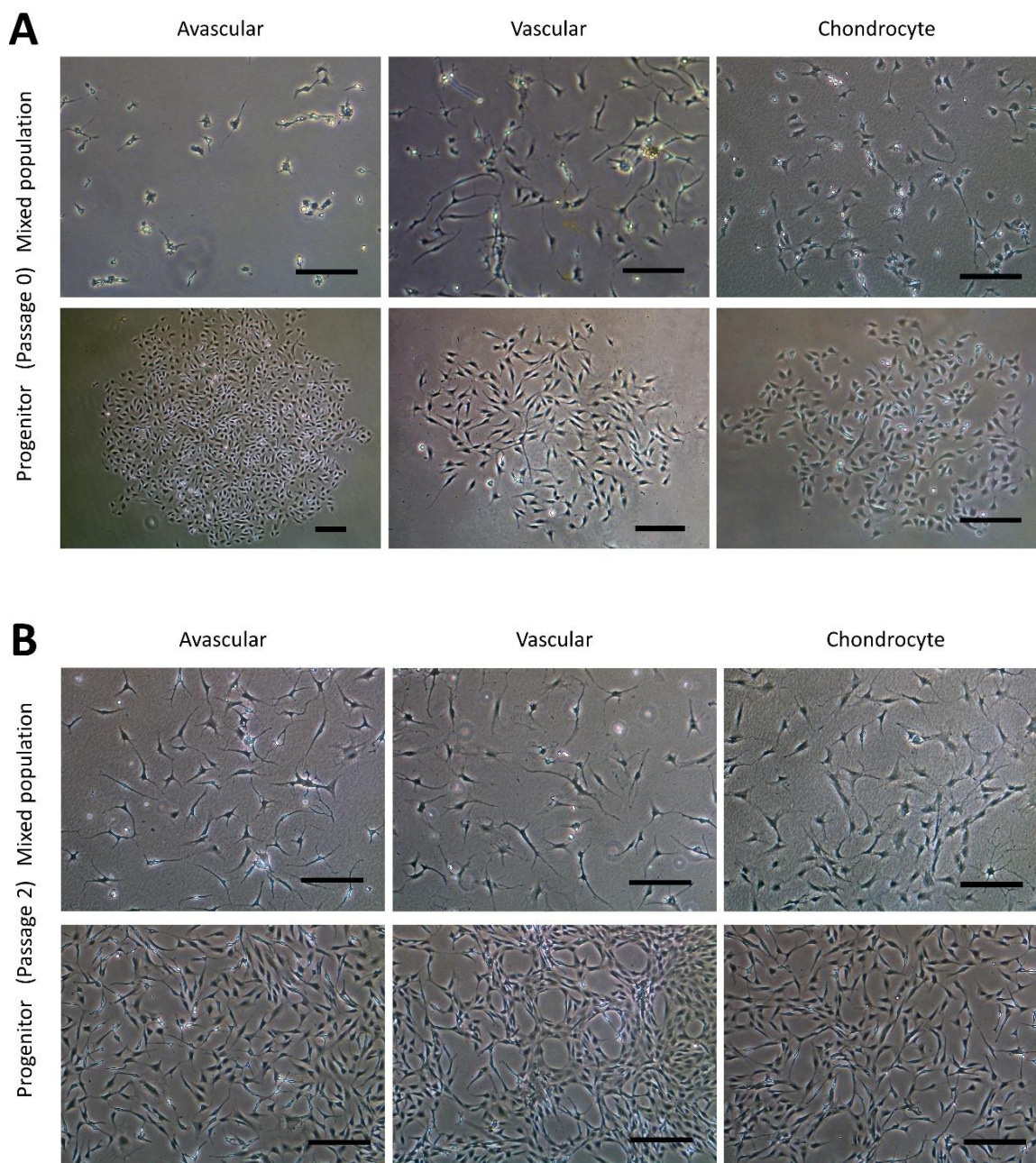


Figure 4.2: Comparison of progenitor cells morphology on monolayer culture.

Representative images from mixed population and progenitor cells at passage 0 (A) and passage 2 (B) in avascular and vascular meniscal cells and chondrocytes. Scale bars represent 250 μm .

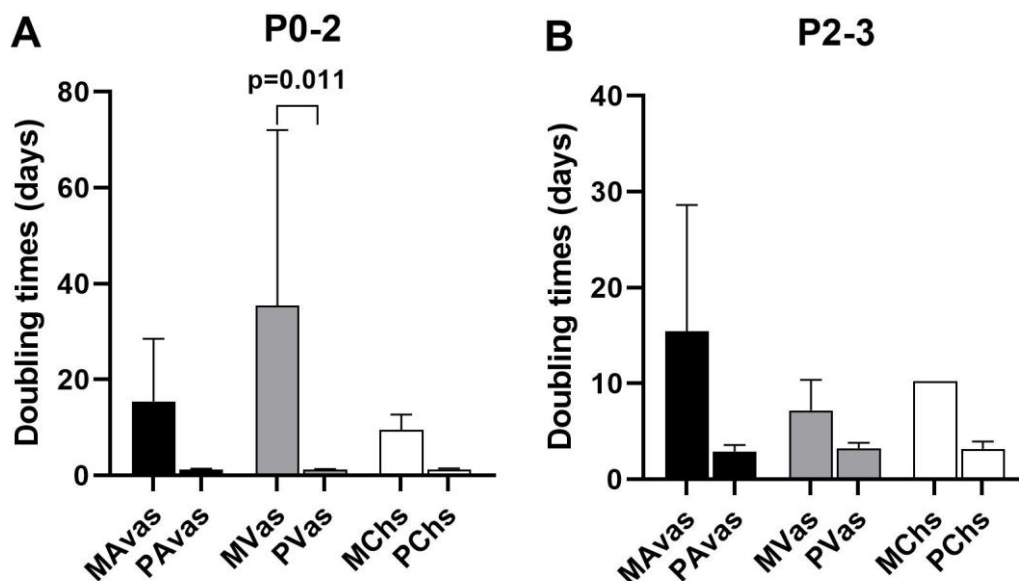


Figure 4.3: Population doubling time (PDT) of progenitor cells

MAVas: mixed avascular meniscal cells, MVas: mixed vascular meniscal cells, MChs: mixed chondrocytes. PAVas: progenitor avascular meniscal cells, PVas: progenitor vascular meniscal cells, PChs: progenitor chondrocytes

4.3.2 Cell-IQ® Analysis

Four of five patients' progenitor colonies of PAVas, PVas and PChs were kept under monitoring for 48 hours in the Cell-IQ® live cell imager. For each progenitor cell type from each patient, two or three colonies were selected for colonies proliferation rate analysis. Figure 4.4 showed the results of individual colony proliferation data. The cell numbers of colonies below 32 cells or doubled after 48 hours in culture was not considered as progenitor colonies. Three of 12 colonies for PAVas, 4 of 11 colonies for PVas, 4 of 10 colonies for PChs were characterised as non-progenitor colonies. After excluding non-progenitor colonies (11 of 33 colonies, 33.3%), proliferation data from progenitor colonies only was compared for PAVas, PVas, PChs fractions (Figure 4.5). The comparison analyses (Table 4.2) showed that PVas colonies proliferated

significantly faster than PAVas ($P=0.0022$) and PChs ($P<0.0001$), whilst the PChs colony proliferation rate was significantly slower than the PAVas colonies ($P=0.0026$).

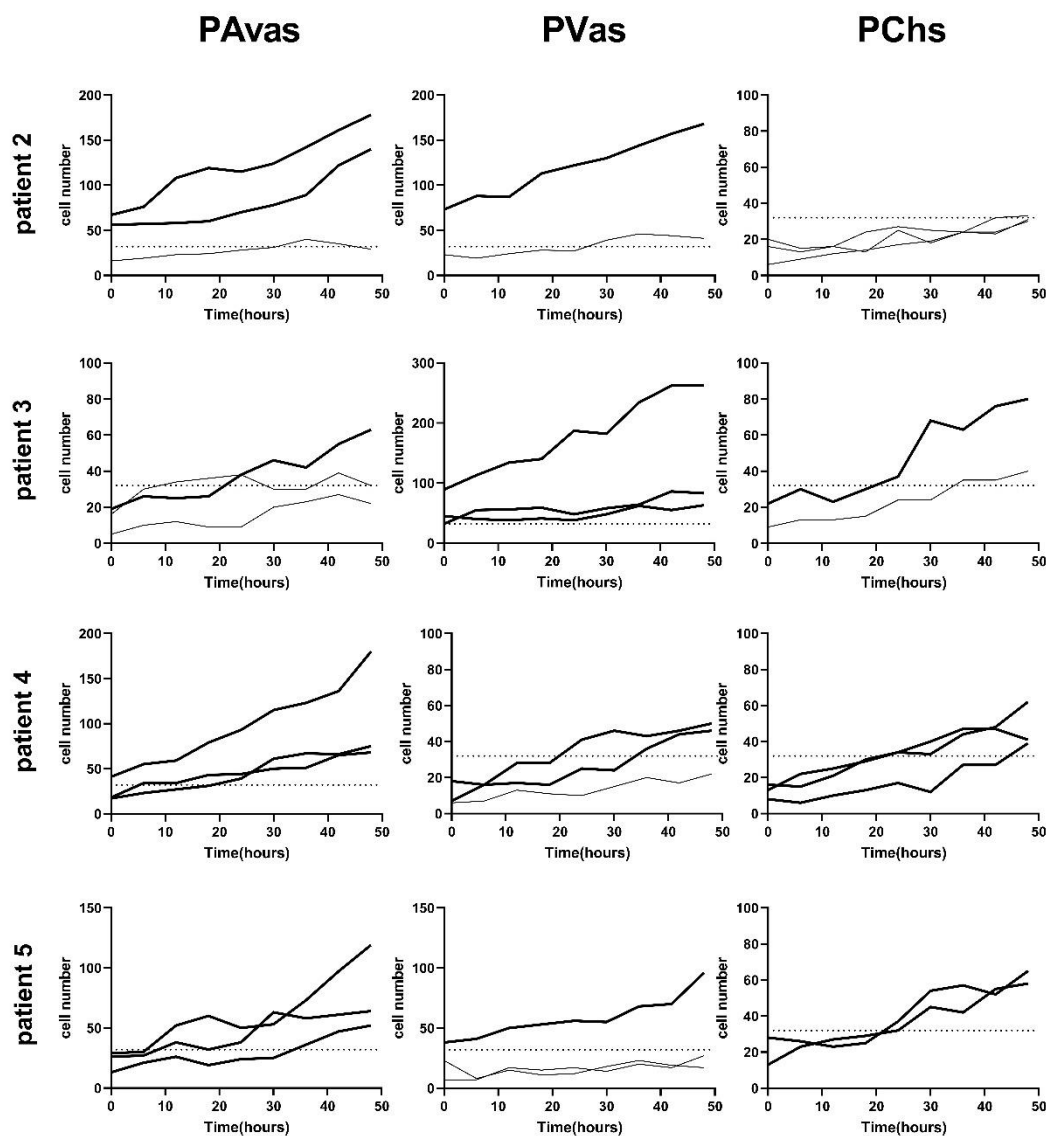


Figure 4.4: Diagram of individual colony proliferation rates over 48 hours in the Cell-IQ®.

Progenitor colonies (cell numbers beyond 32) were highlighted in bold line. The dashed line represents the threshold of minimum cell number as a progenitor colony ($n=32$). PAVas: progenitor avascular meniscal cells, PVas: progenitor vascular meniscal cells, PChs: progenitor chondrocytes

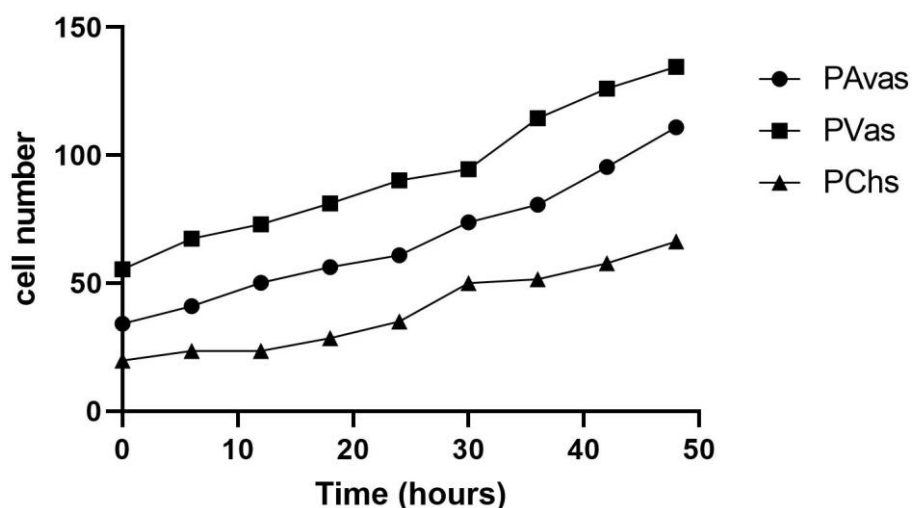


Figure 4.5: The overall comparison of proliferation rate for avascular, vascular meniscal progenitors and chondroprogenitors.

Table 4.2: Tukey's multiple comparisons test

	Predict means, 95% CI	P Value
PAvas vs. PVas	(67.00, 92.98), (-43.83 to -8.127)	0.0022
PAvas vs. PChs	(67.00, 39.53), (8.298 to 46.65)	0.0026
PVas vs. PChs	(92.98, 39.53), (32.45 to 74.45)	<0.0001

PAvas: progenitor avascular meniscal cells, PVas: progenitor vascular meniscal cells,

PChs: progenitor chondrocytes

4.3.3 Cell Surface Markers

Flow cytometry analyses (Figure 4.6) revealed that all cell populations were over 95% positive for the ISCT MSC markers CD73, CD90 and CD105, as well as other markers (CD29 and CD44). CD14 was present on all cell populations, ranging an average from 5.18% to 10.75% positivity. There was no significant difference noted for any of the cell markers examined between mixed population and progenitor cells. However, differences between cell types for integrin markers CD49b, CD49c and the

chondrogenic potency marker CD166 were noted. Progenitor cells showed significantly higher positivity for CD49b compared to their counterpart mixed avascular meniscal fractions ($P<0.0001$), vascular meniscal cells ($P<0.0001$) and chondrocytes ($P<0.0001$). Interestingly, both MAVas and PAVas had significant greater positivity for CD49b compare to MVAs ($P=0.0002$) and PVAs ($P=0.0035$), respectively. Progenitor cells also showed a significantly increased level of CD49c when compared to their paired mixed populations in avascular meniscal ($P=0.0387$), vascular meniscal ($P<0.0001$) and chondrocyte fractions ($P=0.0035$). MAVas also showed significantly higher positivity for CD49c compared to MVAs, whereas no difference was noted in progenitor cell types. For CD166, MChs had a significantly lower positivity compare to MAVas ($P=0.0012$), MVas ($P=0.0144$) and PChs ($P=0.0019$).

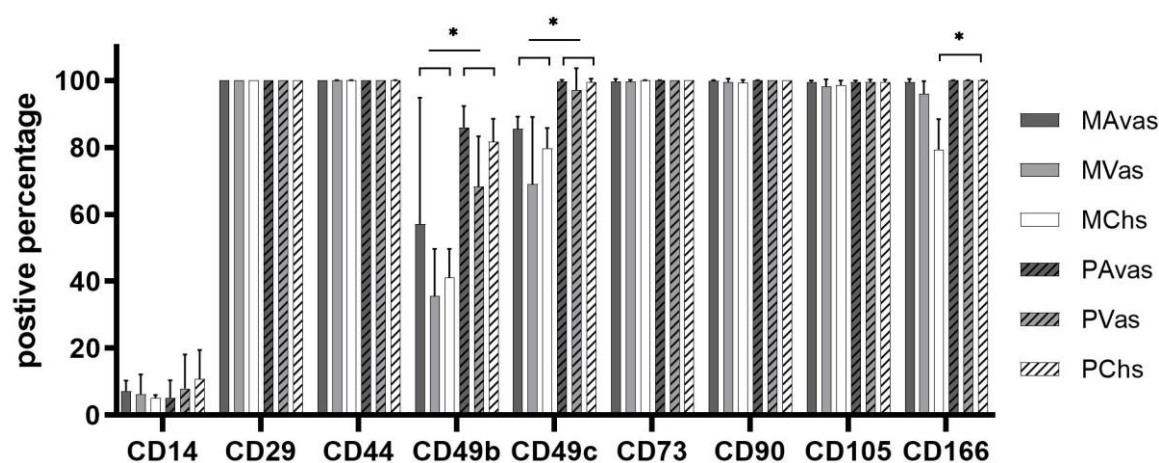


Figure 4.6: Progenitors flow cytometry outcomes

Graphs showing the % immunopositivity of cell surface markers for donor matched mixed or progenitor avascular and vascular meniscal cells and chondrocytes at passage 2-3.

4.3.4 Chondrogenic Gene Expression in Cell Pellets

Figure 4.7 shows relative fold change gene expression levels from 3D pellets of

progenitor cells compared to their mixed population counterparts after 28 days in culture. RT-qPCR analysis of *SOX9* was found to be downregulated in PAVas, PVas and PChs in all five patients compared with mixed population cells, apart from PVas in patient 5. *ACAN* was significantly downregulated in PAVas from patients 1, 4, 5 and in PChs from patient 3, 4, 5. Expression of *COL1A2* was significantly upregulated in PChs from patient 1 and 5 but downregulated in PVas from patient 4 relative to the mixed population cells. *COL2A1* in PVas was significantly downregulated in patient 1 (mean fold change 50 ± 41), patient 4 (mean fold change 5288 ± 3166) and upregulated in patient 2 (mean fold change 7 ± 2) and patient 3 (mean fold change 14 ± 10) compared with PVas. Both PAVas and PChs were significantly downregulated in patient 3-5 compare with MAVas and MChs. Expression of *COL10A1* was found to be downregulated in all three progenitor populations from all five patients relative to their mixed populations, apart from PAVas and PVas which were slightly upregulated in patient 5.

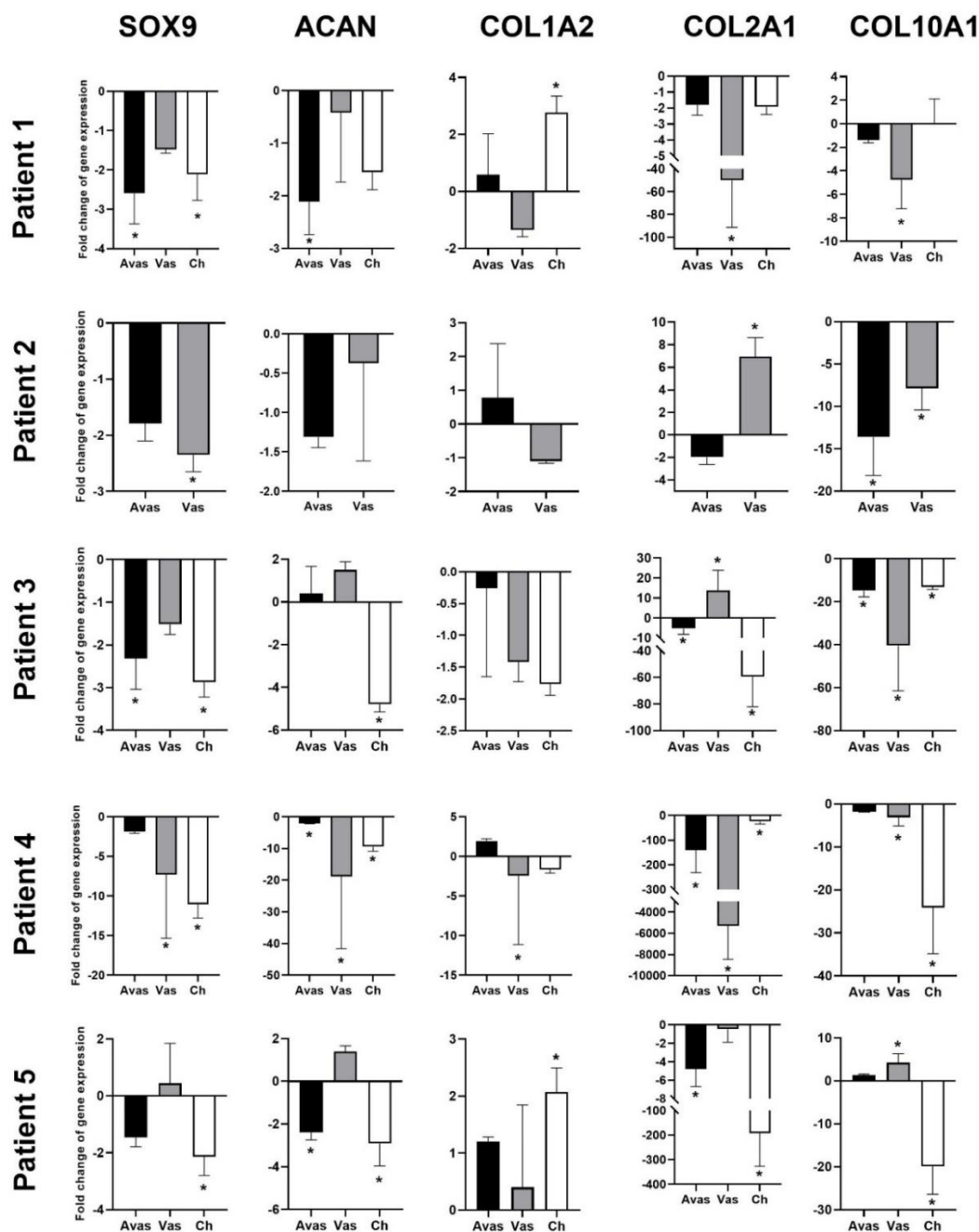


Figure 4.7: RT-qPCR outcomes of progenitor cells.

Graphs showed the genes associated with chondrogenic potency and hypertrophy from 3D pellet culture in mixed or progenitor avascular and vascular meniscal cells and chondrocytes. Gene expression for mixed and progenitor group were normalized to the reference gene GAPDH. Data for progenitor cells are expressed relative to mixed population cells. Significant up- or downregulated genes are indicated with stars.

4.3.5 *In Vitro* Chondrogenic Differentiation Analysis

GAG/DNA analysis (Figure 4.8) demonstrated that progenitor cells generally produced more GAGs than mixed population cells in all three cell types, with significant differences noted only between MVAs and PVas ($P=0.027$). Both MChs and PChs had highest GAGs production across all cell fractions. Progenitor cells formed firmer chondrogenic pellets in terms of their morphology compared with mixed population cells across all three cell types (Figure 4.9). A stronger collagen type I staining trend was observed in all progenitor populations compared with mixed populations without significant difference (Figure 4.10A). A trend for weaker collagen type II staining was detected in all progenitor pellets compared with mixed population pellets (Figure 4.10B), while only MChs pellets were found to be significantly stronger for collagen type II staining compared to PChs pellets ($P=0.0268$).

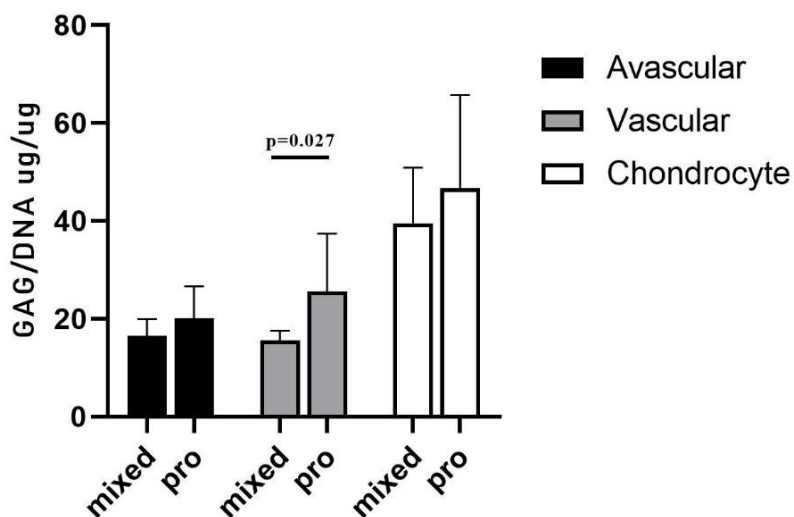


Figure 4.8: GAG/DNA quantitation after 28 days of 3D pellet culture

a comparison of mixed population (mixed) and progenitor (pro) avascular and vascular meniscal cells and chondrocytes from 5 donor matched samples. Error bars indicate the mean \pm SD.

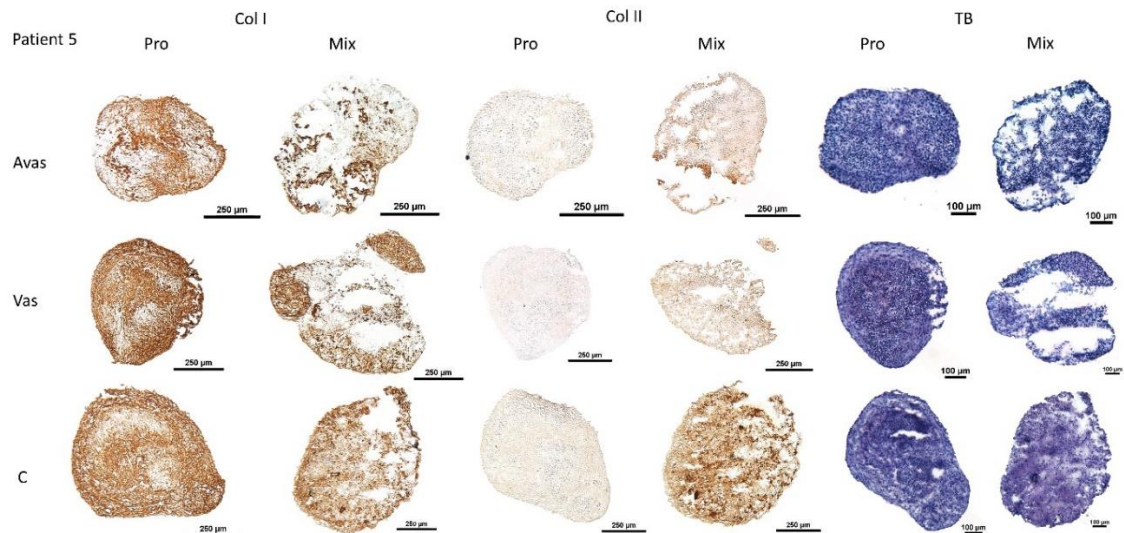


Figure 4.9: Collagen type I and II and toluidine blue staining.

Representative patient 5 chondrogenesis of mixed population and progenitor cells from avascular and vascular meniscus and cartilage, assessed by staining sections using type I and type II collagen by immunohistochemistry.

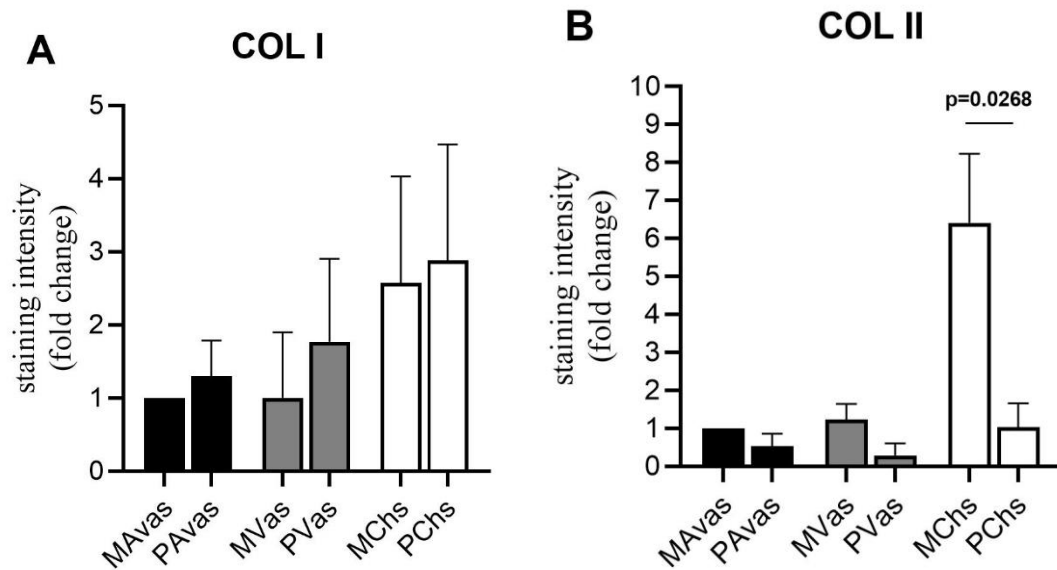


Figure 4.10: Pellets staining intensity

The semi-quantitative IHC analysis of mixed population and progenitor avascular and vascular meniscal cells and chondrocytes in collagen type I (A) and collagen type II, relative fold change to mixed avascular meniscal cells.

4.4 Discussion

Cell-based therapies for meniscus tissue engineering are believed to play a fundamental role in the future meniscus regeneration strategies¹⁸¹. Recent studies have supported the hypothesis that meniscus progenitor cells are the most effective cell type for meniscus regeneration, thought to be due to their tissue specificity and high histocompatibility¹⁷⁷. However, the characteristics of human meniscus progenitor cells including their cell morphology, proliferation rate, surface marker profiles, gene expression and isolation methods have not previously been comprehensively investigated.

Morphologically, primary PAVas and PChs displayed the characteristic cobblestone shaped morphology, whereas PVas had an elongated fibroblast-like morphology. However, in the mixed population, cells presented with more extensive cytoplasmic processes compared to their progenitors. Chondrocytes that displayed cytoplasmic process could be considered to have undergone a hypertrophic change, which is akin to changes observed in late-stage OA cartilage²⁰⁶. Four of the five patient samples used in this study were derived from late-stage OA TKR samples, which might explain this distinct morphological feature noted in the mixed populations. However, the progenitor cells isolated from these OA tissues retained a typical proliferative fibroblastic morphology throughout the culture period assessed.

Clonogenicity is a key feature of all types of stem cells derived from various sources including neural²⁰⁷, hematopoietic²⁰⁸, embryonic stem cells²⁰⁹ and epidermal stem cells²¹⁰. In our study, progenitor cells from vascular meniscus regions were shown to proliferate at a significantly higher rate compared with the mixed population cells at passages 0-2. Cell-IQ[®] live cell imaging analyses of colony forming assays revealed that the PAVas, PVas, PChs isolated using the fibronectin substrate showed a superior

colony forming potential, while the proliferation rate for PVas was significantly higher compared to PAVas and PChs. Seol et al.²⁰² created scratch and punch defects in an explant bovine meniscus, which showed the number of migrated progenitor cells in vascular region was 8.4 times higher than that in avascular region. These results indicated that PAVas, PVas and PChs possess a capacity for self-regeneration and that their endogenous cells display stem-like properties. Our results suggest that vascular meniscal progenitors proliferate faster than avascular meniscal progenitors and chondroprogenitors, which might relate to the higher healing potential observed in the vascular meniscus region¹⁸⁹. However, based on the Cell-IQ[®] live imaging analysis of colony proliferation rates in PAVas, PVas and PChs, not every colony in the fibronectin coated wells showed a superior proliferation capacity. Indeed, 33.3% of colonies were not able to grow beyond 32 cells or doubled after 5 days culture. The cell numbers in these non-progenitor colonies levelled off or even decreased during the 48 hours observed. Possible reasons for the presence of non-progenitor colonies might be that some non-progenitor cells which did not attached to fibronectin remained in the plate wells when media was taken out after 20 minutes. A few more rounds of PBS washing might help to reduce the number of residual non-progenitor cells, but it also poses a risk of washing away any attached progenitor cells. To improve the purity of meniscal progenitor cells in the future, cloning rings could be used to isolate monoclonal progenitor cells¹⁴⁸, although this technique is more cumbersome and doesn't lend itself well to GMP practices for cell therapy manufacture.

Gamer et al.²⁰⁴ reported that progenitor cells migrate from mice meniscus explants and express stem cell markers such as CD44, CD90 and CD73. Shen et al.²¹¹ characterised meniscus stem/progenitor cells by seeding the whole meniscus population at a very low density (300 cells/well) and carried out flow cytometry analysis showed these cells

highly expressed CD44, CD90, CD105, CD166. Our flow cytometry data showed that both whole mixed population and progenitor cells from avascular and vascular regions had high expression levels of CD44, CD73, CD90, CD105, CD166. Thus, these reported progenitor markers might not be specific to meniscus progenitor populations. However, our data supported that progenitor cells had a higher expression of integrin markers including CD49b, CD49c compared to the mixed population from avascular and vascular regions, as well as chondrocytes from donor-matched cartilage. Integrins are cell membrane receptors associated with cell adhesion and recognition that are essential to cell-cell and cell-ECM protein interactions ²¹². CD29 (integrin β 1) is the most abundant integrin expressed by stem cells and chondroprogenitor cells ²¹³. CD105+ BM-MSCs subpopulations with high expression levels of CD29 have been shown to have a superior chondrogenic capacity compared with cells that expression a lower percentage of CD29 ¹⁵⁷. A previous study also demonstrated that BM-MSCs have a high expression level of CD49c ²¹⁴. These findings support our results which indicate that integrin marker expression levels could be used to identify progenitor cells in meniscus tissues. In terms of our flow data the differences between avascular and vascular meniscal cells observed were consistent with the findings in our previous chapter (section 5.3), in that avascular meniscal cells had a higher expression level of the integrin markers CD49b and CD49c compared to vascular meniscal cells from n=10 donor-matched meniscus tissues. The basic principles of the progenitors isolation protocol used in this chapter are based on the selection of cells that highly express β 1 integrins and demonstrate rapid adhesion to ECM proteins¹⁴⁹. Previous studies relevant to meniscal progenitor cells have not reached a consensus on the progenitor cells isolation protocol. Table 4.3 summarizes the meniscus progenitor cells isolation protocols used in previous studies. The table shows that the procedures used vary

widely from FACS sorting, selective adhesion, low seeding, tissue explant isolation etc. all successfully produced colonies. However, which of the protocols produced progenitor cells with a higher colony forming efficiency is unclear.

Table 4.3: Meniscal progenitor cells isolation protocols

Reference	Tissue source	Progenitor cells isolation protocol
Osawa et al. ¹⁸⁹	Meniscus from aborted human foetuses and TKRs	Using FACS to isolate CD34 and CD146 positive meniscal cells after meniscus tissue digestion
Seol et al. ²⁰²	Bovine	Isolate progenitor cells that have migrated into injured sites <i>in vitro</i> , followed by trypsin and collagenase digestion
Shen et al. ²¹¹	Bovine	Meniscal cells were seeded at a very low density to form colonies (300 cells in one 6cm dish)
Gamer et al. ²⁰⁴	Mice	Menisci explant culture: 50 µl essential media for 2 hours for tissue adhesion; 1.5 ml media culture for 3 days with additional 1.5 ml media culture for 5-7 days. Meniscal progenitor cells migrate from explant.
Huang et al. ²⁰³	Rabbit	Suspend digested meniscal cells in stem cell growth media (DMEM, 20% FBS, 100 µl 2-mercaptoethanol, 100 U/ml P/S) to make cell suspension, and culture for 8-10 days to form progenitor colonies.

TKR: total knee replacement; FACS: fluorescence-activated cell sorting

In the chondrogenic analyses undertaken in this study, the immunohistochemistry staining demonstrated that meniscal and chondrocyte progenitor cells were more effective at chondrogenesis compared with the mixed population cells. Type X collagen, a marker of chondrocyte hypertrophy, was found to be highly expressed in

the OA meniscus in a previous study ²¹⁵ and in our work collagen type X gene expression was found to be significantly downregulated in progenitor cells. Together this might indicate that mixed population cells undergo hypertrophic differentiation as part of the progression of OA, whereas their progenitor counterparts do not. In addition, we found that progenitor cells generally produced higher amounts of GAGs compared with mixed population cells in terms of GAG/DNA analyses (significant difference only found between MVas and PVas). These findings suggest that the progenitor population in the meniscus is suitable cell source for use in rebuilding the proteoglycan-rich avascular zone of damaged menisci, which represents key challenge for meniscus repair in the clinic ²⁰¹. Interestingly, we found that the collagen type II staining intensity of PChs was significantly lower than MChs, which matched the gene expression level of collagen type II in PChs chondrogenic pellets, which was significantly down regulated compare with MChs chondrogenic pellets. The downregulation of collagen type II was seen as a sign of chondrocyte dedifferentiation ²¹⁶. Typically, *in vitro* cultured human articular chondrocytes become dedifferentiated and lose their ability to produce hyaline cartilage tissue as their passage number increases ²¹⁷. The dedifferentiation phenomenon of PChs may be caused by the inclusion of FGF2 growth factor in their culture media which is aimed at stimulating the proliferation of progenitor cells. Lee et al. ²¹⁷ cultured costal chondrocytes *in vitro* with or without FGF2 supplementation and demonstrated that the additional of FGF2 accelerated cell expansion and dedifferentiation. However, chondrocytes cultured with FGF2 supplementation showed a better chondrogenic differentiation potential both *in vitro* and *in vivo* compared to chondrocytes cultured without FGF2. Therefore, the addition of FGF2 to culture media may have induced a rapid but reversible dedifferentiation during the *in vitro* expansion phase. Gene expression level of SOX9 and ACAN were

found downregulated in progenitors compared with mixed population cells in most of patients, which may also correlate with the excessive dedifferentiation of progenitor cells. However, no consistent trending was found in the gene expression of collagen type I between progenitors and mixed population, which may be due to the fact of relatively small sample size. This was noted as a limitation in this study.

In conclusion, our study demonstrates that the human meniscus contains meniscal progenitor populations that retains stromal cell-like phenotypes in both the avascular and vascular regions based on clonogenicity and chondrogenic differentiation capacity. Our results also suggested that meniscal progenitors derived from the vascular region of the meniscus exhibit stromal cell characteristics which likely associate with the better meniscal healing potential previously observed in the vascular region. The findings of this study build on the body of evidence which suggests that meniscal progenitors represent an attractive novel cell therapy strategy for the enhancement of meniscal repair and regeneration.

Chapter 5: The influence of fibrin gel on the delivery of autologous meniscal cells in synthetic meniscus scaffold in an ovine meniscus explant model

5.1 Introduction

Partial meniscectomy is the most common procedure to treat an irreparable meniscal tear and quickly relieve a patient's symptoms ²¹⁸. However, knee pain, grinding, clicking and instability are the most common symptoms that develop one year after meniscal surgery ²¹⁸. To pursue a feasible meniscal substitute for a trimmed meniscus, fresh frozen allografts or synthetic meniscus implant such as Actifit[®] or the CMI[®] have been used in the clinic. However, the use of MAT is found to have a high incidence of meniscal graft extrusion without clear evidence of chondroprotective effect ²¹⁹, while both synthetic scaffolds have limitations post-implantation including graft shrinkage, lack of host tissue integration and up to 31.8% failure rate at a mean follow-up of 40 months ⁸⁴. A previous study demonstrated that patients who had a longer time from meniscectomy to meniscal transplantation presented with higher ICRS grades of cartilage damage ²²⁰. The knee joint is already in an early stage of osteoarthritis when meniscal transplantation is considered as a remedial intervention, which could be the main reason leading to graft failure. Therefore, we hypothesise that by performing meniscectomy and filling the gap with a meniscal substitute simultaneously could deliver a better clinical outcome. However, whether to proceed to a meniscectomy or meniscus repair procedure is usually quickly decided by surgeons depending on their experience and also the meniscal tear pattern, assessed during the arthroscopic examination. Thus, meniscal allografts which require matching the donor to the recipient's size and depending on the available resource from a tissue bank are often not suitable in this clinical scenario ²²¹. In addition, the partial synthetic meniscal scaffolds have certain limitations as mentioned above. New meniscus implants are required to withstand the physiological stress, strain and loads that exist within the knee joint. Therefore, the introduction of cell-based meniscal regenerative strategies into

these clinical available scaffolds may overcome these challenges.

Autologous meniscal cells are considered an ideal cell sources to enhance meniscal regeneration ¹⁰⁴, with the major advantage of using in situ derived cells being good histocompatibility ¹⁸¹. Autologous meniscal cells could be isolated from trimming meniscal tissue during a meniscectomy and then reinserted with a carrier back into the patient. To enhance the cell attachment within the scaffolds and to make it easier to manipulate cells during the implantation procedure, a biological cell-delivery vehicle needs to be developed. Fibrin gel is a biocompatible, biodegradable, injectable biomaterial which is generally considered not to be toxic, allergenic or immunogenic ²²². It has been shown to facilitate cell attachment, proliferation, differentiation and tissue formation in a rabbit model of cartilage repair ²²³. Therefore, implanting cells with fibrin glue could induce a synergistic effect for meniscus tissue repair.

The purpose of this chapter was to explore the feasibility of seeding autologous meniscal cells carried by a fibrin gel into the polyurethane scaffold (Actifit[®]) to enhance tissue formation, using an *in vitro* sheep meniscus explant model. We hypothesised that using fibrin gel to deliver autologous meniscal cells combined with the clinical synthetic meniscus scaffold would improve neotissue formation in a meniscal punch defect.

5.2 Experiment design

Fast green dye was mixed with fibrin gel to indicate the fibrin gel distribution within the scaffold as described in chapter 2.9.2. To assess the cell proliferation and viability in the Actifit[®] scaffold with and without fibrin gel, an initial pilot experiment was performed. For this there are three groups, (i) scaffold only (negative control group), (ii) scaffold with chondrocytes (cell group) and (iii) scaffold with chondrocytes

delivered by fibrin gel (fibrin gel group). For the pilot study the constructs were cultured for 14 days, after which cell viability in the scaffold was assessed using a LIVE/DEAD viability/cytotoxicity assay kit and imaged under a confocal microscope as described in chapter 2.9.3. The chondrocytes delivered by fibrin gel using the same protocol were also seeded in CMI® scaffold for 30 minutes and sacrificed for histology analysis to assess the cells distribution within scaffold.

For the main experiment to test our hypothesis that fibrin gel would enhance meniscal cell delivery and function, a sheep meniscus explant model was used for implanting the different groups into, similar to the pilot study but using cells isolated from the avascular region of the meniscus (i) scaffold only, (ii) scaffold with meniscal cells and (iii) scaffold with meniscal cells in fibrin gel. This is shown in Figure 5.1. Five pairs of sheep knee joints (stifle joint) were obtained within 12 hours of sacrifice from animals ranging in age from 11 months to 3 years (Figure 5.2A). Two lateral menisci and two medial menisci were harvested from each sheep (Figure 5.2B), and washed three times with PBS supplemented with 1% P/S. The inner avascular region of each medial menisci was dissected and minced, following by overnight digestion in type II collagenase in serum-free medium at 37 °C. Digested suspensions were passed through a 40µm cell strainer to remove tissue debris and centrifuged at 1000 g for 10 minutes. Avascular meniscal cells were counted with a haemocytometer and trypan blue. Cells were seeded at a density of 5×10^3 cells/ cm² in tissue culture flasks in complete culture media. Cells from the avascular menisci of all five sheep were expanded to passage one prior to seeding into explants.

For all five donors, both lateral menisci were stored at -20°C until cell seeding stage. All menisci were vertically sectioned into quarters. A 3mm core 'defect' was created to simulate a full-thickness tear using a dermal biopsy punch (Figure 5.2C). Subsequently,

samples were incubated in 6 well plates in 3 ml of culture media at 37°C and 5% CO₂. The same size core scaffolds were obtained from the Actifit[®] scaffold and primed in culture media for at least 24 hours on a roller before insertion into meniscus defects. Each of the three groups in the experiment ((i) negative controls, (ii) cells and (iii) fibrin gel) were performed in triplicates for each group). In the cell group, sheep avascular meniscal cells were resuspended in 100µl of media at a concentration of 5 x 10⁶ cells/ml and loaded onto scaffolds. In the fibrin gel group, sheep avascular meniscal cells were resuspended in 75µl of fibrinogen (100mg/ml) at a concentration of 6.7 x 10⁶ cells/ml and injected into the scaffold cores, followed by adding 25µl of thrombin (100U/ml) with 100U/ml aprotinin (A1153, Sigma-Aldrich, UK) supplement. The explant constructs were incubated at 37° C for 30 min to facilitate cellular attachment and polymerisation of the fibrin gel (Figure 5.2D). Subsequently, a further 3 ml of complete culture media was added to all wells. Explants were incubated at 37°C, 5% O₂, and 5% CO₂.

After 28 days of culture, two scaffolds from each group were removed from the meniscal explant. One scaffold was used to extract mRNA and triplicate qRT-PCR tests were performed to assess the gene expression level of collagen type I (COL1A2), collagen type II (COL2A1), aggrecan (ACAN), SOX-9, collagen type X (COL10A1) as described in chapter 4.7. Gene expression level of the fibrin gel group and the cells group were normalised to *GAPDH*, then the relative changes of fibrin gel group to cells group was presented using the comparative threshold method. A 2-fold up- or downregulated change was considered biologically significant. The other scaffold was used to measure the total GAG and DNA content using the DMMB and PicoGreen assay as described in chapter 4.6. Finally, the amount of GAGs were normalised to the corresponding DNA content of the scaffold. The third scaffold and meniscus construct

from each group was fixed and processed for wax embedding and sectioned at 6 μ m thickness (Chapter 2.8.2). Immunohistochemistry staining was performed for collagen type I and II to evaluate the matrix formation (Chapter 2.8.5).

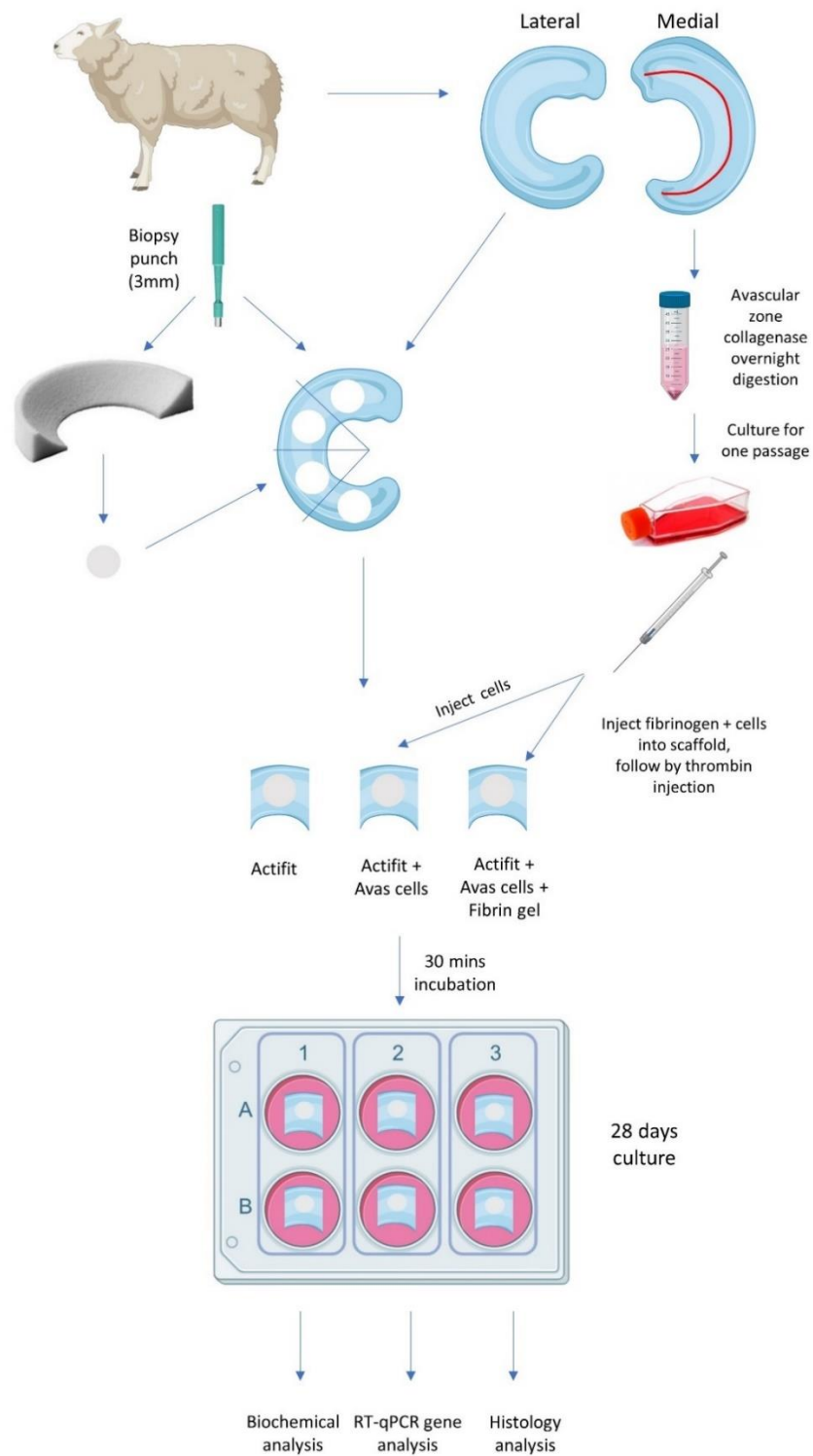


Figure 5.1: Fibrin gel explant experiment workflow diagram.

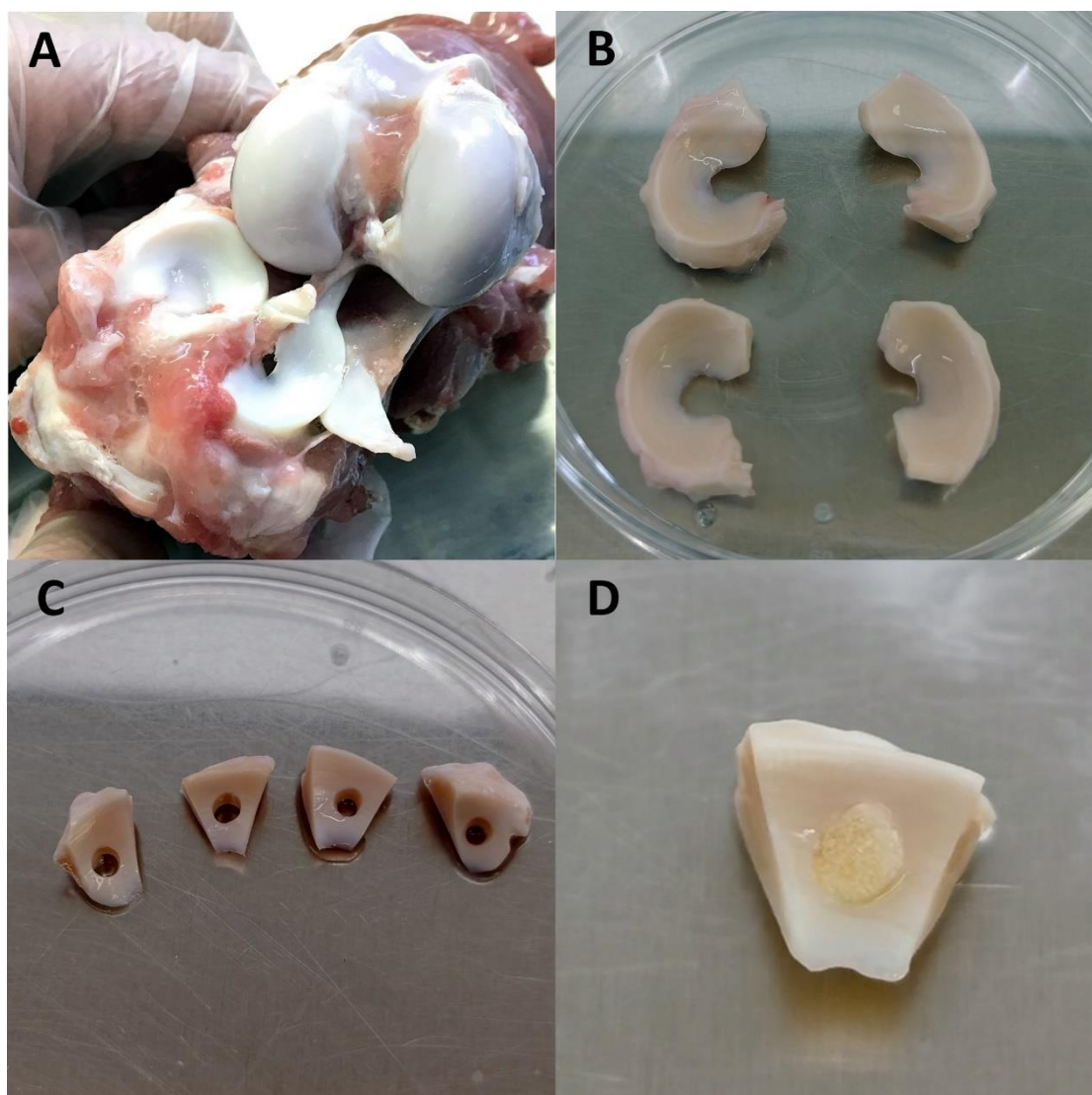


Figure 5.2: Sheep meniscus explant process

(A) Overview of a sheep knee joint (stifle); (B) two pairs of lateral and medial sheep menisci from left and right knees; (C) the lateral meniscus was sectioned into four pieces to create a 3mm diameter punch defect in each; (D) 3mm diameter core of an Actifit[®] scaffold was inserted into the meniscus defect and used for the one of the experimental groups ((i) scaffold only control, or (ii) seeded with cells only or (iii) cells and fibrin gel)

5.3 Results

5.3.1 Fibrin gel distribution and cell viability in the scaffold

After 30 minutes of polymerisation, the Actifit® scaffold was sectioned vertically into halves. The fast green dye indicated that the fibrin gel had penetrated the scaffold throughout, with an even distribution across the whole construct (Figure 5.3). After 14 days in culture, LIVE-DEAD imaging demonstrated that the fibrin gel group had a higher density of chondrocytes in the scaffold compared to the cells alone group, which had lower cell number and diminished viability (Figure 5.4B & Figure 5.4C). Figure 5.5 showed the chondrocytes delivered by fibrin gel in CMI® scaffold evenly distributed with in the scaffold.



Figure 5.3: Fibrin gel penetration test

The fast green dye shows that the fibrin gel had penetrated with complete scaffold within 30 minutes.

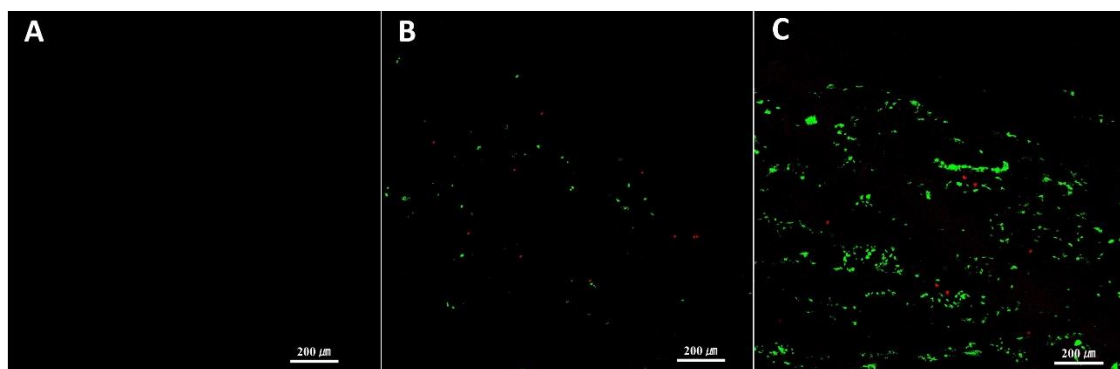


Figure 5.4: Live/dead staining of scaffold

Cell viability demonstrating live cells with green fluorescent staining. No staining was seen in acellular scaffolds (A), some staining was present in the scaffolds seeded with chondrocytes alone (B), but the group that showed the highest number of viable cells retained in the scaffold, was the fibrin seeded scaffolds after 14 days in culture (C). Some red (dead) cells can also be seen in (B) and (C).

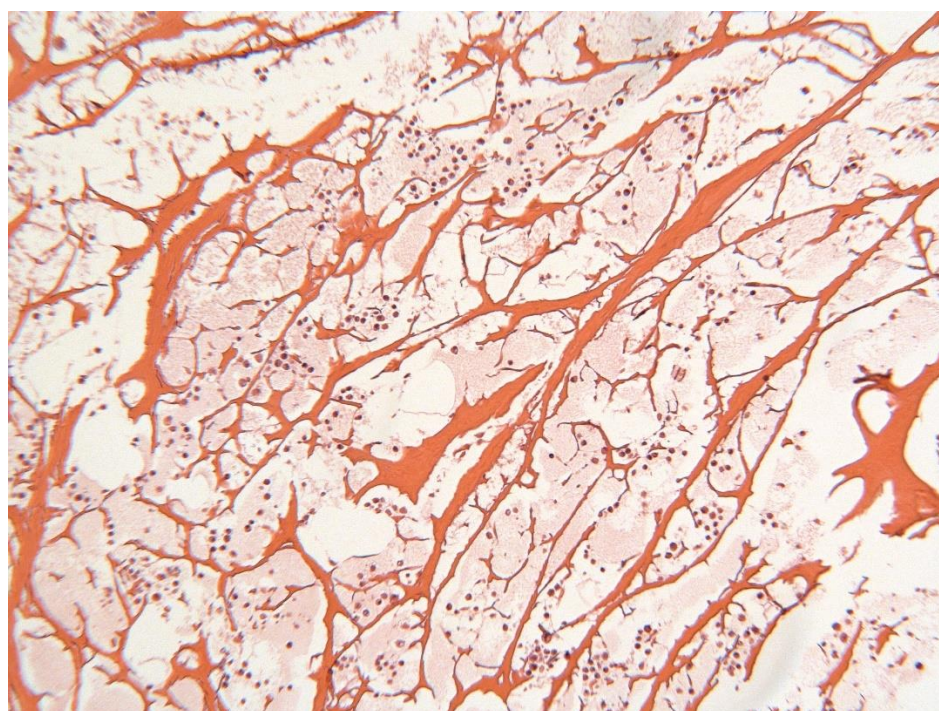


Figure 5.5 Chondrocytes within fibrin gel distribution in CMI® scaffold (H&E staining)

5.3.2 Imaging of cell-seeded scaffolds in the *in vitro* explant model

The ovine meniscal explants with seeded scaffolds were observed and imaged under light microscopy after 14 days and 28 days in culture (Figure 5.6). At day 14, culture expanded avascular meniscal cells were seen mostly growing around the meniscus explant, attached to the tissue culture flask in the cell alone group (Figure 5.6A), whereas cultured avascular meniscal cells were well retained within the fibrin gel seeded scaffold (Figure 5.6B). At day 28, there was no evidence of the meniscus explant tissue attaching to the scaffold (Figure 5.6C). Seeded avascular meniscal cells were seen migrating out of the fibrin gel seeded scaffold onto the tissue culture plastic (Figure 5.6D).

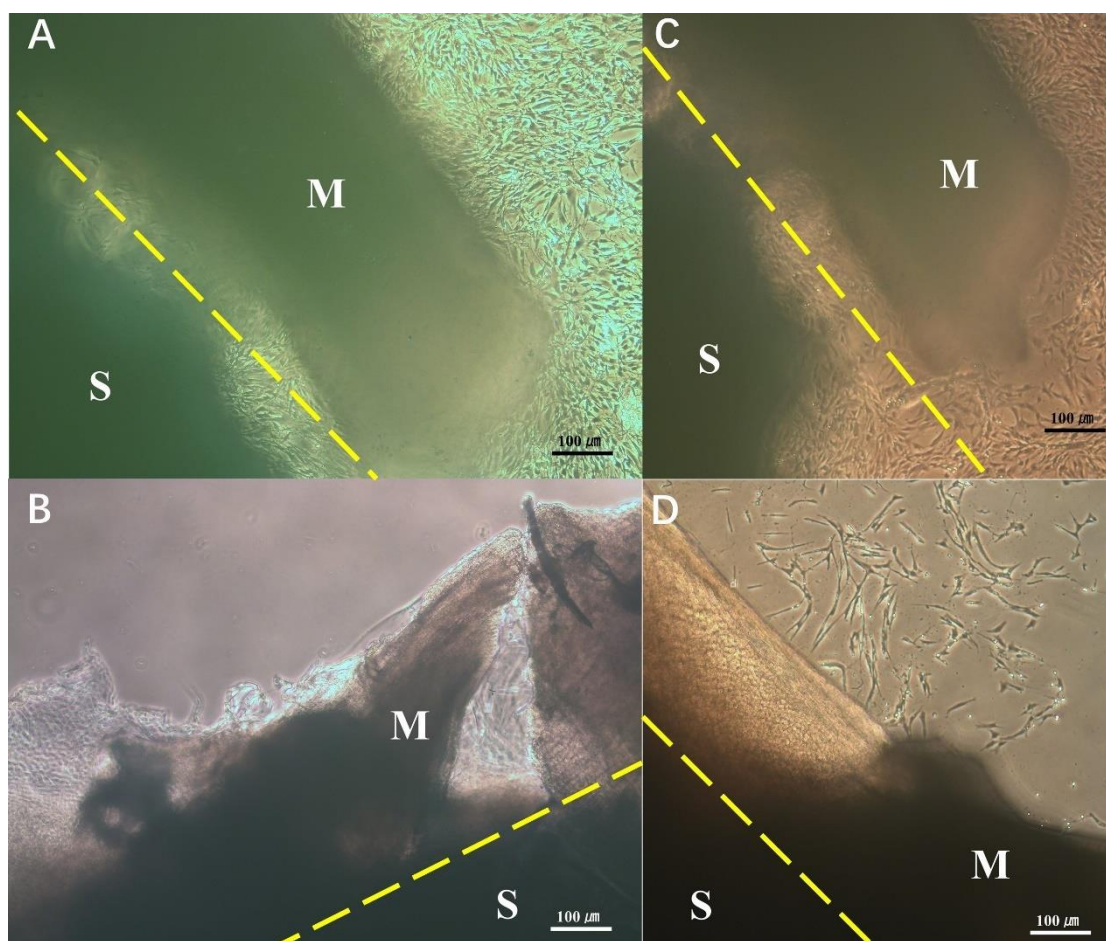


Figure 5.6: Sheep explant culture images

Sheep meniscus explants viewed under a phase contrast light microscope at day 14 (A, B) and day 28 (C, D). Avascular meniscal cells favoured growing on tissue culture plastic in the cell only seeded group (A, C) compared to the fibrin gel seeded group, where the cells appeared generally be retained within the fibrin gel initially (B), before migrating out at day 28 (D). M: meniscus tissue, S: commercial scaffold cores. Yellow dashed line: margin between meniscus and scaffold

5.3.3 Gene expression of meniscal cells in the meniscus explant model

After 28 days, RT-qPCR analysis of RNA extracted from the meniscus explant cultures was performed. Figure 5.7 shows the gene expression of the fibrin gel group relative to that of the cell group. The levels of gene expression for SOX 9 and collagen type X

were significantly upregulated in sheep 1, 2 and 4, but downregulated in sheep 3. The expression level of aggrecan significantly downregulated in sheep 1 and upregulated in sheep 2. Levels of expression for collagen type I were significantly upregulated in sheep 3 and downregulated in sheep 4, while the levels of collagen type II were significantly upregulated in sheep 1 and 3.

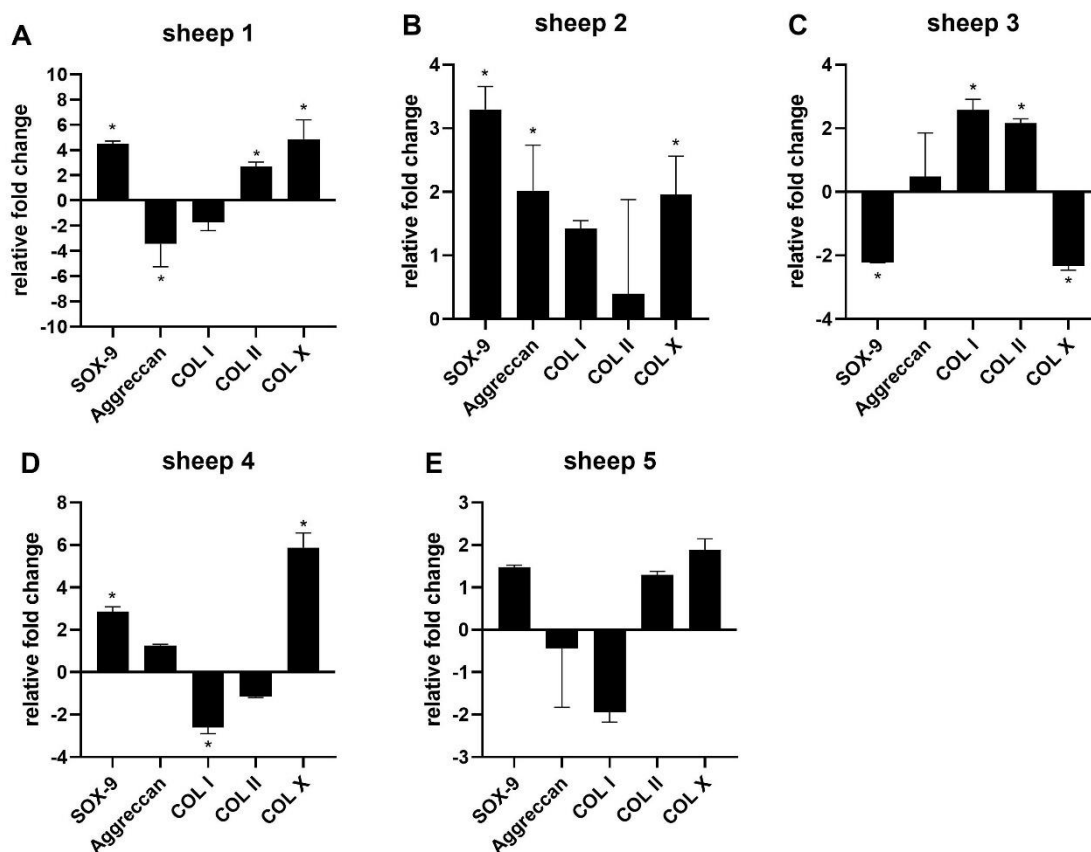


Figure 5.7: Gene expression profiles of extracted mRNA in cell only group and fibrin gel seeded scaffold in the meniscus explant model.

Data shown are the expression levels of the fibrin seeded group expressed relative to cell only seeded group.

5.3.4 Matrix formation assessments in the sheep meniscus explant model

After 28 days in culture, the total GAG and DNA production in the scaffolds were measured in the 3 groups (acellular, cell only and fibrin gel seeded scaffolds). The total

amount of GAGs in the group fibrin gel seeded group were twofold higher than cell only group ($p<0.001$) and eightfold higher than the acellular group ($p<0.001$) (Figure 5.8A). The total DNA was also highest in the fibrin seeded group, being significantly higher than both the cell only and acellular group ($p<0.001$) (Figure 5.8B). Avascular meniscal cells delivered by fibrin gel had a higher production of GAGs compared to those in the cell only group, in which cells were applied directly to the scaffold without a carrier, in terms of GAG/DNA ($p=0.0085$) (Figure 5.8C). Additionally, the evaluation of collagen type I deposition via immunochemistry demonstrated more matrix formation in the fibrin gel seeded scaffolds (Figure 5.9 E&F) compared to the cell only group (Figure 5.9 C&D), with no staining present in the acellular negative control (Figure 5.9 A&B).

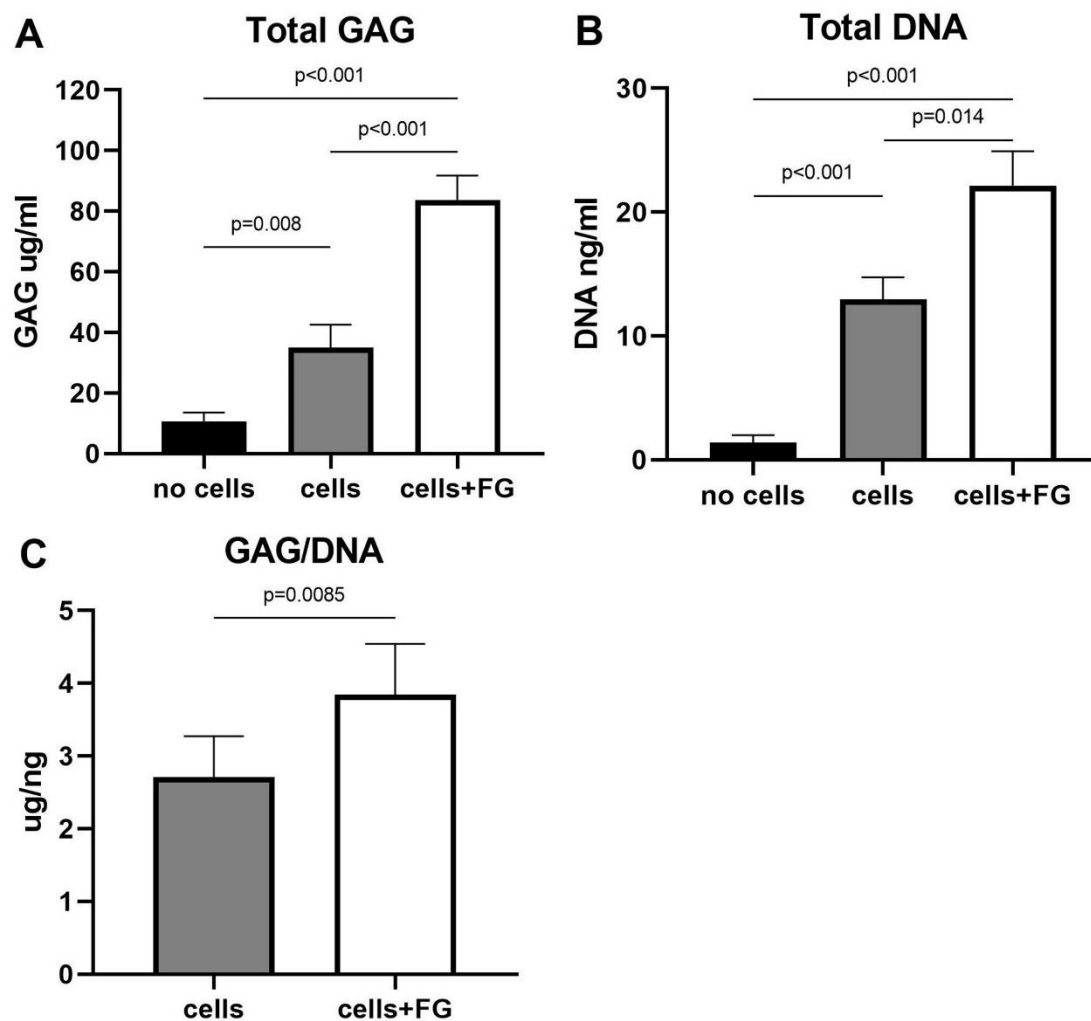


Figure 5.8: Biochemical component analysis of sheep explant models

Quantitation of GAG (A), DNA (B) and GAG/DNA (C) in explant cultures of no cell, cell only and cells and fibrin gel groups after 28 days in culture (n=5).

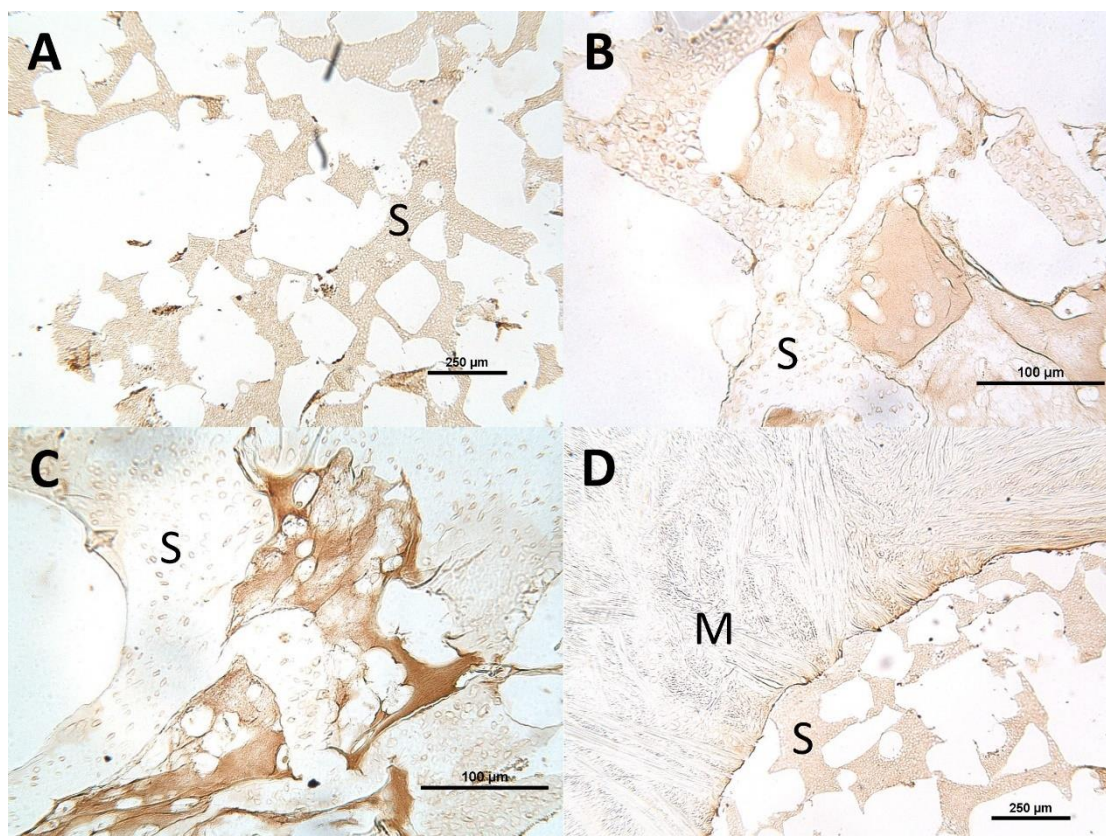


Figure 5.9: Immunohistochemistry staining of collagen type I in explants and scaffolds.

(A) Acellular negative control sample showed no matrix formation within scaffold; Cell only group (B) showed less collagen formation within scaffold compare to fibrin gel seeded group (C); (D) IgG negative control staining; S: Actifit[®] scaffold, M: sheep meniscus tissue.

5.4 Discussion

The goal of this *in vitro* study was to assess the feasibility of delivering autologous meniscal cells together with a fibrin gel carrier to enhance meniscus regeneration for partial meniscus replacement. The study firstly examined the cell distribution and viability with or without fibrin gel delivery in the polyurethane scaffold. Contiguously, we used a sheep meniscus explant model to assess cell seeded scaffold matrix formation in autologous meniscal cell seeded scaffolds with or without fibrin gel as a carrier. Many of findings suggest that fibrin gel could be used as a cell delivery vehicle in meniscus scaffolds as a treatment strategy that could be applicable for use in the clinic for promoting meniscus regeneration.

Whilst the Actifit[®] meniscal implant is used clinically and provides relief of symptoms and benefit for 87.6% patients, it is not usually a permanent solution and pain and disability commonly return within years post-treatment²²⁴. If this scaffold could be successfully populated with cells, they may be able to ensure longer or perhaps even a permanent benefit to patients. Actifit[®] is a PU and PCL based scaffold previous studies have demonstrated that PU by itself is a poor substrate for cells to adhere to²²⁵. Fibrin gel as a biopolymeric material provides various advantages including excellent biocompatibility, promoting cells attachment, degrading in a controllable way and is commonly used clinically²²⁶. Scotti et al.¹³¹ bonded two swine meniscal slices with chondrocyte in a fibrin gel hydrogel and implanted it in a nude mouse model for 4 weeks. They found a firm bonding at the interface with new fibrocartilaginous tissue formation. Our pilot experiment with LIVE-DEAD imaging of the cell group and fibrin gel group demonstrated that delivering cells within a fibrin gel resulted in significantly more live cells being retained within the PU scaffold. Imaging of the meniscus explants also demonstrated that the seeded cells were retained in the scaffolds with fibrin gel

carrier before day 13 and gradually migrated out from fibrin gel up to day 28. Therefore, fibrin gel fulfils the objective of retaining cells implanted within scaffold; this is likely to be important in the clinical scenario where it would keep the cells in position allowing them to maximise the cells function for meniscus tissue regeneration. In addition, fibrin gel as a cell carrier could also improve the implanted cell integration to the host tissue. Previous study has demonstrated that chondrocytes delivered by fibrin gel into a porous poly(vinyl alcohol) hydrogel (PVA-H) significantly enhanced the integration strength of three-layered constructs (PVA-H between devitalized cartilage)²²⁷. However, we didn't compare the integration strength between fibrin gel group and cells groups in our study. A push out mechanical test could be implemented in the future study.

The varies gene expression level in fibrin gel groups compare to cell groups in different donors were noted in our results. Only SOX-9 showed a consistent upregulation in most donors in fibrin gel group. One of the possible reasons may be due to the wide range of donor age (11 month – 3 years old). Clark et al.²²⁸ reported the large diversity of gene expression level in different developmental stages in the domestic sheep. We will select the similar age donor for the future study to have comparable results. This was also noted as a limitation of the study.

Improved matrix-forming capacity of cells implanted within fibrin gel was also indicated, with higher levels of GAGs measured within the polyurethane scaffold loaded with fibrin gel compared to when cells were applied alone. In addition, the higher DNA content in the fibrin gel group proved that this delivery system promoted increased meniscal cell proliferation, whilst the higher GAG/DNA ratio demonstrated that individual cells contributed greater matrix production when delivered in fibrin. On the contrast, the cell group showed significant lower GAG and DNA production

compared with fibrin gel group. Our observation during the explant culture demonstrated that the majority of seeded cells adhered to culture flask instead of the scaffold. Tarafder et al.²²⁹ demonstrated that without the growth factors stimulation in meniscus explant defect site, no migrated synovial MSCs seeded underneath explant could migrate into injury site. Therefore, in our experiment, the exceeded cells growing on the flask unlikely contribute to the matrix production in cells group as previous study. Pawelec et al.²³⁰ seeded ovine meniscal cells into aligned or isotropic collagen type I scaffold with or without fibrin gel delivery. This study showed a similar increase in cell metabolism and cell proliferation in aligned collagen scaffolds when the cells were delivered with fibrin. They also reported on the proliferation of cells within the fibrin gel alone, which didn't show the encouragement of high proliferation or metabolic activity over three weeks which probably due to the early dissolution of fibrin gel²³⁰. In our experiment, we mixed thrombin with aprotinin which could significantly reduce fibrin degradation²³¹. Aprotinin is a serine protease inhibitor to prohibit fibrinolysis by blocking plasmin formation²³². Aprotinin is also a key component of a clinically approved fibrin sealants (TISSEEL, Baxter, Deerfield, IL) which has been widely used in the cell therapy for cartilage repair (ACI)^{233,234}.

The current experiment proved the feasibility of using autologous avascular meniscal cells in an ovine explant model. In the clinic these autologous meniscal cells could be derived from discarded meniscus tissue of patients undergoing partial meniscectomy. One of the major controversies of using autologous meniscal cells for cell-based meniscal therapy is donor site mobility¹⁰⁴. Unlike in ACI, where a biopsy of 'healthy' cartilage is harvested to source the chondrocytes, the rim of meniscus is, which the ideal source of meniscal cells is essential for meniscus replacement suturing²³⁵. However, by performing meniscectomy and cell-based meniscal transplantation simultaneously,

the trimmed meniscus tissue, which is usually from the avascular region, can be used as is an ideal cell source to obtain autologous avascular meniscal cells. Jiang et al.²³⁶ showed that immediate MAT after meniscectomy led to more satisfactory subjective outcomes, including less joint degeneration and less muscle strength deficits compared to delayed MAT (average 35 months after meniscectomy) with 4-6 year follow-up. This combined procedure fills the time gap usually experienced between meniscectomy and meniscus transplantation, during which many patients develop further pain and return for further treatment.

There remain many further questions to answer, for example, what number of meniscus cells will be required? If more are needed than the number obtainable from discarded tissue is not sufficient, coculture with other cell populations could be a possibility. Coculture of primary meniscal cells with BM-MSCs has been considered as a strategy to maintain the differentiated phenotype of primary meniscal cells with the additional benefit that MSCs may contribute to produce functional matrix components of the meniscus and downregulate hypertrophic differentiation of MSCs^{118,237}. A recent clinical study has shown the safety and feasibility of using a combination of chondrons with allogeneic BM-MSCs for cartilage repair²³⁸. Hagmeijer et al.²³⁹ co-cultured human meniscal cells and BM-MSCs in different ratios in pellets with a type I collagen hydrogels. They reported that coculturing 20% meniscal cells and 80% MSCs produced the highest GAGs and collagen content.

A one-stage procedure for meniscus cell therapy would be cost effective and a lower patient burden. To achieve that, a rapid digestion of meniscus tissue during the surgical procedure is required. Numpaisal et al.²⁴⁰ rapidly dissociated bovine meniscus tissue with different concentration collagenase type II for 30 mins and then fragmented with a tissue pulveriser followed by another 30 mins digestion of the same concentration of

collagenase. Their results suggested that 0.2% (w/v) rapidly digested cells had highest cellular metabolism up to day 7. This finding could be combined with the *in vitro* results in this chapter, allowing the design of a more strategic experiment in the future which could use fibrin gel to deliver a mixture of rapidly digested meniscal cells and BM-MSCs to the PU scaffold for a one-stage cell-based therapy for meniscal regeneration.

In the current study, histological processing of the Actifit[®] scaffold was problematic. Our histopathology laboratory regularly uses xylene in processing the tissue ready for wax embedding and it also uses it to deparaffinise wax sections. However, when we used xylene to prepare the Actifit[®] scaffold in an automated processor, the scaffold was severely affected and appeared with holes and cracks when embedded in paraffin. The reason for this may reflect Actifit[®] composition of 20% PU and 80% PCL which could be dissolved in the xylene and subsequently cause the collapse of the scaffold during the vacuum phase used in the embedding process ²⁴¹. The cracks surrounding the scaffold in the paraffin wax was caused by the incomplete dehydration of water and penetration of paraffin probably due to the hydrophobic property of the polymer material. To overcome these difficulties, we carefully transferred the samples between xylene and IPA to maintain the structure before wax embedding. In addition, we increased the dehydration time in IPA to completely remove the water content and the time emerged in paraffin to encourage the thorough penetration of the scaffold. Another issue we found was that the Actifit[®] scaffold peeled off the slides when dewaxing in xylene. To address this issue, we used Histo-Clear II (aliphatic hydrocarbons and d-limonene) which is less brittle, non-toxic and non-volatile as a xylene substitute ¹⁰¹. Cryosectioning was also attempted for the Actifit[®] scaffold. However, the scaffold shattered during cryosectioning.

In conclusion, in this study we proved the feasibility of using fibrin gel to deliver

autologous avascular meniscal cells in a clinical grade meniscus substitute *in vitro*. Cells delivered by fibrin gel showed an increased cell proliferation and more matrix production within the scaffold compared to cells directly seeded into the scaffold in the absence of fibrin. The results of these experiments represent the foundation of this approach of augmenting the benefit of a commercially available meniscal implant with the addition of a cellular component; this biological approach may to increase the longevity of the initial benefit gained from the scaffold alone if it contributes to the biological integrity of the meniscal scaffold.

**Chapter 6: Concomitant autologous
chondrocyte implantation with synthetic
meniscus scaffold or allograft
transplantation: Mid to long term follow up**

6.1 Introduction

Meniscal and chondral lesions are common consequences of acute or chronic musculoskeletal trauma²⁴². These injuries often lead to joint pain and instability, which can trigger the early onset of knee OA. In addition, patients with combined meniscal and chondral lesions have shown an increased risk of developing knee OA compared to patients with a single tissue pathology²⁴³. The most widely used treatments for patients who present with meniscus deficiency and unicompartment arthritis include osteotomy, unicondyle or total knee replacement²⁴⁴.

Meniscus allograft transplantation (MAT) has shown promising results in the treatment of patients who had partial or complete meniscectomy and has been suggested to delay articular cartilage degeneration in a mean of 12.3 years follow-up study²⁴⁵. An alternative procedure to manage pain developed after partial meniscectomy, restore knee biomechanics and delay the onset of OA is the use of a polyurethane (Actifit®) or collagen (CMI®) meniscal substitute, which can be implanted arthroscopically⁸⁴. ACI has been used at our centre for over 20 years and in over 500 patients for the treatment of knee cartilage injuries and early OA. We have previously reported the mid-term to long-term outcome of ACI²⁴⁶, showing that knee function rapidly improves over the first 15 months, after which functionality remained constant for up to 9 years. More recently, others have shown ACI survival rates of 78% at mid-term and 51% beyond ten years following ACI²⁴⁷.

Untreated cartilage defects can lead to excessive loading of meniscus implants, which is frequently responsible for early meniscus graft failure²²⁰. We hypothesise that performing a multi-faceted surgical/biological treatment by combining either MAT or meniscus substitute implantation with ACI could slow the progression of OA without limiting the option for arthroplasty in the future. There are two previous studies that

have presented the short to midterm follow up data on patients who have undergone combined MAT and ACI procedures^{248,249}. Farr et al²⁴⁸ reported 36 patients with four failures at a minimum of 2 years follow up, while Ogura et al²⁴⁹ presented 18 patients with six failures at an average of 7.9 years follow-up. Both studies demonstrated a significant improvement in both symptoms and knee function. However, to the best of our knowledge, no study has reported any clinical outcome on the combined treatment of partial meniscus implantation with concomitant ACI.

Our group has previously reported a small pilot study of eight patients treated with a combination of MAT and ACI with an average of 3 years follow-up²⁵⁰. Longer-term follow-up is needed to determine the full potential of this technique. This study therefore aims to present the mid to long-term follow-up on these first eight and subsequent cases, as well as investigating patients who have received concurrent ACI and a polyurethane partial meniscus replacement.

6.2 Methods and Materials

6.2.1 Patient Information

We reviewed the data from all patients who had undergone ACI with MAT (20 patients) or a polyurethane meniscus scaffold implantation (8 patients, Actifit[®], Orteq Ltd, London, UK) between 1999 and 2018 (Table 6.1). Patients with less than 2 years follow-up were excluded. All patients provided informed consent before surgery. All patients consented to an ethically approved project (REACT 09/H1203/90, approved by South Staffordshire Local Research Ethics Committee, UK).

6.2.2 Surgical Techniques

The procedure was performed in two-stages. In the first stage, the partial or complete absence of a meniscus and the presence of cartilage lesions were confirmed. A cartilage harvest for ACI was obtained from the femoral trochlea, which was transported to our MHRA (Medicines and Healthcare Products Regulatory Agency)-licensed GMP manufacturing facility. Chondrocytes were isolated and expanded *in vitro* to a second/third passage as previously described¹⁴⁷.

In the second stage, an arthrotomy was performed via either a medial or a lateral parapatellar incision depending on the compartment involved. Chondral defects were trimmed to stable edges and covered with periosteum or by a resorbable porcine collagen membrane (Chondro-Gide[®]-Geistlich Pharma AG, Division Biomaterials, Switzerland). The patches were sutured onto the peripheral cartilage and sealed with fibrin glue (Tisseel, Immuno AG, Vienna, Austria). The cultured autologous chondrocytes were injected beneath the patch in a suspension of the patient's own serum.

For allograft transplantation procedures, prior to 2012, conventional open arthrotomy

was performed and an allogeneic cryopreserved meniscus with small bone plugs at either end was placed on top of the tibia and secured by sutures in the bone tunnels. Further sutures were used to secure the allograft to the capsule laterally in order to hold the allograft in the load-bearing position²⁵⁰. From 2012 on, the allograft transplantation was performed using an arthroscopic technique. For medial meniscal transplant, the anterior and posterior horn of allograft was fixed through the tibial tunnel. For lateral meniscal transplant, the central roots were arthroscopically secured with a dovetail bone technique, while the body of the meniscus for both were fixed to the capsule with a combination of all inside, inside-out and outside-in sutures.

For Actifit[®] scaffold implantation, all procedures were performed arthroscopically prior to open arthrotomy for ACI. Briefly, the residual meniscus was debrided while the peripheral rim was preserved. Following the measurement of the meniscus defect, the Actifit[®] scaffold was shaped to the required size + 10% and secured with a combination of meniscal repair kit (FasT-FixZR[®], Smith&Nephew, Andover, USA) and inside-out and outside-in sutures.

The size and site of the treated concomitant cartilage defect was documented using the validated Oswestry Knee Map²⁵¹. The OsCell Rehabilitation protocol for the ACI procedure was followed post-operatively, limiting knee flexion to 45° for three weeks and allowing full weight bearing after 12 weeks²⁵².

6.2.3 Outcome Assessments

All patients were evaluated pre-operatively and post-operatively with a modified Lysholm score (range 0-100 where 0 is worst and 100 best) (appendix IV)²⁵³. Scores were collected at yearly intervals post-operatively during an outpatient follow-up or by a postal questionnaire. The overall survival rate of the two groups of patients was evaluated using the Kaplan-Meier method with failure as the endpoint. Failure was

defined as ACI and/or MAT graft failure with revision of either cartilage repair or MAT or total knee arthroplasty. Patients also answered a question regarding their one-year satisfaction score with the procedure (1-4, 1 poor, 4 satisfied).

Post-operative MRI scans were evaluated by a musculoskeletal radiologist. A previously validated measurement was used to assess the relative meniscal extrusion (rME), coronal cartilage coverage index (cCCI) and sagittal cartilage coverage index (SCCI)²⁵⁴. Briefly, the absolute meniscal extrusion (aME) was measured on the coronal plane through the centre of the tibiofemoral joint, as the distance from the meniscal margin to tibial margin, excluding any osteophytes (Figure 6.1A). On the same view, the rME was calculated as the ratio of aME over total meniscus width. On the sagittal view through the centre of the tibiofemoral compartment, the extrusions of the anterior and posterior meniscal horns were also measured (Figure 6.1B). On the same sagittal and coronal views, CCCI and SCCI were measured as the percentage of tibial cartilage covered by the graft.

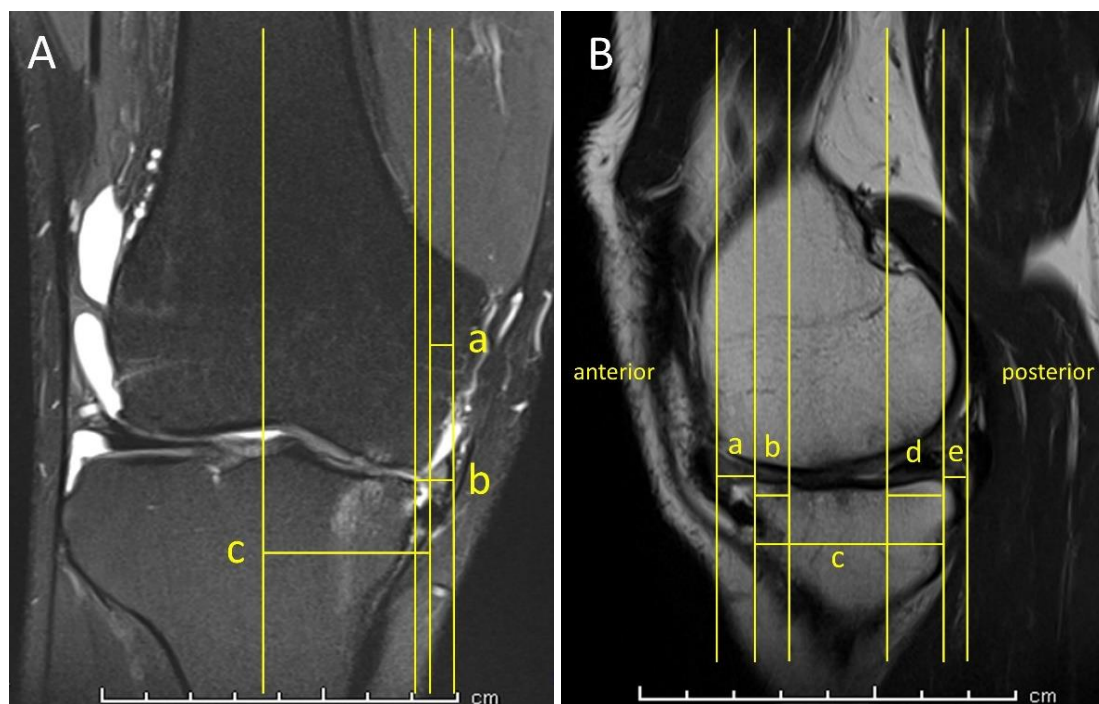


Figure 6.1: Illustration of meniscus extrusion measurement.

(A) Measurements of absolute meniscal graft extrusion (aME) in the coronal plane (a), meniscus graft width (b), coronal width of tibia plateau (c); relative meniscal extrusion (rME) = a/b , coronal cartilage coverage index (cCCI) = $[b-a]/c$. (B) measurement of extrusion (a, e) and non-extrusion (b, d) of anterior and posterior meniscus graft, sagittal width of tibia plateau (c); sagittal cartilage coverage index (sCCI) = $[b+d]/c$.

Biopsies of meniscus were taken at arthroscopy using a Jamshedi juvenile bone marrow biopsy needle (1.8mm diameter), with a video recording of the procedure for 13 out of 20 patients in the MAT treated group between 12 and 24 months postoperatively. A full-depth cartilage biopsy was taken through to the subchondral bone, where possible. Meniscus biopsies were taken radially in the horizontal plane from the outer surface to the centre. Samples were snap frozen in liquid nitrogen-cooled hexane and cryosectioned (7 μ m) and stained with H&E and TB or safranin O & fast green to assess general morphology and proteoglycan content respectively as described previously²⁵⁵.

6.2.4 Statistical Analysis

Mann-Whitney U tests and unpaired Students t tests were used to compare the age, BMI, length of follow-up, rME, cCCI and sCCI of the two groups. One-way ANOVAs were used to compare the improvement in Lysholm scores with time. Kaplan-Meier survival curves were used for survival analyses. A multilevel model was used to estimate mean Lysholm scores for the two groups at 2-, 5- and 10-year follow up. For this model, treatment group and preoperative Lysholm scores were considered as fixed effects and patients as random effects. GraphPad Prism (Version 8.30, San Diego, USA) was used for all statistical analyses other than the multilevel model, for which we used R vs 4.0.2 (R Foundation for Statistical Computing, Vienna, Austria) and the packages nlme and Emmeans. For all statistical tests, a two-tailed p -value below 0.05 was considered statistically significant.

6.3 Results

6.3.1 Patient Demographics

The MAT group comprised 17 males and 3 females (5 medial, 15 lateral) with a mean age at surgery of 40.2 ± 9.0 years (range, 28-58 years). The Actifit[®] group had 7 males and 1 female (4 medial, 4 lateral) with a mean age at surgery of 42 years (range, 31-65 years) (Table 6.1). The mean follow-up for the MAT and Actifit[®] groups was 7.94 years (range, 2-20 years) and 7.2 years (range, 2-10 years), respectively. No significant difference was found in Body Mass Index (BMI) between the two groups ($p=0.058$).

There were 11 patients in the MAT group and three patients in the Actifit[®] group who had bipolar (kissing) lesions. In the MAT group, the mean size of the femoral defects was 6.6 cm^2 (range, 1-12.3 cm^2) and on the tibia was 5.7 cm^2 (range, 1.1-10.5 cm^2). In the Actifit[®] group, the mean size of femoral defects was 2.7 cm^2 (range, 0.25-8 cm^2) and on the tibia was 6.6 cm^2 (range, 0.5-12 cm^2).

Table 6.1: Patient Demographics

	MAT	Actifit [®]
Age at surgery, y, mean \pm SD	40.2 ± 9.0	42.0 ± 11.0
Sex: male/female, n	17/3	7/1
Right/left knee, n	16/4	5/3
Body mass index, kg/m^2 , mean \pm SD (range)	29.4 ± 5.2 (22.3 – 45.6)	25.7 ± 2.8 (22.4 - 30.5)
Follow-up, years, mean \pm SD	7.9 ± 6.1	7.2 ± 3.5
Unipolar / Bipolar cartilage lesion, n	9/11	5/3
Cartilage lesion size, cm^2 , mean \pm SD	6.3 ± 3.3	4.1 ± 5.1
Meniscus lesion location, medial/lateral, n	6/14	4/4
Patch used	5 Periosteum 15 Chondrogide	8 Chondrogide

6.3.2 Concomitant and Subsequent Surgical Procedures

Three patients in the MAT group had concomitant procedures (3 osteotomy) and two patients in the Actifit[®] group (2 osteotomy, 1 ACL reconstruction) at the same time as ACI and meniscal replacement. Eleven of the 20 patients (55%) in the MAT group and 1 of the 8 patients in the Actifit[®] group (12%) required subsequent surgical procedures (43% in total), including osteotomy, microfracture and joint debridement. Six of the 11 patients in the MAT group requiring subsequent procedures had a failure of their MAT procedure later and needed a TKR.

6.3.3 Clinical Outcomes Analysis

In the MAT cohort, the mean pre-operative Lysholm score was 48 ± 17 , which significantly increased to a mean of 66 ± 16 at one-year post-treatment ($p=0.0002$) (Figure 6.2A). Similarly, in the Actifit[®] group, the mean pre-operative Lysholm score was 54 ± 21 which significantly rose to 79 ± 11 at one-year post-operation ($p=0.0073$) (Figure 6.2B). The mean one-year satisfaction scores for the MAT and Actifit[®] groups were 2.8 ± 1.1 and 2.5 ± 1.2 , respectively. At the latest follow up to 2020, a total of 6 procedures were considered failures in the MAT group at a mean of 7.2 ± 3.3 years (range, 3-12 years; Table 6.2), while no patient had revision or arthroplasty procedure in the Actifit[®] group. All 6 of the failed MAT procedures had converted to a total knee replacement due to the progression of OA. Overall, the survival rate for the MAT group was 95% at 5 years and 71% at 10 years, while for the Actifit[®] group, survival was 100% at 5 years and 83% at 10 years (Figure 6.3). However, this difference between the two groups was not significant (log-rank test, $p=0.36$).

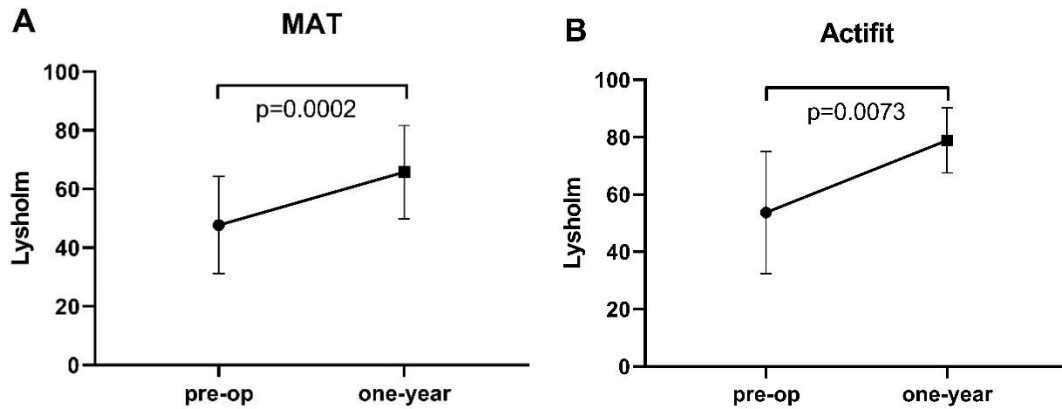


Figure 6.2: Comparison of pre-operative and one-year post-operative Lysholm score for MAT (A) and Actifit® group (B).

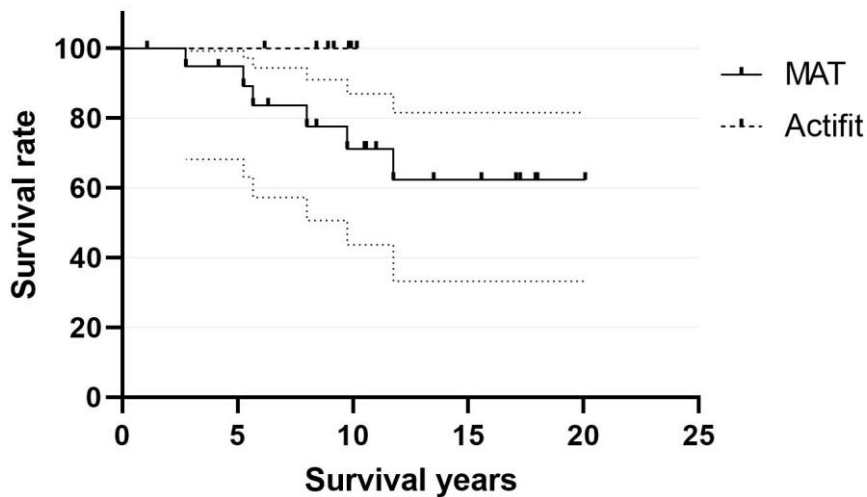


Figure 6.3: Kaplan-Meier survival curves.

Failure was defined as the need for revision surgery or total knee replacement due to ACI and/or meniscus graft failure or as a result of osteoarthritis progression. ACI: autologous chondrocyte implantation. Dash lines indicate 95% confidence intervals.

Table 6.2: Meniscus allograft transplantation failures

Patients	Age/Sex/BMI, kg/cm ²	Cartilage Defect Location/Size, cm ²	Graft location	Unipolar or Bipolar	Concurrent Surgery	Survival years
1	40/M/33.14	LFC/2.04	Lateral	Uni	No	8
2	33/M/32.13	LFC, trochlea/9.45, 2.4	Lateral	Uni	No	12
3	57/M/28.08	MFC, MTP/6, 10.4	Medial	Bi	No	3
4	39/M/27.20	LFC, LTP/N/A	Lateral	Bi	DFO	5
5	48/M/30.07	LTP, LFC, MFC/ 5, 3, 7.5	Lateral	Bi	No	9.75
6	30/M/29.77	LFC, LTP/3.52, 3.08	Lateral	Bi	DFO	5.5

DFO, distal femoral osteotomy; LFC, lateral femoral condyle; LTP, lateral tibial plateau; M, male; MFC, medial femoral condyle; MTP, medial tibial plateau.

6.3.4 Multilevel Modelling and Estimated Clinical Outcome

Multilevel modelling demonstrated that a higher pre-operative Lysholm score was significantly associated with a higher post-operative Lysholm score ($p=0.0034$) (Table 6.3). The estimated post-operative Lysholm score model showed that the two groups had comparable functional scores at 2, 5 and 10-year follow up, with no significant differences (Table 6.4).

Table 6.3: Fixed Effects in the Longitudinal Multilevel Model

Fixed effects	Mean Value of Coefficient (95% CI)	<i>P</i> value
Pre-op Lysholm score	1.83 (0.68, 2.98)	0.0034
Graft type (Allograft-Actifit®)	-0.83 (-15.60, 13.93)	0.9088
Monthly rise after one year	0.02 (-0.12, 0.15)	0.8204
Monthly rise after one year: graft type	-0.04 (-0.19, 0.11)	0.6089

CI: Confidence Intervals.

Table 6.4: Estimated Post-operative Lysholm Scores

Graft type	2-year (95% CI)	5-year (95% CI)	10-year (95% CI)
MAT	64.8 (58.0, 71.5)	63.9 (57.3, 70.5)	62.4 (53.8, 71.0)
Actifit®	66.6 (55.2, 77.9)	67.1 (56.0, 78.3)	68.1 (52.8,83.3)

6.3.5 Radiographic Evaluation

Twelve patients in the MAT group (mean 6.71 ± 4.6 years) and 5 patients in the Actifit® group (mean 2.78 ± 2.0 years) had post-operative MRI evaluation. No significant differences between the two groups were found in rME, cCCI or sCCI (Figure 6.4 A, B and C). Figure 6.5 represent the postoperative MRIs of Actifit implant with ACI patient at one-year (Figure 6.5A) and five-year (Figure 6.5B). The Actifit scaffold has a slightly hyperintense signal with intact morphology at one year follow-up, whereas the signal of scaffold appeared less intensive and the size of scaffold shrunk with a small vertical tear at five years follow-up.

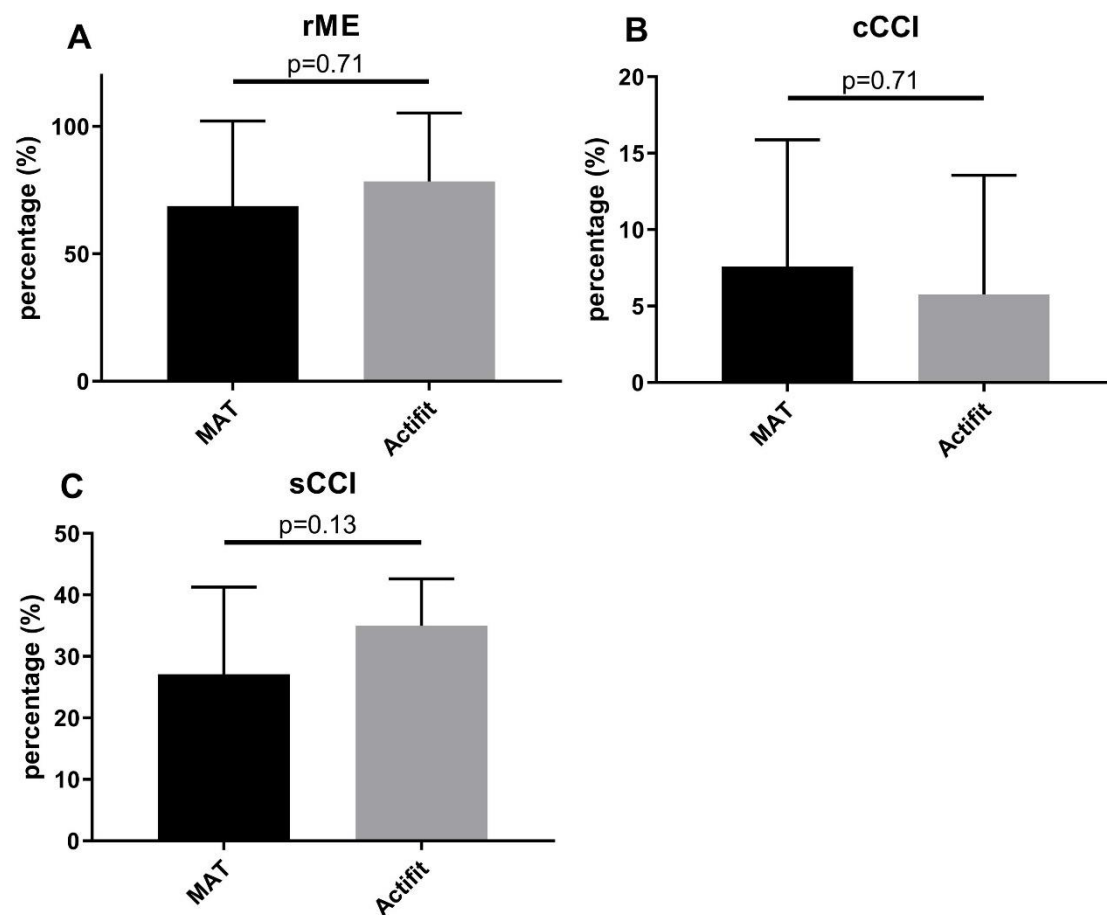


Figure 6.4: MRI assessment of meniscus extrusion.

(A) relative meniscal extrusion and cartilage coverage percentage on coronal (B) and sagittal plane (C) in MAT and polyurethane scaffold groups. rME: relative meniscal extrusion; cCCI: coronal cartilage coverage index; sCCI: sagittal cartilage coverage index

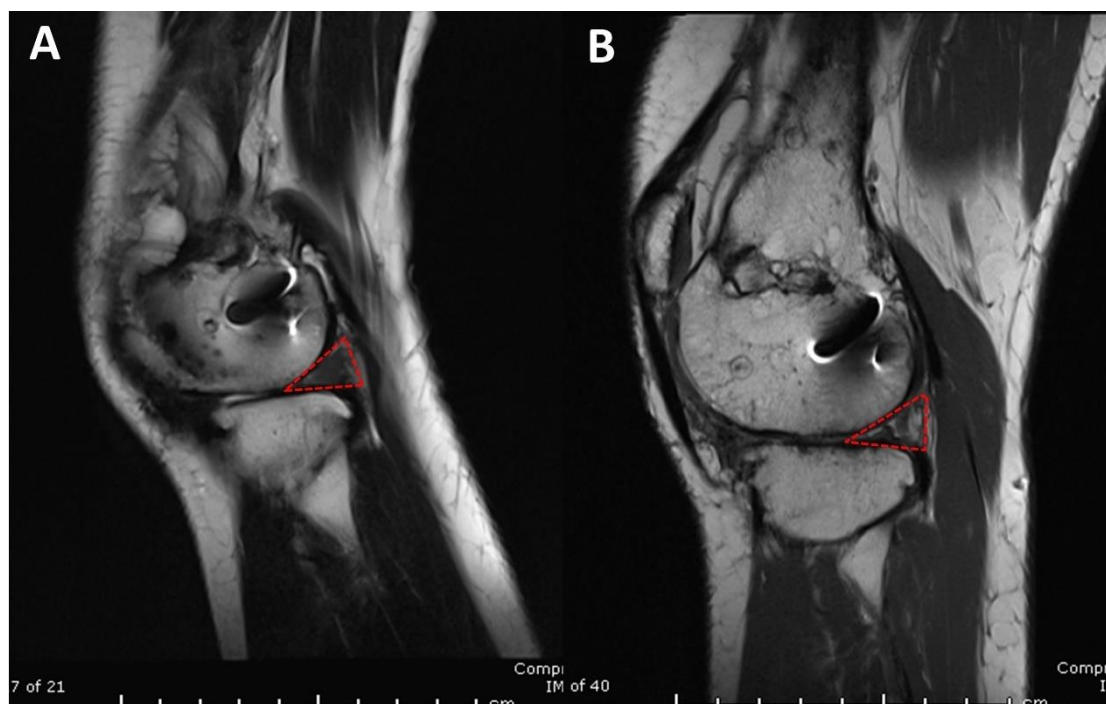


Figure 6.5: *Represent postoperative MRI (sagittal) of Actifit implants with ACI patient.*

(A) One-year postoperative MRI well visualized the intact Actifit scaffold at posterior horn of lateral meniscus. (B) Five years postoperative MRI showed smaller scaffold remnant with a vertical tear on the same plane, but the signal changed less intense compared to one-year postop.

6.3.6 Post-operative Meniscus Allograft Biopsy Histology Evaluation

Thirteen out of 20 patients in the MAT group had a post-operative histological analysis of the meniscus and treated cartilage defect. None of the Actifit® group had post-operative biopsies. H&E staining of allograft implants demonstrated fibrocartilage, which was well populated with cells in all cases. Vascularisation could be observed in some cases (Figure 6.6A). The presence of proteoglycans throughout the tissue was visualised with safranin O & fast green and toluidine blue staining (Figure 6.6B & C).

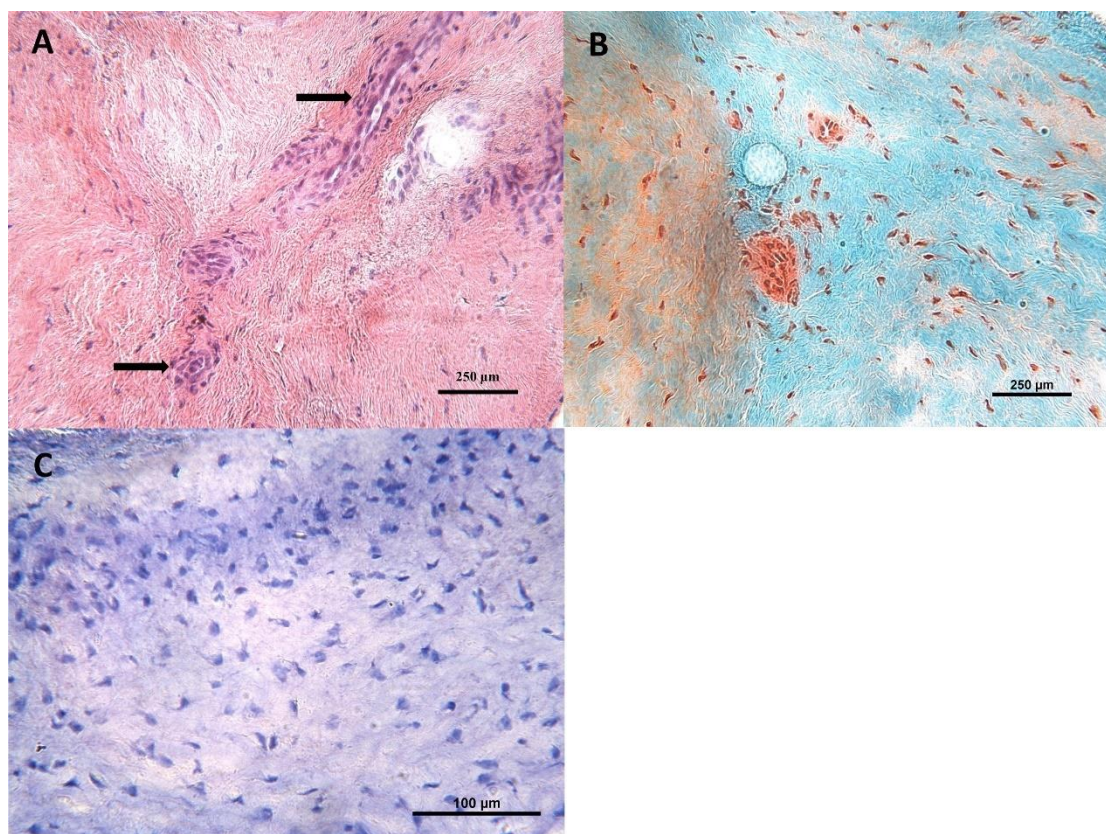


Figure 6.6: Representative histology of biopsies taken 19 months post-operation with allogeneic meniscus

(A-C): H&E staining (A) demonstrated numerous cells in the meniscus matrix with blood vessels (arrow); Safranin O & Fast green (B) and toluidine blue staining (C) showed the presence of sulphated proteoglycans.

6.4 Discussion

In this retrospective case series of mid to long-term follow up, we analysed data from 28 patients who underwent ACI combined with MAT (20 patients) or with a polyurethane meniscus scaffold (Actifit[®], 8 patients) for the treatment of concomitant cartilage lesions and meniscal deficiency. Overall, both groups of patients showed significant improvement in terms of pain relief and functional scores up to 20- and 10-years post-treatment for the MAT and Actifit[®], respectively. Based on clinical outcome analysis and statistical modelling, we found that both groups of patients had a similar recovery pattern, in which the patients' knee function recovered rapidly in the first year, levelling off subsequently. This biphasic recovery pattern was also shown in a cohort study of 80 ACI only-treated patients from our group, which showed a short phase I rapid recovery (in the first 15 months), followed by a longer phase II slow recovery (up to 9 years)²⁴⁶.

To our knowledge, this is the first study that has evaluated the clinical outcomes of combined partial meniscus substitute with concomitant ACI. The polyurethane scaffold was designed for the clinical challenge of treating patients with irreparable, partial meniscal lesions, in an attempt to provide pain relief and restore meniscus function. However, a relatively high failure rate (23-47%) has been noted for the substitute at midterm follow up^{83,256}. Generally, advanced chondral degeneration represents the most common contraindication for meniscus replacement with a scaffold²⁵⁷. In our present study, eight patients in the Actifit[®] group had good midterm clinical outcomes without any revision surgery or knee arthroplasty. The evaluation of postoperative MRI on Actifit[®] scaffold showed well retained morphology at short-term follow-up and less intensive signal change at longer-term follow-up. Our results suggest that if the coexisting cartilage lesion can be repaired using ACI beforehand or simultaneously, a

longer meniscal substitute survival could be achieved.

For the first eight patients who had combined ACI and MAT in our previous short-term follow-up study ²⁵⁰, three were considered to have failed at a relatively early stage, having undergone total knee replacement at 2, 3 and 8 years post-graft. However, the other five patients remained physically active in the long-term (up to 20 years). The common characteristic of the six failure cases in the MAT group for the present study was obesity (mean BMI 30.07 ± 3.24 kg/m²). Jiménez-Garrido et al (2019) reported that obese patients (BMI ≥ 30 kg/m², with four patients a BMI ≥ 30) had higher rates of meniscal transplant failure compared with non-obese patients, while non-obese patients had better knee functional scores compared with obese individuals. The high BMI of at least four of our MAT patients may therefore have contributed to the failure of their procedure. On the other hand, only one of our Actifit[®] patients had a BMI over 30 (BMI = 30.5).

Other previous studies have reported mid- to long-term clinical outcomes of MAT combined with ACI and demonstrated a sustained improvement of knee symptoms and function after a mean of 4.5 and 7.9 years follow-up ^{248,249}. The reported failure rate in these studies were 11% and 33% respectively, with a mean survival time (failure cases) of less than 2 years and 5.4 years post-operatively. Our study of MAT combined with ACI had a comparable failure rate (30%) at longer follow-up and with patients who had a higher rate of bipolar cartilage lesions. Both previous studies suspected that the presence of bipolar lesions could predispose to failure, but these studies had small numbers and were inadequately powered to show any statistical differences. In our study, four out of the six failure cases presented with bipolar lesions, while five out of the 14 non-failed MAT group of patients presented with bipolar lesions; hence the presence of bipolar lesions does not seem to represent a risk factor for failure of this

combined procedure. However, further investigation with a larger sample size will be needed before firm conclusions can be drawn.

Our multilevel modelling analysis showed that baseline Lysholm Score (pre-operative) had a significant positive correlation with post-operative score. Our group's previous study identified pre-operative Lysholm score also as a factor influencing the likelihood of ACI patients progressing to arthroplasty in a cohort of 170 ACI-treated patients ⁹⁹. Such predictors can be incorporated into predictive tools such as ORKA (Oswestry Risk of Knee Arthroplasty, a validated application, <https://www.ork.app/>) ⁹⁹ which can be used to help surgeons and patients evaluate the risks and benefits of surgery, as well as improve planning for post-operative rehabilitation.

Meniscal extrusion is the most commonly reported complication following meniscus transplantation ^{259,260}. Results from our study indicated that a certain degree of meniscal extrusion in both groups was observed without significant differences at midterm radiological assessment. However, the Actifit[®] group tended to have a higher cartilage coverage on the sagittal plane compared to the MAT group. This could be explained by the fact that the anterior and posterior roots of the original meniscus are well preserved in meniscus scaffold implantations ²⁵⁷. In contrast, the Actifit[®] substitute implantation group tended to have poorer cartilage coverage in the coronal plane. This finding has similarly been reported in other studies ^{259,261}. Faivre et al. ²⁵⁹ suggested that the pre-operative coronal absolute meniscus extrusion strongly predicts post-operative meniscus morphological outcomes. Even though the meniscus extrusion is an important outcome measure in meniscus transplantation procedure, the whole joint status evaluation and chondroprotective effect would be more meaningful assessments to investigate the benefits of the implants in long-term follow-up.

There are several limitations in our present study. Firstly, the relatively small number

of patients may introduce a bias in building a multilevel model. Secondly, the fact that most of our cases had multiple pre-operative, concomitant or post-operative procedures, including microfracture, ACL reconstruction, osteotomy, is likely to complicate the data interpretation. Further, many of our patients had complex medical histories. These additional factors make it difficult to isolate the precise clinical effectiveness of concomitant MAT or Actifit® with ACI over time. To evaluate a series of combined procedures sufficient statistical power to achieve narrow confidence intervals, it is likely that a multicentre study will be required.

In conclusion, our study shows for the first time that combining ACI with MAT or Actifit® partial meniscus replacement to treat patients with cartilage defects and meniscal deficiency can provide successful clinical outcomes, with 10-year survival rates of 71% in the MAT group and 100% in the Actifit® group. No significant differences were found between the two groups in terms of clinical and radiographic outcome, though this might be due to the limited patient numbers in the Actifit® group.

Together our findings suggest that these combined surgical treatments might delay or prevent knee OA progression, essentially retaining a biological knee which is particularly relevant in young adult patients. The 30% failure rate noted in the MAT treatment group might relate to the patients' high BMI, low pre-operative Lysholm score or number of cartilage lesions, all which have been indicated to have a negative effect on the outcome. In addition, 43% of patients required subsequent arthroscopic procedures, which needs to be discussed between the surgeon and patient to manage patient expectations before surgery.

Chapter 7: General Discussion

7.1 The role the meniscus plays in progression of knee OA

Meniscus tears are normally caused by an acute injury or as a result of age-related meniscus degeneration, which is considered a significant contributor to knee OA pathology. However, the exact role the meniscus plays in this pathology is still not clear. Many studies have shown that the meniscus is not only a critical mechanical support in the joint, but also has a profound biological influence on the onset and progression of knee OA^{262,263}.

In terms of the role as a “mechanical supporter”, the meniscus distributes loading across the articular surface of the knee joint and maintains the balance of the joint’s biomechanics. Extrusion or deficiency of the meniscus, leading to knee malalignment, was found to be significantly associated with the occurrence and enlarging of bone marrow lesions which closely correlated with the incidence and progression of knee OA^{264,265}. In support of this, patient B in our case report (chapter 1.4.6), who was treated with combined chondrocytes and BM-MSCs and implantation of an Actifit® meniscus scaffold, showed a gradual decrease in the size of BMLs over time. Gait analysis studies report that partial meniscectomy could cause subtle reduction in range of motion, increased external tibial rotation and axial force which leads to altered loading in certain regions of the tibial plateau and subsequent deterioration of the cartilage^{266,267}. However, due to the complexity and heterogeneity of knee-to-knee variability, the mechanisms driving different patient outcomes and affecting different locations of the joint after meniscectomy have yet to be fully identified. Patient based studies, cadaveric models, *in vivo* animal models and bioreactor models which are designed to investigate the meniscus mechanics and mechanobiology have their own advantages and disadvantages, while statistically augmented computational models are considered to have advantages over other models for identifying the mechanical factors

that predispose the knee joint to rapidly develop OA ²⁶⁸.

From the perspective of being a “biological peacemaker” in the joint, meniscal injury and degeneration can affect the balance of the joint’s biologic environment. When an injured meniscus is exposed to a chemical stimulator or mechanical loading, the cells within it can produce pro-inflammatory cytokines, chemokines and matrix-degrading enzymes, potentially leading to ECM breakdown in meniscus, cartilage and synovium during OA pathogenesis. Interleukin-1 β (IL-1 β) and IL-6 are important pro-inflammatory cytokines with increased levels in synovial fluid during early and late stage knee OA ²⁶⁹. Meniscal cells stimulated with pro-inflammatory cytokines have been shown to increase catabolic gene expression, production of MMPs, components of the NF-kB and tumour necrosis factor (TNF) family and decrease collagen and connective tissue growth factor (CTGF) gene expression ²⁷⁰. In our OA meniscus characterisation study (chapter 3), we found the decreased vascularity within the transverse collagen “tree” fibres and increased integrin cells surface markers on meniscal cells at P0 and P2, were associated with increased meniscal degeneration. All these factors may contribute to the inhibition of the intrinsic healing response of the meniscus. Likewise, an increased catabolic activity and degradative enzyme activity were found in the synovial fluid of patients with teared meniscus ²⁶³ and cartilage explants exposed to pro-inflammatory mediators ²⁷¹. Hence, the biologic interactions between meniscus, synovial tissue and articular cartilage can synergistically exacerbate joint inflammation and OA progression.

7.2 The clinical perspective: translation of meniscus regeneration research to clinical practice

The key challenge in the clinic for the treatment of meniscal lesion is the limited ability of the injured meniscus for repair. Factors which contribute to this low or absent self-repair capacity, particularly in the avascular region include poor intrinsic vascularity, hypocellularity, the presence of inflammatory mediators and various proteases in the synovial fluid, as well as complex mechanical loading ²⁰¹. The use of a cell-based strategy for repair or regeneration of the meniscus has great potential, with cells responding to ‘damaged meniscus signals’ and actively responding and altering their metabolic activity to repair the lesions ²⁷². A majority of pre-clinical research models have declared the benefits of using MSCs or allogeneic cells for meniscus tissue engineering ⁸⁵. However, to our knowledge, there appears to be only two MSC injection trials ^{273,274}, two micro-fragmented adipose tissue injection trials using Lipogems[®] ^{275,276} and one meniscal cell bandage trial reported ¹⁰⁵ with none showing clear clinical efficacy to date.

7.2.1 Major obstacles limiting cell therapy for meniscus repair in the clinic

The first limitation preventing the successful translation of the technologies is the various scaffolds as reviewed in chapter 1. Although all the studies showed a superior role of cell and scaffold combinations compared to acellular scaffolds, none of these studies compared different scaffolds with each other. Decellularised scaffolds are limited by their clinical GMP applicability ²⁷⁷. More studies are required to compare the efficacy of using cell-scaffold combinations with the injections of cells alone. In addition, to apply autologous cells seeded on a scaffold, requires *in vitro* cell expansion and availability of a GMP-approved cell therapy facility. The provision and governance of such a facility is a costly undertaking, requiring considerable financial and expertise

investment. The second limitation is that there is no consensus on which cell type has shown the most promising results. Synovial MSCs²⁷⁸ and adipose-derived MSCs¹¹² have both demonstrated to having high proliferation rates and multilineage differentiation capacity. BM-MSCs have been a popular cell source in many studies, having the capability to respond and inhibit inflammation locally as we discussed in the two cases reported with autologous chondrocytes and BM-MSCs treated cartilage defect (chapter 1.4.6). However, harvesting of BM-MSCs can be a painful process and the cells have limited expansion potential *in vitro*²⁷⁹. In our study, we demonstrate that autologous meniscal cells derived from discarded meniscectomy tissue could be a potential cell source (chapter 5). There is no ideal source of cells, with each type having certain advantages and disadvantages. In addition, the literature shows varying differentiation capacities between cell sources using different models and there is lack of evidence to prove one cell type superior to another in meniscal regeneration. The third limitation we have identified is the pathology of the injury model used in research not being comparable to the real ‘pathology’ process in humans. In research injury models such as the sheep explant defect model we used in chapter 5, the treatments are introduced immediately or within two weeks after the defects are created in the meniscus. In addition, the explant model is an isolated tissue, which is not incorporated to adjacent tissues with interconnecting vascularity and no loading is applied as seen in the *in vivo* situation. In clinical practice, patients normally receive the treatment several months or years after trauma, which leads to a different regeneration rate in chronic meniscal lesions compared with acute injuries. Therefore, the development of chronic meniscal injury models, which could reflect the human pathology would be a distinct advantage to help to provide better insights for developing clinically useful regenerative approaches for meniscal repair.

7.2.2 Future perspectives of translating cell-based meniscus tissue engineering to the clinic

To achieve a promising meniscal cell therapy for clinical use in the near future, a single-stage procedure using minimally manipulated autologous cells combined with a clinically approved, off-the-shelf meniscus scaffold is likely to represent the fastest option for clinical translation. Moreover, meniscus injury frequently presented with cartilage lesions in the daily clinic. Our clinical study in chapter 6 demonstrated the mid to long term benefit of using combined meniscus transplantation and ACI to treat co-lesion patients. Therefore, addressing both lesions in cartilage and meniscus with cell-based strategy for the treatment in a single procedure could be an ideal combination in the future. However, in the longer term, perhaps a more cost-effective cell-based meniscal therapy would be the use of an allogeneic approach, although further pre-clinical study is required to demonstrate the safety of this approach. Unlike ACI for cartilage repair where the treated site has subchondral bone as a base and a collagen membrane can be attached as a cover to hold implanted cells in the lesion, the meniscus is an irregularly shaped piece of loosely attached fibrocartilage in the knee joint cavity. Any implanted cells may diminish quickly via joint effusion and inflammatory cytokine influences which may be likely to occur after any surgical procedure. Therefore, a clinically approved hydrogel like Tisseel[®] which could hold cells within a scaffold in the initial post-operative stage and facilitate cell retention and proliferation to enhance matrix formation is essential in the real clinical scenario. In this study we have identified meniscal progenitors in both avascular and vascular regions of the human meniscus, which could be considered as ideal therapeutic cell sources for meniscus tissue engineering. In addition, the work described in this thesis which identified the presence of resident progenitor cells in meniscus tissues, could be used to support

alternative regenerative approaches whereby endogenous progenitors are targeted using biologic augmentation approaches, including mechanical stimulation, injection of platelet-rich plasma and autologous MSCs²⁸⁰.

7.3 Conclusion

In this PhD work, we firstly demonstrated the exclusive cell surface markers (CD49b, CD49c and CD166) to distinguish cells phenotype from avascular or vascular meniscus and cartilage in the OA joint. We also discovered the meniscus “tree-like” collagen fibres pathological changes in degenerated meniscal tissue. The meniscal cells derived from OA meniscus had been approved its chondrogenic capacity *in vitro*. These results filled the gap in the pathology changes in meniscus degeneration and implied the potential treatment target in the future.

Secondly, our study demonstrated that the human meniscus contains meniscal progenitor populations in both the avascular and vascular regions. The vascular progenitor population exhibit better stromal cell characteristics which likely associate with the superior meniscal healing potential in the vascular region. These findings suggested that meniscal progenitors represent an attractive novel cell therapy strategy for the enhancement of meniscal repair and regeneration.

Thirdly, this study proved the feasibility of using fibrin gel to deliver autologous avascular meniscal cells in a clinical grade meniscus substitute *in vitro*. Cells delivered by fibrin gel showed an increased cell proliferation and more matrix production within the scaffold compared to cells directly seeded into the scaffold in the absence of fibrin. The results of the experiment represent the foundation of this approach of augmenting the benefit of a commercially available meniscal implant with the addition of a cellular component.

Lastly, the clinical work demonstrated the combining ACI with MAT or Actifit® partial meniscus replacement to treat patients with cartilage defects and meniscal deficiency can provide successful clinical outcomes, with 10-year survival rates of 71% in the MAT group and 100% in the Actifit® group.

Together, this PhD work presented a comprehensive investigation in meniscus-related research, including meniscus degeneration, meniscal progenitors and cell-based meniscus tissue engineering. This study filled in the gaps of current meniscal biology and pathology, as well as providing a novel cell-based meniscus tissue regeneration strategy as a future treatment option in the clinic.

Reference

1. Kohn D, Moreno B. Meniscus insertion anatomy as a basis for meniscus replacement: A morphological cadaveric study. *Arthrosc J Arthrosc Relat Surg*. 1995;11(1):96-103.
2. Fox AJS, Bedi A, Rodeo SA. The basic science of human knee menisci: structure, composition, and function. *Sports Health*. 2012;4(4):340-351. doi:10.1177/1941738111429419
3. McDermott ID, Sharifi F, Bull AM, Gupte CM, Thomas RW, Amis AA. An anatomical study of meniscal allograft sizing. *Knee Surg Sport Traumatol Arthrosc*. 2004;12(2):130-135.
4. Greis PE, Bardana DD, Holmstrom MC, Burks RT. Meniscal Injury: I. Basic Science and Evaluation. *J Am Acad Orthop Surg*. 2002;10(3):168-176. doi:10.5435/00124635-200205000-00003
5. Kusayama T, Harner CD, Carlin GJ, Xerogeanes JW, Smith BA. Anatomical and biomechanical characteristics of human menisconfemoral ligaments. *Knee Surgery, Sport Traumatol Arthrosc*. 1994;2(4):234-237. doi:10.1007/BF01845594
6. Stein G, Koebke J, Faymonville C, Dargel J, Müller LP, SchiVer G. The relationship between the medial collateral ligament and the medial meniscus: A topographical and biomechanical study. *Surg Radiol Anat*. 2011;33(9):763-766.
7. Clark CR, Ogden JA. Development of the menisci of the human knee joint. Morphological changes and their potential role in childhood meniscal injury. *J Bone Jt Surg*. 1983;65(4):538-47.
8. Bukowiecki A, Hos D, Cursiefen C, Eming SA. Wound-healing studies in cornea and skin: Parallels, differences and opportunities. *Int J Mol Sci*. 2017;18(6):1-24. doi:10.3390/ijms18061257
9. Arnoczky SP, Warren RF. Microvasculature of the human meniscus. *Am J Sports Med*. 1982;10(2):90-95. doi:10.1177/036354658201000205
10. McDevitt CA, Webber RJ. The ultrastructure and biochemistry of meniscal cartilage. *Clin Orthop Relat Res*. 1990;(252):8-18.

doi:10.1097/NCN.0b013e31823ea54e

11. Sweigart MA, Athanasiou KA. Toward tissue engineering of the knee meniscus. *Tissue Eng.* 2001;7(2):111-129.
12. Herwig J, Egner E, Buddecke E. Chemical changes of human knee joint menisci in various stages of degeneration. *Ann Rheum Dis.* 1984;43(4):635-640.
13. Cheung HS. Distribution of type I, II, III, and V in the pepsin solubilized collagens in bovine meniscus. 1987;16:343-356.
14. Spencer Jones R, Keene GCR, Learmonth DJA, et al. Direct measurement of hoop strains in the intact and torn human medial meniscus. *Clin Biomech.* 1996;11(5):295-300.
15. Petersen W, Tillmann B. Collagenous fibril texture of the human knee joint menisci. *Anat Embryol (Berl).* 1998;197(4):317-324.
doi:10.1007/s004290050141
16. Ghosh P, Taylor TK. The knee joint meniscus. A fibrocartilage of some distinction. *Clin Orthop Relat Res.* 1987;(224):52-63.
17. Mcnicol D, Roughley PJ. Extraction and Characterization of Proteoglycan from Human Meniscus. *Biochem J.* 1980;185:705-713.
18. Nakano T, Dodd CM, Scott PG. Glycosaminoglycans and proteoglycans from different zones of the porcine knee meniscus. *J Orthop Res.* 1997;15(2):213-220. doi:10.1002/jor.1100150209
19. Fife RS. Identification of link proteins and a 116,000-Dalton matrix protein in canine meniscus. *Arch Biochem Biophys.* 1985;240(2):682-688.
doi:10.1016/0003-9861(85)90076-1
20. Miller RR, McDevitt CA. Thrombospondin in ligament, meniscus and intervertebral disc. *Biochim Biophys Acta.* 1991;1115(1):85-88.
doi:10.1016/0304-4165(91)90015-9
21. McDevitt CA, Mukherjee S, Kambic H, Parker R. Emerging concepts of the cell biology of the meniscus. *Curr Opin Orthop.* 2002;13(5):345-350.
22. Declercq HA, Forsyth RG, Verbruggen A, Verdonk R, Cornelissen MJ,

- Verdonk PCM. CD34 and SMA expression of superficial zone cells in the normal and pathological human meniscus. *J Orthop Res*. 2012;30(5):800-808. doi:10.1002/jor.21582
23. Verdonk PCM, Forsyth RG, Wang J, et al. Characterisation of human knee meniscus cell phenotype. *Osteoarthr Cartil*. 2005;13(7):548-560. doi:10.1016/j.joca.2005.01.010
24. Makris EA, Hadidi P, Athanasiou KA. The knee meniscus: structure-function, pathophysiology, current repair techniques, and prospects for regeneration. *Biomaterials*. 2011;32(30):7411-7431. doi:10.1016/j.biomaterials.2011.06.037
25. Tsujii A, Nakamura N, Horibe S. Age-related changes in the knee meniscus. *Knee*. 2017;24(6):1262-1270. doi:10.1016/j.knee.2017.08.001
26. Loeser RF, Collins JA, Diekman BO. Ageing and the pathogenesis of osteoarthritis. *Nat Rev Rheumatol*. 2016;12(7):412-420. doi:10.1038/nrrheum.2016.65
27. Vo N V., Hartman RA, Patil PR, et al. Molecular mechanisms of biological aging in intervertebral discs. *J Orthop Res*. 2016;34(8):1289-1306. doi:10.1002/jor.23195
28. Loeser RF. Aging process and the development of osteoarthritis. *Curr Opin Rheumatol*. 2013;25(1):108-113. doi:10.1097/BOR.0b013e32835a9428.Aging
29. Pauli C, Grogan SP, Patil S, et al. Macroscopic and histopathologic analysis of human knee menisci in aging and osteoarthritis. *Osteoarthr Cartil*. 2011;19(9):1132-1141. doi:10.1016/j.joca.2011.05.008
30. Petersen W, Tillmann B. Age-related blood and lymph supply of the knee menisci. A cadaver study. *Acta Orthop Scand*. 1995;66(4):308-312. doi:10.3109/17453679508995550
31. Danzig L, Resnick D, Gonsalves M, Akeson WH. Blood supply to the normal and abnormal menisci of the human knee. *Clin Orthop Relat Res*. 1983;(172):271-276.
32. Sivan SS, Tsitron E, Wachtel E, et al. Age-related accumulation of pentosidine in aggrecan and collagen from normal and degenerate human intervertebral discs. *Biochem J*. 2006;399(1):29-35. doi:10.1042/BJ20060579

33. Sell DR, Nagaraj RH, Grandhee SK, et al. Pentosidine: A molecular marker for the cumulative damage to proteins in diabetes, aging, and uremia. *Diabetes Metab Rev.* 1991;7(4):239-251. doi:10.1002/dmr.5610070404
34. McAlinden A, Dudhia J, Bolton MC, Lorenzo P, Heinegård D, Bayliss MT. Age-related changes in the synthesis and mRNA expression of decorin and aggrecan in human meniscus and articular cartilage. *Osteoarthr Cartil.* 2001;9(1):33-41. doi:10.1053/joca.2000.0347
35. Piperno M, Reboul P, Hellio Le Graverand M-P, et al. Osteoarthritic cartilage fibrillation is associated with a decrease in chondrocyte adhesion to fibronectin. *Osteoarthr Cartil.* 1998;6(6):393-399.
36. Toh WS, Brittberg M, Farr J, et al. Cellular senescence in aging and osteoarthritis: Implications for cartilage repair. *Acta Orthop.* 2016;87(eSuppl 363):6-14. doi:10.1080/17453674.2016.1235087
37. Van Deursen JM. The role of senescent cells in ageing. *Nature.* 2014;509(7501):439-446. doi:10.1038/nature13193
38. Nakata K, Shino K, Hamada M, et al. Human meniscus cell characterization of the primary culture and use for tissue engineering. *Clin Orthop Relat Res.* 2001;391(391):S208-S218.
39. McCulloch K, Litherland GJ, Rai TS. Cellular senescence in osteoarthritis pathology. *Aging Cell.* 2017;16(2):210-218. doi:10.1111/acer.12562
40. Roberts S, Evans EH, Klefsas D, Jaffray DC, Eisenstein SM. Senescence in human intervertebral discs. *Eur Spine J.* 2006;15 Suppl 3(SUPPL. 3):S312-6. doi:10.1007/s00586-006-0126-8
41. Clayton RAE, Court-Brown CM. The epidemiology of musculoskeletal tendinous and ligamentous injuries. *Injury.* 2008;39(12):1338-1344. doi:10.1016/j.injury.2008.06.021
42. Stärke C, Kopf S, Petersen W, Becker R. Meniscal repair. *Arthroscopy.* 2009;25(9):1033-1044. doi:10.1016/j.arthro.2008.12.010
43. Roos H, Laurén M, Adalberth T, Roos EM, Jonsson K, Lohmander LS. Knee osteoarthritis after meniscectomy: prevalence of radiographic changes after twenty-one years, compared with matched controls. *Arthritis Rheum.*

- 1998;41(4):687-693. doi:10.1002/1529-0131(199804)41:4<687::AID-ART16>3.0.CO;2-2
44. Baker BE, Peckham AC, Puppardo F, Sanborn JC. Review of meniscal injury and associated sports. *Am J Sports Med.* 1985;13(1):1-4. doi:10.1177/036354658501300101
 45. Salata MJ, Gibbs AE, Sekiya JK. A systematic review of clinical outcomes in patients undergoing meniscectomy. *Am J Sports Med.* 2010;38(9):1907-1916. doi:10.1177/0363546510370196
 46. Rubman MH, Noyes FR, Barber-Westin SD. Arthroscopic repair of meniscal tears that extend into the avascular zone. A review of 198 single and complex tears. *Am J Sports Med.* 1998;26(1):87-95. doi:10.1177/03635465980260013301
 47. Horibe S, Shino K, Nakata K, Maeda A, Nakamura N, Matsumoto N. Second-look arthroscopy after meniscal repair. Review of 132 menisci repaired by an arthroscopic inside-out technique. *J Bone Jt Surg Br.* 1995;77(2):245-249.
 48. Englund M, Guermazi A, Gale D, et al. Incidental meniscal findings on knee MRI in middle-aged and elderly persons. *N Engl J Med.* 2008;359(11):1108-1115. doi:10.1056/NEJMoa0800777
 49. Kornaat PR, Bloem JL, Ceulemans RYT, et al. Osteoarthritis of the knee: association between clinical features and MR imaging findings. *Radiology.* 2006;239(3):811-817. doi:10.1148/radiol.2393050253
 50. Bhattacharyya T, Gale D, Dewire P, et al. The clinical importance of meniscal tears demonstrated by magnetic resonance imaging in osteoarthritis of the knee. *J Bone Joint Surg Am.* 2003;85-A(1):4-9.
 51. Beaufils P, Becker R, Kopf S, Matthieu O, Pujol N. The knee meniscus: management of traumatic tears and degenerative lesions. *EFORT open Rev.* 2017;2(5):195-203. doi:10.1302/2058-5241.2.160056
 52. Cengiz IF, Pereira H, Espregueira-Mendes J, Oliveira JM, Reis RL. Treatments of Meniscus Lesions of the Knee: Current Concepts and Future Perspectives. *Regen Eng Transl Med.* 2017;3(1):32-50. doi:10.1007/s40883-017-0025-z
 53. Seil R, Becker R. Time for a paradigm change in meniscal repair: save the

- meniscus! *Knee Surgery, Sport Traumatol Arthrosc.* 2016;24(5):1421-1423.
54. Mordecai SC, Al-Hadithy N, Ware HE, Gupte CM. Treatment of meniscal tears: An evidence based approach. *World J Orthop.* 2014;5(3):233-241. doi:10.5312/wjo.v5.i3.233
55. Bryceland JK, Powell AJ, Nunn T. Knee Menisci. *Cartilage.* 2017;8(2):99-104. doi:10.1177/1947603516654945
56. Maffulli N, Longo UG, Campi S, Denaro V. Meniscal tears. *Open access J Sport Med.* 2010;1:45-54. doi:10.2147/oajsm.s7753
57. Beaufile P, Pujol N. Meniscal repair: Technique. *Orthop Traumatol Surg Res.* 2018;104(1S):S137-S145. doi:10.1016/j.otsr.2017.04.016
58. Morgan CD. The “all-inside” meniscus repair. *Arthroscopy.* 1991;7(1):120-125. doi:10.1016/0749-8063(91)90093-d
59. Peltier A, Lording TD, Lustig S, Servien E, Maubisson L, Neyret P. Posteromedial meniscal tears may be missed during anterior cruciate ligament reconstruction. *Arthroscopy.* 2015;31(4):691-698.
60. Peltier A, Lording T, Maubisson L, Ballis R, Neyret P, Lustig S. The role of the meniscotibial ligament in posteromedial rotational knee stability. *Knee Surgery, Sport Traumatol Arthrosc.* 2015;23(10):2967-2973. doi:10.1007/s00167-015-3751-0
61. Sonnery-Cottet B, Conteduca J, Thaunat M, Gunepin FX, Seil R. Hidden lesions of the posterior horn of the medial meniscus: a systematic arthroscopic exploration of the concealed portion of the knee. *Am J Sports Med.* 2014;42(4):921-926. doi:10.1177/0363546514522394
62. Kopf S, Birkenfeld F, Becker R, et al. Local Treatment of Meniscal Lesions with Vascular Endothelial Growth Factor. *J Bone Jt Surgery-American Vol.* 2010;92(16):2682-2691. doi:10.2106/JBJS.I.01481
63. Milachowski KA, Weismeier K, Wirth CJ. Homologous meniscus transplantation. Experimental and clinical results. *Int Orthop.* 1989;13(1):1-11. doi:10.1007/BF00266715
64. Myers P, Tudor F. Meniscal allograft transplantation: how should we be doing

- it? A systematic review. *Arthroscopy*. 2015;31(5):911-925.
doi:10.1016/j.arthro.2014.11.020
65. Rosso F, Bisicchia S, Bonasia DE, Amendola A. Meniscal allograft transplantation: a systematic review. *Am J Sport Med*. 2015;43(4):998-1007.
doi:10.1177/0363546514536021
 66. Smith NA, MacKay N, Costa M, Spalding T. Meniscal allograft transplantation in a symptomatic meniscal deficient knee: a systematic review. *Knee Surg Sport Traumatol Arthrosc*. 2015;23(1):270-279. doi:10.1007/s00167-014-3310-0
 67. Hergan D, Thut D, Sherman O, Day MS. Meniscal allograft transplantation. *Arthroscopy*. 2011;27(1):101-112. doi:10.1016/j.arthro.2010.05.019
 68. Smith NA, Parkinson B, Hutchinson CE, Costa ML, Spalding T. Is meniscal allograft transplantation chondroprotective? A systematic review of radiological outcomes. *Knee Surg Sports Traumatol Arthrosc*. 2016;24(9):2923-2935. doi:10.1007/s00167-015-3573-0
 69. Lee B-S, Kim H-J, Lee C-R, et al. Clinical Outcomes of Meniscal Allograft Transplantation With or Without Other Procedures: A Systematic Review and Meta-analysis. *Am J Sports Med*. 2018;46(12):3047-3056.
doi:10.1177/0363546517726963
 70. Wei G, Liang J, Ru N, Li Y-P, Shang Z-H, Chen J-F. Comparison of medial versus lateral meniscus allograft transplantation. Literature review and meta-analysis. *Saudi Med J*. 2016;37(6):613-623. doi:10.15537/Smj.2016.6.13983
 71. Dalkey NC. The Delphi method: An experimental study of group opinion. In: *Studies in the Quality of Life: Delphi and Decision-Making*. ; 1972:13-54.
 72. Sun J, Vijayavenkataraman S, Liu H. An Overview of Scaffold Design and Fabrication Technology for Engineered Knee Meniscus. *Mater (Basel, Switzerland)*. 2017;10(1). doi:10.3390/ma10010029
 73. Bulgheroni E, Grassi A, Campagnolo M, Bulgheroni P, Mudhigere A, Gobbi A. Comparative Study of Collagen versus Synthetic-Based Meniscal Scaffolds in Treating Meniscal Deficiency in Young Active Population. *Cartilage*. 2016;7(1):29-38. doi:10.1177/1947603515600219

74. Zaffagnini S, Fink C, Grassi A, Marcheggiani Muccioli GM, Marcacci M. Meniscal implants: Indications and outcomes. *Arthroscopie*. 2015;28(1):38-42. doi:10.1007/s00142-014-0837-5
75. Bulgheroni E, Grassi A, Campagnolo M, Bulgheroni P, Mudhigere A, Gobbi A. Comparative Study of Collagen versus Synthetic-Based Meniscal Scaffolds in Treating Meniscal Deficiency in Young Active Population. *Cartilage*. 2016;7(1):29-38. doi:10.1177/1947603515600219
76. Zaffagnini S, Marcheggiani Muccioli GM, Lopomo N, et al. Prospective long-term outcomes of the medial collagen meniscus implant versus partial medial meniscectomy: a minimum 10-year follow-up study. *Am J Sports Med*. 2011;39(5):977-985. doi:10.1177/0363546510391179
77. Monllau JC, Gelber PE, Abat F, et al. Outcome after partial medial meniscus substitution with the collagen meniscal implant at a minimum of 10 years' follow-up. *Arthroscopy*. 2011;27(7):933-943. doi:10.1016/j.arthro.2011.02.018
78. Bulgheroni P, Murena L, Ratti C, Bulgheroni E, Ronga M, Cherubino P. Follow-up of collagen meniscus implant patients: clinical, radiological, and magnetic resonance imaging results at 5 years. *Knee*. 2010;17(3):224-229.
79. Heijkants RGJC, van Calck R V, van Tienen TG, et al. Polyurethane scaffold formation via a combination of salt leaching and thermally induced phase separation. *J Biomed Mater Res A*. 2008;87(4):921-932. doi:10.1002/jbm.a.31829
80. de Groot J. Actifit, Polyurethane meniscus implant: basic science. In: *The Meniscus*. Springer Berlin Heidelberg; 2010:383-387. doi:10.1007/978-3-642-02450-4_48
81. van Minnen B, van Leeuwen MBM, Kors G, Zuidema J, van Kooten TG, Bos RRM. In vivo resorption of a biodegradable polyurethane foam, based on 1,4-butanediisocyanate: a three-year subcutaneous implantation study. *J Biomed Mater Res A*. 2008;85(4):972-982. doi:10.1002/jbm.a.31574
82. Efe T, Getgood A, Schofer MD, et al. The safety and short-term efficacy of a novel polyurethane meniscal scaffold for the treatment of segmental medial meniscus deficiency. *Knee Surg Sports Traumatol Arthrosc*. 2012;20(9):1822-

1830. doi:10.1007/s00167-011-1779-3
83. Dhollander A, Verdonk P, Verdonk R. Treatment of Painful, Irreparable Partial Meniscal Defects With a Polyurethane Scaffold: Midterm Clinical Outcomes and Survival Analysis. *Am J Sports Med.* 2016;44(10):2615-2621. doi:10.1177/0363546516652601
84. Houck DA, Kraeutler MJ, Belk JW, McCarty EC, Bravman JT. Similar clinical outcomes following collagen or polyurethane meniscal scaffold implantation: a systematic review. *Knee Surg Sports Traumatol Arthrosc.* 2018;26(8):2259-2269. doi:10.1007/s00167-018-4838-1
85. Korpershoek J V, de Windt TS, Hagmeijer MH, Vonk LA, Saris DBF. Cell-Based Meniscus Repair and Regeneration: At the Brink of Clinical Translation?: A Systematic Review of Preclinical Studies. *Orthop J Sport Med.* 2017;5(2):2325967117690131. doi:10.1177/2325967117690131
86. Haddad B, Pakravan AH, Konan S, Adesida A, Khan W. A systematic review of tissue engineered meniscus: cell-based preclinical models. *Curr Stem Cell Res Ther.* 2013;8(3):222-231. doi:10.2174/1574888x11308030007
87. Kon E, Filardo G, Tschon M, et al. Tissue engineering for total meniscal substitution: animal study in sheep model--results at 12 months. *Tissue Eng Part A.* 2012;18(15-16):1573-1582. doi:10.1089/ten.TEA.2011.0572
88. Mizuno K, Muneta T, Morito T, et al. Exogenous synovial stem cells adhere to defect of meniscus and differentiate into cartilage cells. *J Med Dent Sci.* 2008;55(1):101-111. <http://www.ncbi.nlm.nih.gov/pubmed/19845155>
89. Port J, Jackson DW, Lee TQ, Simon TM. Meniscal Repair Supplemented With Exogenous Fibrin Clot and Autogenous Cultured Marrow Cells in the Goat Model. *Am J Sports Med.* 1996;24(4):547-555. doi:10.1177/036354659602400422
90. Sanchez-Adams J, Athanasiou KA. Biomechanics of meniscus cells: regional variation and comparison to articular chondrocytes and ligament cells. *Biomech Model Mechanobiol.* 2012;11(7):1047-1056. doi:10.1007/s10237-012-0372-0
91. Baker BM, Nathan AS, Huffman GR, Mauck RL. Tissue engineering with meniscus cells derived from surgical debris. *Osteoarthr Cartil.* 2009;17(3):336-

345. doi:10.1016/j.joca.2008.08.001
92. Gunja NJ, Athanasiou K a. Passage and reversal effects on gene expression of bovine meniscal fibrochondrocytes. *Arthritis Res Ther.* 2007;9(5):R93. doi:10.1186/ar2293
93. Esposito AR, Moda M, Cattani SM de M, et al. PLDLA/PCL-T Scaffold for Meniscus Tissue Engineering. *Biores Open Access.* 2013;2(2):138-147. doi:10.1089/biores.2012.0293
94. Liang Y, Idrees E, Andrews SHJ, et al. Plasticity of Human Meniscus Fibrochondrocytes: A Study on Effects of Mitotic Divisions and Oxygen Tension. *Sci Rep.* 2017;7(1):12148.
95. Adesida AB, Mulet-Sierra A, Laouar L, Jomha NM. Oxygen tension is a determinant of the matrix-forming phenotype of cultured human meniscal fibrochondrocytes. *PLoS One.* 2012;7(6):e39339. doi:10.1371/journal.pone.0039339
96. Adesida AB, Grady LM, Khan WS, Millward-Sadler SJ, Salter DM, Hardingham TE. Human meniscus cells express hypoxia inducible factor-1alpha and increased SOX9 in response to low oxygen tension in cell aggregate culture. *Arthritis Res Ther.* 2007;9(4):R69. doi:10.1186/ar2267
97. Adesida AB, Grady LM, Khan WS, Hardingham TE. The matrix-forming phenotype of cultured human meniscus cells is enhanced after culture with fibroblast growth factor 2 and is further stimulated by hypoxia. *Arthritis Res Ther.* 2006;8(3):R61. doi:10.1186/ar1929
98. Brittberg M, Lindahi A, Nilsson A, Ohlsson C, Isaksson O, Peterson L. Treatment of deep cartilage defects in the knee with autologous chondrocyte transplantation. *N Engl J Med.* 1994;331(14).
99. Dugard MN, Kuiper JH, Parker J, et al. Development of a Tool to Predict Outcome of Autologous Chondrocyte Implantation. *Cartilage.* 2017;8(2):119-130. doi:10.1177/1947603516650002
100. Marsano A, Millward-Sadler SJ, Salter DM, et al. Differential cartilaginous tissue formation by human synovial membrane, fat pad, meniscus cells and articular chondrocytes. *Osteoarthr Cartil.* 2007;15(1):48-58.

- doi:10.1016/j.joca.2006.06.009
101. Vedicherla S, Romanazzo S, Kelly DJ, Buckley CT, Moran CJ. Chondrocyte-based intraoperative processing strategies for the biological augmentation of a polyurethane meniscus replacement. *Connect Tissue Res.* 2018;59(4):381-392. doi:10.1080/03008207.2017.1402892
 102. Weinand C, Peretti GM, Adams SB, Bonassar LJ, Randolph MA, Gill TJ. An allogenic cell-based implant for meniscal lesions. *Am J Sports Med.* 2006;34(11):1779-1789. doi:10.1177/0363546506290666
 103. Angele P, Kujat R, Koch M, Zellner J. Role of mesenchymal stem cells in meniscal repair. *J Exp Orthop.* 2014;1(1):12. doi:10.1186/s40634-014-0012-y
 104. Zellner J, Pattappa G, Koch M, et al. Autologous mesenchymal stem cells or meniscal cells: what is the best cell source for regenerative meniscus treatment in an early osteoarthritis situation? *Stem Cell Res Ther.* 2017;8(1):225. doi:10.1186/s13287-017-0678-z
 105. Whitehouse MR, Howells NR, Parry MC, et al. Repair of Torn Avascular Meniscal Cartilage Using Undifferentiated Autologous Mesenchymal Stem Cells: From In Vitro Optimization to a First-in-Human Study. *Stem Cells Transl Med.* 2017;6(4):1237-1248. doi:10.1002/sctm.16-0199
 106. King D. The healing of semilunar cartilages. 1936. *Clin Orthop Relat Res.* 1990;18(252):4-7. Accessed February 26, 2018. <http://www.ncbi.nlm.nih.gov/pubmed/2406072>
 107. Matsukura Y, Muneta T, Tsuji K, Koga H, Sekiya I. Mesenchymal stem cells in synovial fluid increase after meniscus injury. *Clin Orthop Relat Res.* 2014;472(5):1357-1364. doi:10.1007/s11999-013-3418-4
 108. Horie M, Sekiya I, Muneta T, et al. Intra-articular Injected synovial stem cells differentiate into meniscal cells directly and promote meniscal regeneration without mobilization to distant organs in rat massive meniscal defect. *Stem Cells.* 2009;27(4):878-887. doi:10.1634/stemcells.2008-0616
 109. Hatsushika D, Muneta T, Horie M, Koga H, Tsuji K, Sekiya I. Intraarticular injection of synovial stem cells promotes meniscal regeneration in a rabbit massive meniscal defect model. *J Orthop Res.* 2013;31(9):1354-1359.

- doi:10.1002/jor.22370
110. Hatsushika D, Muneta T, Nakamura T, et al. Repetitive allogeneic intraarticular injections of synovial mesenchymal stem cells promote meniscus regeneration in a porcine massive meniscus defect model. *Osteoarthr Cartil.* 2014;22(7):941-950. doi:10.1016/j.joca.2014.04.028
 111. Nakagawa Y, Muneta T, Kondo S, et al. Synovial mesenchymal stem cells promote healing after meniscal repair in microminipigs. *Osteoarthr Cartil.* 2015;23(6):1007-1017. doi:10.1016/j.joca.2015.02.008
 112. Fraser JK, Wulur I, Alfonso Z, Hedrick MH. Fat tissue: an underappreciated source of stem cells for biotechnology. *Trends Biotechnol.* 2006;24(4):150-154. doi:10.1016/j.tibtech.2006.01.010
 113. Baek J, Sovani S, Choi W, Jin S, Grogan SP, D'Lima DD. Meniscal Tissue Engineering Using Aligned Collagen Fibrous Scaffolds: Comparison of Different Human Cell Sources. *Tissue Eng Part A.* 2018;24(1-2):81-93. doi:10.1089/ten.TEA.2016.0205
 114. Ruiz-Ibán MÁ, Díaz-Heredia J, García-Gómez I, Gonzalez-Lizán F, Elías-Martín E, Abraira V. The effect of the addition of adipose-derived mesenchymal stem cells to a meniscal repair in the avascular zone: an experimental study in rabbits. *Arthroscopy.* 2011;27(12):1688-1696. doi:10.1016/j.arthro.2011.06.041
 115. Pak J, Lee JH, Lee SH. Regenerative repair of damaged meniscus with autologous adipose tissue-derived stem cells. *Biomed Res Int.* 2014;2014:436029. doi:10.1155/2014/436029
 116. Gunja NJ, Athanasiou KA. Effects of co-cultures of meniscus cells and articular chondrocytes on PLLA scaffolds. *Biotechnol Bioeng.* 2009;103(4):808-816. doi:10.1002/bit.22301
 117. Wu L, Prins H-J, Helder MN, van Blitterswijk CA, Karperien M. Trophic Effects of Mesenchymal Stem Cells in Chondrocyte Co-Cultures are Independent of Culture Conditions and Cell Sources. *Tissue Eng Part A.* 2012;18(15-16):1542-1551. doi:10.1089/ten.tea.2011.0715
 118. Cui X, Hasegawa A, Lotz M, D'Lima D. Structured three-dimensional co-

- culture of mesenchymal stem cells with meniscus cells promotes meniscal phenotype without hypertrophy. *Biotechnol Bioeng.* 2012;109(9):2369-2380. doi:10.1002/bit.24495
119. Matthies N-F, Mulet-Sierra A, Jomha NM, Adesida AB. Matrix formation is enhanced in co-cultures of human meniscus cells with bone marrow stromal cells. *J Tissue Eng Regen Med.* 2013;7(12):965-973. doi:10.1002/term.1489
 120. McCorry MC, Bonassar LJ. Fiber development and matrix production in tissue-engineered menisci using bovine mesenchymal stem cells and fibrochondrocytes. *Connect Tissue Res.* 2017;58(3-4):329-341. doi:10.1080/03008207.2016.1267152
 121. Wang J, Wright KT, Perry J, et al. Combined Autologous Chondrocyte and Bone Marrow Mesenchymal Stromal Cell Implantation in the Knee: An 8-year Follow Up of Two First-In-Man Cases. *Cell Transplant.* 2019;28(7):924-931. doi:10.1177/0963689719845328
 122. Guo W, Liu S, Zhu Y, et al. Advances and Prospects in Tissue-Engineered Meniscal Scaffolds for Meniscus Regeneration. *Stem Cells Int.* 2015;2015:517520. doi:10.1155/2015/517520
 123. Sandmann GH, Adamczyk C, Grande Garcia E, et al. Biomechanical comparison of menisci from different species and artificial constructs. *BMC Musculoskelet Disord.* 2013;14:324. doi:10.1186/1471-2474-14-324
 124. Park SH, Kim TG, Kim HC, Yang D-Y, Park TG. Development of dual scale scaffolds via direct polymer melt deposition and electrospinning for applications in tissue regeneration. *Acta Biomater.* 2008;4(5):1198-1207. doi:10.1016/j.actbio.2008.03.019
 125. Agrawal CM, Ray RB. Biodegradable polymeric scaffolds for musculoskeletal tissue engineering. *J Biomed Mater Res.* 2001;55(2):141-150. doi:10.1002/1097-4636(200105)55:2<141::aid-jbm1000>3.0.co;2-j
 126. Kang S-W, Son S-M, Lee J-S, et al. Regeneration of whole meniscus using meniscal cells and polymer scaffolds in a rabbit total meniscectomy model. *J Biomed Mater Res A.* 2006;77(4):659-671. doi:10.1002/jbm.a.30579
 127. Kweon H, Yoo MK, Park IK, et al. A novel degradable polycaprolactone

- networks for tissue engineering. *Biomaterials*. 2003;24(5):801-808.
doi:10.1016/s0142-9612(02)00370-8
128. Zhang Z-Z, Wang S-J, Zhang J-Y, et al. 3D-Printed Poly(ϵ -caprolactone) Scaffold Augmented With Mesenchymal Stem Cells for Total Meniscal Substitution: A 12- and 24-Week Animal Study in a Rabbit Model. *Am J Sports Med*. 2017;45(7):1497-1511. doi:10.1177/0363546517691513
129. Tienen TG, Heijkants RGJC, de Groot JH, et al. Replacement of the knee meniscus by a porous polymer implant: a study in dogs. *Am J Sports Med*. 2006;34(1):64-71. doi:10.1177/0363546505280905
130. Rey-Rico A, Cucchiarini M, Madry H. Hydrogels for precision meniscus tissue engineering: a comprehensive review. *Connect Tissue Res*. 2017;58(3-4):317-328. doi:10.1080/03008207.2016.1276576
131. Scotti C, Pozzi A, Mangiavini L, et al. Healing of meniscal tissue by cellular fibrin glue: an in vivo study. *Knee Surg Sports Traumatol Arthrosc*. 2009;17(6):645-651. doi:10.1007/s00167-009-0745-9
132. Narita A, Takahara M, Sato D, et al. Biodegradable gelatin hydrogels incorporating fibroblast growth factor 2 promote healing of horizontal tears in rabbit meniscus. *Arthroscopy*. 2012;28(2):255-263.
doi:10.1016/j.arthro.2011.08.294
133. Rey-Rico A, Klich A, Cucchiarini M, Madry H. Biomedical-grade, high mannuronic acid content (BioMVM) alginate enhances the proteoglycan production of primary human meniscal fibrochondrocytes in a 3-D microenvironment. *Sci Rep*. 2016;6(1):28170. doi:10.1038/srep28170
134. Chen J-P, Cheng T-H. Thermo-responsive chitosan-graft-poly(N-isopropylacrylamide) injectable hydrogel for cultivation of chondrocytes and meniscus cells. *Macromol Biosci*. 2006;6(12):1026-1039.
doi:10.1002/mabi.200600142
135. Simson JA, Strehin IA, Allen BW, Elisseeff JH. Bonding and fusion of meniscus fibrocartilage using a novel chondroitin sulfate bone marrow tissue adhesive. *Tissue Eng Part A*. 2013;19(15-16):1843-1851.
doi:10.1089/ten.TEA.2012.0578

136. Holloway JL, Lowman AM, VanLandingham MR, Palmese GR. Interfacial optimization of fiber-reinforced hydrogel composites for soft fibrous tissue applications. *Acta Biomater.* 2014;10(8):3581-3589.
doi:10.1016/j.actbio.2014.05.004
137. Holloway JL, Lowman AM, Palmese GR. Mechanical evaluation of poly(vinyl alcohol)-based fibrous composites as biomaterials for meniscal tissue replacement. *Acta Biomater.* 2010;6(12):4716-4724.
doi:10.1016/j.actbio.2010.06.025
138. Hayes JC, Curley C, Tierney P, Kennedy JE. Biomechanical analysis of a salt-modified polyvinyl alcohol hydrogel for knee meniscus applications, including comparison with human donor samples. *J Mech Behav Biomed Mater.* 2016;56:156-164. doi:10.1016/j.jmbbm.2015.11.011
139. Hayes JC, Kennedy JE. An evaluation of the biocompatibility properties of a salt-modified polyvinyl alcohol hydrogel for a knee meniscus application. *Mater Sci Eng C.* 2016;59:894-900. doi:10.1016/j.msec.2015.10.052
140. Petri M, Ufer K, Toma I, et al. Effects of perfusion and cyclic compression on in vitro tissue engineered meniscus implants. *Knee Surg Sports Traumatol Arthrosc.* 2012;20(2):223-231. doi:10.1007/s00167-011-1600-3
141. Pillai MM, Gopinathan J, Senthil Kumar R, et al. Tissue engineering of human knee meniscus using functionalized and reinforced silk-polyvinyl alcohol composite three-dimensional scaffolds: Understanding the in vitro and in vivo behavior. *J Biomed Mater Res A.* 2018;106(6):1722-1731.
doi:10.1002/jbm.a.36372
142. Mandal BB, Park S-H, Gil ES, Kaplan DL. Multilayered silk scaffolds for meniscus tissue engineering. *Biomaterials.* 2011;32(2):639-651.
doi:10.1016/j.biomaterials.2010.08.115
143. Crapo PM, Gilbert TW, Badylak SF. An overview of tissue and whole organ decellularization processes. *Biomaterials.* 2011;32(12):3233-3243.
doi:10.1016/j.biomaterials.2011.01.057
144. Chen Y, Chen J, Zhang Z, et al. Current advances in the development of natural meniscus scaffolds: innovative approaches to decellularization and

- recellularization. *Cell Tissue Res.* 2017;370(1):41-52. doi:10.1007/s00441-017-2605-0
145. Maier D, Braeun K, Steinhauser E, et al. In vitro analysis of an allogenic scaffold for tissue-engineered meniscus replacement. *J Orthop Res.* 2007;25(12):1598-1608. doi:10.1002/jor.20405
146. Chen Y-C, Chen R-N, Jhan H-J, et al. Development and Characterization of Acellular Extracellular Matrix Scaffolds from Porcine Menisci for Use in Cartilage Tissue Engineering. *Tissue Eng Part C Methods.* 2015;21(9):971-986. doi:10.1089/ten.TEC.2015.0036
147. Harrison PE, Ashton IK, Johnson WE, Turner SL, Richardson JB, Ashton B a. The in vitro growth of human chondrocytes. *Cell Tissue Bank.* 2000;1(4):255-260. doi:10.1023/A:1010131729208
148. Williams R, Khan IM, Richardson K, et al. Identification and clonal characterisation of a progenitor cell sub-population in normal human articular cartilage. *PLoS One.* 2010;5(10):e13246. doi:10.1371/journal.pone.0013246
149. Jones PH, Watt FM. Separation of human epidermal stem cells from transit amplifying cells on the basis of differences in integrin function and expression. *Cell.* 1993;73(4):713-724. doi:10.1016/0092-8674(93)90251-k
150. Narkilahti S, Rajala K, Pihlajamäki H, Suuronen R, Hovatta O, Skottman H. Monitoring and analysis of dynamic growth of human embryonic stem cells: comparison of automated instrumentation and conventional culturing methods. *Biomed Eng Online.* 2007;6:11. doi:10.1186/1475-925X-6-11
151. Adan A, Alizada G, Kiraz Y, Baran Y, Nalbant A. Flow cytometry: basic principles and applications. *Crit Rev Biotechnol.* 2017;37(2):163-176. doi:10.3109/07388551.2015.1128876
152. Dominici M, Le Blanc K, Mueller I, et al. Minimal criteria for defining multipotent mesenchymal stromal cells. The International Society for Cellular Therapy position statement. *Cytotherapy.* 2006;8(4):315-317. doi:10.1080/14653240600855905
153. Battula VL, Treml S, Bareiss PM, et al. Isolation of functionally distinct mesenchymal stem cell subsets using antibodies against CD56, CD271, and

- mesenchymal stem cell antigen-1. *Haematologica*. 2009;94(2):173-184. doi:10.3324/haematol.13740
154. Chang CB, Han SA, Kim EM, Lee S, Seong SC, Lee MC. Chondrogenic potentials of human synovium-derived cells sorted by specific surface markers. *Osteoarthr Cartil*. 2013;21(1):190-199. doi:10.1016/j.joca.2012.10.005
155. Grogan SP, Barbero A, Diaz-Romero J, et al. Identification of markers to characterize and sort human articular chondrocytes with enhanced in vitro chondrogenic capacity. *Arthritis Rheum*. 2007;56(2):586-595. doi:10.1002/art.22408
156. Niemeyer P, Pestka JM, Salzmann GM, Südkamp NP, Schmal H. Influence of cell quality on clinical outcome after autologous chondrocyte implantation. *Am J Sports Med*. 2012;40(3):556-561. doi:10.1177/0363546511428879
157. Cicione C, Díaz-Prado S, Muiños-López E, Hermida-Gómez T, Blanco FJ. Molecular profile and cellular characterization of human bone marrow mesenchymal stem cells: Donor influence on chondrogenesis. *Differentiation*. 2010;80(2-3):155-165. doi:10.1016/j.diff.2010.06.001
158. Hemler ME. VLA proteins in the integrin family: structures, functions, and their role on leukocytes. *Annu Rev Immunol*. 1990;8(1):365-400. doi:10.1146/annurev.iy.08.040190.002053
159. Bourin P, Bunnell BA, Casteilla L, et al. Stromal cells from the adipose tissue-derived stromal vascular fraction and culture expanded adipose tissue-derived stromal/stem cells: a joint statement of the International Federation for Adipose Therapeutics and Science (IFATS) and the International So. *Cytotherapy*. 2013;15(6):641-648. doi:10.1016/j.jcyt.2013.02.006
160. Johnstone B, Hering TM, Caplan AI, Goldberg VM, Yoo JU. In vitro chondrogenesis of bone marrow-derived mesenchymal progenitor cells. *Exp Cell Res*. 1998;238(1):265-272. doi:10.1006/excr.1997.3858
161. Farndale RW, Buttle DJ, Barrett AJ. Improved quantitation and discrimination of sulphated glycosaminoglycans by use of dimethylmethylene blue. *Biochim Biophys Acta*. 1986;883(2):173-177. doi:10.1016/0304-4165(86)90306-5
162. Dragan AI, Casas-Finet JR, Bishop ES, Strouse RJ, Schenerman MA, Geddes

- CD. Characterization of PicoGreen interaction with dsDNA and the origin of its fluorescence enhancement upon binding. *Biophys J*. 2010;99(9):3010-3019. doi:10.1016/j.bpj.2010.09.012
163. Schmittgen TD, Livak KJ. Analyzing real-time PCR data by the comparative CT method. *Nat Protoc*. 2008;3(6):1101-1108. doi:10.1038/nprot.2008.73
164. Roberts S, Menage J. Microscopic Methods for the Analysis of Engineered Tissues. In: *Biopolymer Methods in Tissue Engineering*. Vol 238. Humana Press; 2004:171-196. doi:10.1385/1-59259-428-X:171
165. Crowe AR, Yue W. Semi-quantitative Determination of Protein Expression using Immunohistochemistry Staining and Analysis: An Integrated Protocol. *Bio-protocol*. 2019;9(24). doi:10.21769/BioProtoc.3465
166. Undas A, Ariëns RAS. Fibrin clot structure and function: a role in the pathophysiology of arterial and venous thromboembolic diseases. *Arterioscler Thromb Vasc Biol*. 2011;31(12):e88-99. doi:10.1161/ATVBAHA.111.230631
167. Li Y, Meng H, Liu Y, Lee BP. Fibrin Gel as an Injectable Biodegradable Scaffold and Cell Carrier for Tissue Engineering. *Sci World J*. 2015;2015:1-10. doi:10.1155/2015/685690
168. Kattula S, Byrnes JR, Wolberg AS. Fibrinogen and Fibrin in Hemostasis and Thrombosis. *Arterioscler Thromb Vasc Biol*. 2017;37(3):e13-e21. doi:10.1161/ATVBAHA.117.308564
169. Titze IR, Svec JG, Popolo PS. Vocal dose measures: quantifying accumulated vibration exposure in vocal fold tissues. *J Speech Lang Hear Res*. 2003;46(4):919-932. doi:10.1044/1092-4388(2003/072)
170. Lord ST. Molecular Mechanisms Affecting Fibrin Structure and Stability. *Arterioscler Thromb Vasc Biol*. 2011;31(3):494-499. doi:10.1161/ATVBAHA.110.213389
171. MacMullan PA, McCarthy GM. The meniscus, calcification and osteoarthritis: a pathologic team. *Arthritis Res Ther*. 2010;12(3):116. doi:10.1186/ar2993
172. Bennett LD, Buckland-Wright JC. Meniscal and articular cartilage changes in knee osteoarthritis: a cross-sectional double-contrast macroradiographic study. *Rheumatology (Oxford)*. 2002;41(8):917-923.

- doi:10.1093/rheumatology/41.8.917
173. Hunter DJ, Zhang YQ, Niu JB, et al. The association of meniscal pathologic changes with cartilage loss in symptomatic knee osteoarthritis. *Arthritis Rheum.* 2006;54(3):795-801. doi:10.1002/art.21724
 174. Battistelli M, Favero M, Burini D, et al. Morphological and ultrastructural analysis of normal, injured and osteoarthritic human knee menisci. *Eur J Histochem.* 2019;63(1):17-23. doi:10.4081/ejh.2019.2998
 175. López-Franco M, Gómez-Barrena E. Cellular and molecular meniscal changes in the degenerative knee: a review. *J Exp Orthop.* 2018;5(1):11. doi:10.1186/s40634-018-0126-8
 176. Ghadially FN, Lalonde JM, Wedge JH. Ultrastructure of normal and torn menisci of the human knee joint. *J Anat.* 1983;136(Pt 4):773-791. <http://www.ncbi.nlm.nih.gov/pubmed/6688412>
 177. Muhammad H, Schminke B, Bode C, et al. Human migratory meniscus progenitor cells are controlled via the TGF- β pathway. *Stem cell reports.* 2014;3(5):789-803. doi:10.1016/j.stemcr.2014.08.010
 178. Grogan SP, Pauli C, Lotz MK, D'Lima DD. Relevance of meniscal cell regional phenotype to tissue engineering. *Connect Tissue Res.* 2017;58(3-4):259-270. doi:10.1080/03008207.2016.1268604
 179. Son M, Levenston M. Discrimination of meniscal cell phenotypes using gene expression profiles. *Eur Cells Mater.* 2012;23:195-208. doi:10.22203/eCM.v023a15
 180. Bloecker K, Wirth W, Hudelmaier M, Burgkart R, Frobell R, Eckstein F. Morphometric Differences between the Medial and Lateral Meniscus in Healthy Men – A Three-Dimensional Analysis Using Magnetic Resonance Imaging. *Cells Tissues Organs.* 2012;195(4):353-364. doi:10.1159/000327012
 181. Niu W, Guo W, Han S, Zhu Y, Liu S, Guo Q. Cell-Based Strategies for Meniscus Tissue Engineering. *Stem Cells Int.* 2016;2016:4717184. doi:10.1155/2016/4717184
 182. Martinek V, Ueblacker P, Bräun K, et al. Second generation of meniscus transplantation: in-vivo study with tissue engineered meniscus replacement.

- Arch Orthop Trauma Surg.* 2006;126(4):228-234. doi:10.1007/s00402-005-0025-1
183. Wang J, Roberts S, Kuiper JH, et al. Characterization of regional meniscal cell and chondrocyte phenotypes and chondrogenic differentiation with histological analysis in osteoarthritic donor-matched tissues. *Sci Rep.* 2020;10(1):21658. doi:10.1038/s41598-020-78757-6
184. Mennan C, Garcia J, McCarthy H, et al. Human Articular Chondrocytes Retain Their Phenotype in Sustained Hypoxia While Normoxia Promotes Their Immunomodulatory Potential. *Cartilage.* 2019;10(4):467-479. doi:10.1177/1947603518769714
185. Howell R, Kumar NS, Patel N, Tom J. Degenerative meniscus: Pathogenesis, diagnosis, and treatment options. *World J Orthop.* 2014;5(5):597-602. doi:10.5312/wjo.v5.i5.597
186. Kumar D, Manal KT, Rudolph KS. Knee joint loading during gait in healthy controls and individuals with knee osteoarthritis. *Osteoarthr Cartil.* 2013;21(2):298-305. doi:10.1016/j.joca.2012.11.008
187. Li L, Yang X, Yang L, et al. Biomechanical analysis of the effect of medial meniscus degenerative and traumatic lesions on the knee joint. *Am J Transl Res.* 2019;11(2):542-556. <http://www.ncbi.nlm.nih.gov/pubmed/30899361>
188. Alsalameh S, Amin R, Gemba T, Lotz M. Identification of mesenchymal progenitor cells in normal and osteoarthritic human articular cartilage. *Arthritis Rheum.* 2004;50(5):1522-1532. doi:10.1002/art.20269
189. Osawa A, Harner CD, Gharraibeh B, et al. The use of blood vessel-derived stem cells for meniscal regeneration and repair. *Med Sci Sports Exerc.* 2013;45(5):813-823. doi:10.1249/MSS.0b013e31827d1e06
190. Fickert S, Fiedler J, Brenner R. Identification, quantification and isolation of mesenchymal progenitor cells from osteoarthritic synovium by fluorescence automated cell sorting. *Osteoarthr Cartil.* 2003;11(11):790-800. doi:10.1016/S1063-4584(03)00167-5
191. Iannone F, Lapadula G. The pathophysiology of osteoarthritis. *Aging Clin Exp Res.* 2003;15(5):364-372. doi:10.1007/BF03327357

192. Almonte-Becerril M, Costell M, Kouri JB. Changes in the integrins expression are related with the osteoarthritis severity in an experimental animal model in rats. *J Orthop Res.* 2014;32(9):1161-1166. doi:10.1002/jor.22649
193. Yang X, Zhao J, He Y, Huangfu X. Screening for characteristic genes in osteoarthritis induced by destabilization of the medial meniscus utilizing bioinformatics approach. *J Musculoskelet Neuronal Interact.* 2014;14(3):343-348. <http://www.ncbi.nlm.nih.gov/pubmed/25198230>
194. Cao L, Lee V, Adams ME, et al. β 1-Integrin–collagen interaction reduces chondrocyte apoptosis. *Matrix Biol.* 1999;18(4):343-355.
195. Tallheden T, Karlsson C, Brunner A, et al. Gene expression during redifferentiation of human articular chondrocytes. *Osteoarthr Cartil.* 2004;12(7):525-535. doi:10.1016/j.joca.2004.03.004
196. Prosser A, Scotchford C, Roberts G, Grant D, Sottile V. Integrated Multi-Assay Culture Model for Stem Cell Chondrogenic Differentiation. *Int J Mol Sci.* 2019;20(4):951. doi:10.3390/ijms20040951
197. McAlindon TE, Snow S, Cooper C, Dieppe PA. Radiographic patterns of osteoarthritis of the knee joint in the community: the importance of the patellofemoral joint. *Ann Rheum Dis.* 1992;51(7):844-849. doi:10.1136/ard.51.7.844
198. Hommen JP, Applegate GR, Del Pizzo W. Meniscus allograft transplantation: ten-year results of cryopreserved allografts. *Arthroscopy.* 2007;23(4):388-393. doi:10.1016/j.arthro.2006.11.032
199. Rath E, Richmond JC. The menisci: basic science and advances in treatment. *Br J Sports Med.* 2000;34(4):252-257. doi:10.1136/bjism.34.4.252
200. Guo W, Xu W, Wang Z, et al. Cell-Free Strategies for Repair and Regeneration of Meniscus Injuries through the Recruitment of Endogenous Stem/Progenitor Cells. *Stem Cells Int.* 2018;2018:5310471. doi:10.1155/2018/5310471
201. Shimomura K, Hamamoto S, Hart DA, Yoshikawa H, Nakamura N. Meniscal repair and regeneration: Current strategies and future perspectives. *J Clin Orthop trauma.* 2018;9(3):247-253. doi:10.1016/j.jcot.2018.07.008
202. Seol D, Zhou C, Brouillette MJ, et al. Characteristics of meniscus progenitor

- cells migrated from injured meniscus. *J Orthop Res.* 2017;35(9):1966-1972. doi:10.1002/jor.23472
203. Huang H, Wang S, Gui J, Shen H. A study to identify and characterize the stem/progenitor cell in rabbit meniscus. *Cytotechnology.* 2016;68(5):2083-2103. doi:10.1007/s10616-016-9949-2
204. Gamer LW, Shi RR, Gendelman A, Mathewson D, Gamer J, Rosen V. Identification and characterization of adult mouse meniscus stem/progenitor cells. *Connect Tissue Res.* 2017;58(3-4):238-245. doi:10.1080/03008207.2016.1271797
205. Bush P., Hall A. The volume and morphology of chondrocytes within non-degenerate and degenerate human articular cartilage. *Osteoarthr Cartil.* 2003;11(4):242-251. doi:10.1016/S1063-4584(02)00369-2
206. Hall AC. The Role of Chondrocyte Morphology and Volume in Controlling Phenotype—Implications for Osteoarthritis, Cartilage Repair, and Cartilage Engineering. *Curr Rheumatol Rep.* 2019;21(8):38. doi:10.1007/s11926-019-0837-6
207. Pitman M, Emery B, Binder M, Wang S, Butzkueven H, Kilpatrick TJ. LIF receptor signaling modulates neural stem cell renewal. *Mol Cell Neurosci.* 2004;27(3):255-266. doi:10.1016/j.mcn.2004.07.004
208. Skobin V, Jelkmann W, Morschakova E, Pavlov AD, Schlenke P. Tumor Necrosis Factor- α and TNF- β Inhibit Clonogenicity of Mobilized Human Hematopoietic Progenitors. *J Interf Cytokine Res.* 2000;20(5):507-510. doi:10.1089/10799900050023924
209. Li L, Wang BH, Wang S, et al. Individual cell movement, asymmetric colony expansion, Rho-associated kinase, and E-cadherin impact the clonogenicity of human embryonic stem cells. *Biophys J.* 2010;98(11):2442-2451. doi:10.1016/j.bpj.2010.02.029
210. Chan RWS, Schwab KE, Gargett CE. Clonogenicity of human endometrial epithelial and stromal cells. *Biol Reprod.* 2004;70(6):1738-1750. doi:10.1095/biolreprod.103.024109
211. Shen W, Chen J, Zhu T, et al. Intra-Articular Injection of Human Meniscus

- Stem/Progenitor Cells Promotes Meniscus Regeneration and Ameliorates Osteoarthritis Through Stromal Cell-Derived Factor-1/CXCR4-Mediated Homing. *Stem Cells Transl Med.* 2014;3(3):387-394. doi:10.5966/sctm.2012-0170
212. Buckley CD, Filer A. Fibroblasts and Fibroblast-like Synoviocytes. In: *Kelley and Firestein's Textbook of Rheumatology*. Elsevier; 2017:231-249.e4. doi:10.1016/B978-0-323-31696-5.00014-0
213. Koelling S, Kruegel J, Irmer M, et al. Migratory Chondrogenic Progenitor Cells from Repair Tissue during the Later Stages of Human Osteoarthritis. *Cell Stem Cell.* 2009;4(4):324-335. doi:10.1016/j.stem.2009.01.015
214. Jayasuriya CT, Hu N, Li J, et al. Molecular characterization of mesenchymal stem cells in human osteoarthritis cartilage reveals contribution to the OA phenotype. *Sci Rep.* 2018;8(1):1-14. doi:10.1038/s41598-018-25395-8
215. Kiraly AJ, Roberts A, Cox M, Mauerhan D, Hanley E, Sun Y. Comparison of Meniscal Cell-Mediated and Chondrocyte-Mediated Calcification. *Open Orthop J.* 2017;11(1):225-233. doi:10.2174/1874325001711010225
216. Benya P. Dedifferentiated chondrocytes reexpress the differentiated collagen phenotype when cultured in agarose gels. *Cell.* 1982;30(1):215-224. doi:10.1016/0092-8674(82)90027-7
217. Lee J, Lee JY, Chae BC, Jang J, Lee EA, Son Y. Fully Dedifferentiated Chondrocytes Expanded in Specific Mesenchymal Stem Cell Growth Medium with FGF2 Obtains Mesenchymal Stem Cell Phenotype In Vitro but Retains Chondrocyte Phenotype In Vivo. *Cell Transplant.* 2017;26(10):1673-1687. doi:10.1177/0963689717724794
218. Petty CA, Lubowitz JH. Does Arthroscopic Partial Meniscectomy Result in Knee Osteoarthritis? A Systematic Review With a Minimum of 8 Years' Follow-up. *Arthrosc J Arthrosc Relat Surg.* 2011;27(3):419-424. doi:10.1016/j.arthro.2010.08.016
219. Waugh N, Mistry H, Metcalfe A, et al. Meniscal allograft transplantation after meniscectomy: clinical effectiveness and cost-effectiveness. *Knee Surgery, Sport Traumatol Arthrosc.* 2019;27(6):1825-1839. doi:10.1007/s00167-019-

05504-4

220. Parkinson B, Smith N, Asplin L, Thompson P, Spalding T. Factors Predicting Meniscal Allograft Transplantation Failure. *Orthop J Sport Med.* 2016;4(8):2325967116663185. doi:10.1177/2325967116663185
221. Roberson TA, Wyland DJ, T.A. R, D.J. W. Meniscal Allograft Transplantation With Soft Tissue in Bone Socket Fixation: Arthroscopic Technique With Technical Pearls. *Arthrosc Tech.* 2017;6(2):e483-e489. doi:10.1016/j.eats.2016.11.009
222. Kim I, Lee SK, Yoon JI, Kim DE, Kim M, Ha H. Fibrin Glue Improves the Therapeutic Effect of MSCs by Sustaining Survival and Paracrine Function. *Tissue Eng Part A.* 2013;19(21-22):2373-2381. doi:10.1089/ten.tea.2012.0665
223. Jang JD, Moon YS, Kim YS, et al. Novel repair technique for articular cartilage defect using a fibrin and hyaluronic acid mixture. *Tissue Eng Regen Med.* 2013;10(1):1-9. doi:10.1007/s13770-013-0361-0
224. Toanen C, Dhollander A, Bulgheroni P, et al. Polyurethane Meniscal Scaffold for the Treatment of Partial Meniscal Deficiency: 5-Year Follow-up Outcomes: A European Multicentric Study. *Am J Sports Med.* 2020;48(6):1347-1355. doi:10.1177/0363546520913528
225. Lin H -B, Sun W, Mosher DF, et al. Synthesis, surface, and cell-adhesion properties of polyurethanes containing covalently grafted RGD-peptides. *J Biomed Mater Res.* 1994;28(3):329-342. doi:10.1002/jbm.820280307
226. Ahmed TAE, Dare E V., Hincke M. Fibrin: A versatile scaffold for tissue engineering applications. *Tissue Eng - Part B Rev.* 2008;14(2):199-215. doi:10.1089/ten.teb.2007.0435
227. Bichara DA, Zhao X, Bodugoz-Senturk H, et al. Porous Poly(Vinyl Alcohol)-Hydrogel Matrix-Engineered Biosynthetic Cartilage. *Tissue Eng Part A.* 2011;17(3-4):301-309. doi:10.1089/ten.tea.2010.0322
228. Clark EL, Bush SJ, McCulloch MEB, et al. A high resolution atlas of gene expression in the domestic sheep (*Ovis aries*). Kijas J, ed. *PLoS Genet.* 2017;13(9):e1006997. doi:10.1371/journal.pgen.1006997
229. Tarafder S, Park G, Lee CH. Explant models for meniscus metabolism, injury,

- repair, and healing. *Connect Tissue Res.* 2019;00(00):1-12.
doi:10.1080/03008207.2019.1702031
230. Pawelec KM, Best SM, Cameron RE, Wardale RJ. Scaffold architecture and fibrin gels promote meniscal cell proliferation. *APL Mater.* 2015;3(1).
doi:10.1063/1.4900885
231. Mühleder S, Pill K, Schaupper M, et al. The role of fibrinolysis inhibition in engineered vascular networks derived from endothelial cells and adipose-derived stem cells. *Stem Cell Res Ther.* 2018;9(1):1-13. doi:10.1186/s13287-017-0764-2
232. Lorentz KM, Kontos S, Frey P, Hubbell JA. Engineered aprotinin for improved stability of fibrin biomaterials. *Biomaterials.* 2011;32(2):430-438.
doi:10.1016/j.biomaterials.2010.08.109
233. Salzmann GM, Calek AK, Preiss S. Second-Generation Autologous Minced Cartilage Repair Technique. *Arthrosc Tech.* 2017;6(1):e127-e131.
doi:10.1016/j.eats.2016.09.011
234. Kearns SM, Kuhar HN, Bohl DD, Levine BR. An Aprotinin Containing Fibrin Sealant Does Not Reduce Blood Loss in Total Hip Arthroplasty. *J Arthroplasty.* 2017;32(11):3445-3448. doi:10.1016/j.arth.2017.05.040
235. Patil S, Shekhar A, Tapasvi S. Meniscal preservation is important for the knee joint. *Indian J Orthop.* 2017;51(5):576-587. doi:10.4103/ortho.IJOrtho_247_17
236. Jiang D, Ao Y-F, Gong X, Wang Y-J, Zheng Z-Z, Yu J-K. Comparative study on immediate versus delayed meniscus allograft transplantation: 4- to 6-year follow-up. *Am J Sports Med.* 2014;42(10):2329-2337.
doi:10.1177/0363546514541653
237. Matthies N-F, Mulet-Sierra A, Jomha NM, Adesida AB. Matrix formation is enhanced in co-cultures of human meniscus cells with bone marrow stromal cells. *J Tissue Eng Regen Med.* 2013;7(12):965-973. doi:10.1002/term.1489
238. de Windt T, Vonk L, Slaper-Crtenbach I, et al. Allogeneic MSCs and recycled autologous chondrons mixed in a one-stage cartilage cell transplantation: a first-in-man trial in 35 patients. *Stem Cells.* 2017;35(8):1984-1993.
239. Hagmeijer MH, Vonk LA, Fenu M, Van Keep YWAM, Krych AJ, Saris DBF.

- Meniscus regeneration combining meniscus and mesenchymal stromal cells in a degradable meniscus implant: An in vitro study. *Eur Cells Mater.* 2019;38:51-62. doi:10.22203/eCM.v038a05
240. Numpaisal P on, Rothrauff BB, Gottardi R, Chien CL, Tuan RS. Rapidly dissociated autologous meniscus tissue enhances meniscus healing: An in vitro study. *Connect Tissue Res.* 2017;58(3-4):355-365. doi:10.1080/03008207.2016.1245727
241. Abbasi N, Lee RSB, Ivanovski S, Love RM, Hamlet S. In vivo bone regeneration assessment of offset and gradient melt electrowritten (MEW) PCL scaffolds. *Biomater Res.* 2020;24(1):1-24. doi:10.1186/s40824-020-00196-1
242. Noyes FR, Bassett RW, Grood ES, Butler DL. Arthroscopy in acute traumatic hemarthrosis of the knee. Incidence of anterior cruciate tears and other injuries. *J Bone Joint Surg Am.* 1980;62(5):687-695, 757. doi:10.2106/00004623-198062050-00001
243. Lohmander LS, Englund PM, Dahl LL, Roos EM. The long-term consequence of anterior cruciate ligament and meniscus injuries: osteoarthritis. *Am J Sports Med.* 2007;35(10):1756-1769. doi:10.1177/0363546507307396
244. Gioe TJ, Novak C, Sinner P, Ma W, Mehle S. Knee arthroplasty in the young patient: Survival in a community registry. In: *Clinical Orthopaedics and Related Research.* Vol 464. Lippincott Williams and Wilkins; 2007:83-87. doi:10.1097/BLO.0b013e31812f79a9
245. Lee SM, Bin S Il, Kim JM, et al. Long-term Outcomes of Meniscal Allograft Transplantation With and Without Extrusion: Mean 12.3-Year Follow-up Study. *Am J Sports Med.* 2019;47(4):815-821. doi:10.1177/0363546518825251
246. Bhosale AM, Kuiper JH, Johnson WEB, Harrison PE, Richardson JB. Midterm to Long-Term Longitudinal Outcome of Autologous Chondrocyte Implantation in the Knee Joint: A multilevel analysis. *Am J Sports Med.* 2009;37(1_suppl):131-138. doi:10.1177/0363546509350555
247. Nawaz SZ, Bentley G, Briggs TWR, et al. Autologous chondrocyte implantation in the knee: mid-term to long-term results. *JBJS.* 2014;96(10):824-830.

248. Farr J, Rawal A, Marberry KM. Concomitant meniscal allograft transplantation and autologous chondrocyte implantation: Minimum 2-year follow-up. *Am J Sports Med.* 2007;35(9):1459-1466. doi:10.1177/0363546507301257
249. Ogura T, Bryant T, Minas T. Biological Knee Reconstruction With Concomitant Autologous Chondrocyte Implantation and Meniscal Allograft Transplantation: Mid- to Long-term Outcomes. *Orthop J Sport Med.* 2016;4(10):2325967116668490. doi:10.1177/2325967116668490
250. Bhosale AM, Myint P, Roberts S, et al. Combined autologous chondrocyte implantation and allogenic meniscus transplantation: A biological knee replacement. *Knee.* 2007;14(5):361-368. doi:10.1016/j.knee.2007.07.002
251. Talkhani IS, Richardson JB. Knee diagram for the documentation of arthroscopic findings of the knee - Cadaveric study. *Knee.* 1999;6(2):95-101. doi:10.1016/S0968-0160(98)00018-0
252. Hirschmüller A, Baur H, Braun S, Kreuz PC, Südkamp NP, Niemeyer P. Rehabilitation after autologous chondrocyte implantation for isolated cartilage defects of the knee. *Am J Sports Med.* 2011;39(12):2686-2696. doi:10.1177/0363546511404204
253. Smith HJ, Richardson JB, Tennant A. Modification and validation of the Lysholm Knee Scale to assess articular cartilage damage. *Osteoarthr Cartil.* 2009;17(1):53-58. doi:10.1016/j.joca.2008.05.002
254. Faivre B, Boisrenoult P, Lonjon G, Pujol N, Beaufils P. Lateral meniscus allograft transplantation: Clinical and anatomic outcomes after arthroscopic implantation with tibial tunnels versus open implantation without tunnels. *Orthop Traumatol Surg Res.* 2014;100(3):297-302. doi:10.1016/j.otsr.2014.01.007
255. Roberts S, McCall IW, Darby AJ, et al. Autologous chondrocyte implantation for cartilage repair: monitoring its success by magnetic resonance imaging and histology. *Arthritis Res Ther.* 2003;5(1). doi:10.1186/ar613
256. Leroy A, Beaufils P, Faivre B, Steltzlen C, Boisrenoult P, Pujol N. Actifit® polyurethane meniscal scaffold: MRI and functional outcomes after a minimum follow-up of 5 years. *Orthop Traumatol Surg Res.* 2017;103(4):609-614.

- doi:10.1016/j.otsr.2017.02.012
257. Winkler PW, Rothrauff BB, Buerba RA, et al. Meniscal substitution, a developing and long-awaited demand. *J Exp Orthop*. 2020;7(1). doi:10.1186/s40634-020-00270-6
258. Jiménez-Garrido C, Gómez-Cáceres A, Espejo-Reina MJ, et al. Obesity and Meniscal Transplant Failure: A Retrospective Cohort Study. *J Knee Surg*. Published online August 21, 2019. doi:10.1055/s-0039-1695041
259. Faivre B, Bouyarmine H, Lonjon G, Boisrenoult P, Pujol N, Beaufils P. Actifit® scaffold implantation: Influence of preoperative meniscal extrusion on morphological and clinical outcomes. *Orthop Traumatol Surg Res*. 2015;101(6):703-708. doi:10.1016/j.otsr.2015.06.016
260. Jang SH, Kim JG, Ha JG, Shim JC. Reducing the size of the meniscal allograft decreases the percentage of extrusion after meniscal allograft transplantation. *Arthroscopy*. 2011;27(7):914-922. doi:10.1016/j.arthro.2011.02.017
261. De Coninck T, Huysse W, Willemot L, Verdonk R, Verstraete K, Verdonk P. Two-year follow-up study on clinical and radiological outcomes of polyurethane meniscal scaffolds. *Am J Sports Med*. 2013;41(1):67-72. doi:10.1177/0363546512463344
262. Cook AE, Stoker AM, Leary E V., Pfeiffer FM, Cook JL. Metabolic responses of meniscal explants to injury and inflammation ex vivo. *J Orthop Res*. 2018;36(10):2657-2663. doi:10.1002/jor.24045
263. Liu B, Goode AP, Carter TE, et al. Matrix metalloproteinase activity and prostaglandin E2 are elevated in the synovial fluid of meniscus tear patients. *Connect Tissue Res*. 2017;58(3-4):305-316. doi:10.1080/03008207.2016.1256391
264. Hayashi D, Englund M, Roemer FW, et al. Knee malalignment is associated with an increased risk for incident and enlarging bone marrow lesions in the more loaded compartments: The MOST study. *Osteoarthr Cartil*. 2012;20(11):1227-1233. doi:10.1016/j.joca.2012.07.020
265. Teichtahl AJ, Cicuttini FM, Abram F, et al. Meniscal extrusion and bone marrow lesions are associated with incident and progressive knee osteoarthritis.

- Osteoarthr Cartil.* 2017;25(7):1076-1083. doi:10.1016/j.joca.2017.02.792
266. Edd SN, Netravali NA, Favre J, Giori NJ, Andriacchi TP. Alterations in Knee Kinematics After Partial Medial Meniscectomy Are Activity Dependent. *Am J Sports Med.* 2015;43(6):1399-1407. doi:10.1177/0363546515577360
267. Sturme DL, Besier TF, Mills PM, et al. Knee joint biomechanics following arthroscopic partial meniscectomy. *J Orthop Res.* 2008;26(8):1075-1080. doi:10.1002/jor.20610
268. Rodeo SA, Monibi F, Dehghani B, Maher S. Biological and Mechanical Predictors of Meniscus Function: Basic Science to Clinical Translation. *J Orthop Res.* 2020;38(5):937-945. doi:10.1002/jor.24552
269. Mabey T, Honsawek S. Cytokines as biochemical markers for knee osteoarthritis. *World J Orthop.* 2015;6(1):95-105. doi:10.5312/wjo.v6.i1.95
270. Stone A V., Loeser RF, Vanderman KS, Long DL, Clark SC, Ferguson CM. Pro-inflammatory stimulation of meniscus cells increases production of matrix metalloproteinases and additional catabolic factors involved in osteoarthritis pathogenesis. *Osteoarthr Cartil.* 2014;22(2):264-274. doi:10.1016/j.joca.2013.11.002
271. Johnson CI, Argyle DJ, Clements DN. In vitro models for the study of osteoarthritis. *Vet J.* 2016;209:40-49. doi:10.1016/j.tvjl.2015.07.011
272. Horie M, Driscoll MD, Sampson HW, et al. Implantation of allogenic synovial stem cells promotes meniscal regeneration in a rabbit meniscal defect model. *J Bone Joint Surg Am.* 2012;94(8):701-712. doi:10.2106/JBJS.K.00176
273. Mesenchymal Stromal Cells for Degenerative Meniscus Injury. Accessed January 15, 2021. <https://clinicaltrials.gov/ct2/show/study/NCT02033525?term=cell+therapy&cond=meniscus&draw=2&rank=1>
274. Safety Observation on hESC Derived MSC Like Cell for the Meniscus Injury. Accessed January 15, 2021. <https://clinicaltrials.gov/ct2/show/NCT03839238?term=cell+therapy&cond=meniscus&draw=1&rank=4>
275. Malanga GA, Chirichella PS, Hogaboom NS, Capella T. Clinical evaluation of

- micro-fragmented adipose tissue as a treatment option for patients with meniscus tears with osteoarthritis: a prospective pilot study. *Int Orthop*. Published online 2020. doi:10.1007/s00264-020-04835-z
276. Ultrasound-Guided Injections for Meniscal Injuries in Active-Duty Military. Accessed January 15, 2021.
<https://clinicaltrials.gov/ct2/show/NCT04274543?term=cell+therapy&cond=m+eniscus&draw=1&rank=5>
277. Yu Y, Alkhwaji A, Ding Y, Mei J. Decellularized scaffolds in regenerative medicine. *Oncotarget*. 2016;7(36):58671-58683.
doi:10.18632/oncotarget.10945
278. Sakaguchi Y, Sekiya I, Yagishita K, Muneta T. Comparison of human stem cells derived from various mesenchymal tissues: Superiority of synovium as a cell source. *Arthritis Rheum*. 2005;52(8):2521-2529. doi:10.1002/art.21212
279. Jacob G, Shimomura K, Krych AJ, Nakamura N. The Meniscus Tear: A Review of Stem Cell Therapies. *Cells*. 2019;9(1):1-17.
doi:10.3390/cells9010092
280. Woodmass JM, LaPrade RF, Sgaglione NA, Nakamura N, Krych AJ. Meniscal Repair: Reconsidering Indications, Techniques, and Biologic Augmentation. *J Bone Joint Surg Am*. 2017;99(14):1222-1231. doi:10.2106/JBJS.17.00297

Appendices

Appendix I



Health Research Authority

NRES Committee North West - Liverpool East

North West REC Centre
Barlow House
3rd Floor
4 Minshull Street
Manchester
M1 3DZ

Telephone: 0161 625 7832
Facsimile: 0161 625 7299

10 January 2012

Professor Sally Roberts
Director of Spinal Research
ISTM, Keele University
ARC/TORCH Building
RJAH Orthopaedic Hospital
SY10 7AG

Dear Professor Roberts

Study title: Investigating the potential for cells and molecules isolated from orthopaedic patients for modelling and understanding pathogenic conditions and developing diagnostic markers and therapies for musculoskeletal disorders and spinal cord injury

REC reference: 11/NW/0875

Protocol number: None

Thank you for your letter of 03 January 2012, responding to the Committee's request for further information on the above research and submitting revised documentation.

The further information has been considered on behalf of the Committee by the Alternate Vice-Chair and Mr Peter Owen.

Confirmation of ethical opinion

On behalf of the Committee, I am pleased to confirm a favourable ethical opinion for the above research on the basis described in the application form, protocol and supporting documentation as revised, subject to the conditions specified below.

Ethical review of research sites

NHS sites

The favourable opinion applies to all NHS sites taking part in the study, subject to management permission being obtained from the NHS/HSC R&D office prior to the start of the study (see "Conditions of the favourable opinion" below).

Conditions of the favourable opinion

The favourable opinion is subject to the following conditions being met prior to the start of the study.

Management permission or approval must be obtained from each host organisation prior to

the start of the study at the site concerned.

Management permission ("R&D approval") should be sought from all NHS organisations involved in the study in accordance with NHS research governance arrangements.

Guidance on applying for NHS permission for research is available in the Integrated Research Application System or at <http://www.rdforum.nhs.uk>.

Where a NHS organisation's role in the study is limited to identifying and referring potential participants to research sites ("participant identification centre"), guidance should be sought from the R&D office on the information it requires to give permission for this activity.

For non-NHS sites, site management permission should be obtained in accordance with the procedures of the relevant host organisation.

Sponsors are not required to notify the Committee of approvals from host organisations

It is the responsibility of the sponsor to ensure that all the conditions are complied with before the start of the study or its initiation at a particular site (as applicable).

Approved documents

The final list of documents reviewed and approved by the Committee is as follows:

<i>Document</i>	<i>Version</i>	<i>Date</i>
REC application: 92858/271334/1/14		01 December 2011
Investigator CV: Sally Roberts		
Protocol	1	28 November 2011
Participant Information Sheet	1.1	03 January 2012
Participant Consent Form	1.1	03 January 2012
Response to Request for Further Information from Sally Roberts		03 January 2012

Statement of compliance

The Committee is constituted in accordance with the Governance Arrangements for Research Ethics Committees and complies fully with the Standard Operating Procedures for Research Ethics Committees in the UK.

After ethical review

Reporting requirements

The attached document "*After ethical review – guidance for researchers*" gives detailed guidance on reporting requirements for studies with a favourable opinion, including:

- Notifying substantial amendments
- Adding new sites and investigators
- Notification of serious breaches of the protocol
- Progress and safety reports
- Notifying the end of the study

The NRES website also provides guidance on these topics, which is updated in the light of changes in reporting requirements or procedures.

Feedback

You are invited to give your view of the service that you have received from the National Research Ethics Service and the application procedure. If you wish to make your views known please use the feedback form available on the website.

Further information is available at National Research Ethics Service website > After Review

11/NW/0875

Please quote this number on all correspondence

With the Committee's best wishes for the success of this project

Yours sincerely


P. **Mrs Jean Harkin**
Chair

Email: helen.penistone@northwest.nhs.uk

Enclosures: "After ethical review – guidance for researchers"

Copy to: Mrs Teresa Jones
Research Office
ARC Building
RJAH Orthopaedic Hospital
Oswestry
SY10 7AG

Ms Nicola Leighton
Research Governance Officer
Keele University
Keele
ST5 5BG

Appendix II

Analysing interrater/intrarater reliability and agreement

Marker	ICC		Accuracy	
	inter	intra	inter	intra
CD34	0.92	0.95	1.63	1.33
CD39	0.58	0.73	45.3	35.97
CD44	0.57	0.38	0.36	0.43
CD49c	1	1	0.85	0.62
CD166	0.94	0.92	8.68	9.96
CD271	0.98	0.99	4.68	3.25

ICC: Intraclass correlation coefficients

Appendix III

Correlation between Surface markers and Histology scores

	Region																			
	Femoral				Tibial				Inner border				Cellularity				GAG intensity			
	p	Z	r	P	Z	r	P	r	p	Z	r	P	p	Z	r	P	p	Z	r	P
CD14	Avas	0.764	0.301	0.095	0.924	0.096	0.030	0.532	1.681	0.093	0.093	0.532	0.575	0.560	0.177	0.846	0.194	0.061	0.061	0.061
	Vas	0.696	0.391	0.124	0.623	0.491	0.155	-	-	-	-	-	0.604	0.518	0.164	0.681	-0.411	-0.130	-0.130	-0.130
CD19	Avas	0.920	0.100	0.032	0.292	1.054	0.333	0.313	-1.008	0.313	0.313	-0.319	0.093	1.681	0.532	0.846	-0.194	-0.061	-0.061	-0.061
	Vas	0.328	0.977	0.309	0.492	0.688	0.218	-	-	-	-	-	0.756	0.311	0.098	0.024*	2.261	0.715	0.715	0.715
CD29	Avas	0.437	-0.777	-0.246	0.288	1.064	0.336	0.047*	1.986	0.628	0.628	0.628	0.619	-0.497	-0.157	0.667	-0.430	-0.136	-0.136	-0.136
	Vas	0.172	-1.364	-0.431	0.598	-0.527	-0.167	-	-	-	-	-	0.657	-0.445	-0.141	0.321	-0.992	-0.314	-0.314	-0.314
CD34	Avas	0.193	-1.302	-0.412	0.151	1.437	0.454	0.093	1.681	0.532	0.532	0.911	0.112	0.035	0.699	-0.387	-0.122	-0.122	-0.122	-0.122
	Vas	0.051	1.955	0.618	0.280	1.080	0.342	-	-	-	-	0.005**	2.800	0.885	0.100	1.644	0.520	0.520	0.520	0.520
CD39	Avas	0.764	0.301	0.095	0.151	1.437	0.454	0.313	1.008	0.313	0.313	-0.319	0.575	-0.560	-0.177	0.699	-0.387	-0.122	-0.122	-0.122
	Vas	0.328	0.977	0.309	0.202	1.277	0.404	-	-	-	-	0.049*	1.970	0.623	0.681	0.411	0.130	0.130	0.130	0.130
CD44	Avas	0.836	0.208	0.066	0.487	-0.695	-0.220	0.642	0.464	0.147	0.147	0.416	0.416	-0.813	-0.257	1.000	0.000	0.000	0.000	0.000
	Vas	0.096	-1.665	-0.527	0.911	-0.111	-0.035	-	-	-	-	0.196	0.196	-1.293	-0.409	0.162	-1.399	-0.442	-0.442	-0.442
CD45	Avas	0.193	-1.302	-0.412	0.292	-1.054	-0.333	0.911	-0.112	-0.035	-0.035	0.433	0.433	0.784	0.248	0.846	0.194	0.061	0.061	0.061
	Vas	0.696	-0.391	-0.124	0.623	0.491	0.155	-	-	-	-	0.604	0.604	0.518	0.164	0.150	1.439	0.455	0.455	0.455
CD49b	Avas	0.841	-0.201	-0.064	0.009**	2.595	0.821	0.018**	2.360	0.746	0.746	-	0.911	0.112	0.035	0.627	-0.486	-0.154	-0.154	-0.154
	Vas	0.241	-1.173	-0.371	0.280	-1.080	-0.342	-	-	-	-	0.756	0.756	0.311	0.098	0.537	-0.617	-0.195	-0.195	-0.195
CD49c	Avas	0.764	-0.301	-0.095	0.924	0.096	0.030	0.218	1.232	0.390	0.390	0.390	0.575	0.560	0.177	0.561	-0.581	-0.184	-0.184	-0.184
	Vas	0.079	-1.759	-0.556	0.377	-0.884	-0.280	-	-	-	-	0.756	0.756	0.311	0.098	0.150	-1.439	-0.455	-0.455	-0.455
CD73	Avas	1.000	0.000	0.000	0.501	0.673	0.213	0.312	1.012	0.320	0.320	0.822	-0.225	-0.071	0.207	-1.263	-0.399	-0.399	-0.399	-0.399
	Vas	0.621	-0.494	-0.156	0.691	0.397	0.126	-	-	-	-	0.753	0.753	0.314	0.099	0.533	-0.623	-0.197	-0.197	-0.197
CD90	Avas	0.686	0.405	0.128	0.439	-0.774	-0.245	0.910	0.113	0.036	0.036	0.734	-0.339	-0.107	0.078	1.761	-0.587	-0.587	-0.587	-0.587
	Vas	0.060	-1.879	-0.594	0.375	-0.888	-0.281	-	-	-	-	0.558	-0.585	-0.185	0.063	-1.857	-0.587	-0.587	-0.587	-0.587
CD105	Avas	0.269	1.105	0.349	0.337	0.961	0.304	0.500	0.674	0.213	0.213	0.911	0.112	0.035	0.771	-0.291	-0.092	-0.092	-0.092	-0.092
	Vas	0.624	0.490	0.155	0.554	0.591	0.187	-	-	-	-	0.119	1.560	0.493	0.837	0.206	0.065	0.065	0.065	0.065
CD151	Avas	0.593	-0.535	-0.169	0.260	-1.127	-0.356	0.720	0.359	0.114	0.114	0.402	-0.838	-0.265	0.255	1.139	0.360	0.360	0.360	0.360
	Vas	0.396	-0.849	-0.268	0.670	0.426	0.135	-	-	-	-	1.000	0.000	0.000	0.824	0.223	0.071	0.071	0.071	0.071
CD166	Avas	0.193	-1.302	-0.412	0.292	-1.054	-0.333	0.575	0.560	0.177	0.177	0.313	-1.008	-0.319	0.846	-0.194	-0.061	-0.061	-0.061	-0.061
	Vas	0.051	-1.955	-0.618	0.623	-0.491	-0.155	-	-	-	-	0.756	-0.311	-0.098	0.064	-1.850	-0.585	-0.585	-0.585	-0.585
CD271	Avas	0.920	-0.100	-0.032	0.774	-0.287	-0.091	0.433	-0.784	-0.248	-0.248	0.313	1.008	0.319	0.081	1.743	0.551	0.551	0.551	0.551
	Vas	0.171	1.368	0.433	0.202	1.277	0.404	-	-	-	-	0.468	-0.726	-0.230	0.150	1.439	0.455	0.455	0.455	0.455
HLADR	Avas	0.367	0.902	0.285	0.028*	2.203	0.697	0.911	0.112	0.035	0.035	0.575	0.560	0.177	0.561	-0.581	-0.184	-0.184	-0.184	-0.184
	Vas	0.241	-1.173	-0.371	0.377	0.884	0.280	-	-	-	-	0.254	1.141	0.361	0.150	1.439	0.455	0.455	0.455	0.455

Appendix 1: Jonckheere-Terpstra test. avascular region was marked with grey background, vascular region was marked with white background. *, p<0.05, **, p<0.01, the significant values were highlighted in bold and italics

Appendix IV

Patient Label

The Robert Jones and Agnes Hunt 
Orthopaedic Hospital
NHS Foundation Trust

OSWESTRY 'OsCell' Cartilage Knee Lysholm Score-Form

Name: _____

CRN: _____

Date of Birth: _____

This questionnaire has been designed to give information as to how your knee has affected your ability to manage in everyday life. Please answer every section and tick the box's to the left of the statement that applies to you for both your left and right knee. If more than one statement applies to you tick the one that most closely describes your situation.

Please complete the questionnaire for both knees

PAIN		LEFT	RIGHT		
25	<input type="checkbox"/>	<input type="checkbox"/>	I have no pain in my knee		5
20	<input type="checkbox"/>	<input type="checkbox"/>	I have intermittent pain in my knee during severe exertion		4
15	<input type="checkbox"/>	<input type="checkbox"/>	I have marked pain in my knee during severe exertion		3
10	<input type="checkbox"/>	<input type="checkbox"/>	I have marked pain in my knee on or after walking more than 2km		2
5	<input type="checkbox"/>	<input type="checkbox"/>	I have marked pain in my knee on or after walking less than 2km		1
0	<input type="checkbox"/>	<input type="checkbox"/>	My knee is in constant pain		0

INSTABILITY

	LEFT	RIGHT		
25	<input type="checkbox"/>	<input type="checkbox"/>	My knee never gives way	5
20	<input type="checkbox"/>	<input type="checkbox"/>	My knee rarely gives way during athletics or other severe exertion	4
15	<input type="checkbox"/>	<input type="checkbox"/>	My knee frequently gives way during athletics or other severe exertion	3
10	<input type="checkbox"/>	<input type="checkbox"/>	My knee occasionally gives way during daily activities	2
5	<input type="checkbox"/>	<input type="checkbox"/>	My knee often gives way during daily activities	1
0	<input type="checkbox"/>	<input type="checkbox"/>	My knee gives way with every step I take	0

LOCKING

	LEFT	RIGHT		
15	<input type="checkbox"/>	<input type="checkbox"/>	I experience no locking or catching sensation	4
10	<input type="checkbox"/>	<input type="checkbox"/>	I do experience a catching sensation but not a locking sensation	3
6	<input type="checkbox"/>	<input type="checkbox"/>	I occasionally have a locking sensation	2
2	<input type="checkbox"/>	<input type="checkbox"/>	I frequently have a locking sensation	1
0	<input type="checkbox"/>	<input type="checkbox"/>	I have a locked knee now	0

Swelling

	LEFT	RIGHT		
10	<input type="checkbox"/>	<input type="checkbox"/>	My knee does not swell	-
6	<input type="checkbox"/>	<input type="checkbox"/>	My knee swells on severe exertion	-
2	<input type="checkbox"/>	<input type="checkbox"/>	My knee swells on ordinary exertion	-
0	<input type="checkbox"/>	<input type="checkbox"/>	My knee is constantly swollen	-

LIMP

	LEFT	RIGHT		
5	<input type="checkbox"/>	<input type="checkbox"/>	I have no limp	2
3	<input type="checkbox"/>	<input type="checkbox"/>	I have a slight limp or periodical limp	1
0	<input type="checkbox"/>	<input type="checkbox"/>	I have a severe and constant limp	0

STAIR-CLIMBING

	LEFT	RIGHT		
10	<input type="checkbox"/>	<input type="checkbox"/>	I have no problems climbing stairs because of my knee	Please turn over and complete page 2
6	<input type="checkbox"/>	<input type="checkbox"/>	My stair-climbing is slightly impaired because of my knee	
2	<input type="checkbox"/>	<input type="checkbox"/>	I climb stairs one foot at a time because of my knee	
0	<input type="checkbox"/>	<input type="checkbox"/>	Stair-climbing is impossible due to my knee	

SQUATTING

	LEFT	RIGHT		
5	<input type="checkbox"/>	<input type="checkbox"/>	I have no problems squatting	3
4	<input type="checkbox"/>	<input type="checkbox"/>	My squatting is slightly impaired because of my knee	2
2	<input type="checkbox"/>	<input type="checkbox"/>	I can't squat beyond 90°	1
0	<input type="checkbox"/>	<input type="checkbox"/>	Squatting is impossible because of my knee	0

SUPPORT

	LEFT	RIGHT		
5	<input type="checkbox"/>	<input type="checkbox"/>	I am not using any kind of support	2
2	<input type="checkbox"/>	<input type="checkbox"/>	I am using a stick or crutch	1
0	<input type="checkbox"/>	<input type="checkbox"/>	Weight-bearing is impossible for me due to my knee(s)	0

PLEASE ENSURE YOU HAVE ANSWERED ALL OF THE ABOVE QUESTIONS FOR BOTH KNEES

Telephone: Email:

**Information collected by OsCell is registered under the Data Protection Act 1998.
By completing and signing this questionnaire, the information you have given will be stored and used**

Please answer the following questions only after you have had your operation

Complication

Has anything gone wrong with your knee, complications such as:-

	No	Yes		Side	
<u>Blood clots</u> (DVT etc)	<input type="checkbox"/>	<input type="checkbox"/>	Date: D D M M M Y Y Y Y	Left	Right
Required blood thinner	<input type="checkbox"/>	<input type="checkbox"/>	____/____/____	<input type="checkbox"/>	<input type="checkbox"/>
Required hospitalisation	<input type="checkbox"/>	<input type="checkbox"/>		Side	
<u>Infection</u>	<input type="checkbox"/>	<input type="checkbox"/>	Date: D D M M M Y Y Y Y	Left	Right
Required antibiotic	<input type="checkbox"/>	<input type="checkbox"/>	____/____/____	<input type="checkbox"/>	<input type="checkbox"/>
Required hospitalisation	<input type="checkbox"/>	<input type="checkbox"/>		Side	
Date of last KNEE operation:			D D M M M Y Y Y Y	Left	Right
			____/____/____	<input type="checkbox"/>	<input type="checkbox"/>

Please list any other issues below

SATISFACTION

4	<input type="checkbox"/>	I am extremely pleased with the operation.
3	<input type="checkbox"/>	I am pleased with the operation.
2	<input type="checkbox"/>	I am no different than before the operation.
1	<input type="checkbox"/>	I am worse than before the operation
0	<input type="checkbox"/>	I am much worse and would not recommend the operation.

Date Form Completed:

Signature:

Thank you very much.

* Smith HJ, Richardson JB, Tennant A. Modification & validation of the Lysholm Knee Scale to assess articular cartilage damage. Osteoarthritis & Cartilage, 2009; 17(1): 53-8.

To convert 0 - 24 total score to 0 - 100 multiply the total score by 4.167

Knee score form v1.8_1 © OsCell July 2009©

Publications associated with this thesis

Combined Autologous Chondrocyte and Bone Marrow Mesenchymal Stromal Cell Implantation in the Knee: An 8-year Follow Up of Two First-In-Man Cases

Jingsong Wang^{1,2,3}, Karina T Wright^{1,2} , Jade Perry^{1,2}, Bernhard Tins^{1,2}, Timothy Hopkins^{1,2}, Charlotte Hulme^{1,2}, Helen S McCarthy^{1,2}, Ashley Brown², and James B Richardson^{1,2}

Cell Transplantation

1–8

© The Author(s) 2019

DOI: 10.1177/0963689719845328

journals.sagepub.com/home/cl



Abstract

Autologous chondrocyte implantation (ACI) has been used to treat cartilage defects for >20 years, with promising clinical outcomes. Here, we report two first-in-man cases (patient A and B) treated with combined autologous chondrocyte and bone marrow mesenchymal stromal cell implantation (CACAMI), with 8-year follow up. Two patients with International Cartilage Repair Society (ICRS) grade III–IV cartilage lesions underwent a co-implantation of autologous chondrocytes and bone marrow-derived mesenchymal stromal cells (BM-MSCs) between February 2008 and October 2009. In brief, chondrocytes and BM-MSCs were separately isolated and culture-expanded in a good manufacturing practice laboratory for a period of 2–4 weeks. Cells were then implanted in combination into cartilage defects and patients were clinically evaluated pre-operatively and postoperatively, using the self-reported Lysholm knee score and magnetic resonance imaging (MRI). Post-operative Lysholm scores were compared with the Oswestry risk of knee arthroplasty (ORKA) scores. Patient A also had a second-look arthroscopy, at which time a biopsy of the repair site was taken. Both patients demonstrated a significant long-term improvement in knee function, with postoperative Lysholm scores being consistently higher than ORKA predictions. The most recent Lysholm scores, 8 years after surgery were 100/100 (Patient A) and 88/100 (Patient B), where 100 represents a fully functioning knee joint. Bone marrow lesion (BML) volume was shown to decrease on postoperative MRIs in both patients. Cartilage defect area increased in patient A, but declined initially for patient B, slightly increasing again 2 years after treatment. The repair site biopsy taken from patient A at 14 months postoperatively, demonstrated a thin layer of fibrocartilage covering the treated defect site. The use of a combination of cultured autologous chondrocytes and BM-MSCs appears to confer long-term benefit in this two-patient case study. Improvements in knee function perhaps relate to the observed reduction in the size of the BML.

Keywords

Knee, cartilage repair, autologous chondrocyte implantation, autologous bone marrow-derived stromal cells

Introduction

Autologous chondrocyte implantation (ACI) is a cell-based therapeutic strategy which has been used for more than 20 years for the treatment of cartilage defects¹. ACI has shown promising clinical outcomes in terms of pain relief and in delaying joint degeneration^{2,3}. ACI has also recently been approved by the National Institute for Health and Care Excellence (NICE TA 477). This historic decision is anticipated to have a profound impact, as ACI is now considered to be the ‘gold standard’ to treat chondral defects (greater than 2 cm in diameter and not previously treated with

¹ Institute of Science and Technology in Medicine (ISTM), Keele University, Staffordshire, UK

² Robert Jones & Agnes Hunt Orthopaedic Hospital, Oswestry, Shropshire, UK

³ Dalian Medical University, Dalian, China

Submitted: February 27, 2019. Revised: March 22, 2019. Accepted: March 28, 2019.

Corresponding Author:

Karina T Wright, Robert Jones & Agnes Hunt Orthopaedic Hospital, Oswestry, Shropshire SY10 7AG, UK.

Email: karina.wright1@nhs.net



Creative Commons CC BY: This article is distributed under the terms of the Creative Commons Attribution 4.0 License (<http://www.creativecommons.org/licenses/by/4.0/>) which permits any use, reproduction and distribution of the work without further permission provided the original work is attributed as specified on the SAGE and Open Access pages (<https://us.sagepub.com/en-us/nam/open-access-at-sage>).

Table 1. Patient Demographic and Treatment Information.

Case	Defects (number and location)	Previous procedures	Preoperative Lysholm score	Operative notes (at cell implantation)
A	I Patella I MTP I MFC	None	50	4 weeks after tissue harvest, intra-articular injection of chondrocytes and BM-MSCs with hyaluronan.
B	I Patella I MTP I MFC	Debridement 12 months previously (absent meniscus noted)	75	2 weeks after tissue harvest, traditional ACI with a BM-MSC-seeded Actifit [®] meniscal transplant.

ACI: autologous chondrocyte implantation; BM-MSC: bone marrow-derived mesenchymal stromal cells; MFC: medial femoral condyle; MTP: medial tibial plateau.

microfracture). However, there are still some unsolved challenges, such as possible donor-site morbidity^{4,5}, and variable structural cartilage regeneration as noted using imaging and histological analyses⁶.

Bone marrow-derived mesenchymal stromal cells (BM-MSCs) have chondrogenic potential which can be enhanced by co-culture with chondrocytes^{7,8}. Orozco et al. have confirmed the safety and feasibility of using autologous BM-MSCs to treat cartilage defects⁹. They reported 65% to 78% improvement in knee pain and knee function after implantation, demonstrating improved outcomes compared with conventional treatment (e.g. acupuncture, placebo, debridement, lavage), at 12 months postoperatively, with maintained improvement up to 2 years¹⁰.

BM-MSCs were initially proposed to maintain their multipotent capacity and contribute directly to repair cartilage formation and engraftment, with MSCs persisting in multiple tissues for as long as 13 months after transplantation¹¹. However, another study showed that BM-MSCs migrate to the site of damaged cartilage and are stimulated by local inflammatory cytokines or hypoxia to produce large quantities of growth factors which promote tissue regeneration¹². Additionally, MSCs have been found to enhance tissue repair by secreting soluble factors which suppress the inflammatory response and stimulate endogenous stem cell proliferation and differentiation¹³.

Combining cultured autologous chondrocytes and BM-MSCs may be of benefit for cartilage regeneration but to our knowledge this has not been reported on in a clinical study. In this first-in-man study we report two cases of such treatment, hereafter referred to as combined autologous chondrocyte and MSC implantation (CACAMI), with 8 years of clinical outcome data.

Materials and Methods

Patient Information

Two male patients are described in the study: Patient A (70 years of age, body mass index (BMI) 25.25) and Patient B (65 years of age, BMI 22.09) both presented with unilateral knee osteoarthritis (OA) and full thickness cartilage loss on their medial femoral condyles (International Cartilage

Repair Society (ICRS) grade III–IV). Patient A, a keen runner, started to feel right knee pain at 61 years of age and was unable to run at all 9 years later, at the time of treatment. His baseline X-ray showed the complete loss of the medial joint space with sclerosis present in the subchondral bone of the tibia and femur. Patient B began to feel pain in his right knee, without any proximate cause, at the age of 62. At 3 years later, at the time of treatment, he was unable to walk more than a quarter of a mile and could not mobilize around a golf course without the use of a buggy. Both patients were offered knee replacement surgeries but, as keen sportsmen, each wished to avoid arthroplasty, hence they were offered CACAMI. Patient demographic and treatment information, which is distinct for each case, is summarized in Table 1.

Both patients were fully informed that although cultured chondrocytes and BM-MSCs had each been used individually for many years to treat chondral defects, the combination had not yet been used clinically. The process was explained in full and the patients provided informed consent. Each patient consented to an ethically approved project (REACT 09/H1203/90, approved by South Staffordshire Local Research Ethics Committee, UK).

Surgical Procedures and Cell Therapy Delivery

The two-stage procedure was performed in both cases by the same surgeon. The first stage was a diagnostic arthroscopy, at which time macroscopically healthy cartilage was harvested from a low load-bearing area of the femoral trochlea in both patients. Additionally, 20 ml of bone marrow was aspirated from the iliac crest.

Isolated chondrocytes and BM-MSCs were expanded in monolayer culture as described previously^{14,15}. Briefly, the cartilage biopsy was dissected into 2 mm³ pieces and digested in collagenase type II (245 IU/mg dry weight, Worthington, USA) for 16 hours at 37°C. Chondrocytes were plated out in Dulbecco's modified Eagle's medium (DMEM)/F12 supplement with 20% autologous serum, 50 µg/ml ascorbic acid (Sigma Aldrich, Poole, UK) and antibiotics at a seeding density of 5 × 10³ cells/cm². Cells were passaged at 70% confluence and reseeded in culture medium containing 10% autologous serum. Then chondrocytes were passaged a further 1 or 2 times and prepared for

Table 2. Bone Marrow and Cartilage Cell Isolation and Growth Kinetic Information.

Case	Bone marrow			Cartilage			Culture time (days)
	Volume (ml)	Cell number		Weight (mg)	Cell number		
		Initial MNC	Implanted BM-MSCs		Initial	Implanted	
A	20	4×10^6	8×10^6	301	4.9×10^5	4×10^6	28
B	20	3×10^6	6×10^6	286	4.0×10^5	4×10^6	14

BM-MSC: bone marrow-derived mesenchymal stromal cell; MNC: mononuclear cell.

implantation within 4 weeks. To culture BM-MSCs, mononuclear cells were isolated by density gradient centrifuge (Lymphoprep™, Fresenius Kabi Norge AS, Norway) were seeded at a density of 20 million cells per 75 cm² flask in DMEM/F12 supplement with 15% autologous serum and antibiotics. BM-MSCs were passaged at 70% confluence and cultured in medium with 10% autologous serum. The cells were subcultured for a further 1–2 passages and implanted within 4 weeks. Cartilage and bone marrow aspiration harvest and final cell yields are summarized in Table 2. Chondrocytes and BM-MSCs were released for implantation upon conformance to expect morphological characteristics and if cell populations were at least 90% viable, as assessed by trypan blue exclusion (as described in detail in a published current clinical trial)¹⁶.

Patient A underwent a second arthroscopic procedure, in which the chondral defect on the medial femoral condyle was debrided. After this, combined autologous chondrocytes and BM-MSCs were injected into the joint, followed by hyaluronic acid (60 mg in 3 ml Durolane; Fig. 1). Patient B's second stage surgery involved a parapatellar arthrotomy, in which the defect edges were cut vertically using surgical blades. A porcine collagen type I/III membrane (Chondro-gide, Geistlich Biomaterials, Wolhusen, Switzerland) was sutured to the surrounding healthy cartilage using 6.0 Vicryl (Ethicon Leeds, UK). The edges of the patch were sealed to the edges of the defect with fibrin glue (Tisseel, ImmunoAG, Vienna, Austria). Finally, a suspension of cultured chondrocytes was injected underneath the patch, after which a BM-MSC-seeded medial Actifit® polyurethane meniscal scaffold (Orteq Sports Medicine, London, UK) was transplanted.

Clinical Assessments

Each patient was evaluated preoperatively and postoperatively up to 8 years, using a modified Lysholm score¹⁷. Actual postoperative scores were compared with scores predicted using the Oswestry risk of knee arthroplasty (ORKA) score. The ORKA score² is a web-based application that uses baseline information about the patient's age and sex, location of and the number of cartilage defects and baseline knee function score to predict a patient's risk of needing knee arthroplasty (Fig. 2). Postoperative magnetic resonance imaging (MRI) scans at 2, 6, 13, 39, 49, 60 and 86 months for Patient A and at 5, 17, 25 and 52 months for Patient B were

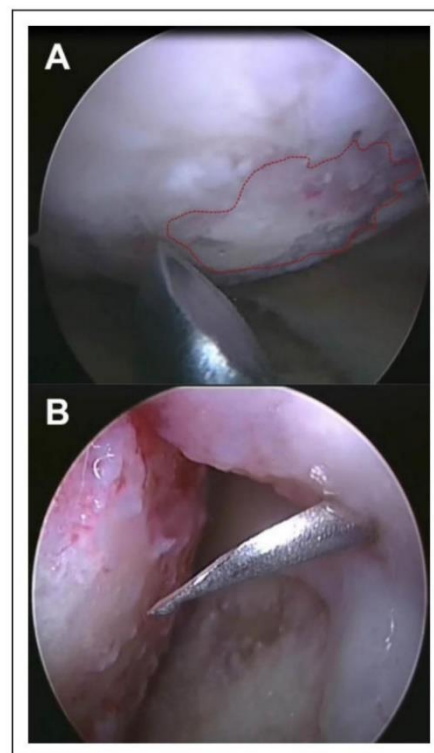


Fig. 1. Arthroscopic images of the medial femoral condyle in Patient A. (A) A full-thickness cartilage defect was observed at the time of cell implantation (red dashed-line). (B) Following the debridement of the lesion, the cultured chondrocytes and MSCs were injected into the synovial cavity, in combination with hyaluronan. MSC: mesenchymal stromal cell.

undertaken to assess the cartilage and bone using two scoring systems. The magnetic resonance observation of cartilage repair tissue (MOCART) score, which evaluates cartilage repair tissue¹⁸ and the whole-organ magnetic resonance imaging score (WORMS). WORMS provides whole-organ evaluation of the total knee joint by assessing not only the cartilage, but also various other structures, including the menisci, ligaments, subchondral bone and bone marrow¹⁹. For each patient, longitudinal postoperative MOCART and WORMS scores were evaluated by a radiologist with significant experience in OA and ACI (Table 3). A higher

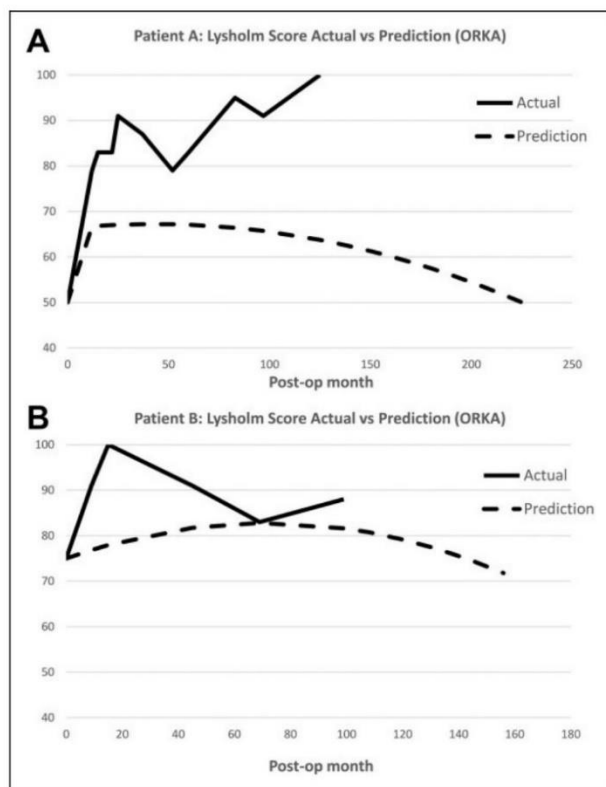


Fig. 2. A comparison of the longitudinal, postoperative actual Lysholm score and ORKA prediction score. (A) For Patient A, the actual score gradually increased to 100, surpassing predicted scores at each time point. (B) For Patient B, the actual score increased initially to 100, after which the score decreased to 83, matching ORKA predictions. Subsequently the actual score then increased again to 88 at the 5-year time point. ORKA: Oswestry risk of knee arthroplasty.

Table 3. A Summary of the MRI Scores (WORMS and MOCART) for Patient A and B.

Patient	Months Post-op	WORMS (0–332)	MOCART (0–100)
A	3	133.5	10
	14	112	15
	61	124	15
B	5	138	75
	17	138	60
	52	143.5	60

MOCART: magnetic resonance observation of cartilage repair tissue; MRI: magnetic resonance imaging; WORMS: whole-organ magnetic resonance imaging score.

MOCART score indicates better cartilage repair, whereas a lower WORMS value indicates a better preserved joint. Bone marrow lesions (BMLs) were also assessed and measured as described previously²⁰ and depicted in Fig. 3.

A second-look arthroscopy was performed in Patient A, 14 months after cell therapy, in which a biopsy of repair cartilage was taken. The sample was snap-frozen in liquid

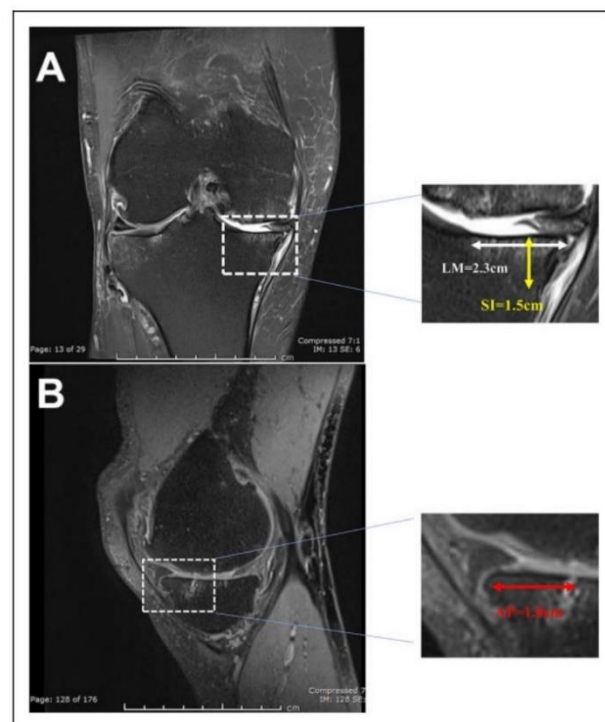


Fig. 3. Measurement of the bone marrow lesion volume on MRI within the medial tibial plateau of patient A. (A) In the coronal image, the LM dimension (2.3 cm) and SI dimension (1.5 cm) of the lesion are measured. (B) In the sagittal image the AP dimension of the same lesion (1.8 cm) is measured. AP: anterior-posterior; LM: lateral-medial; MRI: magnetic resonance imaging; SI: superior-inferior.

nitrogen-cooled hexane and sectioned at 7 μ m thickness onto poly-L-lysine coated glass slides. Sections were stained with hematoxylin and eosin or toluidine blue to assess general morphology and proteoglycan content, respectively. Collagen fiber orientation was examined under polarized light to differentiate between hyaline cartilage and fibrocartilage.

Results

Both patients reported improvements, as measured by pain reduction, within a year of treatment. No complications from surgery were noted in either patient. Further improvements continued up until the time of reporting this study (8-year follow up) and both patients currently remain physically active without joint replacement, with Lysholm scores of 100 and 88, for patients A and B respectively (Fig. 2). Patient A returned to running competitively and has recently taken up swimming. Patient B continues to compete in cycling races. His main residual symptom at final review is pain that develops after driving for more than 1 hour.

Patient A showed progressive enlargement of chondral defects identified on MRI (Fig. 4A), whereas in Patient B

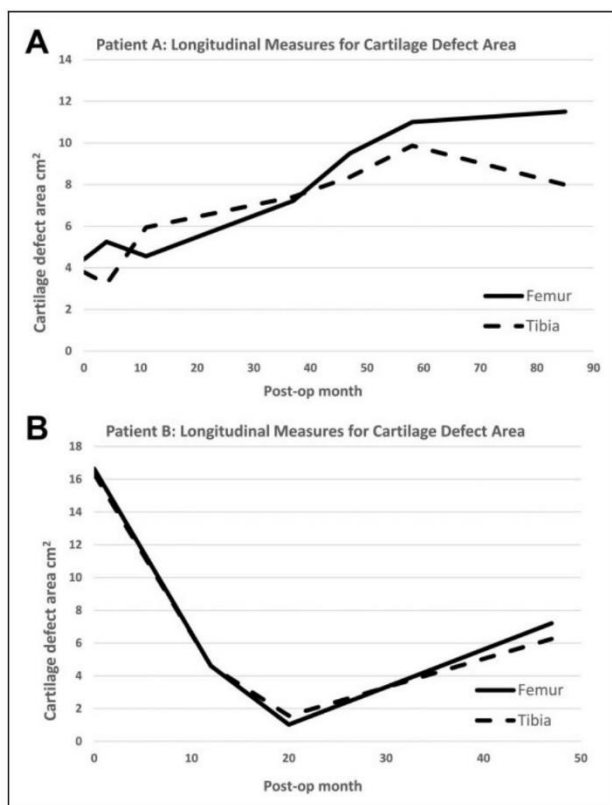


Fig. 4. Cartilage defect size measured from MRIs for Patients A and B. (A) The area of the cartilage defects gradually increased over time for Patient A, whereas the size of cartilage defects decreased for the first 2 years, but increased again thereafter for Patient B (B). MRI: magnetic resonance imaging.

the defect area declined initially and increased slightly 2 years after implantation (Fig. 4B). In both patients, the size of BMLs decreased gradually over time in the tibia as well as the femur. This was especially evident in Patient B, in whom more than 80% of the BMLs disappeared (Fig. 5A and B).

MOCART and WORMS scores at three different times are shown in Table 3. For patient A, the WORMS score fluctuated over time, while the MOCART only marginally improved from 10 to 15. However, for patient B both scores consistently deteriorated over time, but MOCART scores (from 75 to 50) were consistently higher than for Patient A. Additionally, there was no evidence demonstrating the presence of the scaffold or new meniscal tissue in postoperative MRI at 5-month follow up and beyond for patient B.

At second-look arthroscopy for Patient A, 12 months after surgery, the treated defect on the medial femoral condyle was observed to be generally well healed with firm repair tissue on probing, but with a slightly irregular surface. In contrast, the tibial plateau repair cartilage appeared soft but smooth. Histologically, a thin layer of fibrocartilage had formed in the treated defect on the medial femoral condyle.

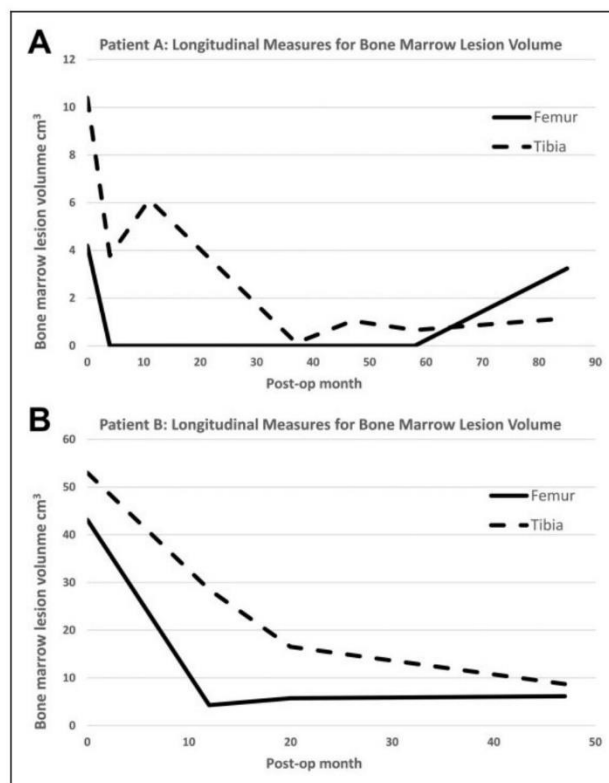


Fig. 5. BML size measured from MRIs for Patients A and B. (A) The BMLs continuously decreased in volume, particularly on the tibial side for Patient A, whereas the BMLs continuously decreased in volume both on the tibial and femoral sides for Patient B (B). BML: bone marrow lesion; MRI: magnetic resonance imaging.

measuring 0.5 mm in depth where previously the bone had been exposed.

Discussion

Our previous case report showed the feasibility of combining ACI with bone graft to treat a major osteochondral defect in the hip following trauma²¹. Combining cultured autologous chondrocytes and BM-MSCs may be of benefit for cartilage regeneration but to our knowledge has not been reported previously in a clinical study. We believe this is the first case report to demonstrate the safety of using combined autologous chondrocytes and autologous BM-MSCs to treat cartilage defects. Clinical symptoms improved dramatically in both patients treated, up to 8 years follow up. We have previously identified six important predictive factors (age, sex, defect number and location, previous surgery, preoperative Lysholm score) in ACI-treated patients, which appear to influence progression to arthroplasty. The combination of these six parameters was used to construct an ORKA index to predict the survival of ACI repair². In this study, both patients were over 60 years old and had multiple defects including patella sites, as well as low preoperative Lysholm

scores, which when using the ORKA assessment indicates a poor prognosis. However, both patients' postoperative Lysholm scores were consistently higher than ORKA predictions.

The patient-reported Lysholm score may have some limitations associated with its subjectivity. However, our group and many others consistently use such a subjective patient-reported outcome as the primary outcome of clinical trials^{16,17,22}. The reason being that ultimately, how the patient feels about their knee function, is the most important clinical observation and metric of treatment success/failure. Moreover, several studies have shown that there is no correlation between subjective functional outcome such as Lysholm score and objective measures such as histological analyses^{23,24}. We have taken measures to help to reduce the limitations associated with the use of subjective scores, including for comparison objective measures (clinical imaging scores) and where possible, histological observations. In addition, we have not relied upon a single Lysholm outcome, but include several, longitudinal postoperative scores for each patient which helps to add further confidence.

The second-look arthroscopy and histological assessments showed that the cartilage defects in Patient A were repaired with a thin layer of fibrocartilage which was not noted at 1-year follow-up MRI. Patient B's cartilage defect sizes were reduced in the early postoperative assessments in contrast to tissue to Patient A, in which the defect sizes increased progressively after treatment. This difference could be attributed to the use of a patch covering the treatment site in Patient A, or to the difference in cell delivery method. Patient B's injected BM-MSCs may have migrated out of the implanted Actifit[®] scaffold and exerted their effects elsewhere within the joint. However, no firm conclusions regarding which cell delivery method represents the better cartilage repair technique can be drawn.

The size of the BMLs in both patients gradually decreased over time. BML is a technical term to describe the high-signal intensity pathological change on MRI²⁵. There are multiple studies demonstrating the positive correlations between BMLs and the pathogenesis of knee pain²⁶⁻²⁸. A large prospective cohort study of 358 patients in Korea showed the prevalence of BMLs in patients with knee OA was 80.3%. After adjusting for age, sex and BMI, the presence and severity of BMLs in the medial compartment were significantly associated with knee pain²⁷. Zhang et al. reported similar results, showing that the changing size of BMLs was related to knee pain fluctuations, and the reduction of BMLs could lower the risk of frequent knee pain²⁹. Although Sower et al. demonstrated a poor relationship between the presence of knee pain and the presence of BMLs on MRI³⁰, a systematic review on 22 studies showed moderate evidence that BMLs were associated with knee OA pain³¹.

In a recent systematic review, the clinical outcome of 347 patients who had undergone Actifit[®] (meniscal) implantation without cells was evaluated and graft failure occurred in 9.9% of patients at a mean follow up of 40 months³². For

Patient B, treated with CACAMI and Actifit[®], postoperative MRI at 5-month follow up demonstrated no obvious signal for the presence of the scaffold or new meniscal tissue, indicating possible resorption of the scaffold. In comparison, Gelber et al. reported that patients with no chondral injuries showed an improved size and morphology of transplanted Actifit[®] scaffolds using MRI at a median follow up of 39 months (range 25–63)³³.

In conclusion, we believe these two case studies suggest that combination of cultured autologous chondrocytes and BM-MSCs appears to confer improved symptoms at least in these two patients. However, despite the improvement in clinical outcome scores, physical joint failure as assessed by MRI is progressing in both patients. Whether this might have progressed with advancing age at a greater rate had the cells not been implanted, will only be resolved in a full clinical trial. In summary, these findings support the hypothesis that autologous BM-MSCs stimulate a beneficial host response, reducing pain, perhaps by influencing the subchondral bone and reducing the size of BMLs.

Authors' Note

Please note that Professor James Richardson (last author) was the initial corresponding author who dedicated his life to the advancement of cell therapy for cartilage repair. Professor Richardson suddenly passed away last year. These two cases were performed by him 10 years ago and we believe these to be the first examples of such a combined treatment. Here we report good clinical outcomes for these first-in-man cases in long-term follow up.

Acknowledgment

We are grateful to the John Charnley Laboratory, RJA Orthopaedic Hospital, UK, for the expansion and preparation of cells used in the procedures.

Ethical Approval

All patients consented to an ethically approved project (REACT 09/H1203/90, approved by South Staffordshire Local Research Ethics Committee, UK).

Statement of Human and Animal Rights

We confirm that the procedures and experiments reported respect the ethical principles for medical research involving human subjects, as set out in the Helsinki Declaration of 1975 (most recently revised in 2008), as well as the national law.

Statement of Informed Consent

All procedures in this study were carried out with informed patient consent. Approvals were acquired from the South Staffordshire Local Research Ethics Committee.

Declaration of Conflicting Interests

The author(s) declared no potential conflicts of interest with respect to the research, authorship, and/or publication of this article.

Funding

The author(s) disclosed receipt of the following financial support for the research, authorship, and/or publication of this article: This work was supported by Versus Arthritis (grant numbers 20815, 19429, and 18480).

ORCID iD

Karina T Wright  <https://orcid.org/0000-0001-8842-5908>

References

- Brittberg M, Lindahi A, Nilsson A, Ohlsson C, Isaksson O, Peterson L. Treatment of deep cartilage defects in the knee with autologous chondrocyte transplantation. *New Engl J Med*. 1994;331(14):889–895.
- Dugard MN, Kuiper JH, Parker J, Roberts S, Robinson E, Harrison P, Richardson JB. Development of a tool to predict outcome of autologous chondrocyte implantation. *Cartilage*. 2017;8(2):119–130.
- Bhosale AM, Kuiper JH, Johnson WE, Harrison PE, Richardson JB. Midterm to long-term longitudinal outcome of autologous chondrocyte implantation in the knee joint: a multilevel analysis. *Am J Sports Med*. 2009;37(suppl 1):131S–138S.
- McCarthy HS, Richardson JB, Parker JC, Roberts S. Evaluating joint morbidity after chondral harvest for autologous chondrocyte implantation (ACI): a study of aci-treated ankles and hips with a knee chondral harvest. *Cartilage*. 2016;7(1):7–15.
- Matricali GA, Dereymaeker GPE, Luvten FP. Donor site morbidity after articular cartilage repair procedures: a review. *Acta Orthop Belg*. 2010;76(5):669–674.
- Roberts S, McCall IW, Darby AJ, Menage J, Evans H, Harrison PE, Richardson JB. Autologous chondrocyte implantation for cartilage repair: monitoring its success by magnetic resonance imaging and histology. *Arthritis Res Ther*. 2002;5(1):60–73.
- Gupta PK, Das AK, Chullikana A, Majumdar AS. Mesenchymal stem cells for cartilage repair in osteoarthritis. *Stem Cell Res Ther*. 2012;3(4):25.
- Hwang NS, Im SG, Wu PB, Bichara DA, Zhao X, Randolph MA, Langer R, Anderson DG. Chondrogenic priming adipose-mesenchymal stem cells for cartilage tissue regeneration. *Pharm Res*. 2011;28(6):1395–1405.
- Orozco L, Munar A, Soler R, Alberca M, Soler F, Huguet M, Sentís J, Sánchez A, García-Sancho J. Treatment of knee osteoarthritis with autologous mesenchymal stem cells: a pilot study. *Transplantation*. 2013;95(12):1535–1541.
- Orozco L, Munar A, Soler R, Alberca M, Soler F, Huguet M, Sentís J, Sánchez A, García-Sancho J. Treatment of knee osteoarthritis with autologous mesenchymal stem cells: two-year follow-up results. *Transplantation*. 2014;97(11):e66–e68.
- Liechty KW, MacKenzie TC, Shaaban AF, Radu A, Moseley AB, Deans R, Marshak DR, Flake AW. Human mesenchymal stem cells engraft and demonstrate site-specific differentiation after in utero transplantation in sheep. *Nat Med*. 2001;6(11):1282–1286.
- Crisostomo PR, Wang Y, Markel TA, Wang M, Lahm T, Meldrum DR. Human mesenchymal stem cells stimulated by TNF- α , LPS, or hypoxia produce growth factors by an NF κ B- but not JNK-dependent mechanism. *AJP Cell Physiology*. 2008;294(3):C675–C682.
- Prockop DJ. Repair of tissues by adult stem/progenitor cells (MSCs): controversies, myths, and changing paradigms. *Mol Ther*. 2009;17(6):939–946.
- Bajada S, Harrison PE, Ashton BA, Cassar-Pullicino VN, Ashammakhi N, Richardson JB. Successful treatment of refractory tibial nonunion using calcium sulphate and bone marrow stromal cell implantation. *J Bone Joint Surg Br*. 2007;89(10):1382–1386.
- Harrison PE, Ashton IK, Johnson WE, Turner SL, Richardson JB, Ashton BA. The in vitro growth of human chondrocytes. *Cell Tissue Bank*. 2000;1(4):255–260.
- Richardson JB, Wright KT, Wales J, Kuiper JH, McCarthy HS, Gallacher P, Harrison PE, Roberts S. Efficacy and safety of autologous cell therapies for knee cartilage defects (autologous stem cells, chondrocytes or the two): randomized controlled trial design. *Regen Med*. 2017;12(5):493–501.
- Smith HJ, Richardson JB, Tennant A. Modification and validation of the Lysholm Knee Scale to assess articular cartilage damage. *Osteoarthritis and Cartilage*. 2009;17(1):53–58.
- Marlovits S, Striessnig G, Resinger CT, Aldrian SM, Vecsei V, Imhof H, Trattnig S. Definition of pertinent parameters for the evaluation of articular cartilage repair tissue with high-resolution magnetic resonance imaging. *Eur J Radiol*. 2004;52(3):310–319.
- Peterfy CG, Guermazi A, Zaim S, Tirman PF, Miaux Y, White D, Kothari M, Lu Y, Fye K, Zhao S, Genant HK. Whole-organ magnetic resonance imaging score (WORMS) of the knee in osteoarthritis. *Osteoarthritis Cartilage*. 2004;12(3):177–190.
- Driban JB, Lo GH, Lee J, Ward RJ, Miller E, Pang J, Price L, McAlindon TE. Quantitative bone marrow lesion size in osteoarthritic knees correlates with cartilage damage and predicts longitudinal cartilage loss. *BMC Musculoskelet Disord*. 2011;12(1):217.
- Akimau P, Bhosale A, Harrison PE, Roberts S, McCall IW, Richardson JB, Ashton BA. Autologous chondrocyte implantation with bone grafting for osteochondral defect due to post-traumatic osteonecrosis of the hip – A case report. *Acta Orthop*. 2006;77(2):333–336.
- Løken S, Heir S, Holme I, Engebretsen L, Årøen A. 6-year follow-up of 84 patients with cartilage defects in the knee: knee scores improved but recovery was incomplete. *Acta Orthop*. 2010;81(5):611–618.
- DiBartola AC, Everhart JS, Magnussen RA, Carey JL, Brophy RH, Schmitt LC, Flanagan DC. Correlation between histological outcome and surgical cartilage repair technique in the knee: a meta-analysis. *Knee*. 2016;23(3):344–349.
- McCarthy HS, Williams JM, Mennan C, Richardson JB, Roberts S. Magnetic resonance imaging parameters at 1 year correlate with clinical outcomes up to 17 years after autologous chondrocyte implantation. *Orthop J Sports Med*. 2018;6(8):232596711878828.

25. Bonadio MB, Ormond Filho AG, Helito CP, Stump XM, Demange MK. Bone marrow lesion: image, clinical presentation, and treatment. *Magn Reson Insights*. 2017;10:1178623X17703382.
26. Joseph GB, Hou SW, Nardo L, Heilmeier U, Nevitt MC, McCulloch CE, Link TM. MRI findings associated with development of incident knee pain over 48 months: data from the osteoarthritis initiative. *Skeletal Radiology*. 2016;45(5):653–660.
27. Kim IJ, Kim DH, Jung JY, Song YW, Guermazi A, Crema MD, Hunter DJ, Kim HA. Association between bone marrow lesions detected by magnetic resonance imaging and knee pain in community residents in Korea. *Osteoarthritis Cartilage*. 2013;21(9):1207–1213.
28. Zhang Y, Nevitt M, Niu J, Lewis C, Torner J, Guermazi A, McCulloch C, Felson DT. Fluctuation of knee pain and changes in bone marrow lesions, effusions, and synovitis on magnetic resonance imaging. *Arthritis Rheum*. 2011;63(3):691–699.
29. Zhang M, Driban JB, Price LL, Lo GH, McAlindon TE. magnetic resonance image sequence influences the relationship between bone marrow lesions volume and pain: data from the osteoarthritis initiative. *BioMed Res Int*. 2015;2015:731903.
30. Sower MF, Hayes C, Jamadar D, Capul D, Lachance L, Jannausch M, Welch G. Magnetic resonance-detected subchondral bone marrow and cartilage defect characteristics associated with pain and X-ray-defined knee osteoarthritis. *Osteoarthritis Cartilage*. 2003;11(6):387–393.
31. Yusuf E, Kortekaas MC, Watt I, Huizinga TW, Kloppenburg M. Do knee abnormalities visualised on mri explain knee pain in knee osteoarthritis? a systematic review. *Ann Rheum Dis*. 2011;70(1):60–67.
32. Houck DA, Kraeutler MJ, Belk JW, McCarty EC, Bravman JT. Similar clinical outcomes following collagen or polyurethane meniscal scaffold implantation: a systematic review. *Knee Surg Sports Traumatol Arthrosc*. 2018;26(8):2259–2269.
33. Gelber PE, Petrica AM, Isart A, Mari-Molina R, Monllau JC. The magnetic resonance aspect of a polyurethane meniscal scaffold is worse in advanced cartilage defects without deterioration of clinical outcomes after a minimum two-year follow-up. *Knee*. 2015;22(5):389–394.



OPEN

Characterization of regional meniscal cell and chondrocyte phenotypes and chondrogenic differentiation with histological analysis in osteoarthritic donor-matched tissues

Jingsong Wang^{1,2,3}, Sally Roberts^{1,2}, Jan Herman Kuiper^{1,2}, Weiguo Zhang⁴, John Garcia^{1,2}, Zhanfeng Cui⁵ & Karina Wright^{1,2}✉

Meniscus degeneration is closely related to the progression of knee osteoarthritis (OA). However, there is currently a lack of quantitative and objective metrics to assess OA meniscal cell phenotypes. In this study we investigated the phenotypic markers and chondrogenic potency of avascular and vascular meniscal cells and chondrocytes from medial OA knee joints (n = 10). Flow cytometry results showed that a significantly greater percentage of meniscal cells were positive for CD49b, CD49c and CD166 compared to donor-matched chondrocytes after 14 days in monolayer culture. The integrins, CD49b and CD29, were expressed at a significantly higher level on avascular meniscal cells derived from tissues with a more degenerated inner border than non-degenerate menisci, suggesting that the integrin family may play an important role in meniscus OA pathology. Collagen fibres arranged in a “tree-like” formation within the meniscus appeared to have less blood vessels associated with them in the vascular region of the most degenerate menisci, which may indicate that such structures are involved in the pathological process. We have demonstrated that meniscal cells derived from the lateral meniscus in medial OA patients have chondrogenic capacity *in vitro* and hence could represent a potential cell source to consider for meniscus tissue engineering.

An increasing number of studies suggest that meniscal degeneration plays a significant role in the pathology of osteoarthritis (OA)¹. Certainly meniscal degeneration is a classical feature of OA knee joints, as seen on Magnetic Resonance Imaging (MRI), contributing to a substantial proportion of joint space narrowing observations². In addition, degenerative tears of the meniscus have important consequences for cartilage loss, as the tears interfere with converting axial loading into horizontal tensile strain and subsequently increasing contact stress on the articular cartilage³. Together, this evidence suggests that pathological changes and extracellular matrix (ECM) degeneration in menisci may play an important role in the disease process of OA.

A series of histological features of the degenerate meniscus were reported in a previous study⁴, including fibrocartilaginous separation of the matrix, fraying, tears, calcification, diffuse hypercellularity, cellular hypertrophy and the presence of abnormal cell clusters within the meniscus matrix. A recent study also demonstrated the severe disorganization of collagen fibers and increased proteoglycan by electron microscopy and histology in late-stage OA patients⁵. In addition, in another study the biochemical composition of the OA meniscus was shown to be altered, in terms of extracellular matrix disorganization, disturbances in collagen and non-collagen protein synthesis and gene expression⁶. However, the mechanism(s) behind these degenerative changes is still

¹School of Pharmacy and Bioengineering, Keele University, Keele ST5 5GB, Staffordshire, UK. ²The Robert Jones and Agnes Hunt Orthopaedic Hospital NHS Foundation Trust, Oswestry SY10 7AG, Shropshire, UK. ³Dalian Medical University, Dalian 116044, China. ⁴Department of Orthopaedic Surgery, First Affiliated Hospital, Dalian Medical University, Dalian 116011, China. ⁵Department of Engineering Science, Institute of Biomedical Engineering, University of Oxford, Oxford OX1 3PJ, UK. ✉email: karina.wright1@nhs.net

ID	Gender	Age	Meniscus	Microscopic grading
Donor 1	Male	46	Lateral	2
Donor 2	Female	53	Lateral	4
Donor 3	Female	66	Lateral	3
Donor 4	Female	66	Lateral	2
Donor 5	Male	66	Lateral	2
Donor 6	Female	67	Lateral	2
Donor 7	Male	69	Lateral	3
Donor 8	Male	69	Lateral	3
Donor 9	Female	75	Lateral	2
Donor 10	Female	87	Lateral	2

Table 1. Demographics of donors from which samples were sourced.

unclear. Investigating the surface marker and gene expression profiles of meniscal cells from OA knees could contribute to this knowledge base.

The meniscus contains a heterogeneous cell population; at least three cell fractions are generally accepted to reside within the tissue⁷. In the inner and middle part of the meniscus (the avascular zone), the main cell type has been defined as having a round or oval shape and the cells have been termed fibrochondrocytes⁸. The outer one-third proportion of the tissue is mainly populated by fibroblast-like cells surrounded by a dense connective tissue⁸. The third population, located in the superficial zone of the meniscus, possess a flattened, fusiform morphology. These cells are suggested to be potential progenitor cells with therapeutic and regenerative properties⁹. Previous studies have characterised these meniscal cell phenotypes and gene expression profiles in normal human and animal tissues^{10–12}. However, to the best of our knowledge, the detailed phenotype of degenerate tissue-derived populations and the surface marker profile of the meniscal cells from the different regions of degenerate menisci have yet to be characterised.

Though human lateral and medial meniscus both are roughly semilunar and wedge-shaped, they have distinct dimensions and morphologies⁷. The lateral menisci display a greater variety in shape, size and thickness than the medial menisci¹³. It also covers a larger proportion of the tibial plateau ($59 \pm 6.8\%$ laterally) in comparison to the medial meniscus ($50 \pm 5.5\%$ medially)¹⁴. However, because of the lack of regular availability of the medial meniscus in degenerate knees, in this study we have only focused on investigating the lateral menisci from the medial compartment of OA patients who underwent total knee replacement (TKR) surgeries.

Cell-based meniscus tissue engineering is considered to represent a promising strategy for meniscus repair and regeneration¹⁵. Meniscal cells from normal human and animal menisci have demonstrated chondrogenic capacity *in vivo* and *in vitro*^{16,17}. However, human meniscal cells derived from the debrided tissue of bucket handle tears showed chondrogenic capacity in pellet culture with significantly less collagen type II and more collagen type I production compared with human bone marrow-derived mesenchymal stem cells (MSCs)¹⁶. This study also demonstrated the successful repair of rabbit meniscus punch defects with autologous meniscal cells delivered in hyaluronan-gelatin scaffolds after 12 weeks. In another defect model, sheep meniscus defects implanted with autologous meniscal cells pre-seeded into a collagen meniscus implant (CMI) demonstrated increased extracellular matrix production and enhanced vascularization after 3 months compared to non-seeded CMI scaffold controls and meniscus-resected controls¹⁷, suggesting that implanted cells contributed to the improved repair noted. However, whether or not meniscal cells derived from OA tissues can retain this therapeutic potential is unclear.

The present study compares the cell characteristics, chondrogenic capacities and phenotypic markers of meniscal cells derived from the inner and outer lateral meniscus (avascular and vascular zones) as well as donor-matched articular chondrocytes from the lateral femoral condyle taken from patients with medial compartment OA knee joints. The study aims to further our knowledge regarding the pathological status of these tissues and to assess the potential of cells derived from OA meniscal tissues for regenerative purposes.

Results

Histological scoring and analysis of meniscus sections. Donors matched samples of cartilage, avascular and vascular meniscus tissue were obtained from 10 patients (6 males and 4 females, ages 46–87 years) undergoing TKR surgery (Table 1). Since the avascular and vascular zones often differed in their morphology and degree of degeneration, we decided to grade them separately. The metachromasia intensity in the matrix of the vascular zone was found to be significantly stronger than in the avascular zone of the tissue (Fig. 1). The inner borders scored either 2 or 3, compared to the other zones which generally had lower scores, suggesting that the inner rim of the meniscus in an OA joint was likely to be the first and most seriously affected structure in the disease process. There were no significant differences observed between regions for other histological parameters.

Several noteworthy histological observations were made. Fibrillation, disrupted tissue structures and/or abnormal cellularity was noted mainly along the inner border, but less frequently elsewhere. These changes appeared to coincide with oedematous changes within the matrix close to surface (Fig. 2a). Cells in the swollen oedematous region showed a chondrocytic appearance. Cell clusters were also observed in these regions and the surrounding extracellular matrix was typicallyacellular. In addition, the toluidine blue (TB) intensity in the corresponding regions appeared stronger (Fig. 2b).

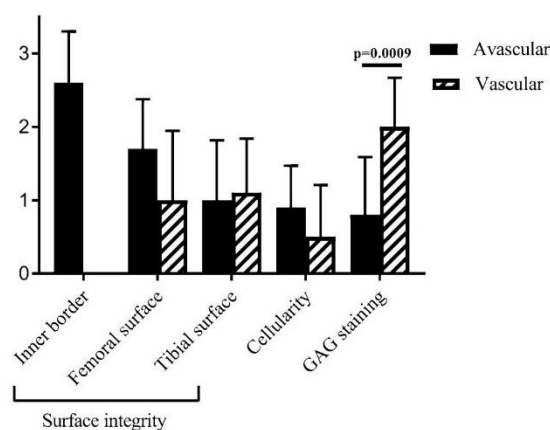


Figure 1. Histological grading results of avascular and vascular regions of the meniscus based on three scoring parameters (n = 10). The glycosaminoglycan (GAG) staining intensity in the vascular region was significantly higher than in the avascular region; (Grade 1: 0–3; Grade 2: 4–7; Grade 3: 8–11; Grade 4: 12–15). Data shown are the means \pm the standard deviation.

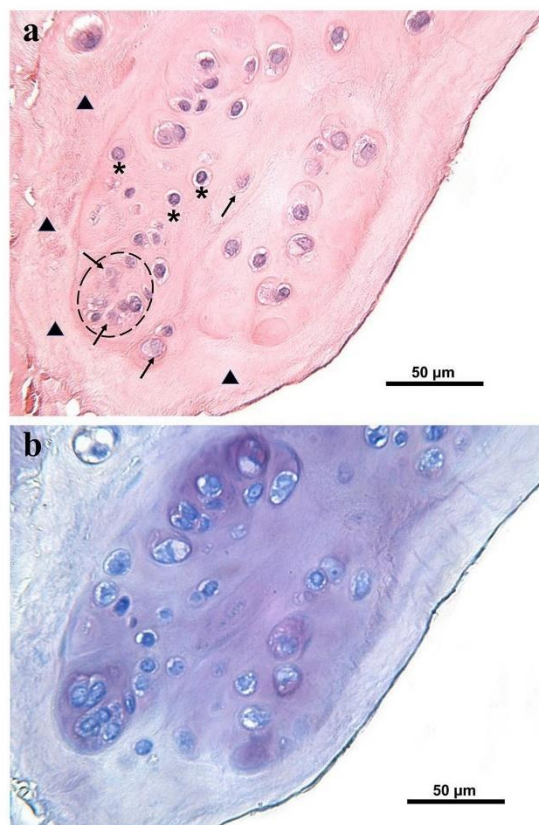


Figure 2. Representative meniscus histology from donor 9 stained with H&E and TB (avascular region, Grade 2): (a) Oedematous changes were observed in the meniscus surface zone, where the cells often appeared chondrocytic (*) sometimes forming clusters (dashed line). The area surrounding the oedematous region was typically acellular (\blacktriangle) Note the necrotic appearance of some cells in this area and within the clusters (\ast); (b) A higher intensity of TB staining was observed in the oedematous region.

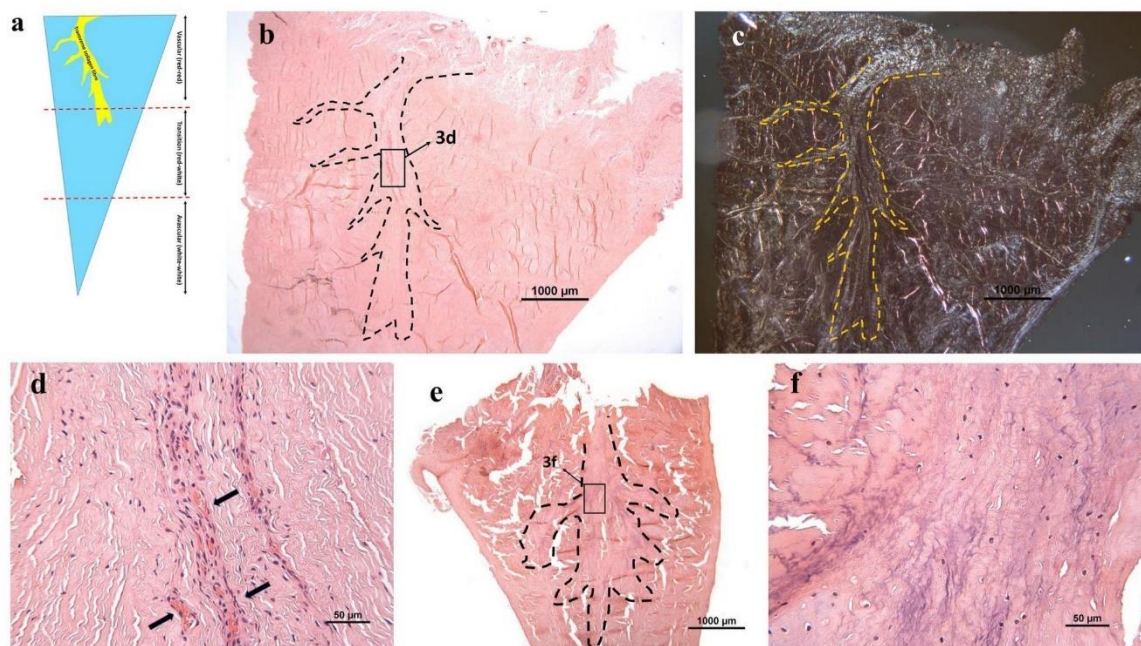


Figure 3. Representative images of Grade 2 (b–d: donor 4) and Grade 3 (e, f: donor 9) menisci with H&E staining: (a) The cross-section diagram of meniscus. The “tree-like” transverse collagen fibre (yellow) runs radially from synovial tissue into vascular region. (b) The collagenous ligament derived from the capsule presented a “tree-like” structure (dotted line); (c) The “tree-like” structure (dotted line) shown in (b) could be visualized easier under polarized light; (d) Blood vessels (arrows) were distributed along the “tree” root; (e) In the Grade 3 menisci where the matrix was fragmented; (f) The “tree-like” structure was more degenerate and without blood vessels in the Grade 3 menisci.

A collection of transverse collagen fibres, referred to as the transverse ligament, were found running from the synovial edge (Fig. 3a) into the vascular region. The ligament presented a “tree-like” formation of fibres interwoven into the avascular region in all 10 patient samples (Fig. 3b), which was most obvious when viewed under polarized light (Fig. 3c). Blood vessels in all six Grade 2 menisci were found associated with this ligament, running alongside the collagen fibres (Fig. 3d). Interestingly, in the Grade 3 and 4 menisci, less blood vessels were found associated with this “tree-like” structure compared to Grade 2 menisci (Fig. 3e,f).

Growth kinetics. Vascular meniscal cells proliferated at a significantly higher rate at passage 0–1 compared to avascular meniscal cells ($p=0.0191$) and chondrocytes ($p=0.0057$) (Fig. 4). Cell population doubling time (PDT) appeared to decrease with increased passage number. However, no significant differences were observed between passage 1–2 and passage 2–3.

Cell surface marker expression levels at passage 0 and prior to chondrogenic differentiation at passage 2: donor-matched analyses of avascular and vascular meniscal cells and chondrocytes.

For all three cell types and for all 10 donors at passage 0, the immunopositivity of the MSC markers CD73, CD90, CD105 was over 95%, which adhered to the International Society for Cellular Therapy (ISCT) criteria; however, around 25% of these cells were CD14 positive which should be lower than 2% in MSCs (according to the ISCT)¹⁸, but is similar to levels we have reported previously in MSCs derived from other musculoskeletal tissues. CD29 (integrin $\beta 1$) and CD44 (hyaluronate receptor) were highly immunopositive on all cell fractions, being over 95% positive in avascular and vascular meniscal cells and over 90% positive on chondrocytes. CD19 (B lymphocyte antigen), CD34 (haematopoietic progenitor cell antigen), CD45 (protein tyrosine phosphatase receptor type C), CD271 (low-affinity nerve growth factor receptor) and HLA-DR (human leukocyte antigen-DR) were consistently below 5%, with no significant difference between groups. However, there was a significant difference in CD49b (integrin $\alpha 2$), CD49c (integrin $\alpha 3$) and CD166 (activated leukocyte cell adhesion molecule) immunopositivity between the three cell types (two-way ANOVA) (Fig. 5a). Similar patterns were found in the 6 donors tested at passage 2, prior to chondrogenic differentiation, with significant differences observed for CD49b and CD49c, but not CD166 (Fig. 5b). For CD49b, at passage 0, the immunopositivity was highest for the avascular cells ($53.89 \pm 17.41\%$) and lowest for the chondrocytes ($16.80 \pm 7.03\%$) with $41.46 \pm 14.95\%$ of cells from the vascular region being immunopositive. In passage 2, levels of CD49b on the three cell fractions followed a similar trend (avascular: $81.47 \pm 11.88\%$, vascular: $73.03 \pm 11.36\%$, chondrocyte: $47.16 \pm 21.81\%$), but the difference between avascular and vascular cells was not significant. CD49c was $73.30 \pm 19.84\%$ immuno-

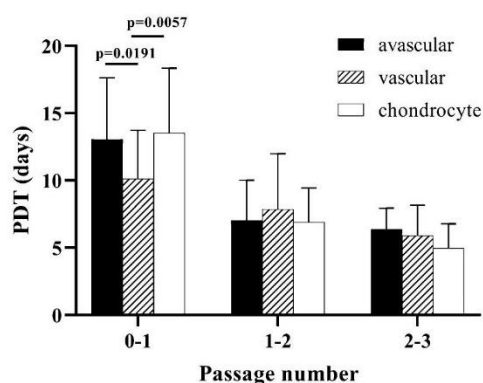


Figure 4. Graph to show the population doubling time (PDT) of avascular, vascular meniscal cells and chondrocytes during cell culture relative to passage number (passage 0–3). Data shown are the means \pm the standard deviation.

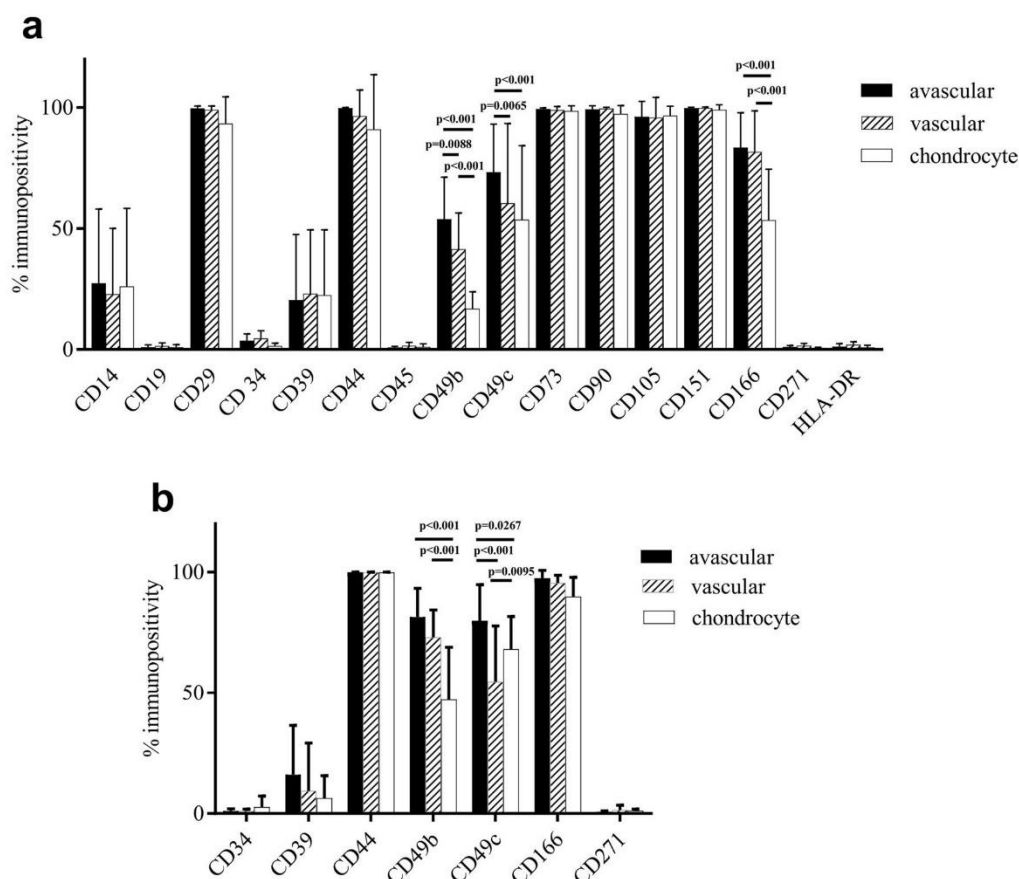


Figure 5. (a) Meniscal cells and chondrocytes exhibited similar immunopositivity for most of the markers investigated at passage 0. A greater percentage of meniscal cells were positive for CD49b, CD49c and CD166 compared with chondrocytes (10 donors); (b) A similar pattern was found for CD49b and CD49c immunopositivity across the cell types at passage 2 (6 donors). Data shown are the means \pm the standard deviation.

	Region	Tibial			Inner border			Cellularity			GAG intensity		
		<i>p</i>	<i>z</i>	<i>r</i>	<i>p</i>	<i>z</i>	<i>r</i>	<i>p</i>	<i>z</i>	<i>r</i>	<i>p</i>	<i>z</i>	<i>r</i>
CD19	Avas	0.292	1.054	0.333	0.313	-1.008	-0.319	0.093	1.681	0.532	0.846	-0.194	-0.061
	Vas	0.492	0.688	0.218	-	-	-	0.756	0.311	0.098	0.024	2.261	0.715
CD29	Avas	0.288	1.064	0.336	0.047	1.986	0.628	0.619	-0.497	-0.157	0.667	-0.430	-0.136
	Vas	0.598	-0.527	-0.167	-	-	-	0.657	-0.445	-0.141	0.321	-0.992	-0.314
CD34	Avas	0.151	1.437	0.454	0.093	1.681	0.532	0.911	0.112	0.035	0.699	-0.387	-0.122
	Vas	0.280	1.080	0.342	-	-	-	0.005	2.800	0.885	0.100	1.644	0.520
CD39	Avas	0.151	1.437	0.454	0.313	1.008	0.319	0.575	-0.560	-0.177	0.699	-0.387	-0.122
	Vas	0.202	1.277	0.404	-	-	-	0.049	1.970	0.623	0.681	0.411	0.130
CD49b	Avas	0.009	2.595	0.821	0.018	2.360	0.746	0.911	0.112	0.035	0.627	-0.486	-0.154
	Vas	0.280	-1.080	-0.342	-	-	-	0.756	0.311	0.098	0.537	-0.617	-0.195
HLADR	Avas	0.028	2.203	0.697	0.911	0.112	0.035	0.575	0.560	0.177	0.561	-0.581	-0.184
	Vas	0.377	0.884	0.280	-	-	-	0.254	1.141	0.361	0.150	1.439	0.455

Table 2. Correlation between surface markers and histology scores. Jonckheere-Terpstra test: Avascular region (marked with grey background); vascular region (marked with white background). Only values that have significant differences are shown in the Table; see the full dataset in the Supplementary Table 1. The significant values are highlighted in bold and italics.

positive on avascular meniscal cells at passage 0, which was significantly higher than vascular meniscal cells ($60.47 \pm 32.99\%$) and chondrocytes ($53.69 \pm 30.60\%$). At passage 2, the immunopositivity of avascular meniscal cells for CD49c was again significantly higher than for the other cell populations, but those from the vascular region were significantly lower than chondrocytes (avascular: $79.99 \pm 14.91\%$, vascular: $54.70 \pm 23.04\%$, chondrocyte: $68.19 \pm 13.46\%$). CD166 positivity was significantly higher on avascular ($83.47 \pm 14.41\%$) and vascular ($81.68 \pm 16.95\%$) meniscal cells compared to chondrocytes ($53.47 \pm 21.09\%$) at passage 0. However, time in culture appeared to upregulate CD166 on chondrocytes, from a mean of 53.47% at P0 to 89.82% at P2. No significant differences were observed for CD166 at passage 2 across the different cell populations (avascular: $97.50 \pm 3.26\%$, vascular: $95.50 \pm 3.22\%$, chondrocyte: $89.82 \pm 7.97\%$).

Comparing flow profiles and histological analyses. The immunopositivity of six markers was significantly related to some histological parameters scored in the avascular and vascular regions (Table 2). Analysis via the Jonckheere-Terpstra test revealed that when the meniscus tibial surface was more severely disrupted in the avascular region, the median number of avascular meniscal cells which were immunopositive for CD49b ($p=0.009$) and HLA-DR ($p=0.028$) increased. In avascular meniscal cells CD49b positivity was also found to be increased when the inner border had more severe disruption ($p=0.018$); the same relationship was found with CD29 ($p=0.047$). Further, when more hypocellularity was observed in the vascular zone, the median immunopositivity for CD34 and CD39 in vascular meniscal cells increased ($p=0.005$ and $p=0.049$, resp.). Finally, it was shown that as GAG intensity increased in the vascular zone, more of the vascular meniscal cells were immunopositive for CD19 ($p=0.024$).

Gene expression profiles: donor-matched analyses of avascular and vascular meniscal cells and chondrocytes. A significantly higher expression level of SOX-9 was found in chondrocytes compared to avascular and vascular meniscal cells (Fig. 6a). Unsurprisingly, the avascular and vascular groups showed a higher expression level of collagen type I compared to donor matched chondrocytes (Fig. 6b). No significant differences were found in the expression levels of collagen type II (COL II), aggrecan (ACAN) or MMP-1 between the cell types (Fig. 6c-e).

In vitro chondrogenic pellet analysis. Chondrogenic capacity across all of the cell types was tested in 6 donors after 28 days of chondrogenic differentiation in pellet culture. In terms of GAG/DNA analyses, chondrocytes consistently produced the highest levels of GAG, while avascular meniscal cells showed lower GAG levels compared to vascular meniscal cells (Fig. 7a). This finding appeared to match the histological grading of TB intensity in the avascular and vascular zones: that is, the vascular regions demonstrated more pronounced matrix metachromasia compared to avascular regions (Figs. 1a, 7a). The donor-matched chondrogenic pellets showed variable chondrogenic capacity across individuals. Overall, strong collagen type I staining was observed in all pellets and across cell types after 28 days of chondrogenic induction, with the highest staining intensity in the vascular meniscal cells (Fig. 7b,c). This observation appeared to match the collagen type I gene expression profile for each cell population (Fig. 6b). However, weak collagen type II staining were detected in all cell types, with a significantly stronger staining intensity produced by chondrocytes pellets compares with vascular meniscal cell pellets (Fig. 7d).

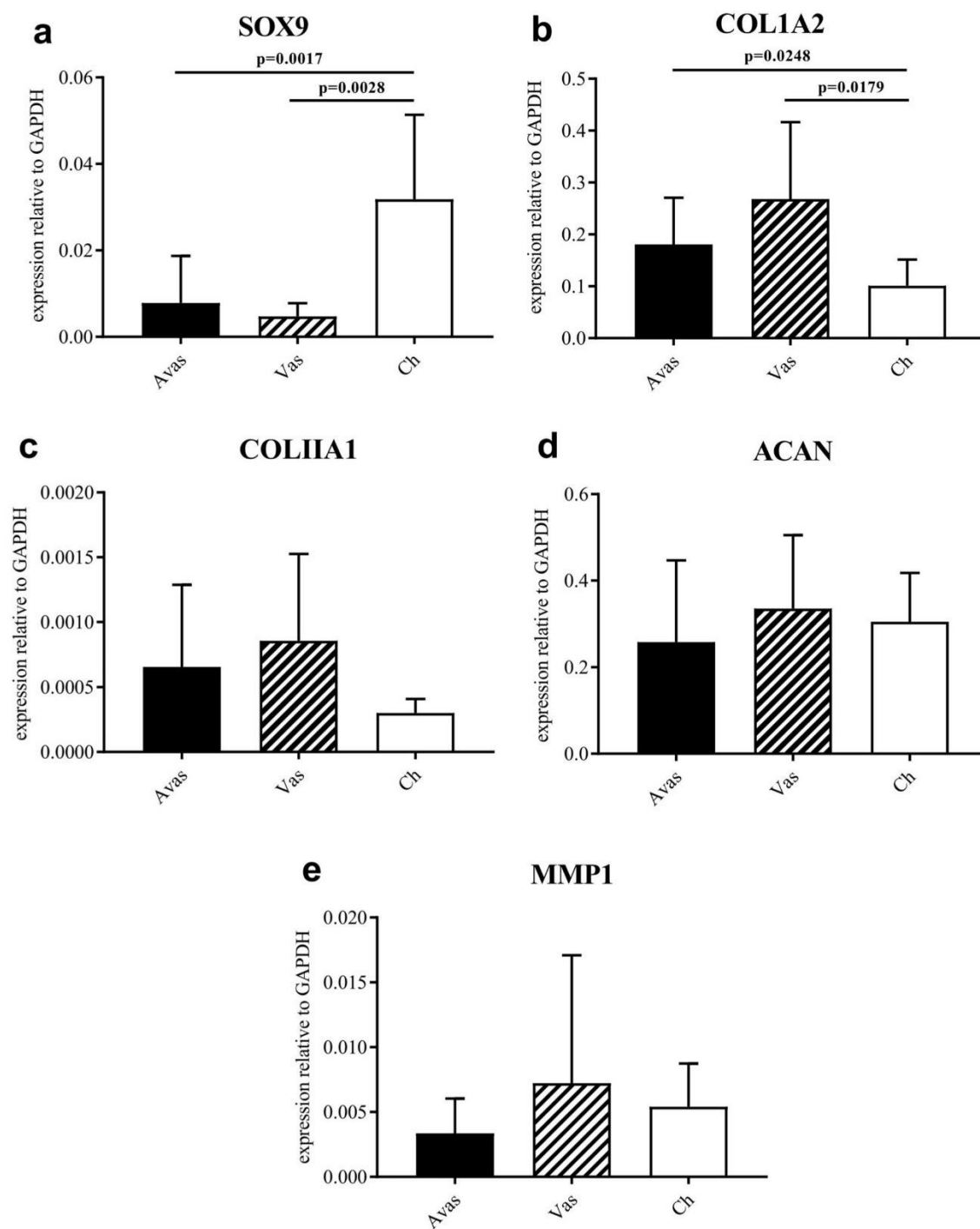


Figure 6. The chondrogenic genes and MMP-1 expression profiles in Avas, Vas and Chondrocytes after 14 days in monolayer culture (a–e). Data shown are the means \pm the standard deviation of triplicate technical replicates and 10 donors for each cell population. Gene expression is shown relative to the reference genes, glyceraldehyde-3-phosphate dehydrogenase (GAPDH).

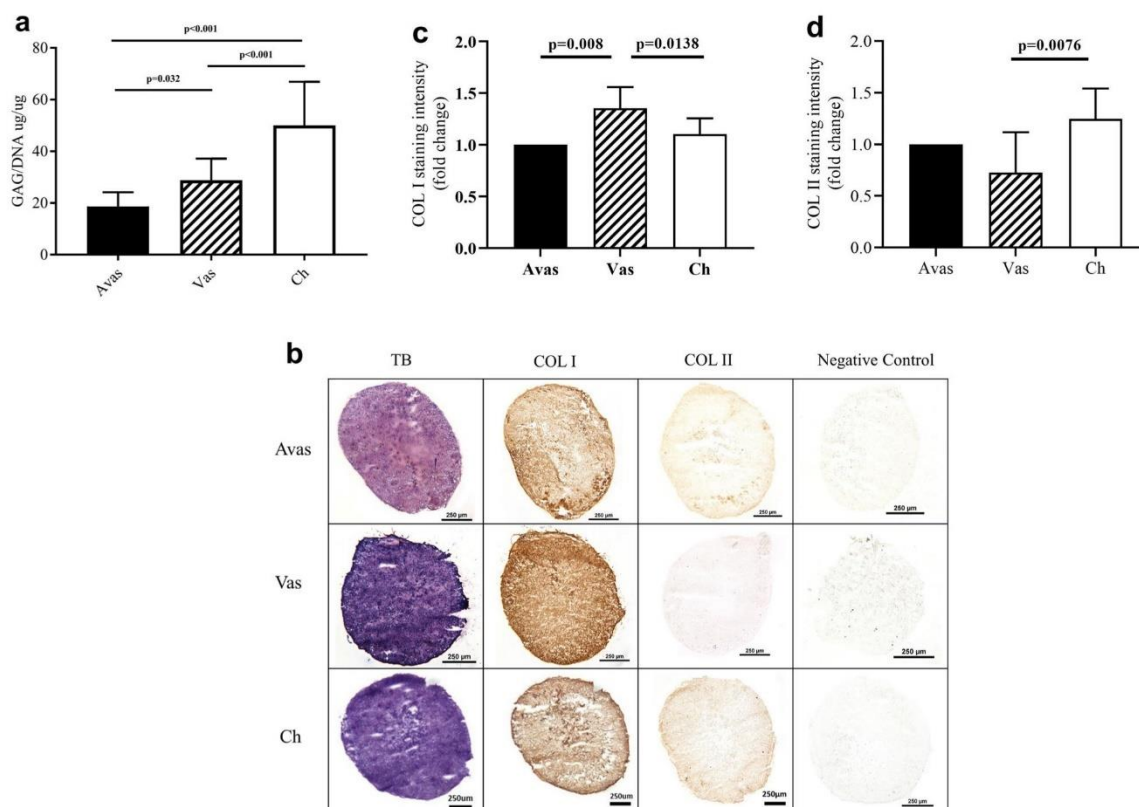


Figure 7. The chondrogenic assessment of avascular and vascular meniscal cells and chondrocytes. **(a)** GAG/DNA quantitation after 28 days of culture in pellets, a comparison of Avascular (Avas) and Vascular (Vas) meniscal cells and chondrocytes (Ch). Data shown are the means \pm the standard deviation of triplicate runs and 6 donors for each cell population. **(b)** Histological analysis of a representative donor 6, chondrogenic pellet sections from Avas, Vas, Ch showing toluidine blue (TB), collagen type I (COL I) and collagen type II (COL II) staining. Scale bars represent 250 μ m. **(c)** Collagen type I and **(d)** collagen type II semi-quantitative immunohistochemical (IHC) analysis, relative fold change to avascular meniscal pellet.

	Coefficient	95% confidence interval		<i>p</i>
		Lower	Upper	
CD34	-0.4543	-1.8915	0.983	0.553
CD39	0.277	-0.0109	0.565	0.096
CD44	-77.5159	-123.7309	-31.301	0.011
CD49b	0.4098	0.0922	0.727	0.035
CD49c	0.0606	-0.1577	0.279	0.601
CD166	-0.2386	-0.6014	0.124	0.233
CD271	-2.911	-6.1629	0.341	0.117
Vascular-avascular	21.0973	11.0721	31.122	0.003
Chondrocytes-avascular	44.3104	29.7228	58.898	<.001

Table 3. Multilevel modelling. The significant values are highlighted in bold and italics.

Chondrogenic potency analysis. Multilevel modelling analysis was conducted to identify chondrogenic potency predictors prior to chondrogenic differentiation (Table 3). CD49b immunopositivity positively associated with GAG quantitation ($p=0.035$). Similar to previous chondrogenic analysis (Fig. 7a), cell types (vascular meniscal cells and chondrocytes) had a significant impact on GAG quantitation compare to avascular meniscal cells ($p=0.003$ and $p<0.001$, resp.). This analysis also showed that CD44 expression negatively associated with GAG quantitation in pellet cultures ($p=0.011$).

Discussion

It is widely accepted that meniscus degeneration leads to the deterioration of articular cartilage and the onset of osteoarthritis⁷. However, the precise mechanisms of the early meniscus degeneration process are still unclear, particularly in terms of cellular phenotypic changes and extracellular matrix alterations¹⁹. We designed this study to undertake a comprehensive characterisation of meniscal cell populations derived from the lateral meniscus obtained from TKR patients. Although we were careful to choose regions with an intact morphology, these tissues were no doubt affected by an OA pathological environment for a prolonged period. In the medial compartment of OA patients, the increased medial loading disrupts the normal medio-lateral load sharing balance. This imbalance leads to lateral compartment lift-off²⁰. Therefore, the lateral meniscus experiences abnormally lower loading which slows down its tissue breakdown²¹. Based on our histological findings, the lateral menisci derived from such joints have experienced varying degrees of deterioration as was demonstrated by our use of the Pauli et al. histological grading system⁴.

Petersen et al. first described the loosely arranged collagen fibres entering the external circumference of the meniscus, originating from the joint capsule and inserting between the circular fibre bundles of the meniscus²². In our study, these “tree-like” shaped structures were identified in all donors. However, to our knowledge, no previous study has described them in relation to the pathological changes observed over time with knee OA. Arnoczky et al. (1982) demonstrated small radial branch of blood vessels which came from the perimeniscal capillary plexus penetrating the meniscal stroma a short distance into the main body of the meniscus²³. The formation of these vessels was seen to associate with the “tree-like” collagen fibres entering into the meniscus. In the present study, histological analyses showed that these blood vessels mainly appear along the collagen fibre “tree root”. However, the vessels were only found in the “tree root” in the vascular area of Grade 2 menisci and were rarely present in the same region in Grade 3 or 4 specimens. This result matches findings from a previous study, which reported blood vessel occurrence only in the dense connective tissue but not in the fibrocartilage²⁴. In this study it was also reported that only a quarter of the meniscus tissue was vascularised in the aged meniscus, whereas the outer one third of the meniscus tissue was vascularised in young adult menisci. Degenerative meniscal tears generally have a complex pattern and are mainly found in the middle and posterior body of the meniscus¹⁹. Partial meniscectomy or non-operative management is normally chosen to treat these patients due to the low healing potential of the degenerate meniscus²⁵. The diminished blood supply noted in the vascular region of the degenerate meniscus may play an important role in its reduced self-healing capacity.

The meniscal cells from the OA joint consist of a heterogeneous population, which has not been well characterised previously. In our study, similarities found in the expression of surface molecules (CD14, CD19, CD29, CD34, CD39, CD44, CD45, CD73, CD90, CD105, CD151, CD271, HLA-DR) from avascular and vascular meniscal cells and chondrocytes indicate their overlapping characteristics and chondrogenic potential. Despite these similarities, differences in CD49b (integrin $\alpha 2$), CD49c (integrin $\alpha 3$) and CD166 (ALCAM) were noted between all cell fractions derived from OA affected tissues. Grogan et al. (2017) reported, in the normal human meniscus, a greater percentage of meniscal cells that were positive for CD14 (LPS-receptor), CD26 (dipeptidyl peptidase IV) and CD49c compared to articular chondrocytes (10 donors)¹⁰. The differences noted in our study in comparison indicate that the OA environment influences the cell surface molecule expression in meniscus and cartilage.

Grogan et al. highlighted that there was positive immunostaining for CD166 (activated leukocyte cell adhesion molecule, ALCAM) on cells that predominately surrounded the blood vessels in the vascular region of the meniscus and on cells at the meniscus surface¹⁰. These cells could be progenitors, as CD166 has previously been used to identify the progenitor populations from chondrocytes in healthy cartilage²⁶. A previous study demonstrated a higher number of CD34 (a stem cell marker) and CD146 (a pericyte marker) positive freshly isolated cells to be found in the vascular region compared with the avascular region of the lateral meniscus in OA patients. This CD34 and CD146 positive cell populations showed multilineage differentiation capacities and contributed to meniscus repair in a rat model²⁷. Our flow cytometry analysis of the different meniscal regions showed higher expression levels of CD166 in the vascular meniscal cell fraction. In addition, our PDT data demonstrated that the vascular meniscal cells possess a higher proliferation rate compared to the other cell types. Together this indicates the presence of progenitors associated with the blood vessels or perhaps that the vasculature in the peripheral region drives a more progenitor-like meniscal cell phenotype in this region. This theory is further supported by our hypothesis that the “tree-like” fibres which “tie” the synovial tissue and meniscus together, not only provide the structural supports for the blood supply into the peripheral meniscus, but may also harbour a conduit for the “progenitor” cells which could originate from synovium, as CD166 positive mesenchymal progenitor populations have been identified in the synovium tissue of osteoarthritic knees²⁸. Ideally, the use of fluorescence-activated cell sorting (FACS) to isolate and quantify CD166 immunopositive populations for further progenitor phenotypic characterisation would be required to validate our hypothesis in future work. In the more degenerate meniscus, we noted the absence of blood vessels with “progenitor” cells in these “tree-like” fibres. We hypothesise that this structure (comprising of collagen fibres, blood vessels and cells) plays an important role in maintaining the meniscus matrix, protecting against the degeneration process in the early OA stages; however, this requires further investigation before firm conclusions may be drawn. In addition, the “tree-root” cell population may have regenerative properties pertinent to the development of meniscus tissue engineering strategies.

Integrins play a key role in mediating chondrocyte-ECM interactions in the OA pathophysiology of articular cartilage degeneration²⁹. However, the role that integrins have in the degeneration of the meniscus is still unclear. CD49b and CD49c are integrin alpha subunits which were first identified as ECM receptors for collagens, laminins and fibronectin³⁰. CD49b was found to have an increased expression in cartilage in the late stage OA mouse model³¹. Unusually, in this animal study CD49b cell signalling was found to be induced by changes in the ECM components which increase the catabolic activity of chondrocytes and favour cell death, as a consequence

of increased metalloproteinase (MMP) activity. Integrin $\alpha 3$ was also identified to be differentially expressed in the whole knee joint in the destabilization of the medial meniscus (DMM) mouse model, which was closely associated with the development of OA³². Our flow cytometry results demonstrate that CD49b and CD49c positivity levels are higher in avascular meniscal cells compared with vascular meniscal cells and chondrocytes in both passage 0 and passage 2 cell populations. This result might be due to the fact that fraying of the avascular region was found in all of the samples included in the study, perhaps indicating a more advanced response to OA progression in the avascular region of the meniscus compared to the other regions examined. The correlation results also demonstrated that with more disrupted tissue structures in the meniscus inner border, the avascular meniscal cells' immunopositivity for CD49b and CD29 (integrin $\beta 1$) increased. $\beta 1$ integrin-collagen interaction is a critical signalling pathway for chondrocyte survival, which prevents apoptosis³³. Therefore, our results could support the hypothesis that the OA-like ECM changes in the avascular region of the meniscus induced the up-regulation of CD49b, CD49c and CD29, although additional mechanistic study will be required to draw firm conclusions.

The multilevel modelling analysis performed to find predictors of chondrogenic potency in this study suggested that higher expression levels of CD49b were significantly associated with higher GAG quantities. A previous study demonstrated that gene expression levels of CD49b were up-regulated in human chondrocyte pellet cultures at day 14 compared to monolayer cultures³⁴. Another study has shown that GAG production significantly increases over time in pellet cultures compared to monolayer cultures³⁵. However, CD49b expression pre-pellet formation has not previously been shown to associate with higher post-pellet GAG levels. Although the higher expression of CD44 was also found to correlate with GAG production, when interpreting this finding it should be kept in mind that in our experiments the CD44 expression ranged from 99.6% to 100% (Fig. 5b). This represented a variation of 0.4%, similar in magnitude to the accuracy by which CD44 could be determined by flow cytometry (Supplementary Table 2). As a consequence, this significant association could well be a "false positive", finding an effect when none actually exists. Multiple regression models can be prone to this type of error³⁶. In addition, such a small variation in CD marker expression is unlikely to have any biological effect. Therefore, CD44 was not considered as a marker associated with GAG production in this case. We should also be cautious when interpreting any results derived from a small sample size. We acknowledge this as a limitation of the study.

Tears of the meniscus are a common sporting injury in fairly young individuals. If they can be repaired biologically, this could avoid the development of OA which is otherwise likely to occur. Autologous meniscal cells derived from the meniscus lesion site could represent a potential cell source for meniscus repair strategies⁷. In the current study, we have shown that extracted and sub-cultured avascular and vascular meniscal cells possess similar chondrogenic capacity with a higher gene expression level of collagen type I compared to donor matched chondrocytes, which more closely matches each of the tissue's native collagen composition. As such meniscal cells may represent a more desirable cell source for cell therapy of the meniscus as they retain their capacity to more specifically reconstitute the native meniscus tissue matrix composition. Such an approach would require two surgical interventions including a biopsy to extract meniscal cells and a second procedure to implant cells or a tissue-engineered meniscus. Moreover, insufficient cell numbers may be obtained from limited "normal" donor tissue. To address these potential issues, human bone marrow stromal cells (BMSCs) were investigated as a supplemental or alternative cell type to meniscal cells for meniscus tissue engineering. Studies have shown that co-culturing BMSCs with meniscal cells resulted in enhanced chondrogenic ECM production under normal and low oxygen in vitro conditions³⁷. Hagmeijer et al. (2018) also demonstrated the feasibility of a one stage procedure by using a rapid digestion for autologous meniscal cells combined with allogenic BMSCs (20:80), applied to a commercial Collagen Meniscus Implant (CMI) scaffold with fibrin glue as carrier in a cadaveric study³⁸. Current treatments for meniscus deficient patients with knee pain that has developed several years after meniscectomy are partial meniscus replacement with a biodegradable scaffold or meniscus allograft transplantation, both of which produce sub-optimal clinical outcomes^{39,40}. The ideal solution is to perform a single stage cell-based partial meniscus replacement when meniscectomy is decided to be the surgical course of action. In this case the surgeon would be able to obtain sufficient meniscus tissue for autologous meniscal cell derivation. Moreover, it is expected that the patient will observe improved outcomes when they receive the treatment at an early stage of disease rather than as a remedial course of action years after the development of OA.

There are several limitations associated with the current study that should be acknowledged. Firstly, we have focused solely on the lateral meniscus from the medial compartment in OA patients, a comparison of medial menisci from lateral OA patients would make for a more complete study. However, insufficient samples for this comparison could be obtained because knee OA is more commonly seen in medial rather than lateral compartment⁴¹. Another limitation of this study is that RNA extraction was not performed to check the gene expression levels of post-chondrogenic pellet but only in monolayer culture because of limited cell numbers. Such chondrogenic related gene expression analysis would complete the chondrogenic potency analysis undertaken in the study.

In conclusion, our study has indicated that CD49b, CD49c and CD166 appear to be important phenotypical markers which can discriminate cells from avascular or vascular meniscus and cartilage in the OA joint. We have observed distinct meniscal cell profiles, which are reflected in corresponding changes in the tissue's structure histologically. The meniscus "tree-like" structure of collagen fibres observed throughout the histological analyses in this study may play an important role in supporting the blood supply to vascular region of meniscus and maintaining the meniscus integrity, protecting against the structural breakdown which can occur as OA progresses. We have also demonstrated that meniscal cells derived from the lateral meniscus of medial compartment OA patients have chondrogenic capacity in vitro and hence could represent a potential cell source to consider for meniscus tissue engineering.

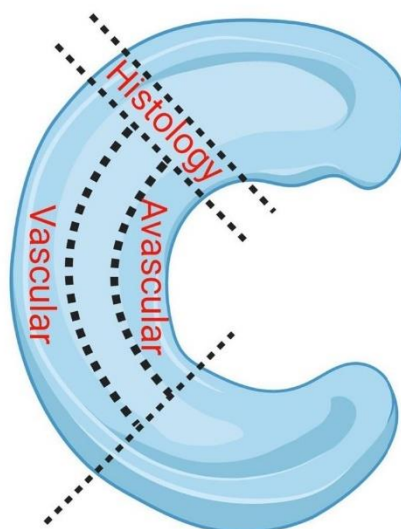


Figure 8. Schematic diagram of the process used for meniscus dissection: The medial body of the macroscopically “normal” meniscus was longitudinally divided into three parts: the inner third was used to extract avascular meniscal cells, the outer third for the extraction of vascular meniscal cells. The adjacent section which composed of the inner and outer regions was dissected for histological grading. Figure was created with BioRender.com.

Methods and materials

Lateral meniscus and cartilage harvest. All the tissue samples used in this study were obtained following the provision of written, informed consent from patients. Favourable ethical approval was given by the National Research Ethics Service Committee Northwest Liverpool East (11/NW/0875) and all experiments were performed in accordance with relevant guidelines and regulations. Macroscopically, intact lateral menisci from the lateral compartment, as well as donor-matched articular cartilage from the lateral femoral condyle, which demonstrated minimal OA changes (macroscopically classified as Outerbridge Grade I or II), were harvested from donors who were undergoing TKR for medial compartment ($n = 10$; mean age 66.4 ± 11.1 ; age range 46–87 years; 4 males, 6 females).

Cell isolation. The middle one third of the lateral meniscus was dissected equally into the inner (avascular zone), middle and outer (vascular zone) in a longitudinal direction (Fig. 8). The middle portion was discarded such that only the definite vascular and avascular zones were studied as such. A section of the meniscus adjacent to that used for cell culture experiments was obtained for histology. Meniscus and cartilage tissues were digested in type II collagenase (245U/ml; Worthington, USA) in Dulbecco’s Modified Eagle Medium (DMEM)/F12 (1:1) (Gibco, USA) and 1% penicillin–streptomycin (P/S) (ThermoFisher Scientific, USA) for 16 h at 37 °C. The digested tissues were filtered through 70 μm cell strainers (ThermoFisher Scientific, USA) and cells were seeded at a density of 5000 cells per cm^2 . The meniscal cells were maintained in monolayer culture in a humidified environment of 5% (v/v) CO_2 and 37 °C for 14 days.

Growth kinetics. Population doubling times (PDT) were calculated for each cell type (from passage 0–3) using the following formula: $\text{PDT} = (t_2 - t_1) \times \ln(2) / \ln(n_2/n_1)$, t_1 = the time of cell seeding, t_2 = the time of cell harvest and n = the cell population at the matching time points.

Histological analysis of meniscus sections. The region of the meniscus adjacent to that used for cell culture from 10 donors was fixed in 10% neutral buffered formalin and embedded in paraffin. Sections (4 μm thick) were stained with haematoxylin and eosin (H&E) for the visualisation of morphological details and with toluidine blue (TB; British Drug Houses, UK) to assess the GAG distribution. All samples were categorised using a modified microscopic meniscus grading system developed by Pauli et al.⁴. Briefly, this modified grading system scored menisci based on the following parameters: (A) Meniscus surface integration of the femoral and tibial side and at the inner border (0: smooth, 1: slight fibrillation and undulation, 2: moderate fibrillation, clefts and undulation, 3: severe fibrillation, clefts and undulation); (B) Cellularity (0: normal, 1: diffuse hypercellularity, 2: diffuse hypo/acellular regions, 3: hypocellularity, empty lacuna, pyknotic cells); (C) Toluidine blue matrix staining intensity (0: none, 1: slight, 2: moderate, 3: strong). The avascular and vascular regions were scored separately by two independent (blinded) assessors. The total score was calculated as follows: $S_{\text{total}} = ((A + B + C)_{\text{Avas}} + (A + B + C)_{\text{Vas}}) / 2 + A_{\text{inner-border}}$. The mean score of the two individual readers was converted to the following grades: Grade 1 represents normal tissue (score 0–3) and Grade 2 indicates mild degeneration

(score 4–7). Moderate degeneration is seen in Grade 3 tissue (score 8–11), while Grade 4 represents the most severe degeneration (score 12–15).

Flow cytometry. After 14 days of monolayer culture expansion (passage 0) each cell type was re-suspended in a PBS buffer of 2% (v/v) bovine serum albumin (BSA; Sigma-Aldrich). Flow cytometry receptors were blocked using a PBS buffer of 10% (v/v) human immunoglobulin (Grifols, Spain) at 4 °C for 1 h. Immunopositivity for 16 molecules which are indicative of mesenchymal stromal cell (MSC) profile (CD14, CD19, CD34, CD45, CD73, CD90, CD105, HLA-DR), chondrogenic potency or cell adhesion molecules (CD29, CD39, CD44, CD49b, CD49c, CD151, CD166, CD271) were targeted. At passage 2, prior to chondrogenic differentiation, a smaller flow panel including chondrogenic potency molecules (CD39, CD44, CD271) and those in which a marked difference was observed between cell populations at passage 0 (CD49b, CD49c, CD166) were investigated in 6 donors.

RNA extraction and quantitative real-time polymerase chain reaction (qRT-PCR). After trypsinisation at passage 0, 100,000 cells were centrifuged (350×g for 8 min), frozen in liquid N₂, and stored at –80 °C temporarily before mRNA extraction. mRNA was extracted using a RNeasy Mini Kit (Qiagen, Hilden, Germany) according to the manufacturer's instructions. A High-Capacity cDNA Reverse Transcriptase Kit (Applied Biosystems, Warrington UK) was used for reverse transcription. qRT-PCR was performed on the Quant Studio 3 Real-Time Quantitative PCR System (Applied Biosystems) using a SYBR Green Reaction Mix. Gene expression levels of collagen type I (COL1A2), collagen type II (COL1A1), aggrecan (ACAN), SOX-9 and matrix metalloproteinase-1 (MMP-1) were normalised against the housekeeping genes glyceraldehyde-3-phosphate dehydrogenase (GAPDH) (Qiagen, QuantiTect Primer Assay). The relative gene expression level of each gene was determined by using the comparative C_T method⁴².

Chondrogenic differentiation. The chondrogenic potency of the three donor-matched cell populations were assessed at passage 2 using a well-established 3D pellet culture system in 6 donors⁴³. Briefly, 2 × 10⁵ cells were centrifuged into a cell pellet with DMEM F12, P/S (1%), ITS (1%), ascorbic acid (0.1 mM) (Sigma-Aldrich), dexamethasone (10 nM), sodium pyruvate (Sigma-Aldrich) and transforming growth factor β-1 (TGF-β-1, PeproTech, London, UK) (10 ng/ml). After 28 days in culture, n = 3 pellets were used for biochemical GAG/DNA quantitation, n = 3 pellets were snap frozen in liquid nitrogen-cooled hexane and stored at –80 °C prior to histological analysis.

GAG/DNA analysis. Pellets were digested in papain to release GAG and DNA. The papain digestion buffer was composed of 50 mM sodium phosphate (BDH), 20 mM EDTA (Sigma-Aldrich), 20 mM N-acetyl cysteine (BDH) and adjusted to pH 6.0. Papain was added to the buffer to reach the final concentration of 125 μg/ml. Each pellet was digested in 200 μl of the papain solution at 60 °C for 3 h. Samples were centrifuged at 1000 g for 5 min and stored at –20 °C prior to use. The GAG content in pellets was measured by 1,9-dimethylmethylene blue (DMMB) assay⁴⁴, with chondroitin sulphate (C9819, Sigma-Aldrich) from bovine trachea used to construct a standard curve. Briefly, 50 μl of each sample was added in duplicate wells of a 96 well plate, with 200 μl of DMMB dye. The results were read immediately at A_{530nm} and A_{590nm}. The standard curve was plotted using the following equation: (A_{530nm}/A_{590nm}) – (A_{530nm blank}/A_{590nm blank}). The total GAG content of each pellet was calculated using the standard curve equation. The DNA content was measured spectrophotometrically using the PicoGreen dsDNA Assay kit (Invitrogen) according to the manufacturer's instructions. Finally, the amount of GAG measured in the chondrogenic pellet was normalised to its DNA content.

Histological and immuno-histochemical analyses of pellets. Three pellets from each cell population were snap frozen in liquid nitrogen and stored at –80 °C prior to use. Pellets were sectioned at a 7 μm thickness and collected onto poly-L-lysine-coated slides. Cryosections were stained with TB (BDH) to assess the general tissue morphology and GAG composition of the extracellular matrix. In addition, immunohistochemistry for collagens type I and II was undertaken. In brief, sections were incubated with ovine hyaluronidase (4800U/ml, Sigma, UK) prior to fixing in 10% formalin. Primary antibodies raised against collagens type I (1:500, clone I-8H5, MP Biomedicals, Cambridge, UK) or type II (1:50, clone CIIC1, DHSB, University of Iowa, USA) were incubated with sections for 1 h. After washing with PBS, sections were incubated with the secondary biotinylated antibody at 50 μg/ml (goat anti-mouse, VECTASTAIN ABC kit, Vector Laboratories, Peterborough, UK), which was added for 30 min. 0.3% hydrogen peroxide in methanol was used to block endogenous peroxidase activity. Enhanced labelling was performed with streptavidin-peroxidase (VECTASTAIN Elite ABC kit, Vector Laboratories, Peterborough, UK) and visualised with diaminobenzidine (DAB, ImmPACT, Vector Laboratories, Peterborough, UK), after the sections were dehydrated. The immunochemistry staining intensity of collagen type I and type II was quantified using ImageJ Fiji Software (version 1.2; WS Rasband, National Institute of Health, Bethesda, MD)⁴⁵.

Statistical analyses. All data were inputted into GraphPad Prism (Version 7.04, USA) and Jamovi (Version 1.1.9.0) for statistical analysis. Differences between cell types were assessed by performing one-way ANOVAs with Tukey's multiple comparisons for population doubling time, positive percentage fluorescence signal, gene expression level, GAG/DNA comparisons and semi-quantitative of collagen type II IHC intensity. Two-way ANOVAs were used to compare the positive percentage fluorescence signal of different cell types and histological scores in avascular and vascular regions. The Jonckheere–Terpstra test was used to assess the correlation

between the positivity of surface markers and meniscus histological scores. Multilevel modelling was performed to determine whether expressions of cell surface markers were associated with chondrogenic outcome as measured by GAG/DNA content. Cell source and cell surface marker positivity were considered as fixed effects, while the donor was considered as a random effect. Our lab previous data from flow marker reliability test (not published) was used to evaluate the reliability of chondrogenic predictors in multilevel modelling results (Supplementary Table 2). For all tests, values of $p < 0.05$ were considered statistically significant.

Received: 2 June 2020; Accepted: 12 November 2020

Published online: 10 December 2020

References

- MacMullan, P. A. & McCarthy, G. M. The meniscus, calcification and osteoarthritis: a pathologic team. *Arthritis Res. Ther.* **12**, 116 (2010).
- Bennett, L. D. Meniscal and articular cartilage changes in knee osteoarthritis: a cross-sectional double-contrast macroradiographic study. *Rheumatology* **41**, 917–923 (2002).
- Hunter, D. J. *et al.* The association of meniscal pathologic changes with cartilage loss in symptomatic knee osteoarthritis. *Arthritis Rheum.* **54**, 795–801 (2006).
- Pauli, C. *et al.* Macroscopic and histopathologic analysis of human knee menisci in aging and osteoarthritis. *Osteoarthr. Cartil.* **19**, 1132–1141 (2011).
- Battistelli, M. *et al.* Morphological and ultrastructural analysis of normal, injured and osteoarthritic human knee menisci. *Eur. J. Histochem.* **63**, 17–23 (2019).
- López-Franco, M. & Gómez-Barrena, E. Cellular and molecular meniscal changes in the degenerative knee: a review. *J. Exp. Orthop.* **5**, 11 (2018).
- Makris, E. A., Hadidi, P. & Athanasiou, K. A. The knee meniscus: structure-function, pathophysiology, current repair techniques, and prospects for regeneration. *Biomaterials* **32**, 7411–7431 (2011).
- Ghadjally, F. N., Lalonde, J. M. & Wedge, J. H. Ultrastructure of normal and torn menisci of the human knee joint. *J. Anat.* **136**, 773–791 (1983).
- Muhammad, H. *et al.* Human migratory meniscus progenitor cells are controlled via the TGF- β pathway. *Stem Cell Rep.* **3**, 789–803 (2014).
- Grogan, S. P., Pauli, C., Lotz, M. K. & D'Lima, D. D. Relevance of meniscal cell regional phenotype to tissue engineering. *Connect. Tissue Res.* **58**, 259–270 (2017).
- Son, M. & Levenston, M. Discrimination of meniscal cell phenotypes using gene expression profiles. *Eur. Cells Mater.* **23**, 195–208 (2012).
- Verdonk, P. C. M. *et al.* Characterisation of human knee meniscus cell phenotype. *Osteoarthr. Cartil.* **13**, 548–560 (2005).
- Greis, P. E., Bardana, D. D., Holmstrom, M. C. & Burks, R. T. Meniscal injury: I. Basic science and evaluation. *J. Am. Acad. Orthop. Surg.* **10**, 168–176 (2002).
- Bloeker, K. *et al.* Morphometric differences between the medial and lateral meniscus in healthy men: a three-dimensional analysis using magnetic resonance imaging. *Cells Tissues Organs* **195**, 353–364 (2012).
- Niu, W. *et al.* Cell-based strategies for meniscus tissue engineering. *Stem Cells Int.* **2016**, 1–10 (2016).
- Zellner, J. *et al.* Autologous mesenchymal stem cells or meniscal cells: what is the best cell source for regenerative meniscus treatment in an early osteoarthritis situation?. *Stem Cell Res. Ther.* **8**, 225 (2017).
- Martinek, V. *et al.* Second generation of meniscus transplantation: in-vivo study with tissue engineered meniscus replacement. *Arch. Orthop. Trauma Surg.* **126**, 228–234 (2006).
- Dominici, M. *et al.* Minimal criteria for defining multipotent mesenchymal stromal cells. The International Society for Cellular Therapy position statement. *Cytotherapy* **8**, 315–317 (2006).
- Howell, R. Degenerative meniscus: Pathogenesis, diagnosis, and treatment options. *World J. Orthop.* **5**, 597 (2014).
- Kumar, D., Manal, K. T. & Rudolph, K. S. Knee joint loading during gait in healthy controls and individuals with knee osteoarthritis. *Osteoarthr. Cartil.* **21**, 298–305 (2013).
- Li, L. *et al.* Biomechanical analysis of the effect of medial meniscus degenerative and traumatic lesions on the knee joint. *Am. J. Transl. Res.* **11**, 542–556 (2019).
- Petersen, W. & Tillmann, B. Collagenous fibril texture of the human knee joint menisci. *Anat. Embryol. (Berl)* **197**, 317–324 (1998).
- Arnoczky, S. P. & Warren, R. F. Microvasculature of the human meniscus. *Am. J. Sports Med.* **10**, 90–95 (1982).
- Petersen, W. & Tillmann, B. Age-related blood and lymph supply of the knee menisci: a cadaver study. *Acta Orthop. Scand.* **66**, 308–312 (1995).
- Mordecai, S. C. Treatment of meniscal tears: an evidence based approach. *World J. Orthop.* **5**, 233 (2014).
- Alsalamah, S., Amin, R., Gemba, T. & Lotz, M. Identification of mesenchymal progenitor cells in normal and osteoarthritic human articular cartilage. *Arthritis Rheum.* **50**, 1522–1532 (2004).
- Osawa, A. *et al.* The use of blood vessel-derived stem cells for meniscal regeneration and repair. *Med. Sci. Sport. Exerc.* **45**, 813–823 (2013).
- Fickert, S., Fiedler, J. & Brenner, R. Identification, quantification and isolation of mesenchymal progenitor cells from osteoarthritic synovium by fluorescence automated cell sorting. *Osteoarthr. Cartil.* **11**, 790–800 (2003).
- Iannone, F. & Lapidula, G. The pathophysiology of osteoarthritis. *Aging Clin. Exp. Res.* **15**, 364–372 (2003).
- Hemler, M. E. VLA proteins in the integrin family: structures, functions, and their role on leukocytes. *Annu. Rev. Immunol.* **8**, 365–400 (1990).
- Almonte-Becerril, M., Costell, M. & Kouri, J. B. Changes in the integrins expression are related with the osteoarthritis severity in an experimental animal model in rats. *J. Orthop. Res.* **32**, 1161–1166 (2014).
- Yang, X., Zhao, J., He, Y. & Huangfu, X. Screening for characteristic genes in osteoarthritis induced by destabilization of the medial meniscus utilizing bioinformatics approach. *J. Musculoskelet. Neuronal Interact.* **14**, 343–348 (2014).
- Cao, L. *et al.* β 1-Integrin-collagen interaction reduces chondrocyte apoptosis. *Matrix Biol.* **18**, 343–355 (1999).
- Tallheden, T. *et al.* Gene expression during redifferentiation of human articular chondrocytes. *Osteoarthr. Cartil.* **12**, 525–535 (2004).
- Prosser, A., Scotchford, C., Roberts, G., Grant, D. & Sottile, V. Integrated multi-assay culture model for stem cell chondrogenic differentiation. *Int. J. Mol. Sci.* **20**, 951 (2019).
- Hall, D. B. Measurement error in nonlinear models: a modern perspective. *J. Am. Stat. Assoc.* **103**, 427–427 (2008).
- Matthies, N.-F., Mulet-Sierra, A., Jomha, N. M. & Adesida, A. B. Matrix formation is enhanced in co-cultures of human meniscus cells with bone marrow stromal cells. *J. Tissue Eng. Regen. Med.* **7**, 965–973 (2013).

38. Hagmeijer, M. H. *et al.* Surgical feasibility of a one-stage cell-based arthroscopic procedure for meniscus regeneration: a cadaveric study. *Tissue Eng. Part C* **24**, 688–696 (2018).
39. Houck, D. A., Kraeutler, M. J., Belk, J. W., McCarty, E. C. & Bravman, J. T. Similar clinical outcomes following collagen or polyurethane meniscal scaffold implantation: a systematic review. *Knee Surg. Sports Traumatol. Arthrosc.* **26**, 2259–2269 (2018).
40. Van Der Straeten, C., Bytтеbier, P., Eeckhoudt, A. & Victor, J. Meniscal allograft transplantation does not prevent or delay progression of knee osteoarthritis. *PLoS ONE* **11**, e0156183 (2016).
41. McAlindon, T. E., Snow, S., Cooper, C. & Dieppe, P. A. Radiographic patterns of osteoarthritis of the knee joint in the community: the importance of the patellofemoral joint. *Ann. Rheum. Dis.* **51**, 844–849 (1992).
42. Schmittgen, T. D. & Livak, K. J. Analyzing real-time PCR data by the comparative CT method. *Nat. Protoc.* **3**, 1101–1108 (2008).
43. Johnstone, B., Hering, T. M., Caplan, A. L., Goldberg, V. M. & Yoo, J. U. In vitro chondrogenesis of bone marrow-derived mesenchymal progenitor cells. *Exp. Cell Res.* **238**, 265–272 (1998).
44. Farndale, R. W., Buttle, D. J. & Barrett, A. J. Improved quantitation and discrimination of sulphated glycosaminoglycans by use of dimethylmethylene blue. *Biochim. Biophys. Acta* **883**, 173–177 (1986).
45. Crowe, A. & Yue, W. Semi-quantitative determination of protein expression using immunohistochemistry staining and analysis: an integrated protocol. *Bio-protocol* **9**, e3465 (2019).

Acknowledgements

Authors are grateful to Versus Arthritis for supporting this work (Grants 20815, 21156 and 18480). The first author Jingsong Wang is also funded by the China Scholarship Council (CSC 201708210189) and Orthopaedic Institute Limited (RPG169).

Author contributions:

J.W., S.R., W.Z. and K.W. designed the study. J.W. conducted the experiments. J.W., S.R., J.G. and J.H.K. contributed to the analysis of the data. All authors contributed to the drafting of manuscript.

Competing interests

The authors declare no competing interests.

Additional information

Supplementary Information The online version contains supplementary material available at <https://doi.org/10.1038/s41598-020-78757-6>.

Correspondence and requests for materials should be addressed to K.W.

Reprints and permissions information is available at www.nature.com/reprints.

Publisher's note Springer Nature remains neutral with regard to jurisdictional claims in published maps and institutional affiliations.

 **Open Access** This article is licensed under a Creative Commons Attribution 4.0 International License, which permits use, sharing, adaptation, distribution and reproduction in any medium or format, as long as you give appropriate credit to the original author(s) and the source, provide a link to the Creative Commons licence, and indicate if changes were made. The images or other third party material in this article are included in the article's Creative Commons licence, unless indicated otherwise in a credit line to the material. If material is not included in the article's Creative Commons licence and your intended use is not permitted by statutory regulation or exceeds the permitted use, you will need to obtain permission directly from the copyright holder. To view a copy of this licence, visit <http://creativecommons.org/licenses/by/4.0/>.

© The Author(s) 2020